Regulation of pannexin 1 trafficking by adenosine triphosphate

by

Andrew Kenneth Jameson Boyce
B.Sc., University of Victoria, 2012

A Dissertation Submitted in Partial Fulfillment
of the Requirements for the Degree of

DOCTOR OF PHILOSOPHY

in the Division of Medical Sciences

© Andrew Boyce, 2017
University of Victoria

All rights reserved. This dissertation may not be reproduced in whole or in part, by photocopy or other means, without the permission of the author.

Supervisory Committee

Regulation of pannexin 1 trafficking by adenosine triphosphate

by

Andrew Kenneth Jameson Boyce
B.Sc., University of Victoria, 2012

Supervisory Committee

Dr. Leigh Anne Swayne (Division of Medical Sciences)
Supervisor

Dr. Robert Chow (Department of Biology)
Outside Member

Dr. Chris Nelson (Depart of Biochemistry & Microbiology)
Outside Member

Dr. Christian Naus (University of British Columbia)
Additional Member

Abstract

The ubiquitously expressed pannexin 1 (Panx1) ion- and metabolite-permeable channel is capable of mediating ATP release in a multitude of cells and tissues. This leads to activation of nearby purinergic (P2X/P2Y) receptors in an autocrine/paracrine manner. Stimulation of P2 receptors also triggers Panx1 activation, leading to the formation of a positive feedback loop. Although the focus of Panx1 research has primarily been on its expression at the cell surface, there is robust and stable expression of Panx1 on intracellular membranes. Whether intracellular Panx1 was the consequence of direct diversion from the secretory pathway or internalization from the cell surface was unknown at the onset of my studies. I postulated that Panx1 internalization to these membranes would require a ubiquitous constitutively or episodically released stimulus to allow stable intracellular expression. ATP, a potent signalling molecule released via exocytosis (constitutive or regulated) or large pore channels, fit this criterion. *My hypothesis was that ATP triggered Panx1 internalization to intracellular compartments*. Upon elevation of extracellular ATP, I observed P2X7R-mediated non-canonical internalization of Panx1 via macropinocytosis. This involved upstream cholesterol-dependent P2X7R-Panx1 clustering via a physical interaction between P2X7R-Panx1 ectodomains and possible contribution of phospholipid (PA, PIP, PIP_2) interactions localized to the Panx1 C-terminus. Physical P2X7R-Panx1 interaction may promote Panx1 association with actively endocytosing regions of the membrane. Internalized Panx1 was targeted to slow recycling Rab14/Rab11-positive endosomes in an Arf6-dependent mechanism. The data I presented here provides an additional negative feedback layer to P2X7R-Panx1 crosstalk in the many cell types where they are co-expressed. Further, this is the first evidence demonstrating that Panx1 surface expression is labile to changes in the cellular environment, which contributes to the understanding of the regulation of Panx1 and associated behaviours through trafficking mechanisms.

Table of Contents

Supervisory Committee ii
Abstract iii
Table of Contents iv
List of Tables vii
List of Figures viii
List of Abbreviations x
Publications xv
Acknowledgments xvii
1 Introduction 1
1.1 Dissertation Overview 1
1.2 Introduction to Pannexins (Panxs) 6
1.2.1 Discovery 6
1.2.2 Distribution 10
1.3 Panx1 11
1.3.1 Regulation of activity 12
1.3.2 Crosstalk with other receptors 13
1.3.3 Purinergic signalling 14
1.3.3.1 Purinergic receptors 15
1.3.3.2 P2X receptors 17
1.3.3.3 P2X7R 19
1.3.3.4 Crosstalk between P2X7R and Panx1 21
1.3.3.5 P2Y receptors 26
1.3.3.6 Contributors to extracellular ATP: Panx1-independent ATP release 27
1.3.3.7 Extracellular ATP hydrolysis 31
1.3.3.8 Negative regulation by extracellular ATP 31
1.3.4 Subcellular distribution 33
1.3.5 Regulation of stability and trafficking 34
1.3.5.1 Stability 36
1.3.5.2 Anterograde trafficking mechanisms 37
1.3.5.3 N-linked glycosylation 38
1.3.5.4 Role of the C-terminus 39
1.3.5.5 Retrograde trafficking mechanisms 41
1.4 Non-canonical mechanisms of endocytosis 46
1.4.1 Phagocytosis 49
1.4.2 Macropinocytosis 50
1.4.3 CLIC/GEEC endocytosis 52
1.4.4 Flotillin-mediated endocytosis 52
1.5 Summary 53
2 Methods 55
2.1 Cell culture 55
2.1.1 Plasmids 55
2.1.2 Transfection and generation of stable cell lines 56

2.1.3 Reagents for cellular treatments ... 57
2.2 Imaging assays ... 59
2.2.1 Live cell confocal microscopy ... 59
2.2.1.1 Live cell Panx1 tracking ... 59
2.2.1.2 Ca^{2+} imaging ... 60
2.2.2 Fixed cell confocal microscopy ... 60
2.2.2.1 Antibodies ... 61
2.2.2.2 Intracellular Panx1 distribution ... 62
2.2.2.3 Panx1 codistribution with subcellular compartment markers ... 64
2.2.2.4 Visualizing P2X7R-Panx1 interactions ... 67
2.2.2.5 Proximity ligation assays (PLA) ... 67
2.3 Biochemical assays ... 69
2.3.1 Western blotting ... 69
2.3.2 Reverse transcriptase-polymerase chain reaction (RT-PCR) ... 70
2.3.3 GST-fusion protein expression and purification ... 71
2.3.4 Pull-down assays ... 72
2.3.5 Membrane lipid strip interaction assays ... 73
2.4 Statistical analysis ... 74
3 ATP modulates Panx1 plasma membrane stability ... 75
3.1 Overview ... 75
3.2 ATP stimulates dose-dependent Panx1 internalization ... 78
3.3 ATP-evoked internalization is dependent on P2XRs ... 81
3.4 Selective inhibition of P2X7R disrupts Panx1 internalization ... 84
3.5 Alanine substitution of W74 in the Panx1 EL1 abrogates ATP-evoked internalization ... 85
3.6 ATP triggers internalization of Panx1 to recycling endosomes ... 86
3.7 Discussion ... 93
4 An extracellular P2X7R-Panx1 interaction regulates downstream internalization ... 102
4.1 Overview ... 102
4.2 Extracellular ATP addition induces P2X7R-Panx1 clustering ... 105
4.3 Endogenous ATP release triggers P2X7R-Panx1 clustering and internalization 107
4.4 Panx1 EL1 interacts with P2X7R ... 108
4.5 W74 within the Panx1 EL1 is essential for ATP-induced P2X7R-Panx1 clustering ... 111
4.6 P2X7R activation (independent of Ca^{2+} and Src) triggers P2X7R-Panx1 clustering and internalization ... 111
4.7 Discussion ... 117
5 Endocytic machinery involved in Panx1 internalization ... 126
5.1 Overview ... 126
5.2 ATP-evoked Panx1 internalization is independent of clathrin and caveolin, but dependent on cholesterol ... 129
5.3 Amiloride disrupts ATP-evoked Panx1 internalization ... 133
5.4 Internalized Panx1 is sorted by Arf6 GTPase ... 134
5.5 Peripheral P2X7R-Panx1 clustering is regulated by membrane cholesterol ... 136
5.6 The Panx1 C-terminus interacts with several phospholipids ... 137

5.7 Discussion 140
6 General Discussion: 149
6.1 ATP-mediated regulation of other Panxs? 151
6.2 Role of other P2X receptors in Panx1 internalization? 153
6.3 Regulatory roles of the C-terminus in Panx1 trafficking and beyond 156
6.4 Investigation of novel regulators of Panx1 trafficking 160
6.5 P2X7R-Panx1 crosstalk in the nervous system 162
6.5.1 In the adult SVZ 169
6.5.2 In chronic pain 171
6.6 Summary 174
Bibliography 176
Appendix 202

List of Tables

Table 1.1 P2X7R sequence variants impact Panx1 crosstalk 25
Table 1.2 Physical interaction between P2X7R and Panx1 26

List of Figures

Figure 1.1 Panxs share structural similarity with Cxs but do not form gap junctions..... 17
Figure 1.3 Regulation of extracellular ATP and purinergic signalling..... 29
Figure 1.4 ATP-sensitive residues in the Panx1 extracellular loops 33
Figure 1.5 Panx1 trafficking 35
Figure 1.6 Panx1 structural elements involved stability and trafficking 39
Figure 1.7 Mechanisms of endocytosis..... 42
Figure 1.8 Research questions 54
Figure 2.1 Panx1-EGFP and endogenous Panx1 demonstrate similar subcellular distribution in N2a cells 56
Figure 2.2 Subcellular compartments are distinguishable using confocal microscopy and codistribution analysis 66
Figure 2.3 Controls for PLA specificity 69
Figure 3.1 Elevated extracellular ATP stimulates internalization of Panx1 79
Figure 3.2 Panx1 is selectively internalized by P2X receptor agonists 83
Figure 3.3 Selective P2X7R inhibition disrupts ATP-evoked Panx1 internalization..... 85
Figure 3.4 Panx1 internalization is impaired in Panx1W74A-expressing cells..... 86
Figure 3.5 ATP triggers transient co-distribution of Panx1 and markers for the early endosome 88
Figure 3.6 ATP transiently reduces distribution of Panx1 with markers for the degradative pathway 90
Figure 3.7 ATP triggers latent increase in Panx1 co-distribution with components of the recycling endosome 92
Figure 3.9 ATP evokes Panx1 endocytosis and targeting of internalized Panx1 to recycling endosomes..... 100
Figure 4.1 ATP triggers P2X7R-Panx1 clustering 106
Figure 4.2 Endogenous ATP release stimulates and is required for P2X7R-Panx1 clustering and regulates Panx1 internalization 108
Figure 4.3 An extracellular interaction of the Panx1 EL1 with P2X7Rs is required for ATP-induced internalization..... 110
Figure 4.4 P2X7R activation, independent of Ca^{2+} signalling pathways, is critical for P2X7R-Panx1 clustering and internalization..... 113
Figure 4.5 P2X7R-Panx1 clustering and internalization is independent of upstream P2X7R-Src signalling 116
Figure 4.6 ATP triggers an extracellular interaction between P2X7R and Panx1, sensitive to Panx1 W74A mutation, upstream of internalization 124
Figure 5.1 Panx1 internalization is clathrin-independent, but sensitive to membrane cholesterol modulation..... 130
Figure 5.2 ATP-evoked Panx1 internalization is clathrin-, caveolin-, and dynamin-independent..... 133
Figure 5.3 Panx1 internalization is amiloride-sensitive..... 134
Figure 5.4 Sorting of internalized Panx1 is dependent on Arf6 135
Figure 5.5 Peripheral P2X7R-Panx1 clustering is cholesterol-dependent..... 137

Figure 5.6 The Panx1 C-terminus interacts with specialized phospholipids 139
Figure 5.7 ATP triggers P2X7R-dependent macropinocytosis reliant on membrane cholesterol internalizes Panx1 into Arf6-positive vesicles 148
Figure 6.1 Regulation of Panx1 trafficking by ATP: summary of my dissertation 151
Figure 6.2 Conservation of ATP-sensitive residues between Panxs..... 153
Figure 6.3 Potential regulators of Panx1 trafficking are enriched in the C-terminus 160
Figure 6.4 Context-specific P2X7R-Panx1 crosstalk in the nervous system..... 168

List of Abbreviations

$^{-/-}$ – knockout

A23187 – Ca^{2+} ionophore

A438079 – selective P2X7R inhibitor

aa – amino acid

ADP – adenosine diphosphate

ADPβS – adenosine-5'-(β-thio)-diphosphate

ANOVA – analysis of variance

AP2 – adaptor protein 2

Arf – ADP ribosylation factor

ARL 67156 – ectonucleotidase inhibitor

Arp2/3 – actin-related protein 2/3 complex

ATCC – American Type Culture Collection

ATP – adenosine triphosphate

ATPγS – adenosine-5'-(γ-thio)-triphosphate

ATPase – ATP hydrolase

BARS – BFA-dependent ADP ribosylation substrate

BFA – brefeldin A

BICR-M1R_k – rat mammary tumour cell line

BSA – bovine serum albumin

BzATP – 2'(3')-O-(4-benzoylbenzoyl) adenosine 5'-triphosphate

Ca^{2+} – calcium

CALHM – Ca^{2+} homeostasis modulator

cAMP – cyclic adenosine monophosphate

Cav-1 – caveolin-1

Cav-2 – caveolin-2

Cav-3 – caveolin-3

Cdc42 – cell division control protein 42

CHOL – cholesterol

CFP – cyan fluorescent protein

CHX – cycloheximide

CL – cardiolipin

CLIC/GEEC – clathrin-independent carrier/GPI-anchor enriched endosomal compartments

CLPZ – chlorpromazine

CNS – central nervous system

COPII – coatomer protein II

CT – carboxyl-terminus

Cx – connexin

Da – Dalton

DAG – diacylglycerol

DMEM – Dulbecco's modified Eagle's medium

DMSO – dimethyl sulphoxide

Dyn II K44A – dominant-negative dynamin II

EEA1 – early endosomal antigen 1

EGFP – enhanced green fluorescent protein

EL – extracellular loop

ER – endoplasmic reticulum

Fil III – filipin III

FRAP – fluorescence recovery after photobleaching

G418 – geneticin 418

GFAP – glial fibrillary acid protein

GFP – green fluorescent protein

Gly0 – core glycosylation

Gly1 – high mannose glycosylation

Gly2 – complex glycosylation

GPI – glycosylphoshatidylinositol

GST- glutathione S-transferase

GT – glyceryl tripalmitate

GTP – guanosine triphosphate

GTPase – GTP hydrolase

HBSS – Hank's buffered saline solution

HEK – human embryonic kidney

HRP – horseradish peroxidase

ICL – intracellular loop

IgG – immunoglobulin G

IP_3 – inositol triphosphate

IP – immunoprecipitation

Ix – innexin

K^+ – potassium

kDa – kilodalton

Lamp1 – lysosomal-associated membrane protein 1

LPAAT-α – lysophosphatidic acid acyltransferase-α

LRRC8 – leucine rich repeat containing 8

M6PR – mannose-6-phosphate receptor

MβCD – methyl-β-cyclodextrin

mPanx1 – mouse Panx1

N2a – Neuro-2a mouse neuroblastoma cells

NA – numerical aperture

NMDAR – N-methyl-D-aspartate receptor

NT – amino-terminus

NTDPase – nucleoside triphosphate diphosphohydrolases

E-NPP – ecto-pyrophosphatase/phosphodiesterase

OGD – oxygen-glucose deprivation

P2XR – ionotropic purinergic receptor

P2YR – metabotropic purinergic receptor

PA – phosphatidic acid

PAK1 – p21-activated kinase

Panx - pannexin

Panx1 – pannexin 1

Panx1Δ307 – C-terminal truncation mutant of Panx1

Panx2 – pannexin 2

$Panx2^{Panx1CT}$ – Panx2-Panx1 C-terminus chimer

Panx3 – pannexin 3

PBS – phosphate buffered saline

PBS-T – phosphate buffered saline with 0.1% Tween-20

PC – phosphatidylcholine

PDL – poly-D-lysine

PE – phosphatidylethanolamine

PFA - paraformaldehyde

PG – phosphatidylglycerol

PI – phosphatidylinositol

PI(4)P – phosphatidylinositol 4-phosphate

$PI(4,5)P_2$ – phosphatidylinositol 4,5-bisphosphate

$PI(3,4,5)P_3$ – phosphatidylinositol 3,4,5-triphosphate

PLA – proximity ligation assay

PLD – phospholipase D

PS – phosphatidylserine

PTM – post-translational modification

PVDF – polyvinyl fluoride

Rab – Ras-related protein

Rac1 – Ras-related C3 botulinum toxin substrate 1

RFP – red fluorescent protein

RT-PCR – reverse transcriptase-polymerase chain reaction

Sar1 – small COPII coat GTPase 1

SDS-PAGE – sodium dodecyl sulphate polyacrylamide gel electrophoresis

SFK – Src family kinase

SH3 – Src homology domain 3

SM – sphingomyelin

Src – sarcoma kinase

STED – stimulated emission depletion

SULF – 3-sulfogalactosylceramide

SVZ – subventricular zone

TAT – transactivator of transcription (HIV1)

TNF – tumour necrosis factor

TRITC – tetramethylrhodamine

UDP – uridine diphosphate

UTP – uridine triphosphate

UVIC – University of Victoria

VNUT – vesicular nucleotide transporter

V-ATPase – vacuolar type H+/ATPase

WGA – wheat germ agglutinin

Publications

Original Research:

1. Boyce AKJ, Swayne LA. (2017) P2X7 receptor crosstalk regulates ATP-induced pannexin 1 internalization. Biochemical Journal 474(13): 2133-2144.
2. Boyce AKJ, Kim MS, Wicki-Stordeur LE, Swayne LA. (2015) ATP stimulates Pannexin 1 internalization to endosomal compartments. Biochemical Journal 470(3): 319-330.
3. Wicki-Stordeur LE, Boyce AKJ, Swayne LA. (2013) Analysis of a Pannexin 2-pannexin 1 chimeric protein supports divergent roles for Pannexin C-termini in cellular localization. Cell Communication & Adhesion 3(4): 73-79.

Reviews:

1. Boyce AKJ**,** Epp AE, Naharajan A, Swayne LA. (2017) Transcriptional and post-translational regulation of pannexins. Biochim Biophys Acta. [ePub ahead of print]
2. Boyce AKJ**,** Wicki-Stordeur LE, Swayne LA. (2014) Powerful partnership: crosstalk between pannexin 1 and the cytoskeleton. Frontiers in Physiology 5(27).
3. Boyce AKJ**,** Prager RT, Wicki-Stordeur LE, Swayne LA. (2013) Pore positioning: Current concepts in Pannexin trafficking. Channels (Austin) 8(2).

Conference Presentation Abstracts:

1. Boyce AKJ, Swayne LA (2016). Molecular mechanisms of ATP-evoked Pannexin 1 internalization. American Society for Cell Biology. San Francisco, California, USA. Poster presentation.
2. Boyce AKJ, Swayne LA (2016). Molecular mechanisms of ATP-evoked Pannexin 1 internalization. University of Virginia Pannexin Conference. Charlottesville, Virginia, USA. Poster presentation.
3. Boyce AKJ, Kim MS, Wicki-Stordeur LE, Swayne LA. (2015). ATP evokes Pannexin 1 endocytosis to endosomal compartments. American Society for Cell Biology. San Diego, California, USA. Oral & Poster presentation.
4. Boyce AKJ, Kim MS, Wicki-Stordeur LE, Swayne LA. (2015). ATP-evoked internalization of Pannexin 1 channels. International Gap Junction Conference. Valparaiso, Chile. Oral & Poster presentation. **Awarded Honourable Mention.**
5. Boyce AKJ, Kim MS, Wicki-Stordeur LE, Swayne LA. (2015). ATP-evoked internalization of Pannexin 1 channels. Canadian Association for Neuroscience (National). Vancouver, British Columbia, Canada. Poster presentation.
6. Boyce AKJ, Prager RT, Wicki-Stordeur LE, Swayne LA. (2014). Stimulus-evoked internalization of Pannexin 1 channels**.** American Society for Cell Biology Annual Meeting (International). Philadelphia, Pennsylvania, USA. Poster presentation.
7. Boyce AKJ, Prager RT, Wicki-Stordeur LE, Swayne LA. (2014). Stimulus-evoked internalization of Pannexin 1 channels. Heart & Stroke Foundation Canadian Partnership for Stroke Recovery Annual Meeting (National). Ottawa, Ontario, Canada. Poster presentation.
8. Boyce AKJ, Wicki-Stordeur LE, Prager RT, Swayne LA. (2013). Investigating a novel intracellular localization and mode of trafficking of Pannexin 1 with

implications for neural cell viability in the post-stroke brain environment. Microscopical Society of Canada Annual Meeting. Victoria, BC, Canada. Oral presentation.

9. Boyce AKJ, Wicki-Stordeur LE, Prager RT, Swayne LA. (2013). Investigating a novel localization and mode of trafficking of Pannexin 1 with implications for neural cell viability in the post-stroke brain environment. Society for Neuroscience Annual Meeting. Toronto, Ontario, Canada. Poster presentation.
10. Boyce AKJ, Wicki-Stordeur LE, Prager RT, Swayne LA. (2013). A novel perinuclear localization of the Pannexin-1 channel could play an additional role in neural cell response to post-stroke stimuli. Loon Lake Cell Biology Retreat. Vancouver, BC, Canada. Oral Presentation.

Acknowledgments

I owe thanks to so many people for their support and encouragement in completing my dissertation work. First and foremost, I want to thank my supervisor Dr. Leigh Anne Swayne. Without her, I would absolutely not be where I am today. I started off in her lab as a wide-eyed undergraduate student, who loved science, but didn't know the first thing about how to do it. So I must thank her for her patience and troubleshooting advice during challenging times, but also for her encouragement, support, and shared excitement when we were on a scientific roll! I also owe thanks to my committee members, Dr. Bob Chow, Dr. Christian Naus, and Dr. Chris Nelson, who provided expert insight, as well as both encouragement and critique over the duration of my project. I would also like to thank Dr. Ian Winship, who acted as an external examiner during my defense.

Funding for this work was provided by the Natural Sciences and Engineering Research Council (NSERC) [RGPIN-2016-04579], infrastructure support from the Canada Foundation for Innovation (CFI) [grant number 29462] and the BC Knowledge Development Fund (BCKDF) [grant number 804754] and start up funds from the University of Victoria (UVic). I was supported by an NSERC Alexander Graham Bell Canada Graduate Scholarship-Master's, an NSERC Postgraduate Scholarship-Doctoral (3 years), and donor awards from UVic (Dr. Howard E. Petch Research Scholarship, President's Research Scholarship, and Dr. Julius F. Schleicher Memorial Scholarship).

Thanks to the many Swayne Lab members who provided experimental and moral support throughout my project. Leigh Wicki-Stordeur helped to perform the cell-surface

luminometry experiments and performed immunostaining and imaging for Figure 2.1 used in the Methods section. She was also an excellent student mentor for me when I was first starting graduate school. Her patience, intrigue, and technical skills were a wonderful example for me as a new graduate student and her continued support throughout my project was greatly appreciated. There were a few other lab members that helped in the generation of some key tools used in my project. Michelle Kim performed the site-directed mutagenesis involved in creating the Panx1 W74A mutant construct. Rose Swansburg performed RT-PCR for the P2X receptors. Finally, I would like to thank Juan Sanchez-Arias, Lena Chen, Catherine Choi, Anna Epp, and Naomi Fuglem for the excellent scientific atmosphere and tremendous support as I worked to finish my project.

Thank you to Dr. Dale Laird and Dr. Silvia Penuela who provided the Panx1-EGFP and Panx1-RFP constructs, as well as the Panx1 EL2 and Panx1 CT antibodies used in this project.

Thank you to my friends who kept asking about my work even though for the first few years I had trouble explaining it to them. They have all helped me become a better science communicator and encouraged and supported me through the trials and tribulations of grad school.

Thank you to my two amazing sisters who are my best friends and a constant inspiration to me. Finally, to my Mom and Dad, thanks for all the love as well as moral support (and financial support when I needed it) that allowed me to pursue my passion for science and focus on academics, which has been a true privilege.

1 Introduction

1.1 Dissertation Overview

Pannexin 1 (Panx1) is a large pore ion and metabolite channel permeable to molecules up to approximately 1 kilodalton (kDa) in size (including adenosine triphosphate, ATP). It is expressed nearly ubiquitously in mammalian cells and tissues (reviewed in Boyce et al. 2017). Panx1 is activated by both physiological [i.e. mechanical stretch (Bao et al. 2004; Xia et al. 2012), G-protein coupled receptor (GPCR) signalling (Locovei, Wang, et al. 2006; Billaud et al. 2015)] and pathophysiological [i.e. ischemia (Weilinger et al. 2012; Thompson et al. 2006), and excitotoxicity (Thompson et al. 2008)] stimuli. In these diverse cells and tissues, Panx1 activation regulates cellular behaviours including neuronal development (Wicki-Stordeur et al. 2012; Wicki-Stordeur & Swayne 2013; Wicki-Stordeur et al. 2016), modulation of synaptic activity (Prochnow et al. 2009; Ardiles et al. 2014; Weilinger et al. 2016; Vroman et al. 2014), regulation of seizure activity (Kim & Kang 2011), propagation of calcium (Ca^{2+}) waves (Locovei, Wang, et al. 2006), inflammasome activation (Crespo Yanguas et al. 2017), cell death (Weilinger et al. 2012; Gulbransen et al. 2012), recruitment of immune cells (Chekeni et al. 2010), and regulation of vascular tone (Lohman et al. 2015, reviewed in Swayne & Bennett 2016; Sanchez-Arias et al. 2016). Many are regulated by crosstalk with other receptors upstream of Panx1 activation including ionotropic purinergic P2X7 receptors (P2X7R), N-methyl-D-aspartate receptors (NMDAR), α-adrenergic receptors, and tumour necrosis factor (TNF)-α receptors (reviewed in Isakson & Thompson 2014; Bravo et al. 2015). A standout amongst these receptor interactions is the interaction with

the ATP-sensitive P2X7R. Notably, not only does ATP released through Panx1 activate P2X7R and other purinergic receptors, but also P2X7R activation stimulates the opening of Panx1 channels (Pelegrin & Surprenant 2006; Iglesias et al. 2008), leading to the establishment of a positive feedback loop in cells where they are co-expressed (reviewed in Baroja-Mazo et al. 2013). These positive feedback loops permit escalating activation, which promotes constitutive Panx1 activation unless countered by some negative feedback mechanism. The first evidence of negative feedback was that elevated extracellular ATP inhibited Panx1 channel function (Ma et al. 2009; Qiu et al. 2012; Qiu & Dahl 2009). I became interested in whether ATP promoted Panx1 internalization because although cell surface Panx1 expression was critical for Panx1-mediated ATP release, several reports observed significant and stable populations of intracellular Panx1 (Bhalla-Gehi et al. 2010; Cone et al. 2013; Lai et al. 2007; Vanden Abeele et al. 2006). As ATP is constitutively or episodically released in many cell types, in this dissertation **I investigated the hypothesis that ATP modulates the cell surface stability of Panx1 by triggering endocytosis to intracellular compartments.**

In the subsequent sections of chapter 1, I briefly introduce and elaborate on the history and current knowledge of the Panx family (Panx1, Panx2, Panx3), including discovery, relationship to gap junction-forming large pore channels, structural features, and cell- and tissue-specific expression. Following this, I focus on Panx1, the most ubiquitous and well-studied Panx and the focus of the work described in my dissertation. I discuss the regulation of its activity and highlight its role as an ATP release channel in purinergic signalling. I then explore the receptor crosstalk involved in Panx1 signalling with a focus on P2X7R, in particular. As my dissertation work identified ATP-mediated

internalization of Panx1, I detail the discovery of ATP as a paracrine- and autocrine-signalling molecule and its regulation. Following this, I summarize the existing knowledge on Panx1 subcellular distribution, stability, and both anterograde and retrograde trafficking mechanisms. I then introduced the possible internalization mechanisms, based on what was known about Panx1 trafficking prior to commencing my dissertation work. In chapter 2, I lay out the methods used throughout this dissertation.

In chapter 3, I investigated *the hypothesis that elevated extracellular ATP promotes Panx1 endocytosis.* Exogenous ATP application stimulated dose- and time-dependent endocytosis of Panx1. I also determined that Panx1 internalization was specific to ATP and was unaffected by other stimuli known to modulate cellular excitability and excitotoxicity. Further, using ATP analogues and metabolites, I determined that Panx1 internalization was regulated by ionotropic purinergic P2X receptors. This was likely through the P2X7R, as a selective P2X7R inhibitor (A438079) disrupted Panx1 internalization. I also demonstrated that an ATP-sensitive residue (W74) in the Panx1 first extracellular loop (Panx1 EL1) was involved in triggering internalization. Using confocal microscopy, I tracked internalized Panx1 through the endosomal system over time using subcellular compartment-specific markers and determined that it was targeted to recycling endosomes.

In chapter 4, I followed up on my earlier finding that Panx1 internalization was dependent on P2X7R activation and investigated the hypothesis that *extracellular ATP promotes a P2X7R and Panx1 interaction, upstream of Panx1 internalization.* I first discovered that elevation of extracellular ATP triggered transient P2X7R-Panx1 clustering at the cellular periphery with a subsequent increase in P2X7R-Panx1 clusters

in intracellular compartments. This observation suggested that P2X7R-Panx1 clusters subsequently internalized. Next, I explored the role of endogenous ATP release in regulating both P2X7R-Panx1 clustering and Panx1 internalization. Baseline P2X7R-Panx1 clustering was enhanced by inhibition of ATP hydrolysis (ectonucleotidase activity) and ablated by enzymatic degradation of endogenous extracellular ATP. I also observed that endogenous ATP release promoted internalization of Panx1. I next identified a physical extracellular interaction between P2X7R and the first extracellular loop of Panx1 (Panx1 EL1). ATP-evoked P2X7R-Panx1 clustering and internalization was disrupted in cells expressing a Panx1 W74A mutant. I also determined that P2X7R activation was required for P2X7R-Panx1 clustering. However, clustering was unaffected by modulation of intracellular P2X7R [Ca^{2+} and sarcoma kinase (Src)-dependent] signalling pathways associated with positive P2X7R-Panx1 crosstalk. Taken together, I identified that P2X7R and Panx1 interacted through their extracellular domains with mutation of Panx1 W74A disrupting ATP-evoked P2X7R-Panx1 clustering and internalization.

In chapter 5, I explored the endocytic machinery involved in regulating P2X7R-Panx1 clustering and Panx1 internalization, linked to my findings in chapters 3 and 4. Based on these findings and preliminary evidence from the literature, I investigated the hypothesis that *ATP stimulated P2X7R-Panx1 clustering and internalization via non-canonical mechanisms dependent on membrane cholesterol.* I first demonstrated that ATP-evoked Panx1 internalization occurred independent of the canonical mechanisms of endocytosis (clathrin, caveolin, and dynamin proteins), yet was dependent on membrane cholesterol. P2X7Rs were previously associated with signalling through lipid

microdomains (reviewed in Robinson & Murrell-Lagnado 2013) that was disrupted by cholesterol depletion, so these findings were not particularly surprising. After describing these findings, I investigated potential non-canonical mechanisms of endocytosis. As Panx1 internalization occurred in relatively large vesicles associated with dynamic membrane regions and Panx1 had been previously shown to interact with actin (Wicki-Stordeur & Swayne 2013; Bhalla-Gehi et al. 2010) and an actin-regulatory protein (Arp3) (Wicki-Stordeur & Swayne 2013), I next investigated regulated macropinocytosis, an actin and Arp3-dependent internalization pathway, as a potential route for Panx1 endocytosis. ATP-dependent Panx1 internalization was disrupted by amiloride, a selective inhibitor of macropinocytosis. In chapter 3, internalized Panx1 was predominantly targeted to recycling endosomes, consequently it would be expected that Panx1 would require sorting in the early endosome upon internalization. A common protein associated with sorting of cargo from non-canonical endocytosis is the GTPase, ADP ribosylation factor 6 (Arf6). Co-expression with a constitutively active (GTP-bound) mutant of Arf6 (Arf6 Q67L), linked to disruption of the sorting event at the early endosome, accumulated intracellular Panx1 in enlarged early-endosome-like vacuoles. Next, I determined that aggregation of membrane cholesterol, as well as cholesterol depletion, disrupted both peripheral P2X7R-Panx1 clustering upstream of internalization. Cholesterol-dependent P2X7R activity was previously reported to regulate lipid metabolism. The Panx1 C-terminus interacted with several phospholipids associated with P2X7R-mediated lipid metabolism and endocytic trafficking. Taken together, these data suggested that ATP-evoked Panx1 internalization via macropinocytosis with endosomal sorting by the Arf6 GTPase.

In summary, I identified that Panx1 surface expression is reduced by an increase in extracellular concentrations of ATP. Panx1 was susceptible to ATP-evoked, P2X7R-regulated internalization, through the early endosome into recycling endosomes, in a dose- and time-dependent mechanism. ATP induced an extracellular interaction between P2X7R and Panx1. Both clustering and internalization were disrupted by mutation of W74 in Panx1 EL1. I then showed that ATP regulates P2X7R-Panx1 cholesterol-dependent clustering upstream of Panx1 internalization through a non-canonical macropinocytic mechanism involving endosomal sorting by Arf6. Finally, the Panx1 C-terminus interacted with phospholipids linked to P2X7R-mediated lipid metabolism involved in regulating membrane curvature in endocytosis, suggesting that this domain may be pivotal for clustering of Panx1 into actively-endocytosing regions of the membrane. This has vast and diverse consequences for P2X7R-Panx1 crosstalk in the many cell types and physiological/pathophysiological scenarios where these two proteins are co-expressed. This is discussed in Chapter 6, along with future directions to follow up on several of the findings I made over the course of my studies.

1.2 Introduction to Pannexins (Panxs)

1.2.1 Discovery

Panxs (Panx1, Panx2, and Panx3) are large pore channels (capable of mediating passage of molecules < 1 kDa) expressed in vertebrates, first discovered by Panchin *et al.* due to their sequence homology to the invertebrate gap junction forming proteins, innexins (Ixs; Panchin et al. 2000). Interestingly, despite sharing sequence homology with Ixs, Panxs did not exhibit sequence homology with the gap junction forming

proteins in vertebrates, connexins (Cxs). Without a high resolution crystal structure available, Panxs were predicted to share structural similarity with Cxs (reviewed in Penuela et al. 2013), which had been described using X-ray crystallography (Maeda et al. 2009; Oshima et al. 2007). Like Cxs, Panxs were predicted to be four pass transmembrane (TM) proteins (Penuela et al. 2013; Figure 1.1), with a cytosolic N-terminus, two extracellular loops (EL), a single intracellular loop (ICL) and a cytosolic C-terminus, yet the boundaries of each domain in Panx have not been precisely determined and varied slightly between sources (Penuela et al. 2009; Wang & Dahl 2010; Spagnol et al. 2014; Dourado et al. 2014; D'hondt et al. 2013). Although Cxs hexamerized to form functional channels, Panxs varied in their oligomerization stoichiometry: Panx1 formed hexamers (Ambrosi et al. 2010; Chiu et al. 2017; Boassa et al. 2007), Panx2 formed heptamers or octamers (Ambrosi et al. 2010), and Panx3, although not experimentally determined, was predicted for hexameric channels like Panx1 thanks to sequence similarities (reviewed in Sosinsky et al. 2011).

The overall protein size and domain length varies between each of the three Panx family members (Penuela et al. 2009). Panx family members exhibit multiple species on Western blot; Panx1 (~41-18 kDa) and Panx3 (~43 kDa) were similar in size, whereas Panx2 is significantly larger (~80 kDa), due to an elongated C-terminus. Each Panx protein is subject to diverse post-translational modifications (PTMs) that regulate both channel function, as well as localization, trafficking, and stability, including phosphorylation (Weilinger et al. 2016; Iglesias et al. 2008; Billaud et al. 2011; Lohman et al. 2015), N-linked glycosylation (Boassa et al. 2007; Penuela et al. 2007), S-nitrosylation (Lohman, Weaver, et al. 2012), palmitoylation (Swayne et al. 2010), and

proteolytic cleavage by caspases (Chekeni et al. 2010; Sandilos et al. 2012, reviewed in Boyce et al. 2017). As the work discussed in my dissertation focuses on regulators of Panx1 trafficking, N-glycosylation, a critical regulatory of Panx1 anterograde trafficking and stability, will be discussed in more depth in a subsequent section.

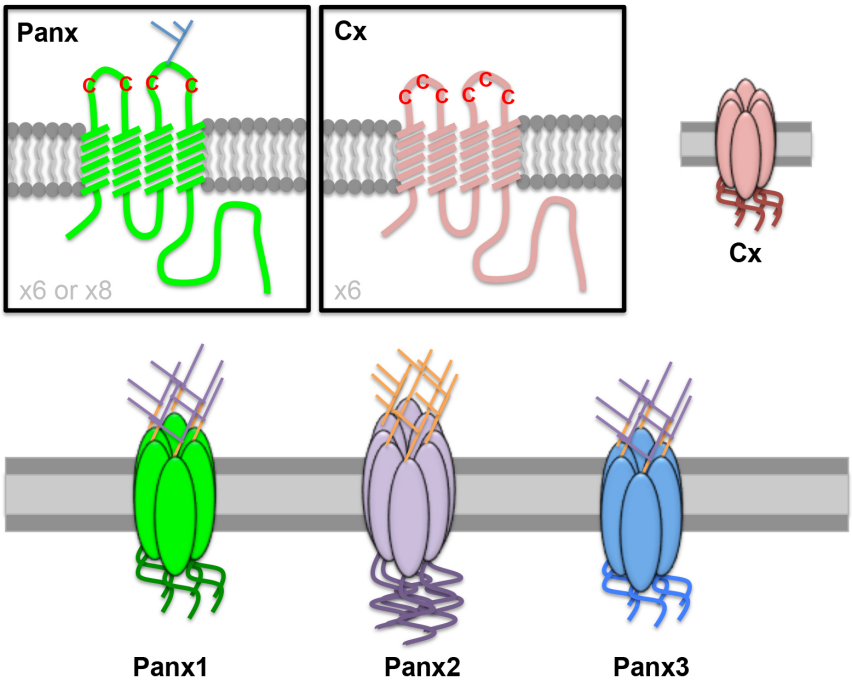

Figure 1.1 Panxs share structural similarity with Cxs but do not form gap junctions. Panxs and Cxs share four-pass transmembrane domain structure with intracellular termini. While Cxs are able to form gap junctions, Panxs are not, likely due to fewer extracellular cysteines (C) involved in forming intramolecular disulphide bonds and the presence of an N-glycosylation on their exofacial surface that would sterically hinder junctional docking. Like Cxs, Panx1 is a hexameric protein, while Panx2 are most likely octameric. Due to similarity with Panx1, Panx3 is predicted to form hexamers.

Based on sequence and structural similarities, Panxs were initially assumed to be a novel gap junction protein (Panchin 2005). Gap junctions, traditionally formed by Cxs (vertebrates) and Ixs (invertebrates), are intercellular channels made up of docked large-

pore channels expressed in neighbouring cells. They are capable of mediating transfer of ions, as well as small molecules and second messengers, including, glutamate, glutathione, glucose, inositol triphosphate (IP_3), cyclic adenosine monophosphate (cAMP), and ATP (Alexander & Goldberg 2003). To date, the sparse evidence that Panxs were capable of forming gap junctions came from ectopic expression systems (Bruzzone et al. 2003; Lai et al. 2007; Vanden Abeele et al. 2006; Ishikawa et al. 2011; Sahu et al. 2014) and has yet to be identified with endogenous Panx1 in physiological conditions. There were several key differences between Cxs and Panxs, which contributed to a growing consensus that Panxs did not form gap junctions (reviewed in Sosinsky et al. 2011). In Cxs, each extracellular loop contained three conserved cysteines requisite for the intramolecular disulphide bonds establishing the secondary structure necessary for junctional formation (Foote et al. 1998; Dahl et al. 1991). This allowed Cx monomers to form stable intercellular channels by docking with apposing Cxs on neighbouring cells (reviewed in Laird 2006). First, Panxs possessed two fewer extracellular cysteines than Cxs, which likely disrupted junctional capabilities (Ambrosi et al. 2010). Unlike Cxs, Panxs were glycosylated on their exofacial surface (Boassa et al. 2007; Penuela et al. 2007), which likely provided steric hindrance to disrupt junctional coupling (reviewed in Sosinsky et al. 2011). Finally, Panxs were expressed in non-junctional cells, such as erythrocytes (Locovei et al. 2006). This suggested that they had a physiological role outside of gap junctional communication (reviewed in Sosinsky et al. 2011).

1.2.2 Distribution

Each Panx family demonstrates differential cell and tissue type-specific expression patterns indicating differential regulation of gene expression. Panx1 exhibited nearly ubiquitous expression across mammalian cells (Penuela et al. 2007; Baranova et al. 2004; Dvoriantchikova et al. 2006; Ivanov et al. 2006; Turmel et al. 2011; Wang et al. 2009; Pelegrin & Surprenant 2006; Sridharan et al. 2010; Lohman, Billaud, et al. 2012; Riquelme et al. 2013; Dolmatova et al. 2012), with enrichment in the nervous system, at both the transcript (Baranova et al. 2004) and protein (Penuela et al. 2007) levels. The expression of *PANX2* transcript was initially reported exclusively in the nervous system (Baranova et al. 2004); however, more recent studies have identified less restricted expression of transcripts in rats (Bruzzone et al. 2003) and transcripts and protein in mice (Le Vasseur et al. 2014). In the central nervous system (CNS) of rats, Panx1 and Panx2 co-expression was observed in most cell types during detailed inspection (Bruzzone et al. 2003; Vogt et al. 2005). Unlike Panx1 and Panx2, Panx3 was not expressed in cells of the nervous system (Penuela et al. 2007), but was present in multiple other cell types (Penuela et al. 2007; Baranova et al. 2004; Bruzzone et al. 2003; Langlois et al. 2014; Turmel et al. 2011). Overall, the research focus on Panx1 (Penuela et al. 2008; Wang et al. 2009; Dvoriantchikova et al. 2006; Celetti et al. 2010; Wicki-Stordeur et al. 2012; Penuela et al. 2009; Lai et al. 2007; Cone et al. 2013) and Panx3 (Penuela et al. 2007; Penuela et al. 2009; Celetti et al. 2010; Penuela et al. 2008; Iwamoto et al. 2010; Ishikawa et al. 2011) has surrounded their localization at the cell surface, although a portion of their distribution was in intracellular compartments, while Panx2 was localized

primarily to intracellular compartments (Swayne et al. 2010; Boassa et al. 2014; Wicki-Stordeur et al. 2013), with some exceptions (Swayne et al. 2010).

1.3 Panx1

Following the discovery of the Panx family of large pore channels (Panchin et al. 2000), Panx1 in particular has piqued the interest of many researchers due to its ubiquitous expression (reviewed in Boyce et al. 2017) and role as a mechanism for regulated ATP release in many physiological and pathophysiological scenarios (reviewed in Lohman & Isakson 2014). ATP release via Panx1 was observed in diverse neuronal populations (Thompson et al. 2006; Weilinger et al. 2016; Kim & Kang 2011; Ohbuchi et al. 2011), neural stem and progenitor cells (Wicki-Stordeur et al. 2012) and glial cells (Burma et al. 2017) of the CNS, erythrocytes (Sridharan et al. 2010; Locovei, Bao, et al. 2006), cells of the immune system (Pelegrin et al. 2008; Pelegrin & Surprenant 2006; Schenk et al. 2008), taste buds (Huang et al. 2007), airway epithelial cells (Ransford et al. 2009), as well as vascular endothelial cells (Lohman et al. 2015), and many other cell types (reviewed in Boyce et al. 2017). In these diverse cells and tissues, a large body of literature established the importance of signalling via Panx1 channels to regulate cellular behaviours including neuronal development (Wicki-Stordeur et al. 2012; Wicki-Stordeur & Swayne 2013; Wicki-Stordeur et al. 2016) and modulation of synaptic activity (Prochnow et al. 2009; Ardiles et al. 2014; Weilinger et al. 2016; Vroman et al. 2014) in the CNS, propagation of Ca^{2+} waves (Locovei, Wang, et al. 2006), cancer progression (Furlow et al. 2015; Penuela et al. 2012), activation of the cellular inflammasome (Crespo Yanguas et al. 2017), phagocytic cell recruitment towards dying cells (Chekeni et al.

2010), regulation of vascular tone (Lohman et al. 2015) and cell death (Weilinger et al. 2012; Gulbransen et al. 2012, reviewed in Swayne & Bennett 2016; Sanchez-Arias et al. 2016). In the following subsections, I will outline the mechanisms of regulating Panx1 channel activity with a focus on purinergic signalling, followed by a detailed description of the subcellular distribution of Panx1 subcellular distribution. I will then outline our understanding of Panx1 stability, as well as trafficking mechanisms, highlighting the knowledge gaps that existed prior to commencing the studies described in my dissertation.

1.3.1 **Regulation of activity**

The hallmarks of Panx1 channel activation include an outwardly-rectifying ionic current (Chiu et al. 2017) and the formation of a pore permeable to large molecules including fluorescent dyes [i.e. ethidium bromide (Pelegrin & Surprenant 2006), YO-PRO-1 (Chekeni et al. 2010), sulforhodamine B (Penuela et al. 2009)] and nucleotides [notably ATP (Sandilos et al. 2012; Chiu et al. 2017, reviewed in Dahl 2015)]. In many studies, due to the difficulty of directly measuring channel-mediated ATP release, dye flux has been used as an alternative for understanding Panx1 pore formation. Panx1 activation occurred in response to several (patho)physiological stimuli including mechanical stretch (Bao et al. 2004), GPCR-mediated signalling (Billaud et al. 2015; Billaud et al. 2011), elevated extracellular potassium (K^+; Santiago et al. 2011) or intracellular Ca^{2+} (Locovei et al. 2006), oxygen and glucose deprivation (OGD)/hypoxia (Thompson et al. 2006; Bargiotas et al. 2011), and excitotoxic NMDAR stimulation (Santiago et al. 2011; Thompson et al. 2008; Weilinger et al. 2016). Although the precise

activation mechanisms are not known for all modulatory stimuli, channel activity was regulated through interactions between the distal C-terminus and pore-lining residues of the TM1 and EL1 (Wang & Dahl 2010; Sandilos et al. 2012) which suggested a "ball-and-chain" mechanism [as occurs with voltage-gated ion channels (Hoshi et al. 1990; Armstrong et al. 1973)]. Much of what is known about the role of the C-terminus in regulating Panx1 activity stemmed from the identification of proteolytic cleavage of the distal C-terminus for caspase 3/7/11 at D378 [mouse (Spagnol et al. 2014; Sandilos et al. 2012; Yang et al. 2015; de Gassart & Martinon 2015)] or D379 [human (Sandilos et al. 2012; Chekeni et al. 2010)] that constitutively activated Panx1 (Chekeni et al. 2010; Sandilos et al. 2012; Yang et al. 2015; de Gassart & Martinon 2015; Chiu et al. 2017). The constitutive activity of the cleaved channel was blocked by co-expression of the free C-terminus (Sandilos et al. 2012). The same group later created a concatameric channel to interrogate the stoichiometry of C-terminal cleavage (Chiu et al. 2017). They observed progressive incremental C-terminal-cleavage-associated increases in single channel current amplitudes, whole cell current densities, and ATP release. Notably, while current was observed in concatameric channels missing a single C-terminus, ATP release required the cleavage of at minimum two C-termini.

1.3.2 **Crosstalk with other receptors**

Panx1 activity was also regulated by interactions with other receptors including purinergic receptors (both P2X and P2Y) to regulate inflammation, neuronal activity, induction of Ca^{2+} waves, or cell death (Ohbuchi et al. 2011; Locovei, Wang, et al. 2006; Iglesias et al. 2008; Kim & Kang 2011; Gulbransen et al. 2012; Draganov et al. 2015), α-

adrenergic receptors to regulate vascular tone (Billaud et al. 2011; Billaud et al. 2015), TNF-α receptors to recruit immune cells during vascular inflammation (Lohman et al. 2015), and NMDA receptors following anoxia or excitotoxic stimulation (Weilinger et al. 2016; Weilinger et al. 2012). These receptors triggered Panx1 activation through signalling leading to PTM, physical coupling, or a combination of both. Notably, several of these receptors triggered Src-mediated signalling and phosphorylation of sites in the Panx1 intracellular loop (Lohman et al. 2015) or C-terminus (Weilinger et al. 2016). During investigation of the channel gating of the concatameric channel, Chiu *et al.* proposed that receptor-mediated activation would induce PTM- and interaction-dependent conformational changes in the pore-blocking C-termini that would induce a "flapping" motion and allow for non-constitutive, physiological Panx1 activation (Chiu et al. 2017).

As the initial finding that inspired the work described in my dissertation was that extracellular ATP, specifically, triggered the internalization of cell surface Panx1, the focus of this dissertation will be on Panx1 crosstalk with purinergic receptors. Here, I will introduce purinergic signalling and the receptors involved with a focus on crosstalk between Panx1 and its most common purinergic receptor interaction partner, P2X7R. In this context, it is important to understand regulation of extracellular ATP release and breakdown, so these topics will be discussed in a follow up section.

1.3.3 Purinergic signalling

ATP was first discovered in 1929 (Fiske & Subbarow 1929), where it was initially proposed as a necessary mediator of muscle contraction. For decades, it was solely

considered as a source of energy for intracellular processes (reviewed in Khakh & Burnstock 2009); however, in 1972, Burnstock *et al.* identified a role for this purine in extracellular paracrine signalling (Burnstock et al. 1972). Purine compounds produced a rapid and transient contraction of isolated rat and guinea pig urinary bladders, with ATP demonstrating the strongest response, which closely mimicked nerve-mediated contractions. This group had previously identified ATP release following stimulation of inhibitory innervation of the gut of both guinea pigs and toads, but had not determined its effects on cell behaviours (Burnstock et al. 1970). Since then, purinergic signalling has been linked to many physiological and pathophysiological phenomena in almost every cell and tissue type (reviewed in Burnstock 2011). Upon release into the extracellular environment, ATP acts as an autocrine or paracrine signalling molecule via activation of cell surface purinergic receptors, the effectors of purinergic signalling (reviewed in Dubyak & el-Moatassim 1993; Burnstock et al. 2011; Abbracchio et al. 2009; Burnstock 2016); however, this event is typically transient as ATP is rapidly broken down into its metabolites by extracellular nucleotidases, negative regulators of purinergic signalling (reviewed in Schetinger et al. 2007). The rapid breakdown of ATP allows for stringent spatial and temporal regulation of purinergic signalling. Further, cell type-specific expression of both purinergic receptors and ectonucleotidases expressed on the surface creates a diverse possibility of outcomes to extracellular ATP elevation.

1.3.3.1 Purinergic receptors

The effectors of extracellular ATP signalling, purinergic receptors, were identified by Burnstock in 1976 (Burnstock 1976), and two years later, they were divided

into two subgroups based on agonist sensitivity (Burnstock 1978, reviewed in Dubyak & el-Moatassim 1993; Burnstock et al. 2011; Abbracchio et al. 2009; Burnstock 2016), P1 (sensitive to adenosine) and P2 (sensitive to primarily ATP and ADP). The P1 family was made up of metabotropic G-protein coupled receptors (GPCRs) with four subtypes (A_1, A_{2A}, A_{2B}, A_3), evoking either G_s or G_i signalling in a subunit-specific mechanism. P1 triggered adenylyl cyclase activation and subsequent modulation of intracellular cAMP levels. As they are exclusively sensitive to adenosine, P1 receptors will not be a focus of this dissertation. P2 receptors, however, were described as an ATP/ADP-activated family of purinergic receptors existing as two major families: ionotropic P2X receptors (with 7 isoforms) and metabotropic P2Y receptors (with 8 isoforms). Panx1 formed feedback loops via purinergic signalling with both P2X and P2Y receptors (Figure 1.2), which will be discussed below.

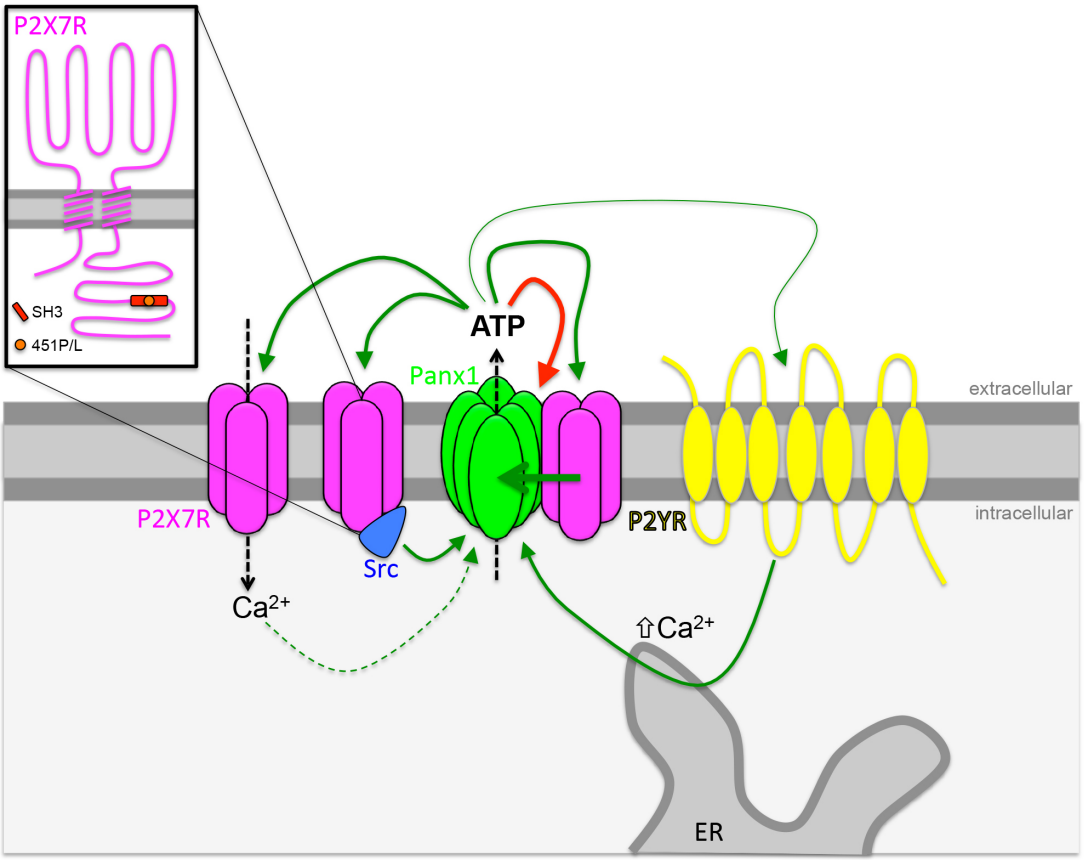

Figure 1.2 Feedback loops in P2 receptor-Panx1 crosstalk. ATP released through Panx1 and other mechanisms activates P2 receptors in a dose dependent manner (demonstrated by thickness of green arrows). P2Y receptor activation stimulates release of intracellular Ca^{2+} stores, which activate Panx1. At higher concentrations of extracellular ATP, the P2X7R is activated and leads to downstream Panx1 activation through a number of possible mechanisms: (1) physical association with the Panx1 channel, (2) P2X7R/Src-mediated signalling upstream of Panx1 activation, and possibly (3) Ca^{2+} influx through P2X7R. P2X7R/Panx1 pore formation is sensitive to a P451L polymorphism in the SH3 domain of P2X7R (the locus of P2X7R-Src interaction). With further increase in extracellular ATP concentration, Panx1 is inhibited through an unresolved mechanism.

1.3.3.2 P2X receptors

P2X receptors (P2X1-7R) are trimeric cation-permeable channels (Ca^{2+}, Na^{+}, K^{+}) (reviewed in North 2002) capable of mediating cation flux down their concentration gradient. This excluded P2X6R, which was retained in the endoplasmic reticulum [ER,

(North 2002; Vial et al. 2004)]. Each subunit consisted of two transmembrane domains, with intracellular N- and C- termini, as well as a large extracellular loop. There was a wide range in subunit size between the seven mammalian isoforms of P2XRs from 379 amino acid (aa; P2X6R) to 595 aa (P2X7R), based on highly divergent C-termini (Habermacher et al. 2016). The structure of crystallized P2X monomers was likened to a dolphin (Hattori & Gouaux 2012), with the body of the dolphin represented by the glycosylated and highly conserved extracellular loop. The head and fins of the dolphin represented the more flexible regions of the P2X ectodomain, while the tail was made up of the two transmembrane domains. The structure of the cytosolic domains are not well understood, as the initial crystal structures were generated from receptors with truncated C-termini (Hattori & Gouaux 2012; Kawate et al. 2009). Within the extracellular loop existed a highly conserved intersubunit ATP-binding pocket, which was originally identified using site-directed mutagenesis (Browne et al. 2010; Chataigneau et al. 2013; Evans 2009; Ennion et al. 2000; Fischer et al. 2007; Zemkova et al. 2007; Yan et al. 2006; Wilkinson et al. 2006; Roberts et al. 2008; Jiang et al. 2000) and later confirmed with the high resolution structures of zebrafish P2X4R in the presence and absence of ATP (Kawate et al. 2009; Hattori & Gouaux 2012). In response to ATP-binding, P2XRs underwent a shift in conformational state that opens the pore, allowing for cation flux across the membrane. With prolonged agonist exposure, all P2X receptors excluding P2X7R were desensitized and enter into an inactivatable conformational state despite ATP remaining bound to the receptor (North 2002). Dissociation of ATP from the binding pocket in P2X receptors allowed for these receptors to enter the activatable resting state.

ATP release via Panx1 led to autocrine/paracrine activation of P2X receptors in many cell types (reviewed in Baroja-Mazo et al. 2013). In turn, stimulation of several P2X receptor subtypes activated Panx1, including possibly P2X1 and P2X4Rs (Taylor et al. 2014; Woehrle et al. 2010), but most commonly P2X7R (Draganov et al. 2015; Hung et al. 2013; Iglesias et al. 2008; Xu et al. 2012; Kanjanamekanant et al. 2014; Negoro et al. 2014). Together, these interactions formed a positive feedback loop of purinergic signalling in many cell types where they were co-expressed (reviewed by Jackson 2015; Baroja-Mazo et al. 2013).

1.3.3.3 P2X7R

Not only were P2X7R exceptional among the P2X receptor family in their relatively prolific association with Panx1, they also exhibited unique structural and functional characteristics (reviewed in Volonté et al. 2012). Due to their unique functional characteristics, they were initially described as a separate family of P2 receptors, “P2Z receptors.” P2X7Rs possessed the highest molecular weight of all purinergic receptors as a result of a C-terminal domain that is more than double the length of other P2X receptor C-termini; however, P2X7R maintained ~35-40% homology with other P2X receptors for the overall protein (Habermacher et al. 2016), due to a large- and highly conserved ectodomain containing the critical ATP-binding pocket (Karasawa & Kawate 2016). Although a crystal structure of P2X7R was recently uncovered (Karasawa & Kawate 2016), it too was performed using a C-terminally truncated receptor. Consequently, the structure of the extended C-terminus was not determined, although it mediated many of its unique functional features (Surprenant et al.

1996; Adriouch et al. 2002) including unique protein-protein interaction and activation of several P2X7R-specific signalling cascades (reviewed in Costa-Junior et al. 2011).

Although particularly enriched in the immune cells in the blood (Surprenant et al. 1996) and glial cells in the nervous system (Sperlagh & Illes 2014), P2X7Rs were expressed in many other cells and tissues of the body (reviewed in Habermacher et al. 2016), including many neuronal subtypes (Able et al. 2011; Yu et al. 2008) and precursor cells (Tsao et al. 2013). P2X7R expression was very stable with a reported half-life of >54 h (Gonnord et al. 2009). In terms of subcellular distribution, they trafficked slowly through the secretory pathway to the plasma membrane (Robinson & Murrell-Lagnado 2013), where several groups have identified two independent populations of P2X7R, one that is localized to and the other excluded from lipid microdomains (Garcia-Marcos, Pérez-Andrés, et al. 2006; Bannas et al. 2005; Pfleger et al. 2012; Barth et al. 2007; Barth et al. 2008; Weinhold et al. 2010, reviewed in Robinson & Murrell-Lagnado 2013). Localization within or outside these lipid microdomains promoted differential P2X7R-mediated signalling pathways (Garcia-Marcos et al. 2006). Here, P2X7R activation played a role in triggering phospholipid metabolism (reviewed in Garcia-Marcos et al. 2006) and was also regulated by membrane lipids (Robinson et al. 2014; Zhao et al. 2007).

It is common for a single cell type to express several subtypes of both P2X receptors (reviewed in North 2002). Here, many P2XR subtypes formed heteromeric channels amongst P2X family members; however, P2X7Rs are distinct in that they only formed homomeric channels. Further, P2X7Rs demonstrated relatively low agonist affinity (≥10-fold relative to other P2XRs; Surprenant et al. 1996), requiring a high

concentration of extracellular ATP to be activated (EC_{50}>100 μM; reviewed in North & Surprenant 2000). One key aspect of P2X7R function (shared with P2X2R and P2X4R; Khakh et al. 1999) was its ability to mediate the formation of a large pore following prolonged stimulation (reviewed in Alves et al. 2014). In some contexts, the P2X7R itself were observed to dilate and allow passage of molecules <900 Da in size (Yan et al. 2008; Yan et al. 2010). While in other scenarios, P2X7R activation led to Panx1-dependent pore formation (Pelegrin & Surprenant 2007; Pelegrin & Surprenant 2006), in part regulated through a polymorphism in the distal P2X7R C-terminus (Sorge et al. 2012; Xu et al. 2012; Adriouch et al. 2002). This apparent discrepancy was potentially resolved by evidence suggesting that, when co-expressed, large pore formation occurred in a mechanism dependent on both channels. Following P2X7R stimulation, there was first rapid and robust Panx1-dependent dye-uptake followed by latent and less significant Panx1-independent dye-uptake (Pelegrin & Surprenant 2009). P2X7R-Panx1 pore formation along with other details of the relationship between P2X7R and Panx1 will be discussed in depth below.

1.3.3.4 Crosstalk between P2X7R and Panx1

There is robust evidence of P2X7R-dependent Panx1 signalling in a multitude of cell types including immune cells (Pelegrin et al. 2006; Iglesias et al. 2008; Sorge et al. 2012; Pelegrin & Surprenant 2007; Pelegrin et al. 2008), neurons and glia of the nervous system (Garre et al. 2016; Silverman et al. 2009; Poornima et al. 2012a; Gulbransen et al. 2012), as well as others (reviewed in Isakson & Thompson 2014; Bravo et al. 2015). Extracellular ATP released through Panx1, activated P2X7Rs. In turn, activation of

P2X7R was linked with downstream stimulation of Panx1-mediated ATP release (Gulbransen et al. 2012; Pelegrin & Surprenant 2009; Iglesias et al. 2008; Ohbuchi et al. 2011; Silverman et al. 2009). This positive purinergic feedback loop was associated with diverse (patho)physiological scenarios [i.e. maintenance of skeletal integrity (Seref-Ferlengez et al. 2016), chronic pain (Sorge et al. 2012), inflammasome activation and cytokine release (Silverman et al. 2009; Pelegrin et al. 2006), and cell death (Gulbransen et al. 2012; Locovei et al. 2007; reviewed in Baroja-Mazo et al. 2013)]. Although much is known about the cellular contexts where P2X7R and Panx1 crosstalk, whether the mechanism involved a signalling cascade, physical coupling, or both has remained less understood.

The most straightforward signalling mechanism for P2X7R-Panx1 crosstalk would be through P2X7R-mediated Ca^{2+} influx; however, the evidence for Ca^{2+}-dependent signalling between P2X7R and Panx1 is contentious and requires further investigation. P2X7R-Panx1-mediated ATP-induced dye efflux and ATP release was significantly increased in Ca^{2+}-free media (Poornima et al. 2012), which they suggested meant either Ca^{2+} flux through P2X7R or Ca^{2+} binding to the exofacial surfaces of P2X7R/Panx1 was required for Panx1 activation. However, this scenario was non-physiological, so further investigation into this mechanism is warranted. Because intracellular Ca^{2+} elevation through other purinergic receptors had previously been shown to activate Panx1 (Kim & Kang 2011; Locovei et al. 2006), here, the authors proposed Ca^{2+} influx was the likely candidate. However, this finding was contradicted by an earlier study from Ma *et al.* that demonstrated that Panx1 currents were unaffected by modulation of extracellular or intracellular Ca^{2+} concentrations in human embryonic

kidney (HEK) 293 cells (Ma et al. 2009). More recently, P2X7R was demonstrated to evoke Panx1-dependent dye uptake in astrocytes of the spinal cord (Garre et al. 2016). This was abolished by pre-incubation with cell-permeable Ca^{2+} chelators, which also suggested dependence on Ca^{2+} influx. However, in this same study, this mechanism was not conserved in cortical astrocytes, suggesting that Ca^{2+}-mediated P2X7R-Panx1 crosstalk could be a cell- or context-specific signalling pathway.

A more likely pathway for P2X7R-Panx1 crosstalk was a Ca^{2+}-independent mechanism. The first evidence of potential for Ca^{2+}-independent crosstalk between P2X7R-Panx1 came in 2002, when Adriouch *et al.* identified an allelic mutation (P451L) in a proline-rich region of the murine P2X7R C-terminus that impaired downstream pore formation in splenic T-cell in response to ATP (Adriouch et al. 2002). This was later confirmed in thymocytes where P451L disrupted pore formation, but maintained P2X7R-dependent cation flux (Le Stunff et al. 2004). Following these discoveries, Iglesias *et al.* identified a potential connection between this polymorphism and Panx1 activation. A Src homology 3 (SH3) domain, known to interact with Src and other tyrosine kinases, was identified in the that overlapped with residue 451 in the proline-rich region of the P2X7R C-terminus (Iglesias et al. 2008). Incubation with cell-permeable peptides (containing either 451P and 451L) targeted to this region disrupted P2X7R-Src interaction and inhibited downstream Panx1-dependent currents and dye-uptake, while P2X7R-mediated currents were not significantly affected (Iglesias et al. 2008). Consequently, P2X7R-dependent Panx1 activation appeared to be dependent on an intermediate step involving Src kinase and independent of Ca^{2+} influx in some contexts (Iglesias et al. 2008). Despite providing evidence for an interaction between P2X7R and Src, Iglesias *et al.* failed to

show an interaction between Src and Panx1 or a specific P2X7R-dependent Src phosphorylation site in Panx1. Thus, there may be additional intermediate molecules in this pathway. Although the majority of follow-up studies suggested that 451P was associated with Panx1-dependent pore formation, while 451L was unable to form a pore. (Sorge et al. 2012; Suadicani et al. 2009), Xu *et al.* demonstrated that only P2X7R 451L evoked Panx1-dependent dye-uptake that relied on activation of caspase activity (Xu et al. 2012). Consequently, the role of this proline-rich region in the P2X7R C-terminus in P2X7R-Panx1 crosstalk needs to be further investigated in diverse cell types and contexts. A summary of these studies is presented in Table 1.

Table 1.1 P2X7R sequence variants impact Panx1 crosstalk

Isoform	Panx1 crosstalk?	Model	Pore formation ?	Notes	Reference
451P	Yes	Peritoneal Macrophages (endogenous)	Yes	TAT-451P prevents Panx1 activation	Sorge *et al.*, 2012
	Yes	Cortical Astrocytes (endogenous)	Yes	Panx1 activation blocked by PP2	Suadicani *et al.*, 2009
	Yes	J774 macrophages (endogenous)	Yes	Panx1 activation blocked by PP2, TAT-451P	Iglesias *et al.*, 2008
	Yes	J774 macrophages (endogenous)/HEK (exogenous)	Yes	Rapid Panx1-dependent dye uptake, slow Panx1-dependent dye uptake	Pelegrin & Surprenant, 2007
	Yes	J774 macrophage, Human lung alveolar macrophage (endogenous)	Yes		Pelegrin & Surprenant, 2006
	ND	Thymocytes (endogenous)	Yes	Panx1 function not investigated	Le Stunff *et al.*, 2004
	ND	Splenic T cells (endogenous)	Yes	Panx1 function not investigated	Adriouch *et al.* 2002
	No	HEK293 (exogenous)	No		Xu *et al.*, 2012
451L	No	Peritoneal macrophages	Limited		Sorge *et al.*, 2012
	No	Cortical Astrocytes (endogenous)	No		Suadicani *et al.*, 2009
	ND	Thymocytes (endogenous)	No	Panx1 function not assessed	Le Stunff *et al.*, 2004
	ND	Splenic T cells (endogenous)	No	Panx1 function not investigated, maintained PLD activation capability	Adriouch *et al.* 2002
	Yes	HEK293 (exogenous)	Yes	Required intermediate caspase activation	Xu *et al.*, 2012

Finally, P2X7R and Panx1 have also been observed to interact physically using co-IP in a number of studies (Pelegrin & Surprenant 2006; Silverman et al. 2009; Kanjanamekanant et al. 2014; Seref-Ferlengez et al. 2016; Pan et al. 2015; Hung et al. 2013; Poornima et al. 2012; Table 2). One of the initial studies identified P2X7R and Panx1 as interaction partners in a complex with the inflammasome during neuroinflammation (Silverman et al. 2009). This was followed up by the finding that this

interaction was enriched during mechanical stress, a condition known to elevate extracellular ATP (Kanjanamekanant et al. 2014); however, the role of the endogenous ligand, ATP, in regulating this interaction and the precise domains involved were unknown prior to commencing my project.

Table 1.2 Physical interaction between P2X7R and Panx1

P2X7R	Panx1	Model	Method	Modulation?	Reference
Endogenous	Endogenous	Bone tissue and cultured osteoblasts (mouse)	P2X7R IP		Seref-Ferlengez *et al.*, 2016
Endogenous	Endogenous	Primary cortical astrocytes (mouse)	Panx1 IP		Pan *et al.*, 2015
Endogenous	Endogenous	Human periodontal ligament cells	Co-IP (Panx1 & P2X7)	Increased association with mechanical stress	Kanjanmekanant *et al.*, 2013
Endogenous	Endogenous	Gingival epithelial cells (human)	P2X4 IP		Hung *et al.*, 2013
Human P2X7R (exogenous)	Rat Panx1-EGFP	HEK293	EGFP IP	Increased association in Ca^{2+}-free media	Poornima *et al.*, 2012
Endogenous	Endogenous	Primary cortical neurons	Co-IP (Panx1 & P2X7)	Interacted with NRLP1 inflammasome components	Silverman *et al.*, 2009
P2X7R-ee	Panx1-myc	HEK293	Myc IP		Pelegrin & Suprenant, 2006

1.3.3.5 P2Y receptors

Metabotropic purinergic receptors (P2YRs) have also been linked to Panx1 signalling (Locovei et al. 2006). P2YRs (P2Y1R, P2Y2R, P2Y4R, P2Y6R, P2Y11-14R) are seven-pass transmembrane domain G-protein coupled receptors (GPCRs) that

respond primarily to ADP, UTP, and UDP, with lower affinity for ATP (reviewed in Weisman et al. 2012). Mammalian P2YRs are less variable in size than P2XRs, ranging from 328 aa (P2Y6R) to 377 aa (P2Y2R). Activation of each P2Y receptor subtype is regulated by specific nucleotides with varying affinities (reviewed in Von Kügelgen & Hoffmann 2016). Following P2YR activation, receptors elicit either phospholipase C activation via the G_q subunit or stimulate/inhibit adenylyl cyclase activity via the G_s or G_i subunits (reviewed in Erb et al. 2006). This modulates signalling in an isoform-specific manner by modulating inositol triphosphate (IP_3) and cAMP signalling, as well as release of intracellular Ca^{2+} stores. Panx1-mediated ATP release led to paracrine/autocrine activation of P2Y receptor signalling in a wide variety of cell types (reviewed in Baroja-Mazo et al. 2013). Further, activation of P2Y receptor signalling (P2Y1R, P2Y2R, and P2Y6R) has been linked with downstream activation of Panx1 (Locovei et al. 2006; Timóteo et al. 2014). This was demonstrated to occur through elevation of intracellular Ca^{2+} (Locovei et al. 2006; Figure 1.3), suggesting that P2YRs and Panx1 could also form a positive feedback loop.

1.3.3.6 Contributors to extracellular ATP: Panx1-independent ATP release

ATP exists in the 1-200 mM concentration range in intracellular compartments and is released through three mechanisms: (1) exocytosis (constitutive or regulated) of ATP-containing vesicles, (2) through large pore ATP-permeable channels (including Panx1) and (3) during cell lysis (reviewed in Chiu et al. 2014; Lohman & Isakson 2014; Baroja-Mazo et al. 2013). Despite its millimolar concentration in intracellular compartments, when measured in bulk extracellular fluid ATP was typically in the

nanomolar range. However, the actual concentration of ATP in the extracellular microdomains around release sites was predicted to be much higher (up to 500 μM; reviewed in Pankratov et al. 2006) for several reasons. First, most purinergic receptors possessed an EC_{50} of 1-100 μM, suggesting that they required millimolar concentrations for appreciable activation (reviewed in Khakh 2001; Von Kügelgen & Hoffmann 2016). The current mechanisms for detection have not allowed observation of ATP concentrations with high temporal and spatial resolution (reviewed in Praetorius & Leipziger 2009). This is important because ATP is rapidly degraded upon release by hydrolytic enzymes (reviewed in Schetinger et al. 2007), suggesting that measurement in bulk extracellular fluid would drastically underestimate that actual concentration. The sources of extracellular ATP, outside of Panx1, will be briefly introduced in the next section (Figure 1.3). This will be followed by a discussion of the factors that negatively regulate extracellular ATP concentrations, including ATP-hydrolyzing enzymes and early evidence for negative feedback of Panx1 by ATP.

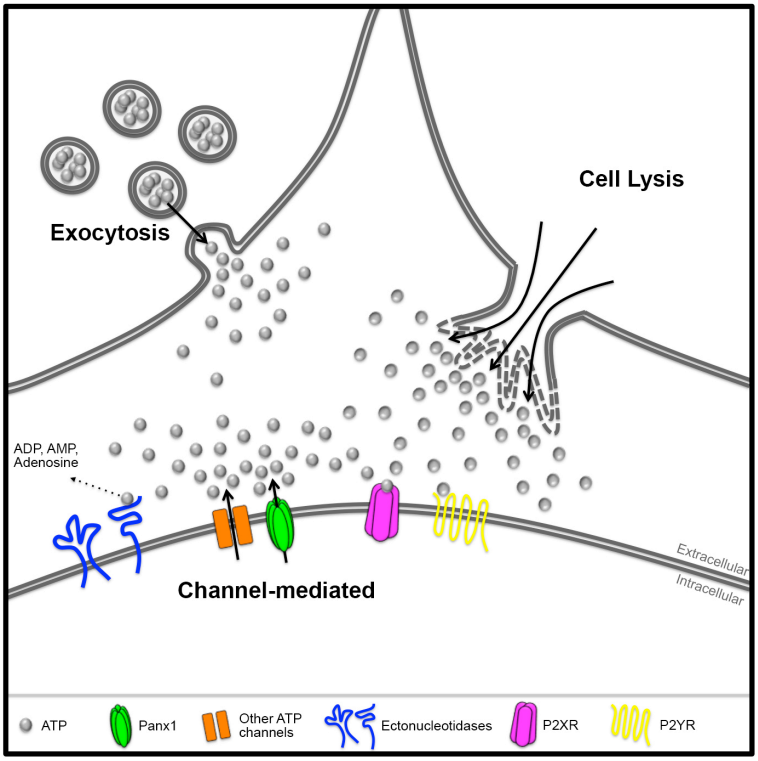

Figure 1.3 Regulation of extracellular ATP and purinergic signalling. ATP is released into the extracellular environment through one of three mechanisms: (1) large-pore channels, like Panx1, (2) regulated or constitutive exocytosis of ATP-containing vesicles, and (3) cell lysis. Upon release, ATP acts through ionotropic P2X and metabotropic P2Y receptors to activate a wide array of cellular signalling pathways with diverse outcomes for cell behaviours. ATP-mediated signalling is typically transient as ATP molecules are rapidly broken down into their metabolites by ectonucleotidases.

Exocytosis of ATP-loaded vesicles occurs through both constitutive and regulated mechanisms. Either regulated or constitutive release in vesicles occurs in a wide variety of cell types, such as osteoblasts (Romanello et al. 2005), lung epithelia (Ahmad et al. 2005), pancreatic β-cells (Aspinwall & Yeung 2005), mast cells (Aspinwall & Yeung 2005), as well as central and peripheral neurons (Jo & Role 2002; Reigada et al. 2003; Morel & Meunier 1981; Stjärne 2001; Sesti et al. 2002; Edwards et al. 1997). ATP is

ubiquitous in all intracellular compartments and organelles (present at 1-10 mM concentrations in the cytoplasm), but is enriched in secretory vesicles by the vesicular nucleotide transporter (VNUT; Sawada et al. 2008). VNUTs rely on the establishment of an electrochemical gradient maintained by the vacuolar type H+/ATPase (V-ATPase; Aberer et al. 1978; Gualix et al. 1996). Vesicular release of ATP was selectively disrupted by inhibition of the V-ATPase (Coco et al. 2003; Feranchak et al. 2010).

It is possible that ATP is also released through several other large-pore channels. Here, large pore channels are classified as channels capable of mediating the passage of large molecules up to 1 kDa in size. There are several candidate channels, which demonstrate structural similarity to Panxs (Siebert et al. 2013; Abascal & Zardoya 2012) that could be capable of ATP release. These include Cxs (reviewed in Lohman & Isakson 2014), Ca^{2+} homeostasis modulator (CALHM) channels (reviewed in Ma et al. 2016), as well as possibly the P2X7R alone (reviewed in Alves et al. 2014) and leucine rich repeat containing 8 (LRRC8) channels (Gaitan-Penas et al. 2016). However, the physiological release of ATP through many of these other channels remains contentious, as ATP release was often observed in non-physiological experimental conditions (reviewed in Dahl 2015; Lohman & Isakson 2014; Lazarowski 2012).

In pathological scenarios, particularly following trauma or during ischemia, cellular lysis leads to dramatic ATP release into the extracellular environment. Here, dying cells undergo membrane breakdown releasing intracellular ATP stores (Braun et al. 1998; Jurányi et al. 1999; Melani et al. 2005). Cell lysis plays a particularly important role as a contributor for extracellular ATP in non-excitable cells. Red blood cells were a particularly interesting example of this, as they lack organelles allowing for vesicular

release; consequently, hemolysis was a major contributing factor to ATP release in the bloodstream during hypoxia or shear stress (Sikora et al. 2014). In response to lysis of nearby cells, ATP levels would be dramatically elevated at discrete cell surface locations of neighbouring viable cells (reviewed in Dubyak & el-Moatassim 1993).

1.3.3.7 Extracellular ATP hydrolysis

Once released, ATP is rapidly hydrolyzed by numerous nucleotidases separated into four major families of ectonucleotidases: (1) nucleoside triphosphate diphosphohydrolases (NTDPases), (2) ecto-pyrophosphatase/phosphodiesterase (E-NPPs), (3) alkaline phosphatases, and (4) ecto-5'-nucleotidases (reviewed in Schetinger et al. 2007), each with different ability to breakdown extracellular ATP into its dinucleoside and mononucleoside metabolites**.** Non-selective inhibition of these enzymes [using common inhibitors like ARL 67156 (Geyti et al. 2008) or α,β-methylene ATP (Joseph et al. 2004)] leads to a steady and sustained increase in extracellular ATP concentration. Interestingly, ectonucleotidase expression and activity are differentially regulated during development (Gómez-Villafuertes et al. 2014) and disease (Lunkes et al. 2003; Bagatini et al. 2011), leading to context-specific regulation of extracellular ATP concentrations (reviewed in Schetinger et al. 2007).

1.3.3.8 Negative regulation by extracellular ATP

Although ATP hydrolysis alone would be sufficient negative feedback for purinergic signalling in some circumstances, the positive feedback loop of ATP-mediated

ATP release created by P2 receptors and Panx1 expressed in the same cell would theoretically lead to a constitutive Panx1 activation and adverse consequences for cell survival (reviewed in Dubyak 2009). However in several circumstances, P2 receptor-dependent Panx1 activation allowed for transient activation (Locovei et al. 2006; Locovei et al. 2007), suggesting the presence of an intrinsic negative feedback mechanism. The first evidence of this was that Panx1 channel activity was inhibited by elevated extracellular ATP concentrations (≥200 μM) in both oocytes (Qiu et al. 2012; Qiu & Dahl 2009) and in mammalian cells (Ma et al. 2009). Several key residues in the first and second Panx1 extracellular loops (EL1 and EL2) were identified that regulated ATP-evoked inhibition. Due to the presence of negatively charged functional groups in the ATP molecule, the basic residues in Panx1 were first investigated for ATP-sensitivity using substitution mutants. Mutation of R75 to basic residues partially conserved ATP-mediated inhibition, while inhibition was disrupted by mutation to negatively-charged or non-polar residues (by >50%; Qiu & Dahl 2009; Kurtenbach et al. 2013). In a follow-up study using alanine-scanning mutagenesis of residues throughout the Panx1 ectodomains, several ATP-sensitive residues in the first and second extracellular loops of Panx1 were subsequently identified (>90% loss of ATP-evoked inhibition – W74, S237, S240, I247, and L266; >50% loss of ATP evoked inhibition – R75, S93, L94, D241, and I267l; Figure 1.4; Qiu et al. 2012). Removal of the ATP-inhibitory effect by mutating key extracellular residues in Panx1 (W74A, 237A, 240A, 266A) led to a five-fold increase in evoked ATP release relative to wildtype-expressing oocytes (Qiu et al. 2012), which suggested disruption of negative feedback. Interestingly, the R75 residue was conserved in non-mammalian species, in a panx1 isoform in zebrafish that was also inhibited by

ATP (≥500 μM; Kurtenbach et al. 2013). There was evidence amongst other channel proteins for negative feedback via permeant molecules [i.e. presynaptic Ca^{2+} channels negatively regulated by Ca^{2+}-sensor proteins (Mochida et al. 2008)], so investigation into the mechanism behind ATP-mediated inhibition including the possible involvement of other ATP-sensitive proteins was warranted.

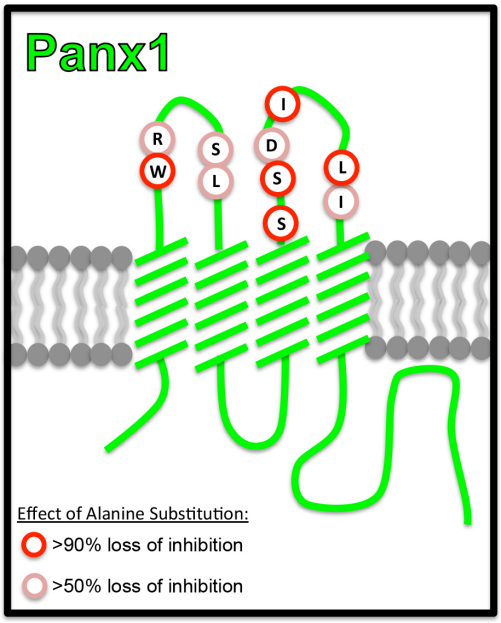

Figure 1.4 ATP-sensitive residues in the Panx1 extracellular loops. ATP-sensitive residues identified in an alanine-scanning mutagenesis study by Qiu, Wang, & Dahl (2012). Alanine substitution of any of the indicated residues led to >90% loss (W74, S237, S240, I247, and L266; red outline) or >50% loss (R75, S93, L94, D241, and I267; pink outline) of ATP-evoked Panx1 inhibition.

1.3.4 Subcellular distribution

Although the function of Panx1 has been linked primarily to its distribution at the cell surface under endogenous (Penuela et al. 2008; Wang et al. 2009; Dvoriantchikova et al. 2006; Celetti et al. 2010; Wicki-Stordeur et al. 2012; Penuela et al. 2009) and exogenous expression (Lai et al. 2007; Cone et al. 2013; Penuela et al. 2008), a portion of Panx1 was

observed in perinuclear compartments (Bhalla-Gehi et al. 2010; Cone et al. 2013; Lai et al. 2007; Vanden Abeele et al. 2006; Penuela et al. 2013; Boassa et al. 2007), including lysosomes (Penuela et al. 2013; Boassa et al. 2007) and the ER (Vanden Abeele et al. 2006). At the cell surface, Panx1 had a uniform and diffuse distribution with regions of enrichment in microdomains (Bhalla-Gehi et al. 2010), including dynamic clusters and plasma membrane protrusions. Higher resolution evidence (electron microscopy) further supported the localization of Panx1 in the plasma membrane (Lohman et al. 2015; Beckmann et al. 2016) where Panx1 did not aggregate into gap junction-like plaques or exhibit periodicity along the membrane (Beckmann et al. 2016). In fact, fluorescence recovery after photobleaching (FRAP) analysis revealed that, unlike the structurally similar Cxs, Panx1 was highly mobile in the plasma membrane and did not require cell-cell contacts for stability or lateral diffusion (Bhalla-Gehi et al. 2010). At the onset of my studies, the mechanisms targeting Panx1 to the cell surface had begun to be exposed; however, the regulatory mechanisms modulating Panx1 stability/turnover, and distribution to intracellular membranes were less clear.

1.3.5 Regulation of stability and trafficking

The research focus on Panx1 function and related behaviours has been on its role at the cell surface (reviewed in Sandilos & Bayliss 2012); consequently, an understanding of the precise mechanisms that regulate cell surface Panx1 distribution, including stability as well as both anterograde and retrograde movement, is critical, yet remains relatively unknown (reviewed in Boyce et al. 2014; Figure 1.5). Anterograde trafficking of Panx1 involves the regulation of membrane protein transport from the ER following translation,

through the Golgi network, destined for the plasma membrane. This portion of the Panx1 lifecycle is best known, as several studies have highlighted critical elements in Panx1 that regulate passage along this pathway including N-linked glycosylation and C-terminal elements. Retrograde trafficking includes transport events regulating the dynamics and turnover of mature Panx1 protein. This portion of the Panx1 life cycle remains less clear, but includes diffusion in the plasma membrane, targeting for degradation, and recycling. The following subsection will highlight the knowns and unknowns of Panx1 stability and trafficking.

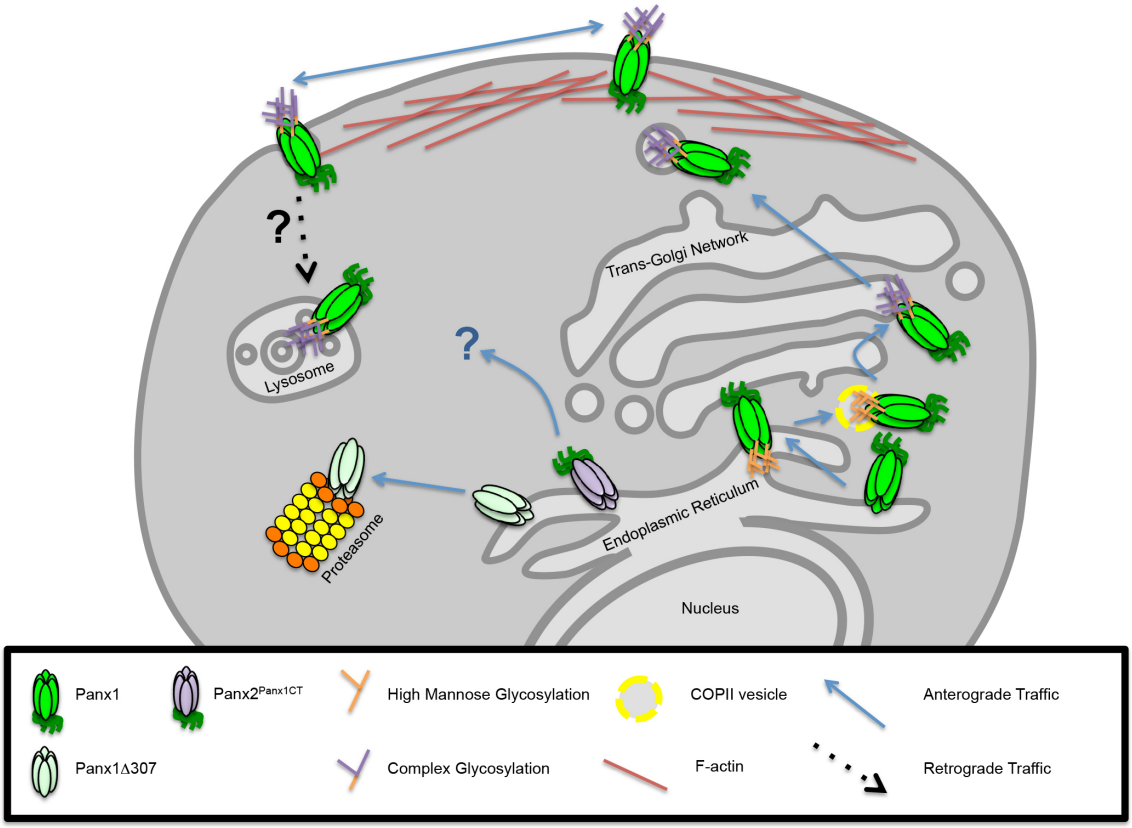

Figure 1.5 Panx1 trafficking. Anterograde trafficking of Panx1 begins in the endoplasmic reticulum (ER), where it receives a high-mannose glycosylation at N254 in the Panx1 EL2, creating the high mannose glycosylation species of Panx1 (Gly1). The Gly1 Panx1 species is transported to the Golgi via COPII vesicles. In the Golgi, the high mannose glycan is modified to

a complex glycosylation (Gly2). Gly2 glycosylation promotes anterograde trafficking and/or stability at the cell surface. An interaction between the Panx1 C-terminus and filamentous actin (F-actin) is critical for stability at the plasma membrane and vesicular trafficking dynamics. Panx1 is degraded within the lysosome, however the internalization mechanisms are unknown, although it is independent of canonical endocytic machinery. Absent of its C-terminus, Panx1Δ307 is retained in the ER then targeted to the proteasome for degradation. However, the C-terminus is not sufficient alone for proper anterograde trafficking of Panx1, as the Panx2^{Panx1CT} chimer is diffusely distributed in intracellular compartments.

1.3.5.1 Stability

There exists plenty of evidence that Panx1 demonstrates long-term stability and is slowly turned over relative to the structurally-related Cxs (reviewed in Penuela et al. 2013). First, Panx1 protein demonstrated an extended half-life (> 8 h; Penuela et al. 2007). Further, treatment with brefeldin-A (BFA), a disruptor of the Golgi apparatus and anterograde transport (Lippincott-Schwartz et al. 1991; Lippincott-Schwartz et al. 1989), demonstrated that a portion of Panx1 cell surface population persisted up to 32 hours after synthesis (Penuela et al. 2013). The remaining population of Panx1 accumulated in intracellular pools. Panx1 was far more stable at the plasma membrane than Cx43, which was turned over rapidly (<4 h; Penuela et al. 2007).This data was supported by FlAsH-ReAsH fluorescence pulse-chase experiments by an independent group, where plasma membrane persisted > 18 h (the final time point of analysis; Boassa et al. 2007). Some of the initially tagged Panx1 was internalized into cytoplasmic vesicles, predominantly lysosomes (Boassa et al. 2007). Degradation of Panx1 in the lysosome was supported by incubation with the lysosomal inhibitor chloroquine, which increased Panx1 accumulation on Western blot (Gehi et al. 2011). As the role for Panx1 in regulating ATP release was dependent on is localization to the cell surface, the regulation of channel

stability at the plasma membrane and trafficking (both to and from the membrane) is of critical importance. Before beginning my dissertation work, studies of Panx1 stability, trafficking, and turnover had been performed in basal, unstimulated conditions (Gehi et al. 2011; Boassa et al. 2007; Penuela et al. 2007; Boyce et al. 2015; Penuela et al. 2013). However, both the turnover and stability of other transmembrane proteins is modulated by ligand-receptor interactions or extrinsic stimuli (reviewed in Sorkin & von Zastrow 2009). Consequently, an aim of my studies was to determine the role of stimuli that modulate Panx1 activity and general cellular excitability on Panx1 cell surface stability and trafficking.

1.3.5.2 Anterograde trafficking mechanisms

Like other transmembrane proteins, Panx1 was synthesized in the ER, where it was inserted into the membrane and folded into its native state prior to commencing its journey through the secretory pathway (reviewed in Ellgaard et al. 2016). From here, it was transported to the Golgi apparatus in coatomer protein II (COPII)-coated vesicles, the canonical route of ER-Golgi transport (Bhalla-Gehi et al. 2010). This was determined by the co-expression of a dominant negative mutant of the small COPII coat GTPase 1 (Sar1 GTPase), a critical regulator of COPII coat assembly (reviewed in Lee & Miller 2007), which led to Panx1 retention in the ER (Bhalla-Gehi et al. 2010). Finally, following transport through the trans-Golgi network, Panx1 was targeted to the cell surface. Interestingly, the proper targeting of *de novo* synthesized Panx1 to the plasma membrane was regulated by a PTM (Boassa et al. 2007; Penuela et al. 2007) and several

key elements within the Panx1 C-terminus (Wicki-Stordeur et al. 2013; Bhalla-Gehi et al. 2010). These findings will be described in detail below.

1.3.5.3 N-linked glycosylation

Shortly after the discovery of Panx1, site-directed mutagenesis and de-glycosylation revealed that the apparent diversity in molecular weight species was the result of N-linked glycosylation. N-linked glycosylation involves the co-translational or post-translational addition of sugar moieties to an exposed asparagine residue by oligosaccharyltransferases. Three different Panx1 glycosylation species were identified: core, unglycosylated (Gly0) localized to the ER, high-mannose (Gly1) transiting between the ER and Golgi, and complex glycosylated (Gly2) associated with cell surface distribution (Penuela et al. 2007; Boassa et al. 2007; Penuela et al. 2009). The relative expression of each glycosylation species was cell and tissue type-specific (Boassa et al. 2007; Penuela et al. 2007). In other proteins, this PTM impacted several properties including folding and stability, trafficking, turnover, and function (reviewed in Shrimal et al. 2015). N-glycosylation of Panx1 at N254 occurred during transit between the ER and Golgi and promoted anterograde trafficking and cell surface stability (Penuela et al. 2007; Penuela et al. 2009; Boassa et al. 2008; Figure 1.5, Figure 1.6). Deglycosylation of wildtype Panx1 or expression of glycosylation-deficient Panx1 mutants promoted localization in intracellular compartments (Penuela et al. 2009; Penuela et al. 2007), although a small proportion of the glycosylation-deficient mutant was still able to reach the cell surface and mediate dye-uptake. The reduced cell surface stability of non-glycosylated Panx1 was supported by studies of other glycosylated proteins, where

reduction or loss of glycosylation reduced cell surface expression (Woo et al. 2013; Haga et al. 2011). Taken together, these findings indicated that N-glycosylation either promoted anterograde trafficking or stabilized Panx1 at the cell surface. The latter could have occurred through several mechanisms including altered interactions with the extracellular matrix or neighbouring cells, or stabilization in a specific membrane microdomain (Torreno-Pina et al. 2014).

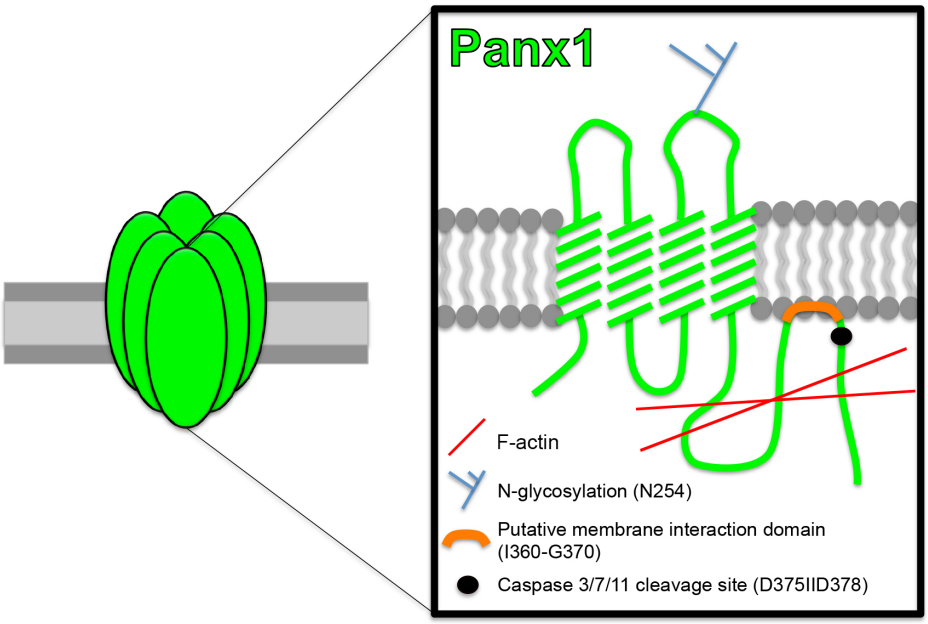

Figure 1.6 Panx1 structural elements involved stability and trafficking. Both N-glycosylation at position 254 and C-terminal elements are critical for proper cell surface expression of Panx1. Complex (Gly2) glycosylation of the Panx1 EL2 promotes anterograde trafficking and/or cell surface stability. Filamentous actin, which regulates Panx1 trafficking dynamics, interacts with the C-terminus, although the precise residues are unknown. A putative lipid membrane interacting domain (orange rectangle) was found upstream of the caspase 3/7/11 cleavage site (black circle) in the Panx1 C-terminus that may play a role in Panx1 stability and trafficking.

1.3.5.4 Role of the C-terminus

Among Panx family members, the C-termini were the most divergent in both amino acid sequence and length (Gehi et al. 2011), which suggested that this was likely

the domain responsible for Panx1-specific PTMs and protein-protein interactions, allowing for fine-tuning of trafficking dynamics, localization, and function, as occurred for other protein families (Coussen 2009; Haitin & Attali 2008; Snyder 2005; Leithe & Rivedal 2007; Feng & Zhang 2009). Several studies demonstrated that the Panx1 C-terminus was critical for regulating subcellular distribution (Figure 1.5). For example, in cell surface biotinylation experiments, a Panx1 mutant with a truncated C-terminus (Panx1Δ307) had drastically reduced surface expression relative to full-length Panx1 and was unable to received complex glycosylation (Gehi et al. 2011). Evidence for the role of the C-terminus in regulating Panx1 trafficking was further supported by the creation of a Panx2-Panx1 C-terminus chimeric protein ($Panx2^{Panx1CT}$) in a report I co-authored (Wicki-Stordeur et al. 2013). $Panx2^{Panx1CT}$ did not codistribute with Panx1 or Panx2; instead it had diffuse intracellular distribution and was unable to reach the cell surface. This both confirmed that the C-terminus was critical for cell surface targeting of Panx1 and suggested that sequence features of the Panx1 C-terminus alone were insufficient to target Panx2 to the plasma membrane (Wicki-Stordeur et al. 2013). The secondary structure of the Panx1 C-terminus was uncovered using a combination of predictive tools and subsequent circular dichroism of short peptides generated that spanned the length of the C-terminus (Spagnol et al. 2014). The C-terminus was primarily made up of random coiled structures, particularly in the distal portion of the domain; however, the middle portion of the C-terminus contained a combination of α-helix and β-strand structure. Within this region was a putative membrane interacting region (I360-G370) in the middle region of the Panx1 C-terminus (Figure 1.6). In a previous study, co-incubation with mimetic detergent micelles led to altered more α-helical structure of this region,

suggesting that interactions with membrane lipids might impact on the structure of this C-terminal region (Spagnol et al. 2014). Finally, a C-terminus localized interaction was identified with actin by a combination of co-sedimentation assays and Panx1 immunoprecipitation (IP) in both exogenous (Bhalla-Gehi et al. 2010) and endogenous (Wicki-Stordeur & Swayne 2013) expression systems. A functional actin cytoskeleton was critical for cell surface expression of Panx1, as actin depolymerization with cytochalasin B led to retention in perinuclear compartments (Bhalla-Gehi et al. 2010). Taken together, these findings highlighted the critical role of the Panx1 C-terminus in regulating cell surface targeting and stability.

1.3.5.5 Retrograde trafficking mechanisms

Although the anterograde trafficking mechanisms of Panx1 have begun to be uncovered, the regulation of retrograde trafficking and Panx1 turnover remains less understood. Gehi *et al.* (2011) were the initial group to investigate the molecular mechanisms regulating Panx1 turnover using BICR-M1R_k and HEK293T cells. A number of potential pathways for membrane protein internalization existed involving diverse proteins and lipid players (reviewed in Kumari et al. 2010; Figure 1.7); however, Gehi *et al.* began their investigation by exploring whether Panx1 internalized through one of the canonical mechanisms: either clathrin- or caveolin-mediated endocytosis.

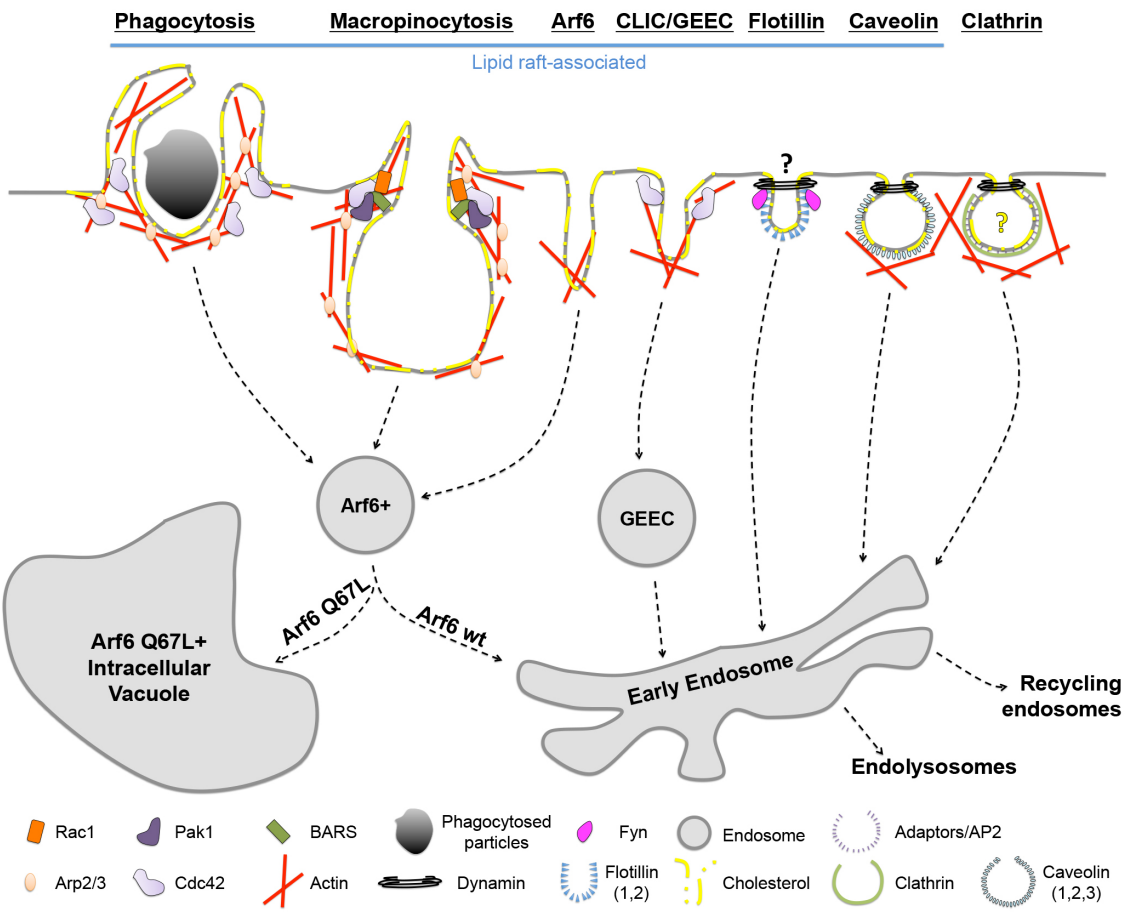

Figure 1.7 Mechanisms of endocytosis. Both large-scale (>0.2 μm vesicles; phagocytosis and macropinocytosis) and small-scale (<0.2 μm vesicles; clathrin, caveolin, flotillin, Arf6, and CLIC/GEEC) endocytic mechanisms rely on a combination of shared and distinct machinery. Most endocytic processes are associated with signalling through cholesterol-rich specialized lipid microdomains, excluding clathrin-mediated endocytosis, although there are some examples of clathrin-mediated endocytosis being sensitive to cholesterol modulation (indicated by yellow '?'). For large-scale endocytosis, phagocytosis is differentiated from macropinocytosis by the presence of large phagocytosed particles and insensitivity to amiloride, which targets submembranous pH-sensitive GTPases and kinases. Both processes are highly reliant on actin-dependent filipodial generation. These pathways, along with the small-scale Arf6-dependent internalization pathway, are distinct from canonical pathways as they share a Arf6-positive vesicle upon internalization before reaching the sorting endosome. The canonical mechanisms, clathrin- and caveolin-mediated endocytosis, involved the formation of a coated vesicle. In clathrin-mediated endocytosis, the coat is formed by a clathrin triskelia connected to cargo proteins via adaptors (commonly AP2). In caveolin-mediated endocytosis, the coat is formed by caveolin proteins,

which interact directly with their cargo. Following vesicular formation, these pathways share a dynamin-dependent scission step. Flotillin-mediated endocytosis is a non-canonical pathway that, like clathrin- and caveolin-, involves the formation of a coated vesicle (by fyn kinase-mediated phosphorylation of flotillin proteins) and in some circumstances vesicular scission by dynamin (indicated by black '?'). Finally, GPI-anchored proteins cluster and are internalized together in tubular structures through a Cdc42-, actin-dependent mechanism. Each of these internalization pathways targets vesicles to the early endosome where the cargo is then sorted for degradation or recycling.

Clathrin-mediated endocytosis (reviewed in McMahon & Boucrot 2011) involves the packaging of cargo proteins into endocytic vesicles with the aid of a vesicular coat composed of polymerized clathrin triskelia (named for their three-pronged structure) and clathrin-associated adaptor proteins. As soluble clathrin proteins do not interact with receptor cargo or the membrane directly, clathrin-adaptor proteins (i.e. adaptor protein 2, AP2) interact with membrane receptors (Ohno et al. 1995), leading to receptor clustering and the genesis of clathrin-coated pits. Clathrin triskelia then interact with adaptor proteins and polymerize to form a basket-like structure promoting membrane curvature and pit formation (Hinrichsen et al. 2006). This pathway is highly versatile, as a wide array of clathrin-associated adaptor proteins interact with different receptors (reviewed in Traub 2009), allowing for both ligand-dependent and constitutive endocytosis .

Caveolin-mediated endocytosis involves recruitment of membrane proteins destined for internalization into caveolin-rich lipid microdomains (reviewed in Kumari et al. 2010). Caveolins directly interact with two key components of these specialized lipid microdomains, cholesterol and sphingolipids (Murata et al. 1995; Fra et al. 1995), Importantly, depletion or aggregation of cholesterol abolishes caveolae formation (Rothberg et al. 1992). Membrane proteins internalized through this mechanism typically

interact with caveolin directly or through an accessory protein (see Gracia et al. 2011). The high density of caveolin oligomers, spanning only the inner leaflet of the plasma membrane, as well as interaction with membrane cholesterol leads to curvature of the membrane and formation of cup-shaped invaginations of the membrane (reviewed in McMahon & Gallop 2005).

Following the formation of either clathrin- or caveolin-mediated invaginations, a scission step completed by the dynamin protein leads to internalization of a vesicle (Van der Bliek et al. 1993; Henley et al. 1998). The coat proteins are then disassembled and recycled to the plasma membrane, while the internalized vesicle is targeted to the early endosome for sorting toward either the lysosome for degradation or the recycling endosome to be returned to the cell surface (reviewed in Jovic et al. 2010). Intracellular vesicular trafficking involves the continuous budding off of vesicles from one compartment and fusing with the next in a highly organized and directional manner. This process is regulated by a number of compartment-specific proteins, including the vast Ras-related protein (Rab) GTPase family (Diekmann et al. 2011), which insert themselves into specific compartmental membranes upon binding GTP and are subsequently released upon GTP hydrolysis (reviewed in Stenmark 2009). GTP hydrolysis alters the interactions between Rabs, molecular motors, and other effector proteins, allowing for regulated cytoskeletal transport of vesicles to and from discrete intracellular compartments (reviewed in Grosshans et al. 2006). The rich diversity of Rabs has made them excellent markers for specific subcellular compartments and spatiotemporal tracking of protein trafficking (Diekmann et al. 2011).

Gehi *et al.* first investigated whether Panx1 in a steady state (unstimulated) was internalized through either of the canonical endocytic mechanisms, clathrin or caveolin-dependent endocytosis (Gehi et al. 2011). Relative Panx1 overlap with clathrin-mediated (clathrin heavy chain, AP2) and caveolin-mediated (Cav-1, Cav-2) endocytic machinery was not affected following a prolonged disruption of anterograde trafficking with BFA. Further, relative levels or Panx1 glycosylation species and subcellular distribution were not affected by co-expression with the dominant-negative dynamin II (DynII K44A) in BICR-M1R_k cells. Additionally, treatment with a dynamin inhibitor, Dynasore, had no additive effect on altering glycosylation species expression profile. Further, Panx1 did not co-IP with any of this canonical endocytic protein machinery (clathrin heavy chain, AP2, Cav-1, Cav-2, dynamin II). These findings suggested that Panx1 endocytosis occurred through a non-canonical internalization mechanism (Gehi et al. 2011). Many non-canonical internalization processes involved signalling through specialized lipid microdomains dependent on cholesterol (reviewed in Mayor et al. 2014). Gehi *et al.* (2011) suggested that incubation with the cholesterol-depleting agent methyl-β-cyclodextrin (MβCD; up to 24h) had no effect on altering glycosylation species nor Panx1 subcellular localization; however, representative confocal micrographs appeared to show an accumulation of Panx1 at the cell periphery following MβCD treatment (6 and 24 h time points) that was not addressed nor quantified (Gehi et al. 2011). The authors concluded that, based on the long-term stability of Panx1 at the membrane and the absence of canonical internalization mechanisms, Panx1 function would be regulated predominantly by modulating channel gating rather than governing the oligomerization, trafficking, and stability of Panx1 channels (Gehi et al. 2011). However these previous

studies did not determine whether the stimuli and signalling pathways that modulate Panx1 channel activity also regulated trafficking, stability, and turnover.

1.4 Non-canonical mechanisms of endocytosis

Although Gehi *et al.* clearly observed Panx1 internalization independent of clathrin- and caveolin- mediated pathways (Gehi et al. 2011), the precise non-canonical internalization mechanism (of which there are many) was not identified. Most non-canonical endocytic mechanisms elicit membrane curvature and vesicular formation independent of traditional coat-adaptor-receptor interactions (reviewed in Mayor et al. 2014). Instead, they require the clustering of critical regulatory proteins in specialized membrane microdomains (often referred to as lipid rafts or lipid microdomains; Chadda et al. 2007; Rollet-Labelle et al. 2004; Mayor et al. 2014; Otto & Nichols 2011), which allow for complex spatial and temporal regulation of internalization machinery. The Fluid Mosaic model, proposed by Singer and Nicholson (Singer & Nicolson 1972), was the initial theory underlying the distribution of proteins in the plasma membrane. In this theory, the composition of lipids and proteins in the plasma membrane was random, based on dynamic rotational and lateral diffusion patterns. However, experimental evidence from early studies of plasma membrane diffusion identified that protein and lipid mobility might be partially restricted. First, Simons and van Meer observed that sphingolipids were enriched at the apical surface of epithelial cells (van Meer & Simons 1988), suggesting a lipid sorting mechanism at the level of the trans Golgi network. A portion of plasma membrane lipids were later determined to be partially insoluble by the non-ionic detergent Triton X-100 at cold temperatures, indicating that these membrane

lipids may be tightly packed in a complex structure (Brown & Rose 1992). In addition to this, work with model membranes highlighted that a combination of saturated lipids and cholesterol were able to form transient, tightly-packed, but laterally dynamic clusters independent of protein components (Hjort Ipsen et al. 1987). These clusters were insoluble in Triton X-100, consistent with observations made in cell-based assays (Ahmed et al. 1997; Schroeder et al. 1994). Finally, sequestration of membrane cholesterol disrupted physiological processes in a multitude of cell types, suggesting a role for membrane cholesterol in signalling complexes at the plasma membrane (Rothberg et al. 1990). This gave rise to the lipid raft hypothesis, proposed by Simons and Ikonen (Simons & Ikonen 1997), which suggested that this phenomenon was the result of an intricate network of protein-protein, protein-lipid, and lipid-lipid interactions resulting in highly ordered specialized microdomains, distinct from the surrounding disordered membrane.

Controversy arose in the scientific community shortly after the proposal of the lipid raft hypothesis based on: (1) the indirect, perturbing techniques used to study them that were initially available (i.e. detergent-resistant fractionation) and (2) the inconsistency in their size and distribution observed with imaging techniques used to study them *in situ* (see reviews Edidin 2003; Munro 2003). However, the advent of super resolution microscopy has confirmed the presence of rafts *in situ*, which are typically smaller and more heterogeneous and dynamic than initially anticipated (Simons & Gerl 2010).

The protein components of these cholesterol-containing, detergent-insoluble ‘rafts’ were progressively discovered (reviewed in Laude & Prior 2004) and include

glycosylphoshatidylinositol (GPI)-anchored proteins and acylated signalling proteins including Src family kinases, integrins, nitric oxide synthase, GPCRs, growth factor receptors, and cholesterol-binding proteins including, famously, caveolins. Lipidomic analysis soon revealed a complement of lipids enriched in rafts in addition to cholesterol and sphingolipids, including arachadonic acid, phosphatidic acid (PA) and its metabolites, as well as $PI(4,5)P_2$ (Pike & Casey 1996; Pike et al. 2002; Fridriksson et al. 1999; Ogiso et al. 2015). However, thanks to high-resolution imaging and refined fractionation, we now know that when a raft assembles, only a subset of these markers is enriched in a given raft. Only in specific cell types (including polarized epithelial cells or oligodendrocytes; Danielsen & Hansen 2003) or when rafts are artificially enlarged (via antibody crosslinking or enrichment in detergent-insoluble fractions) are a full complement of raft proteins observed, suggesting the presence of several raft subtypes with unique signalling properties.

The likelihood of Panx1 being internalized through non-canonical mechanisms (many of which involve signalling through lipid microdomains) was supported by the early trafficking work by the Laird lab (Gehi et al. 2011). Further, ATP-sensitive P2 receptors rely on raft-localization for key aspects of their signalling (Garcia-Marcos et al. 2006). In rafts, the clustering of critical regulatory proteins allows for complex spatial and temporal regulation of internalization machinery, which is particularly important for many of the non-canonical endocytic mechanisms that emerge independent of traditional coat proteins (Chadda et al. 2007; Rollet-Labelle et al. 2004; Mayor et al. 2014; Otto & Nichols 2011). Underlying these complex protein-lipid microdomains is cortical actin,

which is necessary for membrane rearrangement and recruitment of endocytic machinery into these specialized microdomains (Gowrishankar et al. 2012; Römer et al. 2010).

In the next section, I will introduce several of the possible non-canonical mechanisms of endocytosis (reviewed in Mayor et al. 2014) that could regulate Panx1 internalization including the large scale endocytic pathways (0.2 μm to ~5 μm-sized vesicles): phagocytosis and macropinocytosis; as well as small-scale endocytic pathways (<200 nm-sized vesicles) including Arf6-dependent endocytosis, clathrin-independent carrier-GPI-enriched early endosomal compartments (CLIC-GEEC endocytosis), and flotillin-mediated endocytosis.

1.4.1 Phagocytosis

Phagocytosis is the receptor-mediated cellular ingestion of large particles typically associated with immune cells (≥0.5 μm; reviewed in Flannagan et al. 2012). Here, it plays a role in the clearance of foreign bodies (i.e. invading bacteria) or dead/dying cells (i.e. Chekeni et al. 2010). As the presentation of foreign bodies is very diverse, it is not surprising that phagocytosis is initiated through a wide complement of receptors (reviewed in Flannagan et al. 2012). Typically, ligand-receptor interactions trigger receptor oligomerization that initiates the signalling cascade involved in the internalization event (Odin et al. 1991). Receptor clusters are then targeted to lipid microdomains in a cholesterol-dependent manner (Rollet-Labelle et al. 2004). Internalization involves the activation of SFKs or other lipid raft-localized tyrosine kinases (Jaumouille et al. 2014), as well as actin polymerization mediated by cell division control protein 42 (Cdc42) and other small GTPases (Hoppe & Swanson 2004) and

enrichment of the phospholipid PI(4,5)P_2. In fact, inhibition of PI(4,5)P_2 production disrupts phagocytosis (Botelho et al. 2000).

1.4.2 Macropinocytosis

Macropinocytosis is the regulated internalization of extracellular fluid commonly known as "cell drinking." The generation of large heterogeneous endocytic vesicles (0.2-5 μm), associated with actin-dependent membrane ruffling, absent of phagocytosed particles (Swanson & Watts 1995), is characteristic of the macropinocytic internalization pathway. Internalization is triggered by soluble antigenic molecules in immune cells (Sallusto et al. 1995) or growth factors and other signalling molecules in other cell types [i.e. epidermal growth factor (West et al. 2000), macrophage colony-stimulating factor (Racoosin & Swanson 1989); reviewed in (Bohdanowicz & Grinstein 2013)]. Membrane ruffles are generated through filipodial outgrowth regulated by dynamic actin polymerization and dependent on cholesterol (Grimmer et al. 2002). There are several critical actin-regulatory proteins involved including Rho kinases and the actin-related protein 2/3 (Arp2/3) complex (reviewed in Ridley 2006). In addition to these actors, this process is regulated by the p21-activated kinase Pak1 (Dharmawardhane et al. 2000) and the GTPases Cdc42 and Ras-related C3 botulinum toxin substrate 1 [Rac1 (Zhang et al. 1995)], which regulate actin polymerization into filopodia and stimulate Pak1 activation. Pak1 then triggers BFA-dependent ADP ribosylation substrate (BARS), a protein strongly associated with macropinosome genesis. BARS initiates membrane curvature and endocytosis through metabolic generation of phosphatidic acid from lysophosphatidic acid, promoting invagination of the plasma membrane (Kooijman et al.

2003). Expression of a dominant negative mutant of BARS disrupts this pathway (Liberali et al. 2008). Many of the aforementioned enzymes are uniquely sensitive to submembranous pH, consequently, inhibition of the Na^+/H^+ exchanger with amiloride selectively inhibits macropinocytic endocytosis (West et al. 1989; Koivusalo et al. 2010). Arf6 is a GTPase localized to both the plasma membrane and endosomal compartments (Radhakrishna & Donaldson 1997) that has been linked to macropinocytosis. Internalization pathways reliant on Arf6 are classically both clathrin- and dynamin-independent and include both macropinocytosis (Sannerud et al. 2011; Tang et al. 2015), phagocytosis (Beemiller et al. 2006), as well as small-scale endocytic events (reviewed in Mayor et al. 2014). Like Rabs, Arf6 cycles between an active GTP-bound and an inactive GDP-bound state (Brown et al. 1993). During Arf6-mediated endocytosis, GTP-bound Arf6 activates PI(4)P 5-K (Naslavsky et al. 2003), which triggers the conversion of PI(4)P into PI(4,5)P_2. PI(4,5)P_2 recruits GTPases and other effectors involved in vesicle formation (reviewed in Bohdanowicz & Grinstein 2013). Upon internalization, subsequent PI(4,5)P_2 dephosphorylation is required for fusion of cargo-containing vesicles into a common sorting endosome with internalized vesicles from other pathways. From here, cargo are subsequently sorted for either degradation or recycling (Naslavsky et al. 2003). As GTP-bound Arf6 activates the phosphatidylinositol-4-phosphate 5-kinase, constitutively-active Arf6 mutants (Arf6 Q67L) cause accumulation of cargo proteins within large PI(4,5)P_2-positive intracellular vacuoles (Naslavsky et al. 2003), which can be used to distinguish from cargo undergoing canonical clathrin-dependent endocytosis.

1.4.3 CLIC/GEEC endocytosis

GPI-anchored proteins are internalized through the CLIC (clathrin-independent carrier) pathway to specialized endosomes enriched in GPI-anchored proteins (GEEC; GPI-enriched early endosomal compartments; Sabharanjak et al. 2002). GPI moieties are membrane anchors for a diverse group of proteins including immune and parasitic antigens, enzymes, and membrane receptors (Ferguson 1999). This process is significantly slower than traditional endocytic pathways often taking up to several hours (Mayor & Riezman 2004). CLIC/GEEC endocytosis is insensitive to inhibition of dynamin II, RhoA, Rac1, and Arf6 (Sabharanjak et al. 2002; Lundmark et al. 2008). However, it is blocked by Cdc42 inhibition, which promotes the redistribution of GPI-anchored proteins into the clathrin-dependent pathway (Sabharanjak et al. 2002), or cholesterol depletion (Chadda et al. 2007), indicating some shared molecular players with other non-canonical mechanisms (Kumari & Mayor 2008). CLIC/GEEC endocytosis is also dependent on lipid signalling, as alteration of cholesterol and sphingolipid levels modulate this pathway (Sharma et al. 2004; Chadda et al. 2007).

1.4.4 Flotillin-mediated endocytosis

Flotillin proteins are responsible for yet another mechanism of clathrin- and caveolin-independent endocytosis (reviewed in Otto & Nichols 2011). Fyn kinase-mediated phosphorylation of flotillins triggers aggregation of flotillin proteins in the plasma membrane (Riento et al. 2009). This clustering induce invagination in a dose-dependent manner (Frick et al. 2007). Although it is clear that flotillin-mediated internalization is independent of canonical coat proteins, both dynamin (Aït-Slimane et

al. 2009; Payne et al. 2007) and cholesterol (Strauss et al. 2010; Schneider et al. 2008) regulate the endocytosis of flotillin-mediated pits in certain circumstances. Consequently, it shares some potential overlap with canonical internalization pathways and can be modulated with associated inhibitors.

1.5 Summary

Panx1 is predominantly known as a cell surface ATP release channel; however, there remains a significant and stable population of intracellular Panx1 in many cell types. Whether intracellular Panx1 is the result of divergence from the secretory pathway prior to reaching the plasma membrane or internalization from the cell surface was previously unknown. If it were the result of internalization, it would likely need a constitutive or episodic stimulus that exists across cell and tissue types; extracellular ATP fits this criterion. Prior to the genesis of my project, ATP was observed to negatively regulate Panx1 channel function although the mechanisms of negative feedback were not well understood. The following chapters aim to uncover how elevating extracellular ATP and other stimuli known to modulate Panx1 activity or alter cellular excitability affect Panx1 cell surface stability (Figure 1.8). Herein, I investigate ATP-triggered internalization, as well as the destination of endocytosed Panx1 and the molecular mechanisms involved with a particular focus on the role of P2X7Rs. Finally, I investigate the endocytic machinery (including both protein and lipid components) involved in internalizing and sorting Panx1 between endosomal compartments.

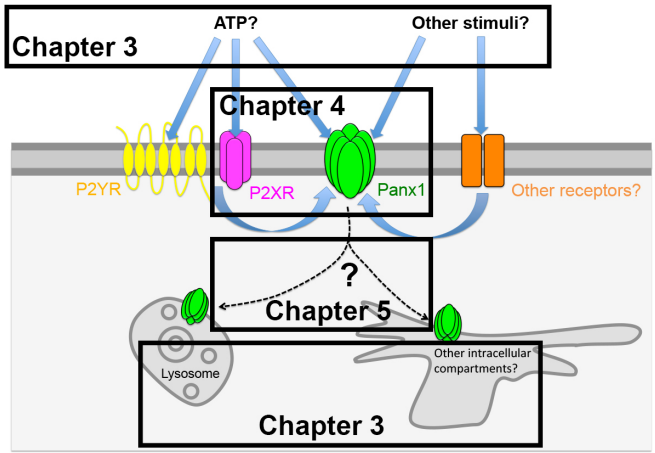

Figure 1.8 Research Questions. The aim of my dissertation is to address whether intracellular Panx1 expression is regulated through endocytosis. In chapter 3, I will ask whether ATP or other stimuli known to modulate Panx1 activity or cellular excitability trigger endocytosis. Following this, I will also explore the destination of endocytosed Panx1 and whether it is specifically targeted for lysosomal degradation or shuttled to additional intracellular compartments. In chapter 4, after finding that Panx1 is internalized in response to ATP and sensitive to P2X7R inhibition, I will investigate the role of extracellular ATP in modulating P2X7R-Panx1 interactions upstream of internalization. Finally, in chapter 5, I will uncover the endocytic machinery (including both protein and lipid components) involved in internalizing and sorting Panx1 into endosomal compartments.

2 Methods

2.1 Cell culture

Neuro2a (N2a) mouse neuroblastoma cells (procured from the American Type Culture Collection, ATCC) were cultured in Dulbecco's modified Eagle's medium (DMEM)/F12 supplemented with 10% FBS, 100 units/mL penicillin, and 100 μg/mL streptomycin (all obtained from Gibco/Life Technologies). Human Embryonic Kidney (HEK)-293T cells (procured from the ATCC) were cultured in DMEM supplemented with 10% FBS, 100 units/mL penicillin, and 100 μg/mL streptomycin.

2.1.1 Plasmids

The Panx1-EGFP and Panx1-RFP plasmids (Penuela et al. 2007) were generous gifts from Drs. Dale Laird and Silvia Penuela. A mutant Panx1W74A-EGFP plasmid was created by Michelle Kim using site-directed mutagenesis of the Panx1-EGFP plasmid (Penuela et al. 2007) with the following primers (forward: 5'-CGAGTTCTTTCTCCGCGCGACAGGCTGCCTTTG-3'; reverse: 5'CAAAGGCAGCCTGTCGCGCGGAGAAAGAACTCG-3') using the QuikChange II site-directed mutagenesis kit following manufacturer's protocols (Agilent Technologies) and confirmed by sequencing (Eurofins MWG Operon). The pARF6-CFP (Plasmid #11382) and pARF6-Q67L-CFP (Plasmid #11387) were acquired from Addgene, courtesy of Dr. Joel Swanson (Beemiller et al. 2006).

2.1.2 Transfection and generation of stable cell lines

Where indicated, N2a and HEK293T cells were transfected using jetPEI reagent (Polyplus transfection/VWR) according to the manufacturer's protocol. N2a cells stably expressing equivalent levels of Panx1-EGFP or Panx1W74A-EGFP were maintained in DMEM/F12 containing 10% FBS, and 100 units/mL penicillin, 100 µg/mL streptomycin, and 400 µg/mL geneticin 418 (all obtained from Gibco/Life Technologies). EGFP-tagging of Panx1 did not affect subcellular distribution (Figure 2.1).

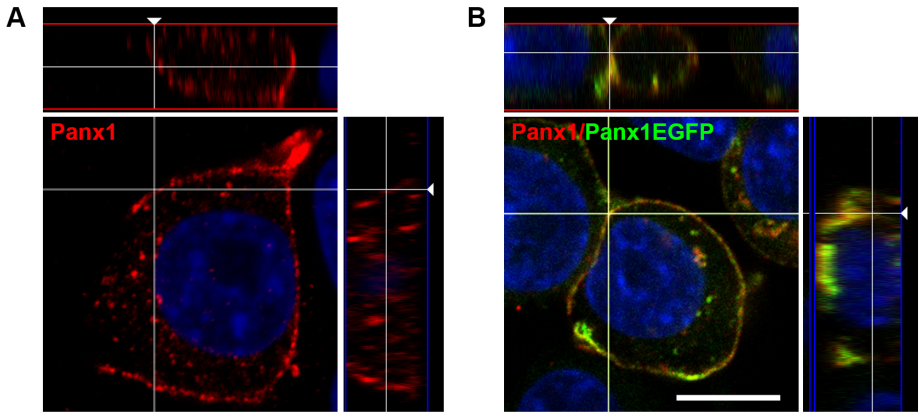

Figure 2.1 Panx1-EGFP and endogenous Panx1 demonstrate similar subcellular distribution in N2a cells. (A) Confocal micrograph with merged orthogonal side views of endogenous Panx1 distribution in N2a cells or (B) Panx1-EGFP (green)-expressing N2a cells labelled with anti-Panx1 CT (red). Modified images from Wicki-Stordeur, Boyce, & Swayne, 2012 (http://www.tandfonline.com/doi/full/10.3109/15419061.2013.791681). Hoechst 33342 (blue) was used as a nuclear counterstain. Scale bar, 10 µm.

Stable cell lines were generated as follows: N2a cells were transfected with Panx1-EGFP or Panx1W74A-EGFP using the jetPEI reagent (Polyplus transfection/VWR) according to the manufacturer's protocol. Panx1-EGFP or Panx1W74A-EGFP N2a cells, stably expressing either one of these constructs, were generated by selecting a clonal colony from N2a cells transfected with Panx1-EGFP or Panx1-W74A-EGFP, respectively. Using

a kill dose of the mammalian selection antibiotic geneticin 418 (G418, 800 μg/mL) eliminated any confounding untransfected cells. Colonies were used that expressed equivalent levels of transfected protein. Cells were plated on poly-D-lysine (PDL, Sigma)-coated coverslips. For all internalization-related experiments, protein translation was briefly inhibited by treatment with 20 μg/mL cycloheximide (CHX; Sigma) for 8 h, coincident with other treatments. Cells were fixed with 4% paraformaldehyde (PFA) washed three time in phosphate buffered saline (PBS) prior to mounting for imaging or processing for immunostaining or proximity ligation assay (PLA).

2.1.3 Reagents for cellular treatments

We investigated the role of ATP (100, 200, or 500 μM, Sigma) versus vehicle control (equal volume of water) on Panx1 cell surface stability and trafficking. We evaluated the effects of other modulators of cellular excitability/excitotoxicity using 30 mM potassium chloride (K^+), 10 μM Ca^{2+} ionophore A23187, and chemical OGD (100 μM potassium cyanide and 1 μg/mL oligomycin) for 30 minutes. We investigated nucleotide specificity of ATP-induced Panx1 internalization using 100 μM or 500 μM 2'(3')-O-(4-benzoylbenzoyl) adenosine 5'-triphosphate triethylammonium salt (BzATP), 500 μM UTP Tris salt, 500 μM adenosine-5'-(β-thio)-diphosphate trilithium salt (ADPβS; all obtained from Sigma-Aldrich) or 500 μM adenosine-5'-(γ-thio)-triphosphate tetralithium salt (ATPγS; Tocris Bioscience). For the P2X7 inhibitor experiments, cells were pre-treated for 1 h prior to ATP or vehicle treatment with 100 μM A438079 (Tocris Bioscience) or vehicle (equal volume of dimethyl sulphoxide, DMSO). For experiments

using modulators of endocytic pathways, cells were pre-treated for 1 h prior to ATP or vehicle treatment with 10 μg/mL chlorpromazine (CLPZ), 1 μg/mL filipin III (Fil III), 10 mM methyl-β-cyclodextrin (MβCD) or vehicle control (equal volume of DMSO; all endocytosis inhibitors obtained from Sigma-Aldrich) respectively. We modulated extracellular ATP levels with apyrase (50 U/mL, Sigma) or ARL 67156 (250 μM, Tocris Biosciences). Inhibition of the P2X7R was performed using A438079 (100 μM, Tocris Bioscience). For experiments examining the role of extracellular Ca^{2+}, cells were incubated in Hank's buffered saline solution (HBSS; 137 mM NaCl, 5.36 mM KCl, 4.17 mM $NaHCO_3$, 0.44 mM KH_2PO_4 monobasic, 0.34 mM Na_2HPO_4 anhydrous, 5.56 mM dextrose) supplemented with Ca^{2+} (1.05 mM) or without Ca^{2+} and in the presence of 5 mM EGTA. To chelate intracellular Ca^{2+}, cells were bathed in media containing EGTA-AM (50 μM, Calbiochem), BAPTA-AM (50 μM, Molecular Probes), or vehicle (equal volume of DMSO). For Src inhibition experiments, we used PP2 (10 μM, Enzo Life Sciences) or its inactive analogue PP3 (10 μM, Calbiochem). For P2X7R-Src peptide interference assays, cells were pre-treated with TAT (transactivator of transcription)-conjugated membrane-permeable peptides (10 μM, GenScript, >90% purity) corresponding to the SH3 domain in the murine human P2X7R C-terminus (Iglesias et al. 2008) (TAT-mP2X7R-451P (NH_2-SLHDSPPTPGQYGRKKRRQRRR-COOH), TAT-mP2X7R-451L (NH_2-SLHDSPLTPGQYGRKKRRQRRR-COOH), or TAT-hP2X7R (NH_2-ALHDTPPIPGQYGRKKRRQRRR-COOH) along with a TAT only control (NH_2-YGRKKRRQRRR-COOH)). We disrupted macropinocytosis by pre-treating cells with amiloride (300 μM; Sigma) or vehicle (DMSO) for 1 h.

2.2 Imaging assays

Confocal imaging and analysis were performed blinded to the experimental conditions. Images were acquired with a Leica TCS SP8 confocal microscope. Quantification was performed using Leica Application Suite (version 3.1.3) and in the confocal plane displaying the largest plane of the nucleus. Comparisons were made between images acquired under identical conditions. Representative confocal micrographs were adjusted for contrast uniformly using Adobe Photoshop (CC 2015.1.2) for display purposes only; no contrast adjustments were made prior to analysis.

2.2.1 Live cell confocal microscopy

Panx1-EGFP N2a cells were plated on 100 μg/mL PDL-coated eight-well chambered coverglass (Nunc LabTek/ ThermoScientific) and maintained at a temperature of 37 °C and 5 % CO_2. Images were captured (Leica TCS SP8) using a 20X (dry) or 63X (water-immersion) objective, where indicated.

2.2.1.1 Live cell Panx1 tracking

Tetramethylrhodamine (TRITC)-conjugated wheat germ agglutinin (WGA; 1 μg/mL; Life Technologies) was added 5 min prior to imaging. ATP (100 μM, 200 μM, 500 μM; Sigma-Aldrich) or vehicle control (water) was added to individual wells and images were collected at 1-min intervals for 30 min using a 20x [0.7 numerical aperture (NA)] objective. Quantification of Panx1-EGFP fluorescence intensity to describe ‘intracellular Panx1’ was performed at time zero and each 5-min interval thereafter, as follows: a

polygonal trace was drawn 1 μm inside of the peak WGA intensity at the cell periphery and the encapsulated average Panx1-EGFP fluorescence intensity per pixel was computed (Figure 1). Data were normalized to values obtained at time zero. N ≥ 25 cells were analysed per experimental condition per biological replicate. Only cells that were stable in the z-axis for the entire imaging window were counted.

2.2.1.2 Ca^{2+} imaging

Cells were incubated in HBSS with Ca^{2+} or without Ca^{2+} (+ EGTA) 1 h prior to imaging. Cells were supplemented with Fluo4-AM (4 μM) for 30 min prior to imaging. Baseline images were captured at 10 s intervals for 2 min using a 63X (1.2 NA) water-immersion objective. Images of ATP-treated cells (500 μM) were captured at 10 s intervals for 2 min following stimulation.

2.2.2 Fixed cell confocal microscopy

Confocal images (Leica TCS SP8) of fixed cells were acquired using a 40X (1.3 NA) oil immersion objective at 3X optical zoom in 1296 x 1296 format with a pixel area of 71 nm^2 as confocal z-stacks. Stimulated Emission Depletion (STED) confocal microscopy (Klar et al. 2000) was performed on a Leica TCS SP8 STED confocal microscope and deconvolution was performed using the Huygens Professional deconvolution software (Suite 15.05; Schoonderwoert et al. 2013).

2.2.2.1 Antibodies

Primary antibodies (arranged alphabetically) used were: anti-β-actin (1:160,000; Sigma), anti-caveolin-1 (Cav-1; 1:100, Novus Biologicals LLC), anti-clathrin heavy chain (1:50; Novus Biologicals LLC), anti-early endosome antigen 1 (EEA1; 1:200, Cell Signalling Technology Inc.), anti-GFP polyclonal (1:5000 – western blot; 1:500 – immunofluorescence; Roche Applied Science), anti-GFP monoclonal (1:50, Life Technologies), anti-giantin (1: 500, Lifespan Biosciences Inc.), anti- glutathione S-transferase (GST; 1:100, Cell Signalling clone 26H1), anti-HIV1 TAT (1:10, Abcam), anti-lysosomal-associated membrane protein 1 (Lamp1; 1:200), anti-mannose-6-phosphate receptor (M6PR; 1:100, Abcam Inc.), anti-P2X7R (1:800 – western blot, 1:100 – permeabilized, 1:10 – unpermeabilized, Alomone Labs), anti- Rab14 (1:400, Abcam Inc.), anti-Rab4 (1:200, BD Biosciences), anti-Rab7 (1:200, Abcam Inc.), and anti-Rab11 (1:50, Santa Cruz Biotechnology). The Panx1 primary antibodies used were anti-Panx1CT (1:2500; Penuela et al. 2007) and anti-Panx1 extracellular loop 2 (EL2; 1:200; Penuela et al. 2009). Secondary antibodies included horseradish peroxidase (HRP)-conjugated AffiniPure donkey anti-rabbit immunoglobulin G (IgG), HRP-conjugated AffiniPure donkey anti-mouse IgG (both at 1:4000; Jackson ImmunoResearch), Alexa Fluor® 647-conjugated AffiniPure donkey anti-rabbit IgG (1:600; Jackson ImmunoResearch), Alexa Fluor® 568 donkey anti-mouse IgG, and Alexa Fluor® 568 donkey anti-rabbit IgG (both at 1:600; Life Technologies).

2.2.2.2 Intracellular Panx1 distribution

In chapter 3, to identify Panx1 subcellular localization upon ATP stimulation, I quantified the distribution of Panx1-EGFP in cells treated with various pharmacological modulators of internalization. Briefly, Panx1-EGFP N2a cells were plated on PDL-coated coverslips in 24 well plates. Cells were cultured and pre-treated briefly with CHX as described above in the live cell confocal experiments. Where indicated, I added other reagents or drugs in the continued presence of CHX. Following ATP or control treatment, cells were fixed with 4% paraformaldehyde in PBS for 10 min. Coverslips were then incubated with primary antibodies in antibody buffer (3% BSA, 0.3% Triton-X-100 in PBS) overnight at 4°C, washed and incubated with corresponding fluorophore-conjugated secondary antibody and Hoechst 33342 nuclear counterstain in antibody buffer for 1 h at room temperature, then washed and mounted in VectaShield (Vector Labs). $N \geq 30$ cells were analysed per experimental condition per biological replicate. Confocal images were obtained at 4x optical zoom in 1024 x 1024 format with a pixel area of 71 nm^2 at room temperature using a 40x (1.3 NA) oil immersion objective as confocal z-stacks and quantification was performed in the confocal plane displaying the largest central plane of the nuclei in the region of interest.

Intracellular Panx1 was quantified as described above (and in Figure 3.1) and normalized to values obtained for vehicle-treated controls. STED imaging of selected regions of interest was performed to support localization to specific compartments obtained with conventional confocal microscopy with enhanced resolution. STED images were obtained with a pixel area of 39 nm^2 using a 100X (1.4 NA) oil immersion STED white objective. This allowed for a theoretical maximum resolution of approximately 80

nm prior to deconvolution. Deconvolution removes aberrations and increases the contrast of the image allowing for an increase in resolution by a factor of 1.5-2 (Schoonderwoert et al. 2013). Analysis of background speckular structures (reflecting single antibody molecules or aggregates of antibody molecules) revealed an apparent resolution of 42 nm for STED microscopy experiments.

Also in chapter 3, the co-distribution of Panx1 and proteins involved in clathrin or caveolin-mediated endocytosis in either 500 μM ATP or vehicle control treated N2a cells was evaluated using Pearson's correlation coefficient for Panx1-EGFP and antibodies for these proteins. Pearson's correlation coefficient is a pixel-by-pixel measure of the covariance in the intensities of two fluorophores. Pearson's values can range from 1 for linearly related distribution of two intensities to –1 for two intensities that have a perfectly inverse relationship, a value of 0 reflects an uncorrelated relationship (Dunn et al. 2011). Following an 8 h CHX treatment, cells were fixed at 30 min post-stimulus and co-distribution data were collected for each Panx1-EGFP-positive cell in a region of interest within 1 μm of any unopposed plasma membrane. To assay for dynamin-dependent endocytosis, stable Panx1-EGFP N2a cells grown on PDL-coated coverslips were first incubated for 6 h in complete DMEM/F12 containing CHX. The cells were then rinsed and incubated in DMEM/F12 containing CHX supplemented with 2 mg/mL bovine serum albumin (BSA) for 1 h (all at 37 °C). Cells were then incubated for an additional hour in DMEM/F12/CHX/BSA supplemented with 80 μM Dynasore (Sigma-Aldrich) or DMSO control. Following this, cells were pre-incubated at 4 °C for 10 min, then in the same media supplemented 80 μM Dynasore or DMSO control and 25 μg/mL transferrin-Alexa Fluor 647 (Life Technologies) for an additional 45 min at 4 °C. Cells

were then rinsed in ice-cold DMEM/F12/CHX/BSA supplemented with 80 μM Dynasore or DMSO control and fixed immediately or media was replaced with warm media containing 500 μM ATP or vehicle control. Following a 30 min incubation period at 37 °C (internalization period), cells were fixed, and intracellular Panx1-EGFP and transferrin were measured as described above.

2.2.2.3 Panx1 codistribution with subcellular compartment markers

In chapter 3, to determine the pathway followed by internalized Panx1, the co-distribution of internalized Panx1-EGFP with antibody markers for specific subcellular compartments was determined by analysis of confocal micrographs with the Leica Application Suite software (version 3.1.3) Pearson's correlation tool. Following 8 h of CHX treatment, cells were PFA-fixed at 0.5, 1, and/or 2 h after 500 μM ATP stimulus. Vehicle-treated cells (2 h) served as control. Panx1-EGFP -expressing N2a cells were then immunostained with antibodies for subcellular compartment-specific markers. Images were obtained at 4x optical zoom in 1024 x 1024 format with a pixel area of 71.02 nm^2 at room temperature using a 40x (1.3 NA) oil immersion objective as z-stacks and quantification was performed in the confocal plane displaying the largest central plane of the nucleus (Hoechst 33342) in the region of interest. For this analysis we re-named the intracellular analysis region as 'central' and we added a 1 μm thick region of analysis, termed 'peripheral', immediately outside the 'central' region (and bounded by the plasma membrane) because early endosomes are primarily located in the cell periphery (reviewed in Huotari & Helenius 2011). The Pearson's correlation coefficient of Panx1-EGFP and antibodies for subcellular compartment-specific markers was

determined per cell in each region of interest. Figure 2.2 demonstrates that these markers (and their respective subcellular compartments) are spatially distinguishable by confocal microscopy of N2a cells. As expected, EEA1 and giantin, a marker for the Golgi, demonstrated limited co-distribution (Pearson's: 0.029±0.003). EEA1 and Lamp1 shared minor co-distribution (Pearson's: 0.16±0.01). Although these are at opposite ends of the degradation pathway, one would expect a degree of overlap reflecting the constant membrane trafficking between the various endosomal compartments and the lysosome during endosomal maturation (Huotari & Helenius 2011). As anticipated given their shared localization within some recycling endosomes, Rab4 and Rab14 had a much higher degree of co-distribution (0.53±0.03). The data for ≥ 50 cells were averaged for each biological replicate (N = 4).

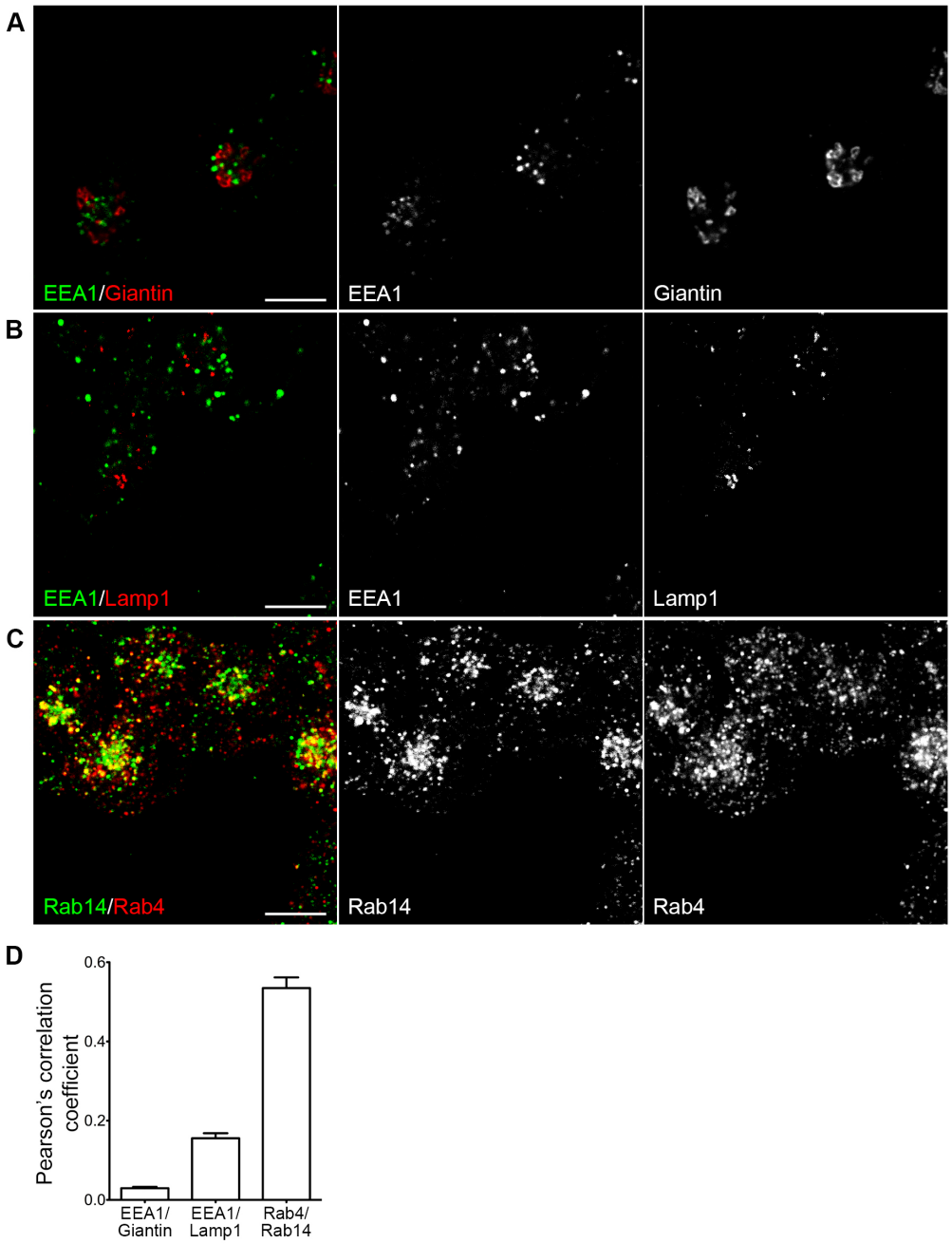

Figure 2.2 Subcellular compartments are distinguishable using confocal microscopy and codistribution analysis. Representative confocal micrographs of CHX-treated Panx1-EGFP N2a cells indicate limited co-distribution between (A) EEA1 (green) and giantin (red) – markers for the early endosome and the Golgi, respectively; minor codistribution between (B) EEA1 (green) and Lamp1 (red), markers for the early endosome and lysosome, respectively; and a high degree of co-distribution between (C) Rab14 (green) and Rab4 (red) – two markers that share some

recycling endosomal compartments. Scale bars = 10 μm. (D) Co-distribution was quantified using Pearson's correlation coefficient. *N* = 4 biological replicates per experimental condition.

2.2.2.4 Visualizing P2X7R-Panx1 interactions

In chapter 4, to visualize surface staining of GST-Panx1^{EL1}, PFA-fixed, CHX-treated Panx1-EGFP N2a cells were incubated with GST-Panx1^{EL1} or GST control, washed and incubated with anti-GST (1:100), washed and incubated in Alexa Fluor 568 donkey anti-mouse IgG (1:300; Fisher Scientific) and Hoechst 33342 (1:300) in immuno PBS (154 mM NaCl, 6.25 mM sodium phosphate monobasic, 18.75 mM sodium phosphate dibasic, pH 7.2), then washed and mounted in VectaShield. For TAT-peptide treatments, cells were fixed and underwent antigen retrieval in sodium citrate buffer (10 mM sodium citrate, 0.05% Tween 20, pH 6.0) for 1 h at 60 °C, washed, then incubated with anti-TAT clone N3 (1:20; Abcam) in antibody buffer (3% BSA, 0.3% Triton-X-100 in PBS) overnight at 4°C. Next, coverslips were washed, then incubated with Alexa Fluor 568 donkey anti-mouse IgG and Hoechst 33342 in antibody buffer for 1 h at room temperature, then washed and mounted. Confocal micrographs shown are representative of ≥ 30 cells imaged per condition.

2.2.2.5 Proximity ligation assays (PLA)

We used the Duolink *In Situ* PLA kit (Sigma) according to the manufacturer's instructions. PFA-fixed cells were incubated overnight with anti-GFP monoclonal (1:50**,** Roche Applied Sciences) and anti-P2X7R extracellular (1:100, Alomone Labs) in antibody buffer at 4°C. In separate experiments, fixed cells were pre-incubated with

purified GST-Panx1^{EL1} or GST alone (10 μM, 45 min at 4 °C), then incubated with anti-GST (1:100, Cell Signalling clone 26H1) and anti-P2X7R (1:100) for 1 h at room temperature. Mouse monoclonal anti-GFP (1:50) and a rabbit polyclonal anti-GFP (1:500, Life Technologies 5) in antibody buffer were used as a positive control, while primary antibody omission served as a negative control (Figure 2.3). Following primary incubation, coverslips were washed in PBS and incubated with PLA probe anti-rabbit PLUS and PLA probe anti-mouse MINUS (each at 1:5 dilution; Sigma) for 60 min at 37 °C in a humid chamber. Cells were then washed in Wash Buffer A (0.01 M Tris, 0.15 M NaCl, 0.05% Tween 20 in water; pH 7.4) twice for 5 min each. PLA probes within <40 nm of each other were ligated using an incubation in 5X ligation buffer and DNA ligase (1:40, Sigma) for 30 min at 37 °C. Following this, coverslips were washed twice for 2 min each in Wash Buffer A then incubated for 100 min at 37 °C in 5x Amplification Red buffer and DNA polymerase. Fluorescent oligonucleotide probes in the Amplification Red buffer hybridize with the amplified DNA allowing for visualization of fluorescent P2X7R-Panx1 PLA clusters. Coverslips were then washed twice for 10 min in 1X Wash Buffer B (0.2 M Tris, 0.1 M NaCl in water; pH 7.5) and once for 1 min in 0.1X Wash Buffer B prior to mounting in VectaShield and subsequent imaging.

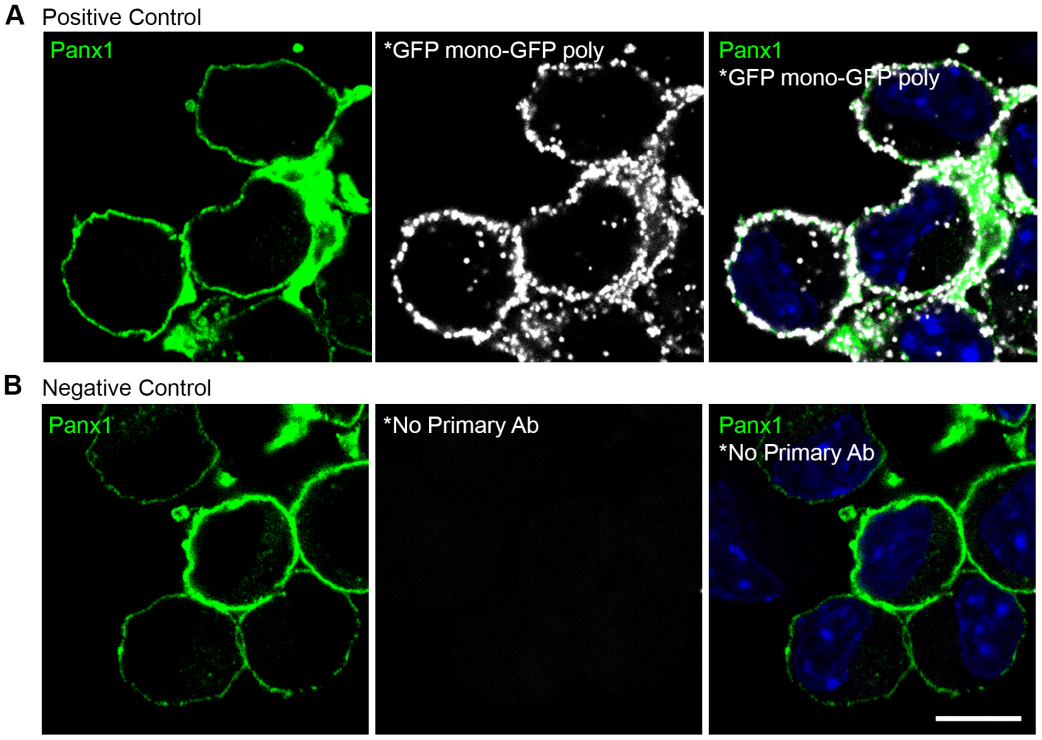

Figure 2.3 Controls for PLA specificity. Confocal micrographs of PLA clusters in Panx1-EGFP N2a cells (green) for (A) positive (*GFP mono-GFP poly; white) or (B) negative (no primary antibodies; white) controls. Hoechst 33342 (blue) was used as a nuclear counterstain. Scale bar, 10 µm.

2.3 Biochemical assays

2.3.1 Western blotting

In chapter 3, to investigate Panx1 protein expression following ATP stimulation, Panx1-EGFP N2a cells were treated with CHX, as described above in the live cell confocal experiments. Cells were either collected immediately (0 h) or stimulated with vehicle-control for 2 h or with ATP for 0.5, 1, or 2 h, and collected at the endpoint. Cells were homogenized in a Tris-based lysis buffer (150 mM NaCl, 1.0% IGEPAL CA-630, 0.5% sodium deoxycholate, 0.1% SDS, 50 mM Tris, pH 8.0), supplemented with protease

inhibitor cocktail at 1 μL/10^6 cells [stock: 0.104 mM 4-(2-aminoethyl) benzenesulfoyl fluoride hydrochloride, 0.08 mM aprotinin, 4 mM bestatin hydrochloride, 1.4 mM n-(trans-epoxysuccinyl)-L-leucine 4-guanidinobutylamide, 2 mM leupeptin hemisulfate salt, 1.5 mM pepstatin A; Sigma-Aldrich], PMSF at 2 μL/10^6 cells, sodium orthovanadate at 2 μL/10^6 cells, and 1 mM EDTA and incubated on ice for 30 min. Homogenates were then passed through a 27-gauge needle three times and centrifuged at 17500 *g* for 15 min. Supernatant was collected as whole cell lysate. Samples were boiled (100°C) for 20 min in SDS-PAGE loading dye under reducing conditions (dithiothreitol and β-mercaptoethanol). Western analysis was performed as previously described (Wicki-Stordeur et al. 2012; Wicki-Stordeur & Swayne 2013; Swayne et al. 2010). Briefly, gels were transferred onto 0.2 μm pore-size polyvinyldene fluoride (PVDF) membrane for 1 h at 85 V, or 16-18 h at 22 V. Ponceau S total protein staining was used to confirm successful transfer of gel contents onto membrane. Blocking and antibody incubations (primary: room temperature for 1 h or 4°C for 16-18 h; secondary: room temperature for 1 h) were performed in blocking buffer (5% skim milk powder in PBS-T; 10 mM Na_2HPO4, 1.25 mM NaH_2PO4, 2.7 mM KCl, 137 mM NaCl, 0.1% Tween 20).

2.3.2 Reverse transcriptase-polymerase chain reaction (RT-PCR)

Total RNA was isolated from N2a cells and first-strand synthesis (Superscript II; according to the manufacturer's protocol; Life Technologies) was performed by Rose Swansburg followed by PCR using cycling parameters of 95 °C for 5 min, 34 cycles of 95 °C for 30 sec, 56 °C for 30 sec, and 72 °C for 1 min, and a final step at 72 °C for 7

min for the following primers: 5'-AGAAGGGCGGGGTGGTTGGT-3', 5'-AGGCCCCATGTCCTCCGCAT-3' defining a 368- base pair (bp) P2X1R amplicon, accession number [GenBank: NM_008771.3], 5'-ATCGTGGTGCGGAATCGGCG-3', 5'- TCCCATCCTCCACCGGGCAC-3' defining a 445-bp P2X2R amplicon [GenBank: NM_153400.4], 5'-AGCCCGGGATTGGAGACCCC-3', 5'-TCAATGGCCGTGTCCCGCAC-3' defining a 460-bp P2X3R amplicon [GenBank: NM_145526.2], 5'-CTTGGCCTTCATTGCGGGTA-3', 5'-GGAAGGCAAGACCATTAGGCA-3' defining a 253-bp P2X4R amplicon [GenBank: NM_011026.3], 5'-CGGTGGCCAAAGTGAGCTGGAG-3', 5'-CACGCTCAGCACAGATGCCCT-3' defining a 388-bp P2X5R amplicon [GenBank: NM_033321.3], 5'- GGCCTCCAGTTCAGCTGCGG-3', 5'-CCACGTCCCACAGCCGGTTC-3' defining a 368-bp P2X6R amplicon [GenBank: NM_011028.2], 5'- AACAGAGCGAGCCTGTCGCC-3', 5'-TGACCTTGGTGTGCACGGAGC-3' defining a 216-bp P2X7R amplicon [GenBank: NM_011027.3], and 5-TGGTGCTGAGTATGTCGTGGAGT-3', 5'-AGTCTTCTGAGTGGCAGTGATGG-3' defining a 292 bp glyceraldehyde-3-phosphate dehydrogenase (GAPDH) amplicon, accession number [GenBank: NM_008084.2]. No bands were detected for P2X5R and P2X6R over an annealing temperature gradient between 56 °C and 67 °C.

2.3.3 GST-fusion protein expression and purification

Panx1 EL1 (mouse Panx1 aa 56-107; Penuela et al. 2009) and Panx1 CT (mouse Panx1 aa 298-426; Penuela et al. 2009) were cloned into in the pGEX-4T-3 plasmid (Amersham

Biosciences) and transformed into BL21 *E. coli* (New England Biolabs). Protein expression was induced using IPTG (200 μM) for 4 h at 37°C with shaking. Cultures were pelleted and resuspended in 10 mM PBS (150 mM NaCl, 9.1 mM dibasic sodium phosphate, 1.7 mM monobasic sodium phosphate) supplemented with 2 mM EDTA, 0.05% Tween 20, 0.1% β-mercaptoethanol and mechanically lysed using a French pressure cell press.

GST fusion proteins were purified using glutathione-sepharose 4B beads (GE Healthcare) in 10 mM PBS for 18 h at 4°C. GST-bound beads were then washed with PBS-RIPA buffer [10 mM PBS, 0.1% sodium dodecyl sulphate (SDS), 0.5% sodium deoxycholate, 1% IGEPAL CA-630], PBS-RIPA buffer without SDS, followed by 10 mM PBS. Glutathione-bound GST-fusion proteins were eluted in serial incubations with buffer (50 mM Tris-HCl, pH 8) containing reduced glutathione (10 mM; Sigma). Eluted samples underwent buffer exchange into 10 mM PBS using 3K Amicon tubes (EMD Millipore).

2.3.4 Pull-down assays

Cells were lysed in 1.0% IGEPAL in TBS (50 mM Tris, pH 8.0, 150 mM NaCl, 1.0% IGEPAL CA-630), supplemented with protease inhibitor cocktail at 1 μL/10^6 cells (Sigma), PMSF at 2 μL/10^6 cells, sodium orthovanadate at 2 μL/10^6 cells, and 1 mM EDTA and incubated on ice for 30 min. Lysates were passed through 27 gauge needle, and centrifuged at 17,500 x g for 20 min. Supernatant was collected as whole cell lysate (input). Equivalent amounts of bead-immobilized GST or GST-Panx1^{EL1} were incubated with 2.5 mg of lysate (30 min; 4 °C with inversion). Beads were washed once in TBS-

RIPA (50 mM Tris, pH 8.0, 150 mM NaCl, 1.0% IGEPAL CA-630, 0.1% sodium dodecyl sulphate, 0.5% sodium deoxycholate), twice in 1% IGEPAL in TBS (4°C with inversion), then briefly three times in TBS at room temperature. Samples were then eluted from beads by boiling (100°C) for 20 min in SDS-PAGE loading dye under reducing conditions (dithiothreitol and β-mercaptoethanol) and analyzed by Western blot, as previously described (Wicki-Stordeur et al. 2012; Wicki-Stordeur & Swayne 2013; Swayne et al. 2010). Pull-down assays were repeated in triplicate.

2.3.5 Membrane lipid strip interaction assays

Membrane Lipid Strips (Echelon Biosciences; hydrophobic membrane spotted with 15 different membrane lipids [GT – glyceryl tripalmitate, DAG – diacylglycerol, PA – phosphatidic acid, PS – phosphatidylserine, PE – phosphatidylethanolamine, PC – phosphatidylcholine, PG – phosphatidylglycerol, CL – cardiolipin, PI – phosphatidylinositol, PI(4)P – phosphatidylinositol 4-phosphate, PI(4,5)P_2 – phosphatidylinositol 4,5-bisphosphate, PI(3,4,5)P_3 – phosphatidylinositol 3,4,5-triphosphate, CHOL – cholesterol, SM – sphingomyelin, SULF – 3-sulfogalactosylceramide] and a blank [xylene cyanol FF]) were blocked for 1 h in blocking buffer (3% BSA in PBS-T). Strips were then transferred to blocking buffer containing purified protein of interest: PI(4,5)P_2 Grip (1 μg/mL; positive control from Echelon Biosciences), GST (5 μg/mL), or GST-fused Panx1 C-terminus (GST-Panx1^{CT}; 5 μg/mL) for 1 h, then washed three times in PBS-T and incubated for an additional hour in blocking buffer with primary antibody. Strips were again washed in PBS-T three times

then incubated in corresponding HRP-conjugated secondary for 1 h. All incubations were performed at room temperature with gentle agitation.

2.4 Statistical analysis

Western blot densitometry was quantified using ImageJ 1.45 [Chapter 3 (Schindelin et al. 2015)) or FIJI (Chapters 4 and 5 (Schindelin et al. 2012)]. Significance was determined using unpaired Student's *t* tests or a one-way analysis of variance (ANOVA) with Dunnett's *post hoc*. Results from live cell imaging experiments were analysed using a two-way ANOVA for time and treatment. Fixed cell confocal microscopy results were analysed using a one-way ANOVA, two-way-ANOVA or a Student's t test, as indicated. Data analysed using ANOVA were subsequently subjected to a Dunnett's post-hoc test, a multiple comparison procedure that compares all treatments to a single control. PLA data (PLA clusters per cell) were analyzed using a one-way ANOVA (with Dunnett's *post-hoc*), two-way ANOVA (with Bonferroni or Dunnett's *post-hoc*, where specified), or Student's t test. A biological replicate was defined as a coverslip obtained from an independent cell passage. All data were presented as mean ± S.E.M. Detailed information about statistical tests is available in the figure legends.

3 ATP modulates Panx1 plasma membrane stability

The data presented here are published in **Boyce AKJ, Kim MS, Wicki-Stordeur LE, Swayne LA (2015) ATP stimulates Pannexin 1 internalization to endosomal compartments. Biochemical Journal 470 (3): 319-330.**

3.1 Overview

Panx1 proteins hexamerize to form ATP-permeable channels in many cells and tissues of vertebrates (reviewed in Penuela et al. 2013). Although functional studies have focused on Panx1 at the cell surface, there was evidence for robust and stable expression of Panx1 in intracellular compartments (Bhalla-Gehi et al. 2010; Cone et al. 2013; Lai et al. 2007; Vanden Abeele et al. 2006). Prior to completing the work described in this chapter, it was unclear whether this population was the consequence of (1) direct diversion from the secretory pathway after the Golgi or (2) endocytosis of mature Panx1 from the cell surface. I postulated that Panx1 internalization to these membranes would require endocytosis through a stimulus that is episodically released. ATP was a potential candidate for this phenomenon as it is constitutively released in episodic bursts via exocytosis and large pore channels (including Panx1) from diverse cell types (Lin et al. 2007; Mishra et al. 2006; reviewed in Pankratov et al. 2006; Praetorius & Leipziger 2009) including N2a cells (Iglesias & Spray 2012). Although predominantly closed under resting conditions, Panx1 channels opened in response to several stimuli including mechanical stretch (Xia et al. 2012; Bao et al. 2004) and proteolytic cleavage of the C-

terminus (Sandilos et al. 2012; Chekeni et al. 2010, reviewed in Chiu et al. 2014) as well as crosstalk with other receptors including P2X and P2Y receptors (Locovei, Wang, et al. 2006; Pelegrin & Surprenant 2006), NMDARs (Weilinger et al. 2012; Weilinger et al. 2016), α-adrenergic receptors (Billaud et al. 2011; Billaud et al. 2015), and TNF-α receptors (Lohman et al. 2015, reviewed in Baroja-Mazo et al. 2013; Isakson & Thompson 2014). Notably, Panx1 functionally interacted in a positive feedback loop with several purinergic receptors. ATP-stimulated P2X and P2Y receptors trigger Panx1-mediated ATP release (Locovei, Wang, et al. 2006; Iglesias et al. 2008; Pelegrin & Surprenant 2006). ATP, in turn, acted as an autocrine/paracrine signalling molecule to activate additional purinergic receptors (reviewed in Baroja-Mazo et al. 2013). Activation of these positive feedback loops would theoretically promote instability by opening the large pore of Panx1 more frequently; however this was not the case in several early studies of Panx1 function, where purinergic activation of Panx1 was transient, suggesting the presence of negative feedback (Locovei et al. 2007; Locovei et al. 2006). The first evidence of a negative feedback mechanism was that elevated extracellular ATP inhibited Panx1 currents and Panx1-mediated dye flux in both oocytes and mammalian cells (Ma et al. 2009; Qiu et al. 2012; Qiu & Dahl 2009). This could have occurred through two putative mechanisms: either by channel inactivation/pore block, by promoting internalization of Panx1 from the cell surface, or through a combination of the two mechanisms. Considering the presence of uncharacterized intracellular Panx1 in combination with an unknown mechanism behind ATP-mediated negative feedback, in this chapter **I investigated the hypothesis that elevating extracellular ATP promotes Panx1 endocytosis to intracellular compartments.**

I used stable expression of Panx1-EGFP in N2a cells as the model system in my study for the following reasons. First, N2a cells express a complement of P2X and P2Y receptors (Gomez-Villafuertes et al. 2009; Masgrau et al. 2009; Chen & Chen 1997), with the primary functional P2X receptor being P2X7R (Gomez-Villafuertes et al., 2009), and are sensitive to Panx1-dependent paracrine signalling (Iglesias & Spray 2012), allowing for the study of the purinergic feedback loop. Second, I was interested in studying Panx1 in neural cells, as Panx1 is enriched in this system at both the transcript and protein level (Baranova et al. 2004; Penuela et al. 2007, reviewed in Boyce et al. 2017). Here, N2a cells provided an excellent model for studying subcellular localization and trafficking due to their relatively large cytoplasm to nucleus ratio relative to primary neural cell cultures. Finally, selection of a clonal N2a population stably expressing Panx1-EGFP allowed us to dynamically track the trafficking dynamics without overwhelming trafficking machinery. Panx1-EGFP demonstrated similar cell surface and intracellular distribution to endogenous Panx1 in N2a cells (see Methods, Figure 2.1) and forms a functional channel (Lai et al. 2007; Bhalla-Gehi et al. 2010; Wicki-Stordeur et al. 2013), thus it was suitable for use in studying Panx1 trafficking.

In this chapter, I determined that ATP stimulated Panx1 endocytosis in a dose- and time-dependent manner at concentrations of ≥200 μM. Based on both imaging and biochemistry results, Panx1 internalization occurred specifically in response to ATP relative to other stimuli that modulate Panx1 activity or general cellular. Internalization was dependent on P2X receptors, based on nucleotide selectivity, and was sensitive to the selective P2X7R inhibitor A438079. Interestingly, mutation of a residue in the first extracellular loop (EL1) of Panx1 led to abrogation of ATP-evoked internalization. Once

internalized, Panx1 transited through the early endosome (peak at 30 min post-stimulation) and was eventually enriched in slow recycling endosomal compartments (between 1-2 h post-stimulation).

3.2 ATP stimulates dose-dependent Panx1 internalization

I tracked the retrograde movement of Panx1 in response to ATP in living N2a cells using a Panx1-EGFP stable line (Panx1-EGFP N2a) that we established to create a homogeneous cell population with Panx1-EGFP expression and distribution similar to endogenous Panx1 (Figure 2.1). Pre-treatment with CHX, a protein synthesis inhibitor that disrupted the translocation event during translation (Schneider-Poetsch et al. 2010), eliminated the confounding fluorescence signal from *de novo* synthesized Panx1-EGFP transiting through the secretory pathway and allowed imaging of mature Panx1 specifically (Figure 3.1A).

I imaged trafficking dynamics of Panx1-EGFP using live cell confocal microscopy after ATP application (25 min; 0, 100, 200, 500 μM; Figure 3.1B). The kinetics of Panx1 trafficking can be easily observed in Movie 3.1**,** where Panx1-EGFP signal overlapped with TRITC-wheat-germ agglutinin (WGA) of the labelled plasma membrane, producing yellow vesicles as ATP (500 μM) evoked internalization of cell surface Panx1 into intracellular compartments. To quantify intracellular Panx1, a 1 μm trace was drawn inside the WGA-labelled plasma membrane and the average EGFP fluorescence intensity per pixel of the encapsulated area was computed (Figure 3.1Bii). ATP stimulated dose (≥200 μM)- and time (≥15 min)-dependent Panx1 endocytosis (increase in intracellular Panx1; Figure 3.1B). ATP treatment had no effect on cell

morphology or viability. Panx1 internalization was not significantly increased by vehicle or 100 μM ATP treatment.

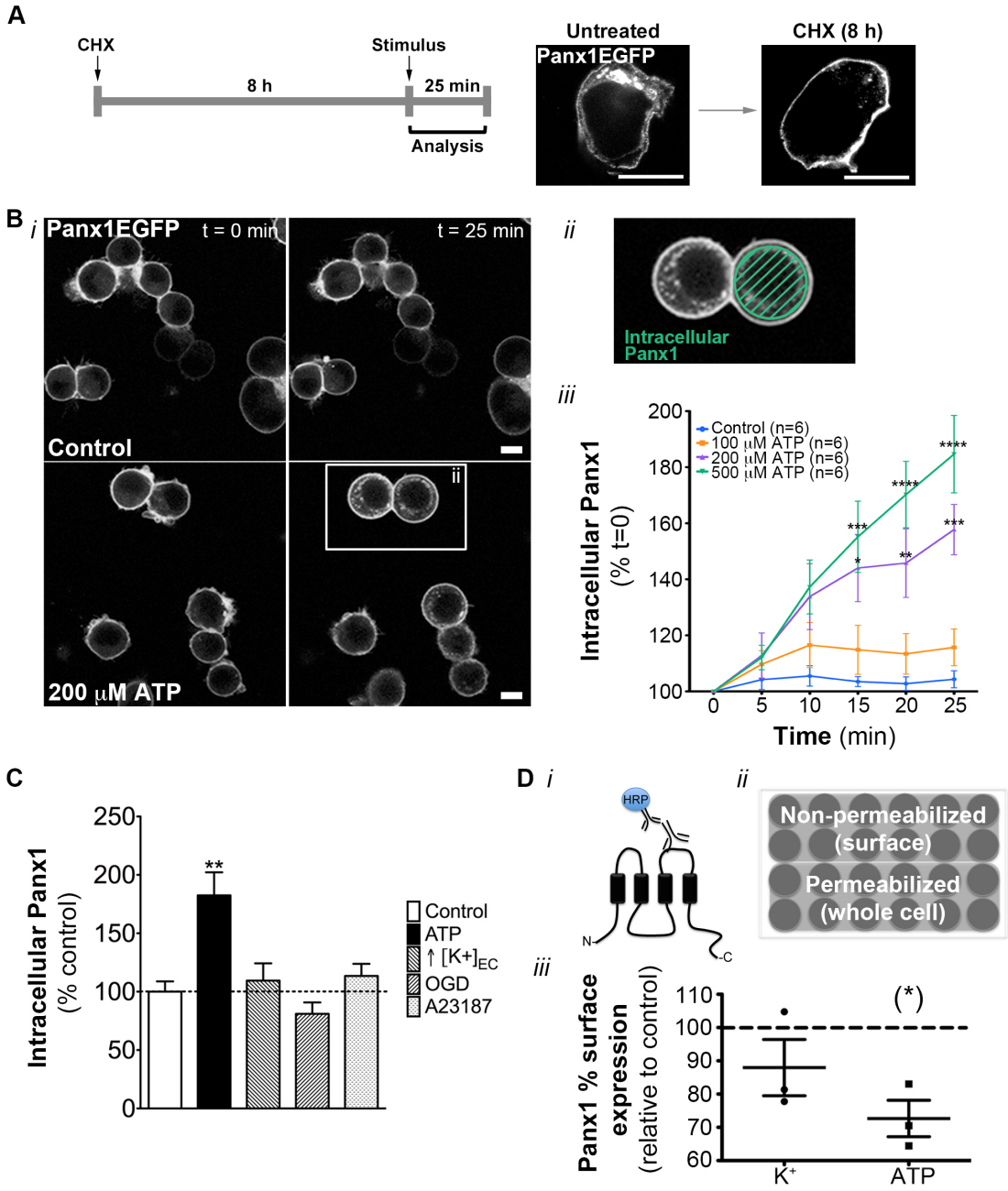

Figure 3.1 Elevated extracellular ATP stimulates internalization of Panx1. (A) Panx1-EGFP N2a cells were treated for 8 h with CHX (20 μg/mL) to observe the mature population of Panx1 and then stimulated with the indicated concentrations of ATP. (B) Representative confocal

micrographs from the 0- and 25-min time points (i) and depiction of the region of analysis from the insets (ii, digital zoom). Intracellular Panx1 fluorescence intensity expressed as a percentage of time zero at each 5-min interval (iii). $N = 6$, two-way ANOVA [time: $F(4, 20) = 26.7$; treatment: $F(3, 20) = 8.35$; interaction: $F(12, 20) = 9.16$] with Dunnett's *post-hoc* (*p<0.05, **p<0.01, ***p<0.001, ****p<0.0001). (C) Effects of 200 μM ATP, 30 mM K^+, 10 μM Ca^{2+} ionophore A23187 and chemical OGD (100 μM potassium cyanide and 1 μg/mL oligomycin) relative to vehicle control on intracellular Panx1 at 30 min post-stimulus. $N = 4$; one-way ANOVA with Dunnett's *post-hoc* (**p<0.01). Scale bars, 10 μm. (D) Cell-surface luminometry utilizes a primary antibody to an extracellular epitope (Panx1-EL2; i) to determine the surface expression in non-permeabilized cells as a percentage of the whole cell expression in permeabilized cells, as depicted in (ii). (iii) Surface expression of Panx1 transiently expressed in HEK293T cells is decreased by ATP (200 μM), but not by elevated K^+ concentration (10 mM). $N = 3$, one sample *t* test compared to hypothetical value of 100% (*p<0.05).

Movie 3.1 (see attached). Panx1 internalizes in response to exogenous ATP. N2a cells stably expressing Panx1-EGFP treated with 500 μM ATP at time zero. Plasma membrane, vesicles, and Golgi are labelled with WGA-TRITC (red). Internalized Panx1-EGFP-positive vesicles appear yellow. Cells were imaged every minute over a 25-minute span. Scale bar, 10 μm.

To investigate the specificity of Panx1 internalization to an ATP stimulus, I compared ATP stimulation for 30 min to equivalent duration of elevated extracellular K^+, chemical OGD (Van Rossum 1976), and Ca^{2+} ionophore (A23187) treatment, which induces an increase in intracellular Ca^{2+} (Dedkova et al. 2000; Figure 1C). Each of these stimuli modulated Panx1 activity in previous studies (Locovei et al. 2006; Silverman et al. 2009; Thompson et al. 2006). Following these treatments (30 min), the cells were fixed and imaged using confocal microscopy to measure intracellular Panx1. As expected from the live cell assay, 200 μM ATP evoked a significant increase in intracellular Panx1 (~180% of control), while K^+ (10 mM), chemical OGD, and A23187 did not significantly alter intracellular Panx1 levels over this same time course. Although in a previous study

(Boyce et al. 2014), I had suggested that these generalized stimuli weakly influenced Panx1 trafficking dynamics or plasma membrane expression, the lack of elevated intracellular Panx1 suggests that these stimuli had no persistent effect on the internal Panx1 pool.

My imaging data was supported by a biochemical cell surface luminometry assay (Dubel et al. 2004) in Panx1-transfected HEK293T cells (Figure 3.1D). Cell surface luminometry assays require a primary antibody with an epitope to the exofacial surface of the protein of interest. Here, an antibody to the second extracellular loop of Panx1 (EL2 - Penuela et al. 2009; Figure 3.1Di) was used. Enhanced chemiluminescence (ECL) for target protein abundance was quantified using a plate reader from unpermeabilized cells (channels at the surface membrane) normalized to the ECL signal from permeabilized cells (channels on all cell membranes; see Figure 3.1Dii). This permitted direct comparison of cell surface Panx1 between different treatment groups. I treated Panx1-expressing HEK293T cells with K^+ (10 mM), ATP (200 μM), or vehicle (water). Elevated extracellular ATP significantly reduced Panx1 surface expression relative to vehicle, while K^+ addition had no observable effect.

3.3 ATP-evoked internalization is dependent on P2XRs

I next sought to determine whether ATP or its metabolites were responsible for stimulating Panx1 endocytosis. This was particularly critical as numerous studies have described both functional and physical interactions between Panx1 and various P2 receptors in a wide variety of cell types (Pelegrin & Surprenant 2006; Iglesias et al. 2008;

Kanjanamekanant et al. 2014; Shoji et al. 2014; Locovei et al. 2006; Maslieieva & Thompson 2014). Investigation of the nucleotide dependence of internalization informed on the possible involvement of a specific subtype of purinergic receptors (i.e. P2X or P2Y; reviewed in Burnstock 2011). P2X and P2Y receptors demonstrated differential ATP metabolite and analogue sensitivity (see Khakh et al. 2001; Von Kügelgen & Hoffmann 2016); as a result of this differential sensitivity, screening for nucleotide dependency provided insight into the potential involvement of specific receptor families and isoforms.

Panx1-EGFP N2a cells were treated with ATP and several of its metabolites and synthetic analogues (ATP, ATPγS, ADPβS, BzATP, UTP) then fixed 30 min after stimulation (Figure 3.2). Intracellular Panx1, relative to vehicle-treated cells, was then assessed using confocal microscopy. ATP (500 μM) evoked the most robust and significant increase in intracellular Panx1 (~280% of control; Figure 3.2A); ATPγS, a non-hydrolyzable ATP analogue (500 μM; selective for primarily P2XRs), also evoked a significant yet lesser intracellular Panx1 accumulation (~150% of control). ADPβS, a non-hydrolyzable ADP analogue (500 μM; selective for primarily P2YRs), did not evoke a significant intracellular Panx1 accumulation relative to vehicle-treated cells. Relative to vehicle, BzATP (selective for some P2XR; Figure 3.2B), UTP (selective for P2YR) did not significantly increase intracellular Panx1 accumulation.

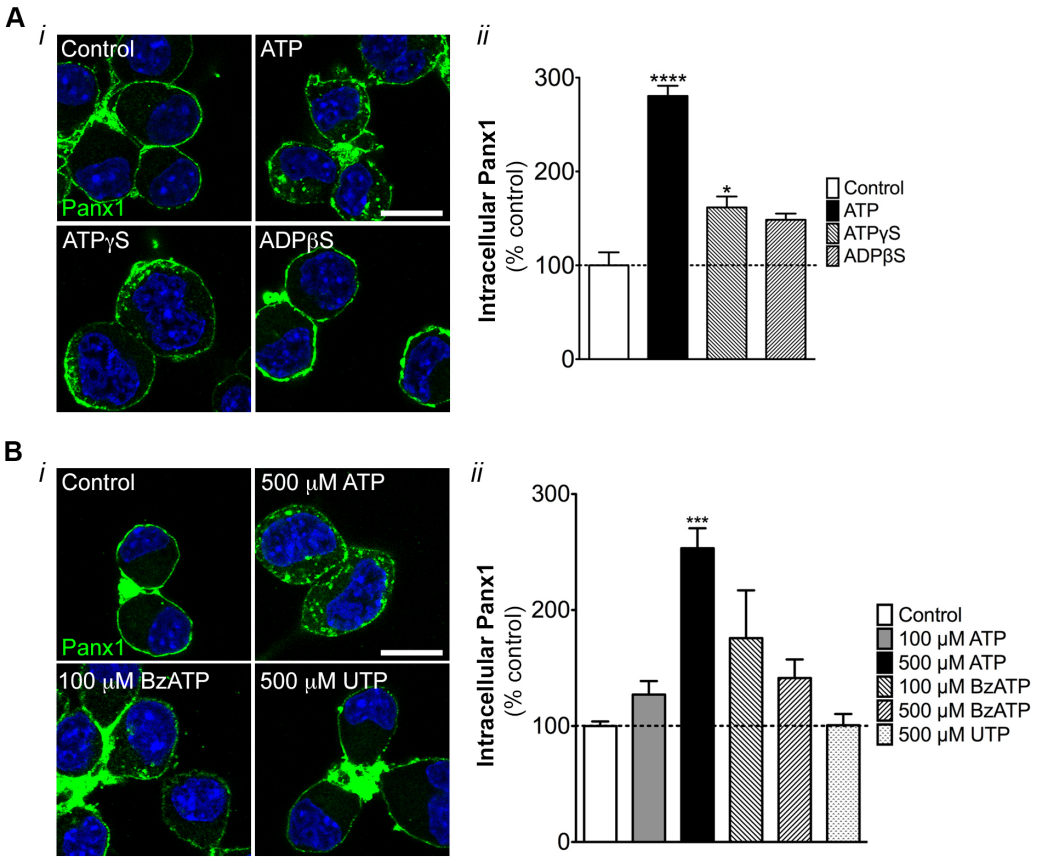

Figure 3.2 Panx1 is selectively internalized by P2X receptor agonists. (A) Confocal micrographs (i) of Panx1-EGFP N2a cells following stimulation with vehicle control or ATP, ATPγS, or ADPβS (each 500 μM, 30 min). (ii) Intracellular Panx1 was quantified relative to vehicle control. $N = 4$, one-way ANOVA with Dunnett's *post-hoc* (****$p<0.0001$). (B) Confocal micrographs (i) of Panx1-EGFP N2a cells 30 min following stimulation with vehicle control, 500 μM ATP, 100 μM BzATP or 500 μM UTP. (ii) Intracellular Panx1 was quantified in cells that had been stimulated with 100 or 500 μM ATP, 100 or 500 μM BzATP, or 500 μM UTP relative to vehicle control. $N = 4$, one-way ANOVA with Dunnett's *post-hoc* (***$p<0.001$). Hoechst (blue) was used as a nuclear counterstain. Scale bars,10 μm.

Both ADPβS and UTP that act primarily on P2Y receptors (von Kugelgen 2006; Jacobson et al. 2012; Weisman et al. 2012) had no effect on intracellular Panx1 accumulation, which indicated that P2YRs were not involved in triggering Panx1

internalization. Prior to my study, Panx1 activation via P2YRs involved P2Y-evoked increase in intracellular Ca^{2+} (Locovei et al. 2006), which was mimicked by treatment with the Ca^{2+} ionophore (A23187). A23187 facilitates transport of Ca^{2+} ions across the plasma membrane and triggers subsequent increases in intracellular Ca^{2+} through a number of mechanisms including activation of some plasma membrane Ca^{2+} channels and phospholipase C-dependent release of intracellular Ca^{2+} stores (Dedkova et al. 2000). A23187 (Figure 3.1C) had no effect on internalization, further supporting the omission of P2YR signalling upstream of Panx1 internalization. Taken together, these findings suggested that P2X receptors were responsible for Panx1 internalization.

3.4 Selective inhibition of P2X7R disrupts Panx1 internalization

Although the nucleotide data ruled out P2YRs, they were inconclusive with regards to the P2XR subtype responsible for triggering Panx1 internalization. Of the P2XR family, N2a cells expressed P2X1R, P2X2R, P2X3R, P2X4R and P2X7Rs at the transcript level (Figure 3.3A; RT-PCR performed by Rose Swansburg). Of those, the primary functional isoform is P2X7R (Gomez-Villafuertes et al. 2009). I had suspected that P2X7Rs are involved in regulating Panx1 internalization as the dose threshold required to initiate internalization was in the range for activation of P2X7R (EC_{50}>100 μM; Surprenant et al. 1996), yet well above the other P2X family members (EC_{50}<10 μM, reviewed in North & Surprenant 2000). Consequently, we made use of the selective P2X7R blocker A438079 (McGaraughty et al. 2007; Nelson et al. 2006) to narrow down

the P2XR subtype. Selective P2X7R inhibition abrogated ATP-evoked internalization of Panx1 (Figure 3.3B), which implicated P2X7Rs upstream of Panx1 endocytosis.

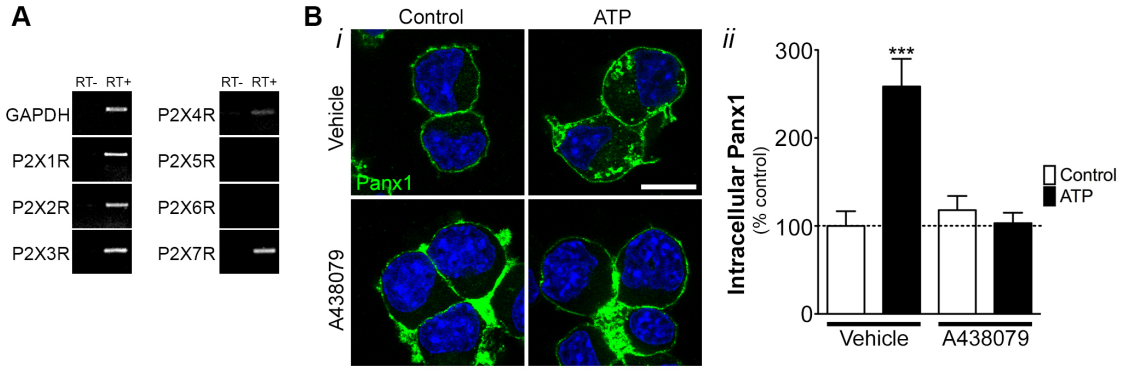

Figure 3.3 Selective P2X7R inhibition disrupts ATP-evoked Panx1 internalization. (A) N2a cells express P2X1-4R and P2X7R transcripts, as indicated by RT-PCR. GAPDH was used as a loading control (RT-PCR performed by Rose Swansburg). (B) Confocal micrographs (i) of Panx1-EGFP N2a cells that were pre-treated for 1 h prior to 500 μM ATP or control treatment with 100 μM A438079 and fixed at 30 min post-stimulus. (ii) Intracellular Panx1 was quantified relative to vehicle control. $N = 4$, one-way ANOVA with Dunnett's *post-hoc* (***$p<0.001$). Hoechst (blue) was used as a nuclear counterstain. Scale bars, 10 μm.

3.5 Alanine substitution of W74 in the Panx1 EL1 abrogates ATP-evoked internalization

Like P2 receptors, ATP-sensitive residues within both of the Panx1 ectodomains have also been identified (Qiu et al. 2012; Qiu & Dahl 2009, reviewed in Dubyak 2009). Qiu and Dahl (Qiu et al. 2012; Qiu & Dahl 2009) discovered these residues using alanine-scanning mutagenesis of mouse Panx1 while investigating ATP-mediated inhibition of Panx1 currents (≥200 μM). Several alanine-substitutions of extracellular loop residues led to >90% loss of ATP-mediated inhibition (W74, S237, S240, I247, L266; Qiu et al. 2012). Only one of these residues in existed in the EL1 of Panx1, a

tryptophan at position 74 (W74), while the others were present in the second extracellular loop (S237, S240, I247, L266). Michelle Kim created an EGFP-tagged alanine substitution mutant construct for W74, Panx1W74A-EGFP, and I generated a stable N2a cell line expressing Panx1W74A-EGFP to test the effect of W74A on Panx1 internalization relative to Panx1-EGFP N2a cells (Figure 3.4). Although Panx1W74A demonstrated equivalent cell surface expression, remarkably the ATP-mediated internalization was dramatically dampened in Panx1W74A-EGFP N2a cells to a non-significant level (Figure 3.4). This suggested that the Panx1 EL1 was also pivotal in regulating Panx1 internalization.

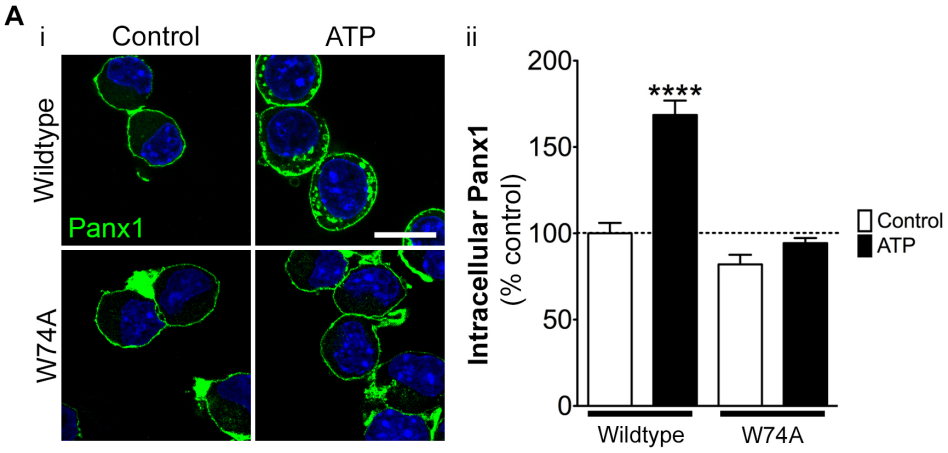

Figure 3.4 Panx1 internalization is impaired in Panx1W74A-expressing cells. (**A**) The extent of intracellular Panx1 is demonstrated in confocal micrographs (**i**) of N2a cells stably expressing Panx1-EGFP (top panels) or mutant Panx1W74A-EGFP (bottom panels) stimulated with vehicle control (left panels) or 500 μM ATP (right panels) for 30 min, quantified relative to control in (**ii**). $N = 4$, one-way ANOVA with Dunnett's *post-hoc* (****$p<0.0001$). Hoechst (blue) was used as a nuclear counterstain. Scale bars, 10 μm.

3.6 ATP triggers internalization of Panx1 to recycling endosomes

Following endocytosis, the initial compartment that internalized transmembrane proteins encounter is the early endosome (for which EEA1 is an established marker), where they are sorted for recycling or degradation (reviewed in Jovic et al. 2010; Figure 3.5A). In the degradation pathway, endosomal compartments become increasingly acidic from the Rab7-positive late endosome (Vitelli et al. 1997), through the M6PR-positive endolysosome (Ghosh et al. 2003; Brown et al. 1986) and finally to the Lamp1-positive lysosome (Eskelinen 2006). Conversely, internalized proteins destined for recycling to the cell surface are diverted to fast-recycling Rab4-positive (Sonnichsen et al. 2000) or slow-recycling Rab14-positive (Linford et al. 2012) and/or Rab11-positive (Ullrich et al. 1996) endosomes. Under control conditions and when present, intracellular Panx1 co-distributed predominantly with markers for the early endosome, late endosome, endolysosome and the lysosome, suggesting that it was primarily targeted to the degradation pathway (Figure 3.5B). To determine the pathway that internalized Panx1 transits through, I tracked the intracellular destination of Panx1 in a temporal manner (0.5, 1 and 2 h) after addition of ATP (500 μM) by comparing relative Pearson's correlation coefficient between Panx1 and subcellular compartment-specific markers (Figure 3.5A).

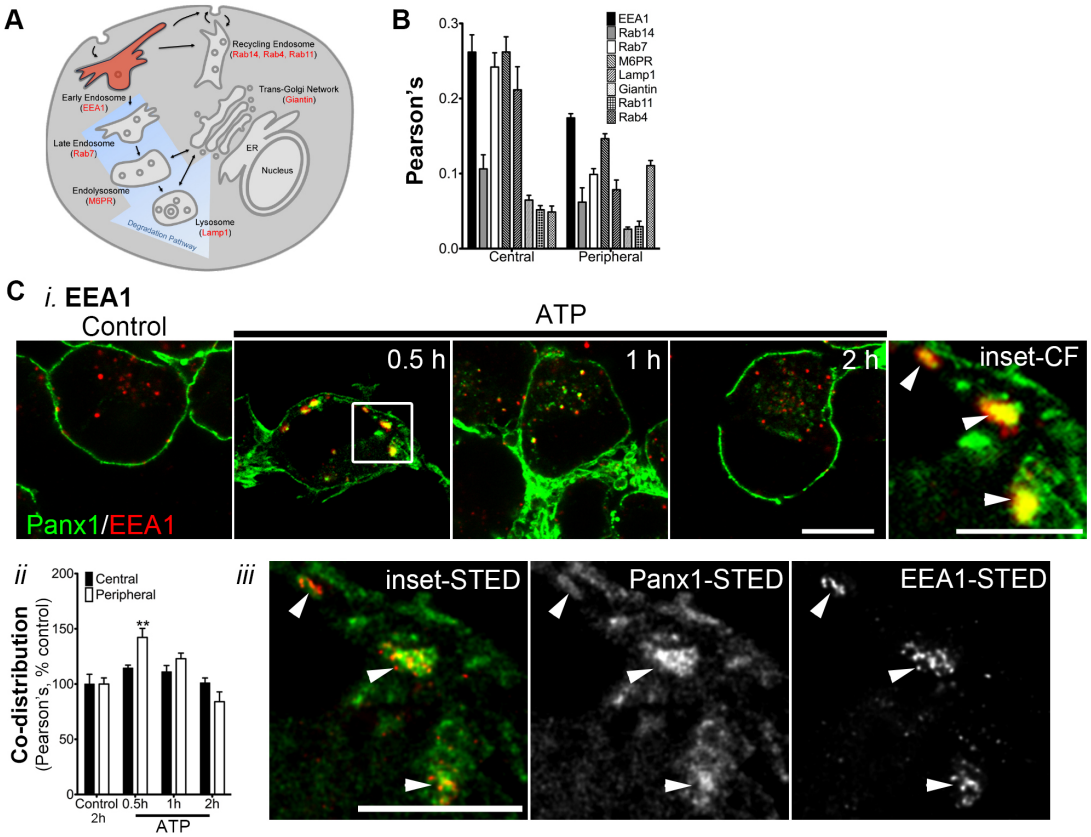

Figure 3.5 ATP triggers transient co-distribution of Panx1 and markers for the early endosome. (A) Diagram of subcellular compartment specific markers highlighting the early endosome and the specific antibody marker used (EEA1; see part C). (B) Pearson's correlation coefficients for Panx1-EGFP and the markers for subcellular compartments in N2a cells stably expressing Panx1-EGFP under control conditions (2 h vehicle) in the central and peripheral regions (see 'Methods'). (C) Confocal micrographs (i) of Panx1-EGFP N2a cells demonstrate Panx1 (green) distribution relative to an early endosome marker (C; EEA1; red) stimulated with ATP (500 μM) for 0.5, 1, and 2 h relative to vehicle control-treated cells (2 h). Panx1 co-distribution with compartment-specific markers was quantified in the central region and peripheral region (ii; see 'Methods'). $N = 4$ per treatment group; central and peripheral regions each analyzed independently with one-way ANOVA and Dunnett's *post-hoc,* **$p < 0.01$. (iii) Representative STED confocal images of selected regions of interest from coverslips used in (ii) obtained using a Leica SP8 STED microscope to confirm localization of Panx1 and EEA1 to common compartments with greater resolution. Hoechst (blue) was used as a nuclear counterstain. Scale bars, 10 μm. Inset scale bars, 5 μm.

As endosomes are internalized, they typically migrate from peripheral to a more central distribution (reviewed in Huotari & Helenius 2011). Therefore, I demarcated a 1 μm region of analysis, 'peripheral', surrounding the intracellular region (defined in Figure 3.1). Based on the resolution limits of traditional confocal microscopy, I expected the 'peripheral' region would include Panx1 distributed to (1) the plasma membrane, (2) directly adjacent to the plasma membrane (either to be inserted or recently internalized) and (3) in early endosomes adjacent to the plasma membrane. I redefined the previously named 'intracellular' region as 'central' from this point onward. Prior to beginning these experiments, I predicted that internalized Panx1 might codistribute initially with peripheral early endosomes in our first post-stimulation time point (0.5 h). This would have been overlooked without including the region of analysis at the cellular periphery, where immature early endosomes are predominantly localized. As expected, at the initial time point following ATP stimulation (0.5 h), peripheral Panx1/EEA1 codistribution was significantly enhanced (~150%) relative to vehicle-treated cells (Figure 3.5C). Moreover, localization of Panx1 to EEA1-positive structures was confirmed using higher resolution STED microscopy (Figure 3.5C).

As transmembrane proteins undergoing regulated endocytosis are often targeted for degradation (reviewed in McMahon & Boucrot 2011), I investigated whether Panx1-EGFP expression in whole cell lysates was reduced following ATP stimulation (500 μM; 0.5, 1 and 2 h after treatment) relative to vehicle (0 and 2 h) in the presence of CHX. Panx1 expression (normalized to β-actin) remained unchanged (Figure 3.6A) in both vehicle and ATP-treated cells suggesting negligible Panx1 degradation occurred over this 2 h treatment period. Concurrent with Panx1 enrichment in early endosomes (0.5 h post-

treatment), central Panx1 codistribution with markers for the degradation pathway (Figure 3.6B) was significantly reduced [Rab7 (Figure 3.6C) and Lamp1 by ~50% (Figure 3.6D)], indicating that Panx1 was not targeted to the degradation pathway in response to elevated extracellular ATP. Further, intracellular Panx1 codistribution with markers for endolysosomal compartments never increased above control levels in time points up to 2 h after ATP stimulation (Figure 3.6).

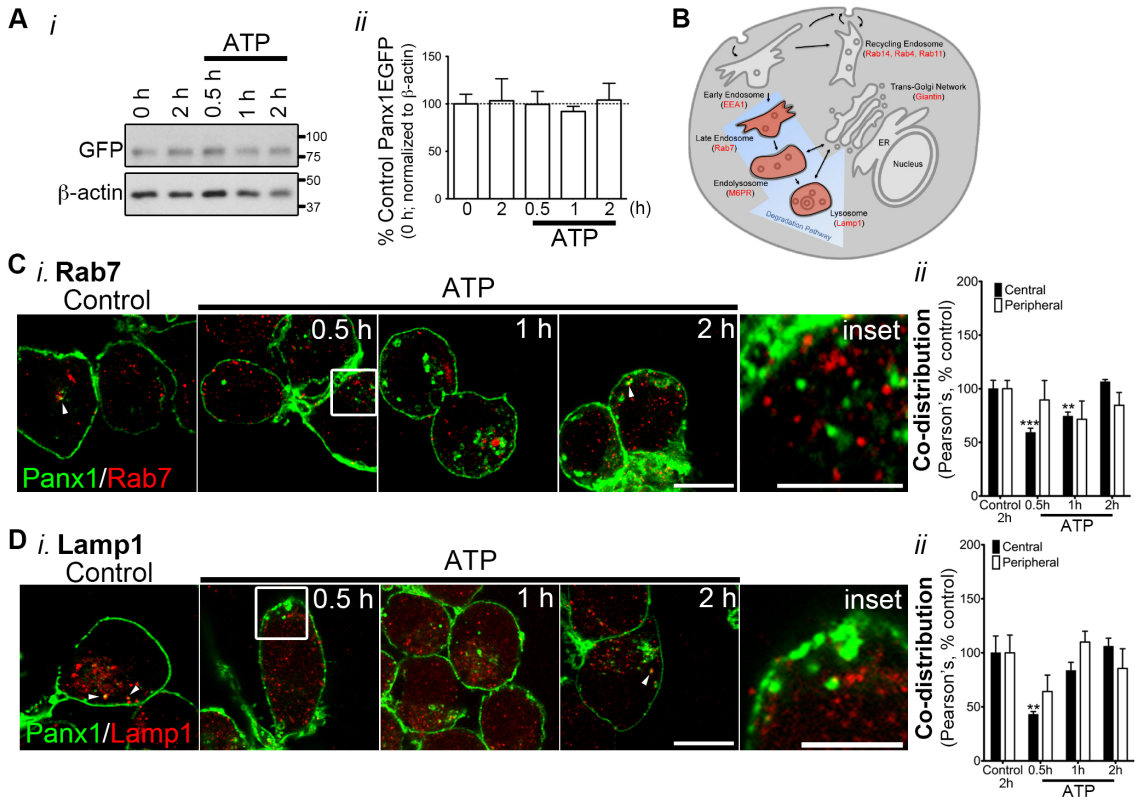

Figure 3.6 ATP transiently reduces distribution of Panx1 with markers for the degradative pathway. (A) Panx1-EGFP expression relative to β-actin assessed by Western blotting was unchanged over a 2 h time course in both 500 μM ATP and vehicle-treated Panx1-EGFP N2a cells (i, Western blot; ii, quantification of three replicates by densitometry). (B) Diagram of subcellular compartment specific markers highlighting the degradative pathway and the specific antibody marker used (Rab7, M6PR, Lamp1; see parts C, D). (C) Representative confocal micrographs (i) of N2a cells stably expressing Panx1-EGFP demonstrate Panx1 (green) distribution relative to the late endosome (C; Rab7; red) and lysosome (D; Lamp1; red)

stimulated with ATP (500 μM) for 0.5, 1, and 2 h relative to vehicle control-treated cells (2 h), central and peripheral co-distribution quantified in (ii). $N = 4$ per treatment group; central and peripheral each analyzed independently with one-way ANOVA with Dunnett's *post-hoc* (**$p<0.01$, ***$p<0.001$). Hoechst (blue) was used as a nuclear counterstain. Scale bars, 10 μm. Inset scale bars, 5 μm.

The alternative pathway for internalized Panx1 was recycling endosomes (Rab14/Rab11/Rab4-positive compartments, Figure 3.7A; reviewed in Bonifacino & Traub 2003; Jovic et al. 2010). During typical transmembrane protein recycling, Rab4 is associated with rapid recycling endosomes (Yudowski et al. 2010), while Rab14 is associated with intermediate compartments (Linford et al. 2012) between sorting endosomes and Rab11-positive slowly recycling endosomes (Ullrich et al. 1996). Interestingly, at later time points after ATP stimulation (1 h and 2 h), central Panx1 and Rab14 codistribution was significantly enhanced (~220% at 1 h; ~240% at 2 h; Figure 3.7B). Panx1 codistribution with Rab14-positive structures was confirmed using STED microscopy (Figure 3.7B). Rab11, another marker for recycling endosomes (Sonnichsen et al. 2000, Figure 3.7C), also exhibited significantly increased latent intracellular Panx1 co-distribution (1 h and 2 h after ATP stimulation). While Panx1-Rab4 codistribution, although increased, was not significant (Figure 3.7D). Considering the time course and marker co-distribution, these data indicated that elevation of extracellular ATP enhanced the targeting of internalized Panx1 to slow recycling endosomes.

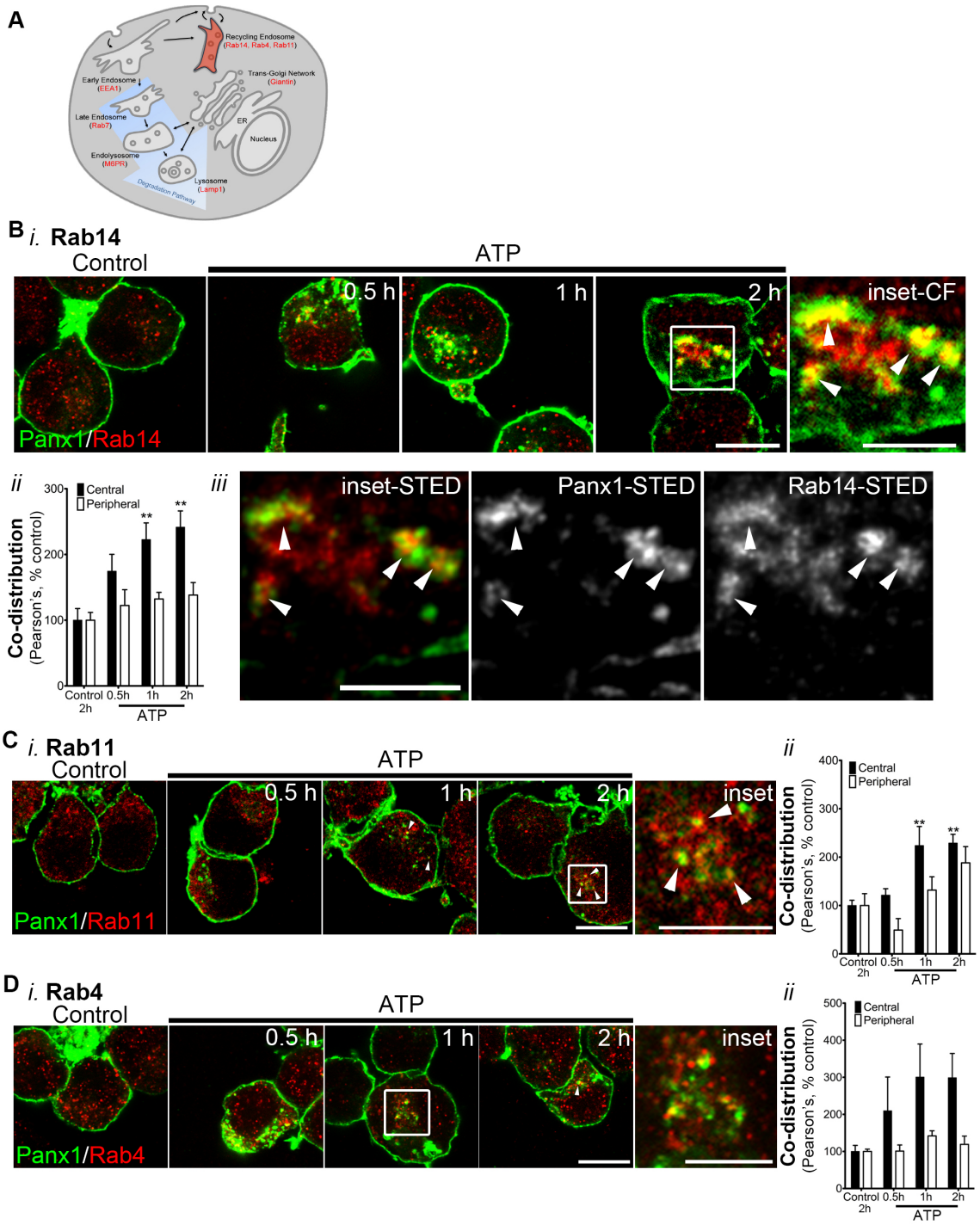

Figure 3.7 ATP triggers latent increase in Panx1 co-distribution with components of the recycling endosome. (A) Diagram of subcellular compartment specific markers highlighting the degradative pathway and the specific antibody marker used (Rab14, Rab11, Rab4, see parts B-D). Representative confocal micrographs (i) of Panx1-EGFP N2a cells demonstrate Panx1 (green) distribution relative to subcellular markers for the recycling endosomes (B - Rab14, C – Rab11, D

– Rab4; red) stimulated with ATP (500 μM) for 0.5, 1, and 2 h relative to vehicle control-treated cells (2 h). Panx1 co-distribution with compartment-specific markers was quantified in the central region and peripheral region (ii; see 'Methods'). (iii) Representative STED confocal images of selected regions of interest from coverslips used in (ii) obtained using a Leica SP8 STED microscope to confirm localization of Panx1 and Rab14 to common compartments with greater resolution. $N = 4$ per treatment group; central and peripheral regions each analyzed independently with one-way ANOVA with Dunnett's *post-hoc,* (**$p<0.01$). Hoechst (blue) was used as a nuclear counterstain. Scale bars, 10 μm. Inset scale bars, 5 μm.

3.7 Discussion

In this chapter, I identified that in response to ATP addition (≥ 200 μM) to the cell culture medium, intracellular Panx1 was increased in N2a cells and co-distributed with markers for recycling endosomes. *Where would physiological ATP levels reach this concentration?* In dimensionally-constrained extracellular environments surrounding vesicular or channel-mediated ATP release, ATP concentrations was up to 500 μM (Pankratov et al. 2006), similar to Ca^{2+} micro- and nano- domains surrounding Ca^{2+}-permeable channels (Tadross et al. 2013; Neher & Almers 1986). For instance, the concentration of ATP in secretory vesicles of mast cells is between 5-50 mM (Bergendorff & Uvnas 1973; Uvnas 1974), while synaptic vesicles are predicted to contain between 150-200 mM ATP (Van Der Kloot 2003). Consequently, in the microdomains adjacent to vesicular release sites or ATP-permeable channels, extracellular ATP could mirror the concentrations used in this chapter. This would be transient, considering ectonucleotidase activity [expressed on the cell surface of most cell types, including N2a cells (Gómez-Villafuertes et al. 2014)]. Thus, ATP-evoked Panx1 internalization could provide an important and novel negative feedback mechanism for regulating ATP release within a range of extracellular concentrations.

My work provides the first evidence of the impact of ATP on Panx1 trafficking and localization. Significant internalization of Panx1 occurred at concentrations well above those required for activation of P2XRs or P2YRs (reviewed in Von Kügelgen & Hoffmann 2016; Khakh et al. 2001). I demonstrated increased sensitivity to P2XR-modulating ligands over P2YR-ligands (Figure 3.2), as Panx1 internalization was not evoked by either UTP or ADPβS. Further, Panx1 internalization was disrupted by A438079 (Figure 3.3), suggesting that it was dependent on P2X7R activation.

Previous studies suggested elevated extracellular ATP also inhibited Panx1 channel activity (Qiu et al. 2012; Qiu & Dahl 2009; Ma et al. 2009; Kurtenbach et al. 2013). Extracellular ATP inhibited mPanx1 in oocytes (≥200 μM; Qiu & Dahl 2009) and in mammalian cells {>200 μM; Ma et al. 2009), as well as zebrafish panx1b (>500 μM; Kurtenbach et al. 2013). Panx1 inhibition shared many similarities with the Panx1 internalization I observed in this chapter, including similar sensitivity to extracellular ATP concentrations (>200-500 μM; Ma et al. 2009; Qiu & Dahl 2009; Kurtenbach et al. 2013), and disruption by the W74A mutation in Panx1 EL1 (Qiu et al. 2012). Like internalization, other nucleotides and nucleoside diphosphates did not inhibit Panx1 in work from the Dahl lab (Qiu & Dahl 2009; Qiu et al. 2012); however, Ma *et al.* observed some inhibitory action of GTP and UTP [although these were less effective than ATP (Ma et al. 2009)]. Panx1 inhibition and internalization demonstrated differential regulation by ATP analogues and ligands for P2XRs. This suggested that internalization and inhibition were regulated by distinct mechanisms with the possibility of shared components. In previous analyses on Panx1 inhibition, the effect of BzATP was variable. It was a more robust inhibitor than ATP of mPanx1 in oocytes (Qiu & Dahl 2009; Qiu et

al. 2012), while it was less effective as an inhibitor in HEK293T cells (Ma et al. 2009). The expression systems used in these studies have evidence of diverse endogenous P2XR expression [*Xenopus* oocytes (Juranka et al. 2001; Paukert et al. 2002), HEK293T cells (Worthington et al. 1999)]. Consequently, ATP-mediated inhibition could have involved interplay with P2X receptors present in these cells. Panx1 inhibition was evoked by both agonists *and* antagonists of P2XRs [including A438079 (Qiu & Dahl 2009)]. Endogenous *Xenopus* P2X7R (xP2X7R) exhibited differential agonist sensitivity and shared <50 % homology with mammalian P2X7Rs (Paukert et al. 2002); consequently, it could be expected that inhibitors of the mammalian isoforms had differential effects on the *Xenopus* receptor. On the other hand, if Panx1 inhibition was triggered by direct interaction with A438079, it is possible that different P2X7R expression levels between oocytes and N2a cells altered the response to A438079 and subsequent Panx1 inhibition or internalization. Finally, the capability of crosstalk between xP2X7R and mammalian Panx1 is unknown and may have impacted on the functionality of P2X7R inhibitors.

The sensitivity of Panx1 internalization to alanine-substitution of W74A in Panx1 EL1 suggested that this domain: (1) directly interacted with ATP to stimulate internalization, (2) interacted with an ATP-sensitive protein to promote internalization and/or (3) allosterically altered Panx1 interactions by changing conformation of the protein. In earlier studies, Qiu *et al.* (2012; 2009) investigated whether ATP-mediated inhibition was the result of direct ATP-binding to mPanx1. Importantly, ATP-mediated inhibition occurred during voltage ramp-evoked Panx1 activation, while internalization was observed in response to ATP alone. The search for an ATP-binding pocket in Panx1 by Qiu *et al.* (2009) began by investigating the amino acid composition of Panx1

ectodomains. Panx1 contains seven basic residues in its extracellular loops; however, cysteine-substitution mutation of only one of the seven reduced the inhibitory effect on channel function at all [R75C (Qiu & Dahl 2009), neighbouring W74 (Figure 3.4)] and only by ~50%. Importantly, ATP-mediated inhibition was unable to be assessed in two of the seven basic residues (K248C, K256C) because mutation resulted in non-functional channels (Qiu & Dahl 2009). The R75 residue was conserved in zebrafish panx1b, yet was absent from panx1a, which was less sensitive to ATP-mediated inhibition, suggesting that this critical residue was evolutionarily conserved (Kurtenbach et al. 2013). Substitution of R75 with basic residues in mPanx1 (Qiu & Dahl 2009) and zebrafish panx1b (Kurtenbach et al. 2013) maintained agonist-mediated inhibition during voltage-mediated activation, while negatively-charged or non-polar substitutions reduced inhibition. This is consistent with a potential interaction between Panx1 and a negatively charged ATP molecule or a negatively charged region of an interaction partner. The structure of the canonical ATP-binding domain, the Walker loop (Walker et al. 1982), a β-strand followed by a glycine-rich loop and an α-helix (reviewed in Hanson & Whiteheart 2005), was not present in EL1. However, the combination of the three basic (R75, K248, K256) residues and these additional non-polar residues that abolished ATP-mediated inhibition could possibly form a non-canonical ATP-sensitive motif. Using alanine-scanning mutagenesis, Qiu *et al.* identified several additional ATP-sensitive residues in the first and second extracellular loops of mPanx1 (>90% loss of inhibition – W74A, S237A, S240A, I247A, and L266A; >50% loss of inhibition S93A, L94A, D241A, and I267A; Qiu et al. 2012). The high concentration of ATP required for inhibition/internalization and the fact that mutation of the key basic residue (R75) only

partially abolished inhibition suggested that if Panx1 did interact with ATP directly, it did so with very low affinity. The hexameric structure of Panx1 channels could allow for an intersubunit ATP-binding pocket, like in P2X receptors (Kawate et al. 2009; Hattori & Gouaux 2012); however, if this was the case, it would require a high resolution crystal structure to resolve. It is also possible that Panx1 EL1 mediates an ATP-dependent interaction with the P2X7R involved in modulating internalization, based on the ATP-Panx1 interaction data from Qiu *et al.* (Qiu & Dahl 2009) and the sensitivity of Panx1 internalization to both P2X7R inhibition and mutation of W74A in Panx1. If true, this phenomenon would be expected in any cell type where P2X7R and Panx1 were co-expressed. The signalling and interaction between P2X7R and Panx1 in response to modulating extracellular ATP concentrations will be further explored in Chapter 4.

In general, the internalization of receptors and membrane proteins can play two possible roles: (1) reduction of signal transduction at the cell surface via transient (via recycling) or terminal (via degradation) processes (Dang & Christie 2012; Avraham & Yarden 2011) or (2) altered signal transduction due to introduction of novel interactions in a subcellular context-specific mechanism (Furthauer & Gonzalez-Gaitan 2009; Thomsen et al. 2016). Together, channel/receptor endocytosis and endosomal trafficking provides an additional layer of complexity to related signalling pathways. Prior to addition of exogenous ATP, I observed intracellular Panx1 primarily localized to the endolysosomal pathway (Figure 3.5). Endolysosomal Panx1 could play a functional role that is unique from its role as an ATP release channel at the cell surface or simply be targeted for degradation in a constitutive process. A unique endolysosomal function was supported by a recent study where probenecid (a commonly-used Panx1 inhibitor

(Silverman et al. 2008)) prevented lysosomal damage during ischemia, suggesting that Panx1 was involved in maintaining lysosomal integrity (Wei et al. 2015). Although there is evidence to suggest that Panx1 is broken down in the lysosome (Gehi et al. 2011), I did not see a significant reduction in Panx1 protein levels over the 2 h observation period in my studies. Previously, an extended period of lysosomal inhibition (20 h) led to Panx1 accumulation (Gehi et al. 2011, albeit in a different cell line). As the half-life of Panx1 was observed to be much greater than the 2 h period of observation (Penuela et al. 2007; Boyce et al. 2015), this discrepancy could be resolved by extending the analysis period for future studies. Together, these data suggested that Panx1 was not targeted for degradation and instead was targeted to recycling endosomal compartments.

There are two diverse pathways for membrane protein recycling: a rapid recycling pathway that occurs on a short time scale (over several minutes) and a slow recycling pathway (over several hours) (Li et al. 2008). In response to elevated extracellular ATP, internalized Panx1 demonstrated significant co-distribution with two markers for recycling endosomes (Rab14, Rab11; Figure 3.7), yet not a third (Rab4; Figure 3.7) at 1 and 2 h time points following ATP stimulation. Rab GTPases (of which there are at least 44 family members in human and mice (Diekmann et al. 2011)) are critical regulators of recycling pathways (reviewed in Stenmark 2009). Crosstalk between a wide array of family members (reviewed in Diekmann et al. 2011) allows for both temporal and spatial regulation of recycling. Rab4 is linked to rapid recycling back to the cell surface (Yudowski et al. 2010), while Rab11 (Ullrich et al. 1996) is typically associated with slow recycling to the plasma membrane. Rab14 is involved in targeting vesicular cargo to slow recycling endosomal compartments (Linford et al. 2012) and shares a family of

effector proteins with Rab11 (Lall et al. 2015). However, it acts upstream of both slow and fast recycling, where due to the intercompartmental transit of Rabs, it partially co-distributes with Rab11 (Lu & Wilson 2016) and Rab4 (Yamamoto et al. 2010). Interestingly, there are differences in the GTPase-dependent sorting mechanisms between clathrin-dependent and clathrin-independent internalization mechanisms (reviewed in Grant & Donaldson 2009). Rab14, which co-distributed strongly with internalized Panx1, was commonly associated with non-canonical sorting mechanisms (Lu & Wilson 2016; Kuijl et al. 2007; Kyei et al. 2006). For instance, it positively regulated the clathrin-independent sorting protein Arf6 GTPase in neurite outgrowth (Lu & Wilson 2016), as well as phagocytosis in macrophages (Kuijl et al. 2007; Kyei et al. 2006). Preliminary evidence suggested that Panx1 endocytosis occurred in a non-canonical mechanism in HEK293T and BICR-M1Rk cells (Gehi et al. 2011), thus co-distribution with Rab14-positive compartments provides further evidence that Panx1 could be internalized in a non-canonical mechanism.

Considering the endolysosomal localization of Panx2 (Boassa et al. 2014; Wicki-Stordeur et al. 2013; Swayne et al. 2010; Cone et al. 2013), it is also possible that Panx1 internalization could lead to co-distribution with Panx2. A recent report demonstrated neuroprotection in the context of stroke was contingent on double knockout of both Panx1 and Panx2, suggesting functional overlap/crosstalk (Bargiotas et al. 2012; Bargiotas et al. 2011, although Panx1$^{-/-}$ in female had a strong neuroprotective effect, Freitas-Andrade et al. 2016); however the subcellular distribution of these proteins is very different under basal conditions (Boassa et al. 2014, reviewed in Boyce et al. 2014). Panx2 co-distributed with Rab4-positive endosomes in HEK293T cells (Boassa et al.

2014). Although ATP did not significantly increase co-distribution with Rab4, basal co-distribution in our study (Figure 3.7); thus, Panx1 and Panx2 could co-distribute discretely in Rab4-positive endosomes. Whether intracellular Panx1 and Panx2 physically or functionally couple in endosomal systems remains to be determined.

In this chapter, I investigated the hypothesis that *exogenous application of extracellular ATP promotes Panx1 endocytosis to intracellular compartments.* I revealed that ATP evoked a dramatic increase in intracellular Panx1 in a dose- and time-dependent mechanism requiring P2X7R activation and an ATP-sensitive residue (W74) in the Panx1 EL1 (Figure 3.9). The mechanism behind elevation of extracellular ATP and P2X7R-Panx1 crosstalk upstream of Panx1 internalization will be further explored in chapter 4. Internalized Panx1 was targeted to slowly recycling endosomes (Rab14/Rab11-positive); the endocytic machinery involved in internalization and sorting to recycling endosomes will be explored in chapter 5.

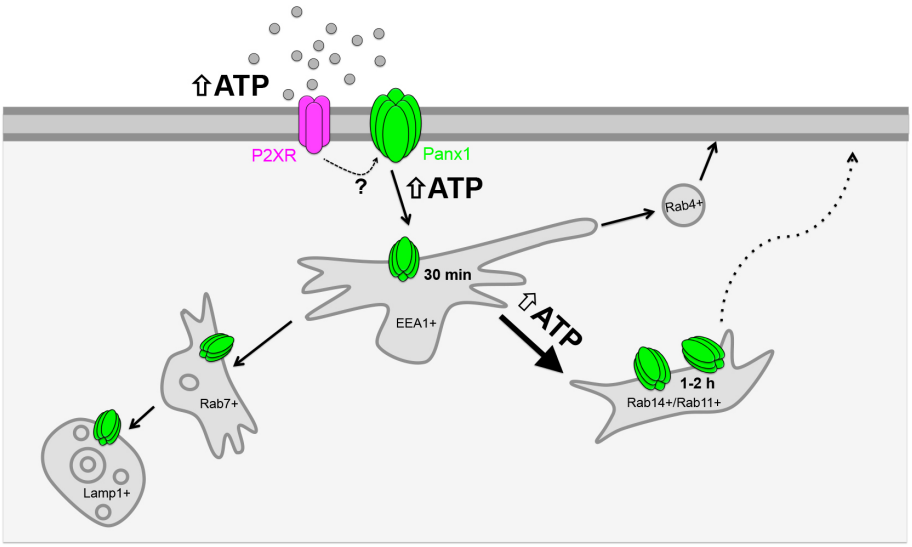

Figure 3.8 ATP evokes Panx1 endocytosis and targeting of internalized Panx1 to recycling endosomes. ATP stimulates Panx1 endocytosis in a dose- and time-dependent manner at

concentrations of ≥200 μM. Internalization was dependent on P2X receptors, likely P2X7R, based on agonist sensitivity and inhibition by the selective P2X7R A438079. Mutation of a residue in the Panx1 EL1 also abrogated ATP-evoked internalization, suggesting either ATP-Panx1 interaction or regulation through an ATP-sensitive receptor (i.e. P2XRs). Once internalized, Panx1 transited through the early endosome (30 min post-treatment) and was subsequently targeted to recycling endosomal compartments (1-2 h post-treatment).

4 An extracellular P2X7R-Panx1 interaction regulates downstream internalization

The data presented here in Chapter 4 are presented in **Boyce AKJ, Swayne LA (2017) - P2X7 receptor crosstalk regulates ATP-induced pannexin 1 internalization. Biochemical Journal 474(13): 2133-2144.**

4.1 Overview

In chapter 3, I demonstrated that extracellular ATP (≥200 μM) triggered significant and sustained Panx1 endocytosis to recycling endosomes (Boyce et al. 2015). This effect required P2X7R activation, but the underlying molecular mechanisms were unresolved. There is robust evidence of crosstalk between P2X7Rs and Panx1 in a multitude of cell types (reviewed in Isakson & Thompson 2014; Bravo et al. 2015). Although much is known about the cellular contexts in which P2X7R-Panx1 crosstalk occurs, the mechanisms linking P2X7R and Panx1 signalling, whether through signalling intermediates and/or physical coupling, are less clear. Extracellular ATP released through Panx1, activates P2X7Rs. In turn, activation of P2X7R has been linked with downstream stimulation of Panx1 activity [release of ATP and other small molecules (Gulbransen et al. 2012; Pelegrin & Surprenant 2009; Iglesias et al. 2008; Ohbuchi et al. 2011; Silverman et al. 2009)].

Several studies have linked P2X7R-mediated intracellular signalling pathways to Panx1 activation (Poornima et al. 2012; Garre et al. 2016; Iglesias et al. 2008). In neural cell types, two independent groups have suggested a role of P2X7R-mediated Ca^{2+} flux in

activating Panx1 (Poornima et al. 2012; Garre et al. 2016), however this was countered by an earlier study that demonstrated no effect of intracellular or extracellular Ca^{2+} modulation on Panx1 function (Ma et al. 2009). Conversely, P2X7R-mediated intracellular signalling also activated Panx1 via Src kinase signalling independent of Ca^{2+} (Iglesias et al. 2008). Iglesias *et al.* identified an SH3 domain, known to interact with Src and other tyrosine kinases, in the proline-rich region in the P2X7R C-terminus (Iglesias et al. 2008), with mutation of this region disrupting P2X7R-mediated Panx1 pore formation (Suadicani et al. 2009; Sorge et al. 2012). Incubation with cell-permeable peptides targeted to this region disrupted P2X7R-Src interaction and inhibited downstream Panx1-dependent currents and dye-uptake, while P2X7R-mediated currents were not significantly affected (Iglesias et al. 2008); however, they failed to show an interaction between Src and Panx1 or a specific P2X7R-dependent Src phosphorylation site in Panx1. Finally, P2X7R and Panx1 have also co-immunoprecipitated in both endogenous and exogenous expression systems (Pelegrin & Surprenant 2006; Silverman et al. 2009; Kanjanamekanant et al. 2014; Seref-Ferlengez et al. 2016; Pan et al. 2015; Hung et al. 2013; Poornima et al. 2012); however, the role of ATP in modulating the interaction of these ATP-sensitive proteins and the precise domains involved in regulating the interaction were unknown. Based on the sensitivity of internalization to P2X7R inhibition and a mutation in Panx1 EL1, if they do interact physically, the parsimonious explanation was that it would occur through their extracellular domains. Consequently, in this chapter, **I tested the hypothesis that extracellular ATP promotes an extracellular P2X7R and Panx1 interaction, upstream of Panx1 internalization.**

Using the proximity ligation assay (PLA) technique to detect Panx1 and P2X7R within 40 nm of one another (referred to as "clustering") *in situ* (Söderberg et al. 2006), I discovered that extracellular ATP positively regulates P2X7R-Panx1 clustering. PLA permits a quantitative measure of clustering between two proteins *in situ*, because signal is only produced when they are separated by <40 nm (Söderberg et al. 2006). Here, an advantage of PLA (over other techniques for studying protein-protein interactions) was that I obtained spatial information regarding the subcellular distribution of protein clustering. In-depth spatiotemporal analysis revealed that ATP evoked an early (5 min) increase in P2X7R-Panx1 clustering at the cell periphery, followed by a later (30 min) increase manifesting in intracellular compartments, suggesting that P2X7R and Panx1 might internalize together in response to ATP. Hydrolysis of endogenous extracellular ATP robustly reduced baseline P2X7R-Panx1 clustering and decreased intracellular Panx1, while inhibition of ectonucleotidases enhanced both clustering and internalization. Physical association was likely involved in clustering as a GST-fusion construct of Panx1 EL1 pulled down P2X7R from N2a lysates. Mutation of the ATP-sensitive residue in the Panx1 EL1, W74 (which was shown to disrupt ATP-induced intracellular accumulation of Panx1 in Chapter 3), abrogated ATP-stimulated clustering. As anticipated, selective P2X7R inhibition with A438079 blocked ATP-induced P2X7R-Panx1 clustering. However, both Panx1 internalization and P2X7R-Panx1 clustering were unaffected by modulation of P2X7R intracellular signalling pathways (Ca^{2+} and Src kinase). Taken together, our results suggested that ATP-mediated P2X7R-dependent clustering of P2X7R-Panx1 clustering via physical interaction between their extracellular domains (independent of Ca^{2+} or Src).

4.2 Extracellular ATP addition induces P2X7R-Panx1 clustering

Addition of ATP (500 μM) to CHX-treated Panx1-EGFP N2a cells evoked a time-dependent increase in P2X7R-Panx1 clustering (5 min post-treatment ~130%; 30 min post-treatment ~170% of unstimulated control; Figure 4.1A). Next, the kinetics of P2X7R-Panx1 clustering was assessed with spatial specificity by differentiating between clustering at the cellular periphery (overlap with peripheral Panx1 signal) and total clustering throughout the cell (Figure 4.1Aiii,iv). Five min after ATP treatment, enhanced peripheral P2X7R-Panx1 clustering was observed relative to control cells (~150% of time 0; Figure 4.1Aiii), which was reduced to control levels 30 min after stimulation. The ratio of peripheral to total clusters initially increased at 5 min, it significantly decreased relative to control by 30 min after exogenous ATP addition (Figure 4.1Aiv), which indicated that P2X7R-Panx1 clusters internalized over time. These findings suggested that extracellular ATP elevation transiently increases peripheral P2X7R-Panx1 clusters, which are then internalized by 30 min. As the most robust increase in clustering was observed at 30 min following stimulation, this time point was used for the remainder of this chapter.

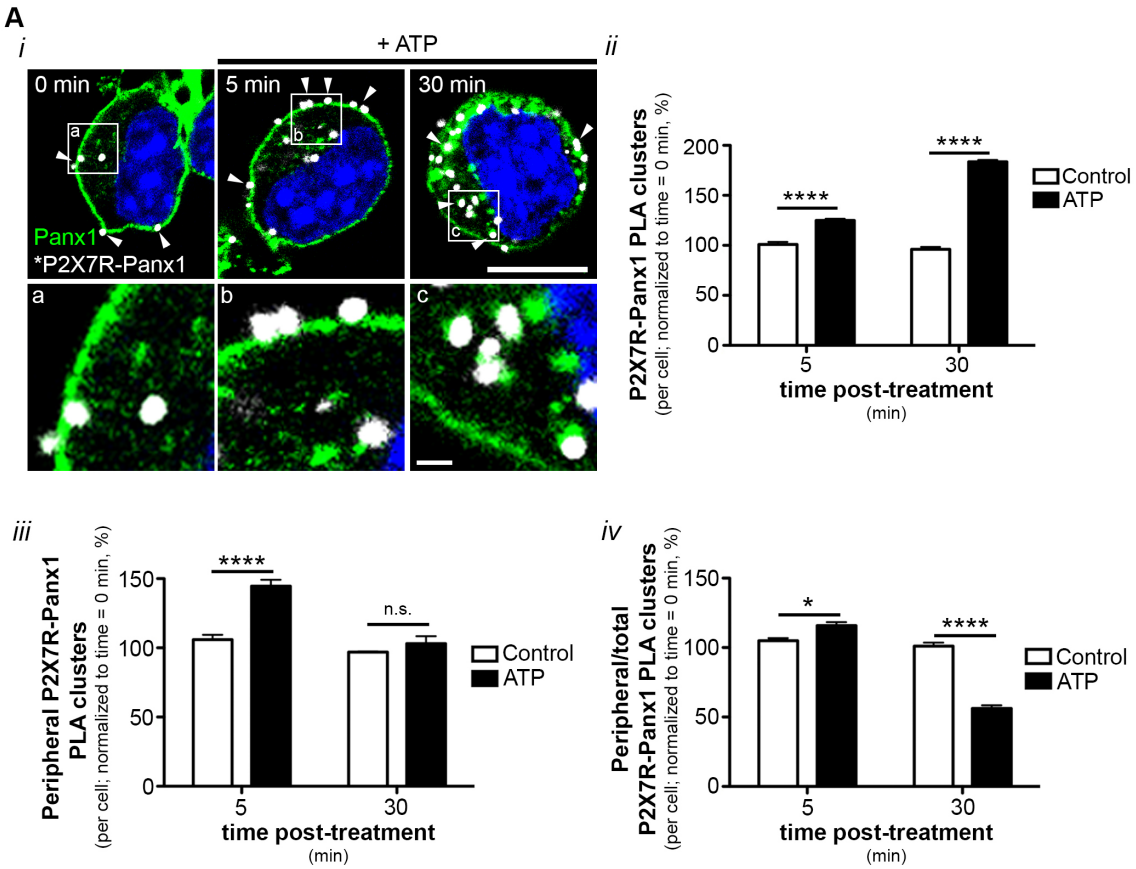

Figure 4.1 ATP triggers P2X7R-Panx1 clustering (A) Representative confocal micrographs (*i*) demonstrating P2X7R-Panx1 PLA clusters (*P2X7R-Panx1; white) in Panx1-EGFP (green) N2a cells without and with ATP (500 μM). Insets (4x digital zoom) demonstrate intracellular Panx1 present in unstimulated conditions (a) and enriched with ATP stimulation (b: 5 min, c: 30 min). Inset scale bar, 1 μm. (*ii*) P2X7R-Panx1 clusters increased at 5 and 30 min following ATP treatment (two-way ANOVA [time: $F(1, 10)=212.4$, $p<0.0001$; treatment: $F(1, 10)=652.8$, $p<0.0001$; interaction: $F(1, 10)=152.7$, $p<0.0001$] with Bonferroni's *post-hoc,* ****$p<0.0001$). (*iii*) Peripheral P2X7R-Panx1 clusters increased at 5 min (two-way ANOVA [time: $F(1, 10)=37.58$, $p=0.0027$; treatment: $F(1, 10)=29.63$, $p<0.0001$; interaction: $F(1, 10)=15.58$, $p=0.0001$] with Bonferroni's *post-hoc,* ****$p<0.0001$). (*iv*) Ratio of peripheral to total P2X7R-Panx1 clusters increased at 5 min and decreased at 30 min (two-way ANOVA [time: $F(1, 10)=182.6$, $p<0.0001$; treatment: $F(1, 10)=52.07$, $p<0.0001$; interaction: $F(1, 10)=139.2$, $p<0.0001$] with Bonferroni's *post-hoc,* *$p<0.05$, ****$p<0.0001$).

4.3 Endogenous ATP release triggers P2X7R-Panx1 clustering and internalization

In the previous chapter, as well as in Figure 4.1, we explored the role of exogenous ATP application on ATP-evoked internalization. We next investigated whether endogenously extracellular ATP release impacted P2X7R-Panx1 clustering and Panx1 internalization. ATP release from N2a cells occurs in part through a Panx1-dependent mechanism (Iglesias & Spray 2012). Earlier work from our lab indicated that N2a cell proliferation, migration, and differentiation were regulated by endogenous Panx1-mediated ATP release (Wicki-Stordeur & Swayne 2013; Wicki-Stordeur et al. 2012). Additionally, N2a cells endogenously expressed ectonucleotidases (Gómez-Villafuertes et al. 2014) allowing for the rapid breakdown of ATP upon release. To determine whether endogenous ATP release impacted on P2X7R-Panx1 clustering and Panx1 internalization, Panx1-EGFP N2a cells were cultured in the presence of apyrase [catalyzes extracellular ATP hydrolysis (Handa & Guidotti 1996)] or an ectonucleotidase inhibitor (ARL 67156; inhibits extracellular ATP hydrolysis by non-selective inhibition of ectonucleotidases; Geyti et al. 2008; Figure 4.2Ai). These results were compared to treatment with exogenous ATP over a 30 min time course, as in my previous experiments (500 μM). Notably, apyrase (50 U/mL; 24 h) completely abolishes P2X7R-Panx1 clustering, while P2X7R-Panx1 clustering is significantly increased following ARL 67156 treatment (250 μM) of the same duration (Figure 4.2Aii). Following a similar trend to P2X7R-Panx1 clustering, apyrase significantly reduced intracellular Panx1 (~75% of control), while ARL 67156 significantly enhanced intracellular Panx1 accumulation (~170% of control; Figure 4.3Aiii). Together, I demonstrated that

endogenous ATP release triggers and is required for P2X7R-Panx1 clustering and influences downstream Panx1 internalization. These findings helped to explain why Panx1 was observed in intracellular compartments in vehicle-treated cells during experiments using exogenous ATP. Exogenous ATP application, however, led to a more robust effect on both clustering and internalization; thus, it was used for the remainder of the study.

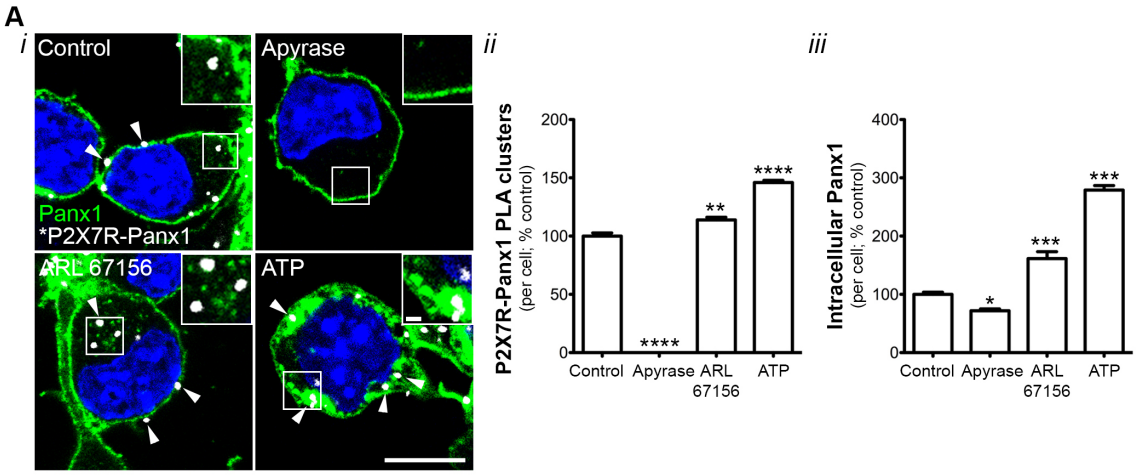

Figure 4.2 Endogenous ATP release stimulates and is required for P2X7R-Panx1 clustering and regulates Panx1 internalization (A) Confocal micrographs (*i*) demonstrating P2X7R-Panx1 clusters (white) in control (water; 24 h), apyrase (50 U/mL; 24 h), ARL 67156 (250 μM; 24 h), or ATP (500 μM; 30 min). Insets (2x digital zoom) demonstrate intracellular Panx1 present in unstimulated conditions and enriched with ATP stimulation. Inset scale bar, 1 μm. (*ii*) Clusters decreased with apyrase and increased with ARL67156 and ATP treatment (one-way ANOVA with Dunnett's *post-hoc,* **p<0.01, ****p<0.0001). (*iii*) Intracellular Panx1 decreased with apyrase and increased with ARL 67156 and ATP (one-way ANOVA with Dunnett's *post-hoc,* *p<0.05, ***p<0.001, ****p<0.0001). All experiments included N = 3-4 coverslips from separate passages per condition (≥ 30 cells analyzed per coverslip). Hoechst 33342 (blue) was used as a nuclear counterstain. Scale bars, 10 μm.

4.4 Panx1 EL1 interacts with P2X7R

PLA allowed for spatial analysis of P2X7R-Panx1 clustering; however, it did not definitively reveal whether these clusters involved a physical interaction between P2X7R and Panx1. P2X7R and Panx1 have co-immunoprecipitated in several contexts (Pelegrin & Surprenant 2006; Silverman et al. 2009; Kanjanamekanant et al. 2014; Seref-Ferlengez et al. 2016; Pan et al. 2015; Hung et al. 2013; Poornima et al. 2012), yet the precise domain involved in mediating this interaction was unknown. Features of the Panx1 EL1, namely W74, were involved in both ATP-dependent Panx1 inhibition (Qiu & Dahl 2009; Qiu et al. 2012) and Panx1 internalization (reported in Chapter 3 & Boyce et al. 2015). With this in mind, I suspected P2X7R and Panx1 interacted through this extracellular domain. To examine whether P2X7R interacts with the Panx1 EL1 (Figure 4.3Ai), cell lysates were incubated with glutathione bead-immobilized GST-Panx1^{EL1} [Figure 3Aii; sequence predicted in Penuela *et al.* (2009)] or GST control alone in a pull-down assay. Full-length P2X7R (~75 kDa) along with lower molecular weight species (notably between 15-50 kDa) were enriched by GST-Panx1^{EL1} (Figure 4.3Aiii). In unpermeabilized Panx1-EGFP cells incubated with GST-Panx1^{EL1} (10 μM), PLA revealed clustering of P2X7R and GST-Panx1^{EL1} at the cell surface that is negligible in cells incubated with equimolar GST (Figure 3B). Taken together, these data indicated that the P2X7R-Panx1 physical interaction was localized to their respective extracellular domains.

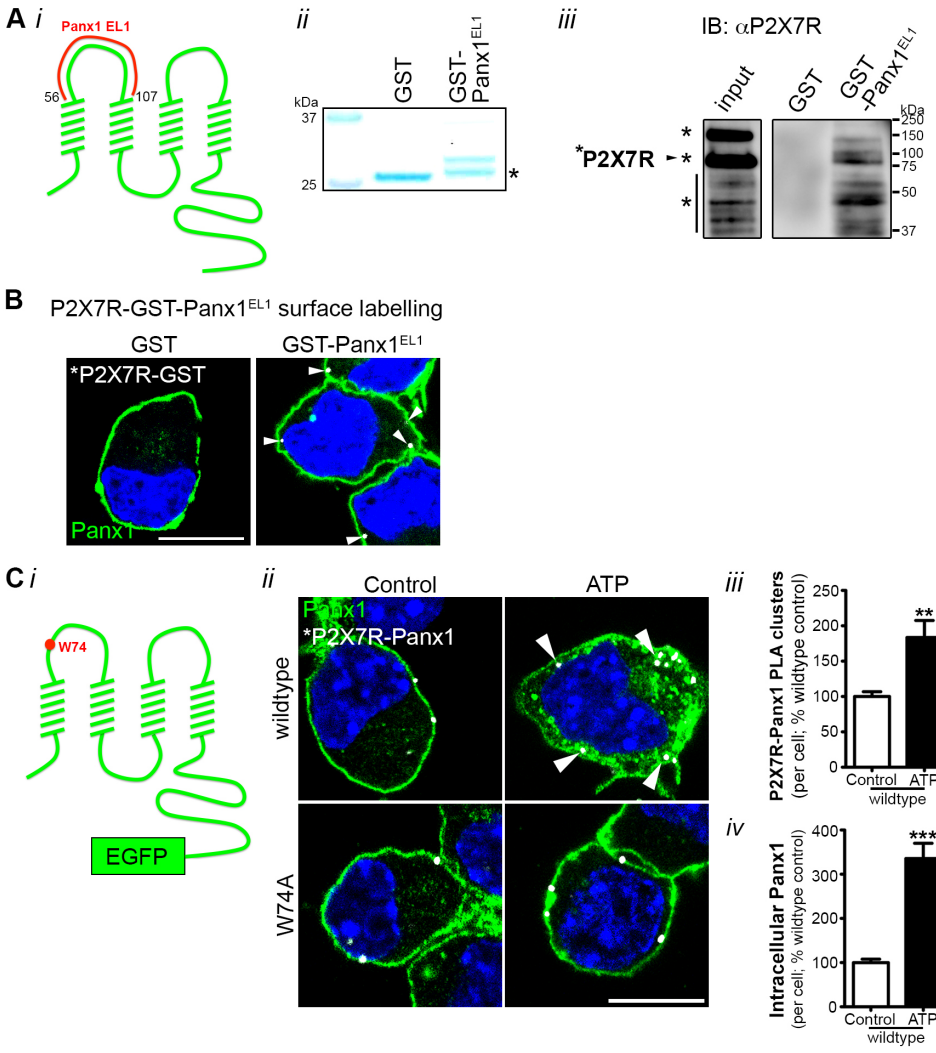

Figure 4.3 An extracellular interaction of the Panx1 EL1 with P2X7Rs is required for ATP-induced internalization (A) Schematic (*i*) of EL1 (red; amino acids 56-107) in mouse Panx1. (*ii)* Colloidal blue-stained SDS-PAGE gel of GST, and GST-Panx1^{EL1}. Asterisk indicate cleavage product. (*iii)* Representative Western blot of pull-down of N2a lysates (input) with immobilized GST-Panx1^{EL1} probed with anti-P2X7R. Pull-down with GST served as a negative control. Blot is representative of three independent experiments. Asterisks indicate non-specific bands remaining with antigen pre-incubation prior to Western blotting. (B) Confocal micrographs demonstrating (*i*) cell surface anti-GST (red) or (*ii*) P2X7R-GST clusters (white) in unpermeabilized Panx1-EGFP (green) N2a cells incubated with GST or GST-Panx1^{EL1} (10 μM). (C) Schematic (*i*) of W74 residue (red) in Panx1 EL1. (*ii*) Confocal micrographs demonstrating P2X7R-Panx1 clusters (white) in Panx1-EGFP or Panx1W74A-EGFP N2a cells stimulated with vehicle or ATP (500 μM; 30 min). (*iii*) P2X7R-Panx1 clusters were unchanged with ATP treatment in Panx1W74A-

EGFP N2a cells (two-way ANOVA [interaction: F(1, 8)=7.007, p=0.0294; genotype: F(1, 8)=11.54, p=0.0094; ±ATP: F(1, 8)=9.23, p=0.0161] with Dunnett's *post-hoc,* **p<0.01). (iv) ATP did not increase intracellular Panx1 in W74A-expressing cells (two-way ANOVA [interaction: F(1, 8)=36.25; p=0.0003; genotype: F(1, 8)=61.25, p<0.0001; ±ATP: F(1, 8)=41.88, p=0.0002] with Dunnett's *post-hoc,* ****p<0.0001). All imaging experiments included $N = 3$ coverslips from separate passages per condition (≥ 30 cells analyzed per coverslip). Hoechst 33342 (blue) was used as a nuclear counterstain. Scale bar, 10 μm.

4.5 W74 within the Panx1 EL1 is essential for ATP-induced P2X7R-Panx1 clustering

To investigate whether alanine-substitution of W74 residue in Panx1 EL1 (Figure 4.3Ci) altered P2X7R-Panx1 clustering, we utilized Panx1W74A-EGFP N2a cells (Figure 4.3Cii). ATP-induced P2X7R-Panx1 clustering was abolished by the W74A mutation (Figure 4.3Ciii). Panx1W74A-EGFP N2a cells that did not exhibit an increase in P2X7R-Panx1 clustering also demonstrated no significant increase in downstream Panx1 internalization (Figure 4.3Civ). These data suggested that this ATP-sensitive residue in the Panx1 EL1 regulated ATP-evoked P2X7R-Panx1 clustering and Panx1 internalization.

4.6 P2X7R activation (independent of Ca^{2+} and Src) triggers P2X7R-Panx1 clustering and internalization

The genesis of this chapter stemmed from the observation that ATP-evoked Panx1 internalization was disrupted by selective antagonism of P2X7R with A438079. Consequently, I was interested in whether P2X7R inhibition also reduced the P2X7R-

Panx1 clustering in the presence of ATP. Pre-incubation with A438079 reduced ATP-evoked P2X7R-Panx1 clustering (Figure 4.4A) and Panx1 internalization (consistent with Chapter 3) to baseline levels, which suggested that activation of P2X7Rs is also critical for P2X7R-Panx1 clustering.

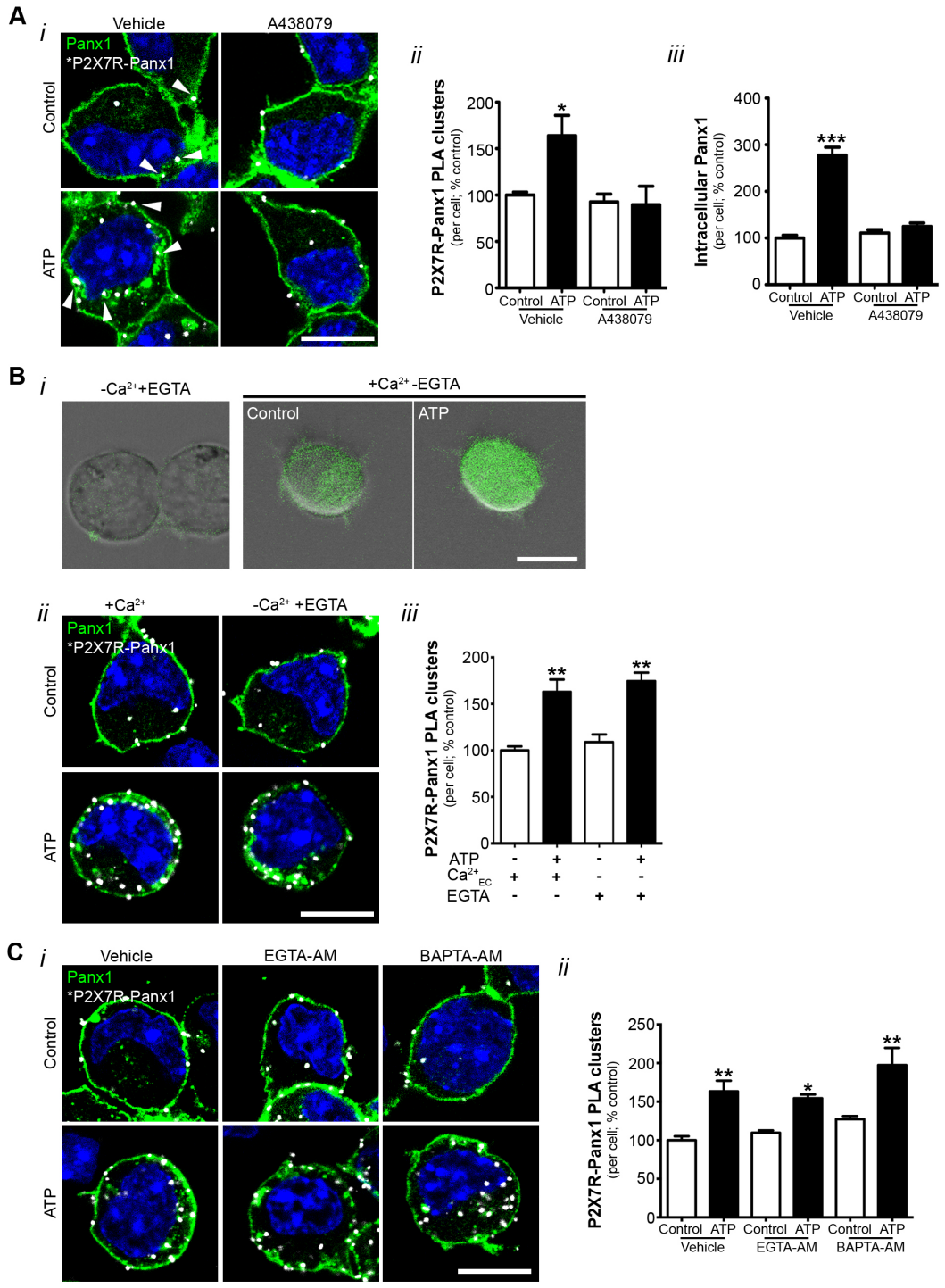

Figure 4.4 P2X7R activation, independent of Ca^{2+} signalling pathways, is critical for P2X7R-Panx1 clustering and internalization (A) Representative confocal micrographs (*i*) demonstrating P2X7R-Panx1 clusters (white) in Panx1-EGFP (green) N2a cells pre-treated with A438079 (100 μM, 1 h) prior to vehicle (water) or ATP (500 μM; 30 min). (*ii*) P2X7R-Panx1

clusters did not increase in the presence of A438079 (*N* = 3, two-way ANOVA [interaction: F(1, 8)=4.682, p=0.0624; inhibitor: F(1, 8)=6.978, p=0.0296; ±ATP: F(1, 8)=3.86, p=0.0851] with Dunnett's *post-hoc*, *p<0.05). (iii) ATP did not increase intracellular Panx1 in the presence of A438079 (N= 3, two-way ANOVA [interaction: F(1, 8)=60.14; p<0.0001; inhibitor: F(1, 8)=45.43, p=0.0001; ±ATP: F(1, 8)=82.55, p<0.0001] with Dunnett's *post-hoc,* ****p<0.0001). (B) Confocal micrographs of Fluo4-AM (4 μM, 30 min prior to imaging) in N2a cells incubated in HBSS with or without Ca2+ (+ 5 mM EGTA) prior to vehicle or ATP addition (500 μM). Transmitted light overlays indicate cellular boundaries. (C) Confocal micrographs (*i*) of P2X7R-Panx1 clusters (white) in cells pre-incubated with or without Ca^{2+} (+ 5 mM EGTA) prior to vehicle or ATP (500 μM; 30 min). (*ii*) P2X7R-Panx1 clusters were not affected by modulating extracellular Ca^{2+} (*N* = 3, two-way ANOVA [interaction: F(1, 8)=0.01989; p=0.8913; ± Ca^{2+}: F(1, 8)=1.201, p=0.3050; ±ATP: F(1, 8)=47.59, p=0.0001] with Dunnett's *post-hoc*, **p<0.01). (D) Confocal micrographs (*i*) demonstrating P2X7R-Panx1 clusters (white) in cells incubated with EGTA-AM (50 μM), BAPTA-AM (50 μM), or vehicle (DMSO) for 1 h prior to vehicle or ATP addition (500 μM; 30 min). (*ii*) P2X7R-Panx1 clusters were not affected by chelating intracellular Ca^{2+} (*N* = 3, two-way ANOVA [interaction: F(2, 12)=0.6839; p=0.5253; chelator: F(2, 12)=4.885, p=0.0281; ±ATP: F(1, 12)=41.66, p<0.0001] with Dunnett's *post-hoc*, *p<0.05, **p<0.01, ***p<0.001)

I next aimed to determine if intracellular signalling mechanisms previously associated with Panx1 pore formation in response to P2X7R activation were also involved. These included ATP-evoked Ca^{2+} flux (Figure 4.4) and Src family kinase (SFK) activation (Figure 4.5; reviewed in Bravo et al. 2015). To determine the impact of P2X7R-dependent Ca^{2+} signalling, we modulated extracellular (by removing Ca^{2+} from culture medium; Figure 4.4Bii) and intracellular Ca^{2+} (by chelating intracellular Ca^{2+}; Figure 4.4Ci). ATP-evoked P2X7R-Panx1 clustering was not affected by removing extracellular Ca^{2+} (Figure 4.4Biii) or chelating intracellular Ca^{2+} (Figure 4.4Cii), suggesting it occurred independent of Ca^{2+} signalling.

To examine the effects of SFK signalling on clustering, cells were treated with the non-selective SFK inhibitor, PP2 (10 μM; Hanke et al. 1996), or its inactive analogue, PP3 (10 μM). Pre-incubation with the SFK inhibitor significantly reduced active Src kinase (pY416Src; Figure 4.5Ai), but did not significantly alter ATP-induced P2X7R-Panx1 clustering (Figure 4.5Aii,iii). To validate this pharmacological data, we next employed cell-permeable competitive peptides that were previously reported to disrupt a P2X7R-Src interaction, targeted to the SH3 domain in the P2X7R C-terminus (Figure 4.5B), upstream of Panx1 activation (Iglesias et al. 2008). N2a cells were derived from the A/J albino mouse strain (Klebe & Ruddle 1969), which carries the 451P allele (pore-forming) in the SH3 domain of the P2X7R (Figure 4.5C; Sorge et al. 2012), so TAT-451P peptides were used in this analysis along with TAT-peptides to the 451L and human P2X7R SH3 domain as controls (Figure 4.5D). Although the TAT-conjugated peptides were able to permeate the cell, none of the peptides significantly affected ATP-induced P2X7R-Panx1 clustering, confirming that Src kinases were not involved in ATP-induced P2X7-Panx1 clustering (Figure 4.5E). The lack of involvement of Ca^{2+} or SFKs suggested that intracellular signalling pathways that mediate P2X7R-Panx1 crosstalk in other physiological processes are not implicated in P2X7R-Panx1 clustering. In addition to the absence of a role for P2X7R-Panx1 intracellular signalling pathways in regulating their clustering, it is important to note that neither modulation of intracellular/extracellular Ca^{2+} nor disruption of Src signalling abrogated Panx1 internalization.

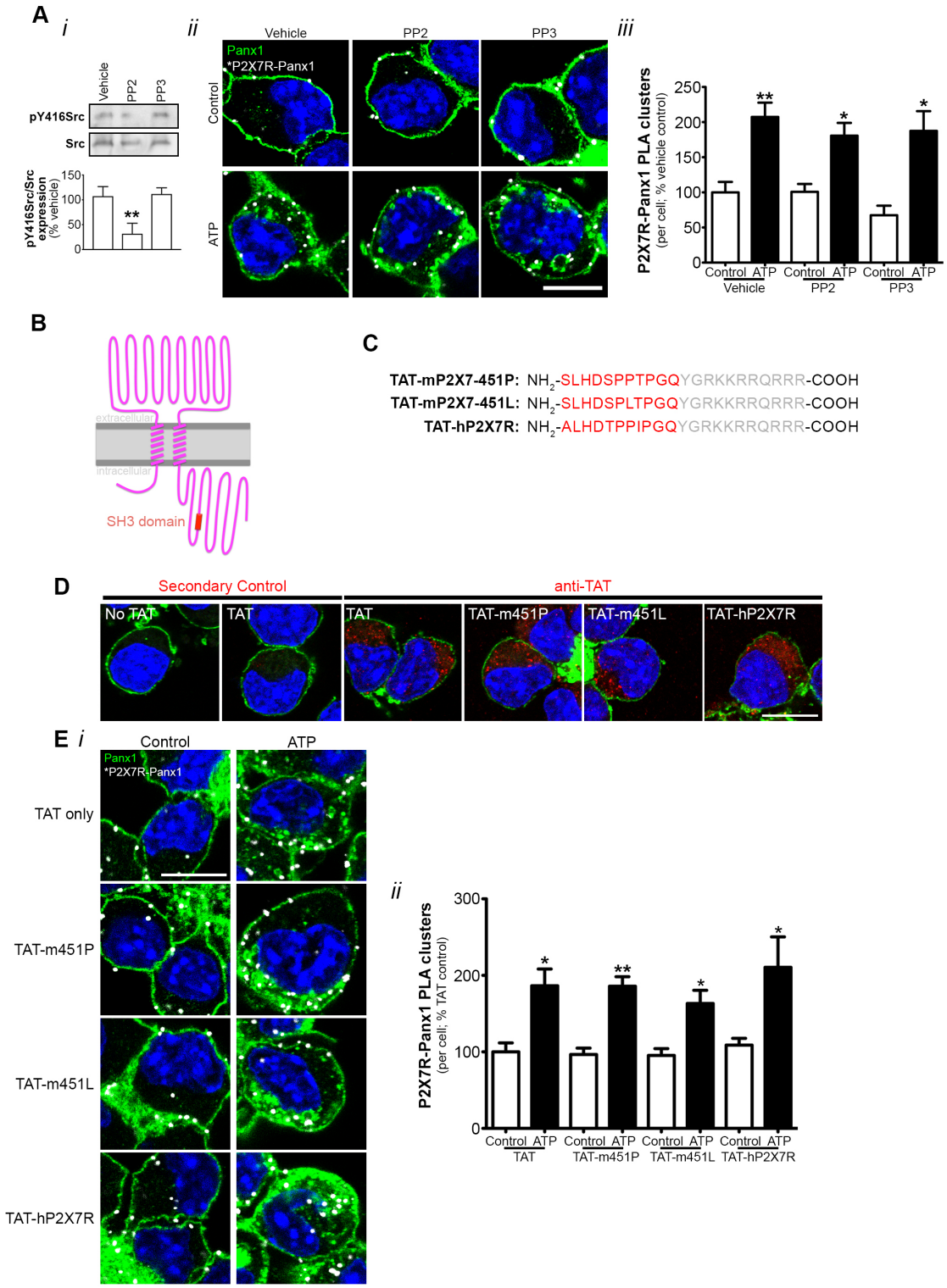

Figure 4.5 P2X7R-Panx1 clustering and internalization is independent of upstream P2X7R-Src signalling. (A) Western blot demonstrated reduced active Src kinase (pY416Src) expression following inhibition with PP2 (10 μM, 1 h) (N =3, one-way ANOVA with Dunnett's *post hoc*,

p<0.01). (B) Confocal micrographs (*i*) of P2X7R-Panx1 clusters (white) in cells treated with vehicle (DMSO), PP2 (10 μM) or PP3 (10 μM) for 1 h prior to vehicle or ATP (500 μM; 30 min). (*ii*) P2X7R-Panx1 clusters were unaffected by PP2 or PP3 ($N = 3$, two-way ANOVA [interaction: $F(2, 12)=0.6088$; $p=0.5600$; inhibitor: $F(2, 12)=0.994$, $p=0.3986$; ±ATP: $F(1, 12)=45.69$, $p<0.0001$] with Dunnett's *post-hoc*, *p<0.05, **p<0.01). *N* refers to the number of coverslips from independent passages (≥ 30 cells analyzed per coverslip). (E) Schematic of the P2X7R with SH3 domain (red). (F) Alignment of cell-permeable P2X7R-Src interfering peptides (TAT-mP2X7R-451P, TAT-mP2X7R-451L, TAT-hP2X7R; red). TAT sequence is in grey. (G) Confocal micrographs of Panx1-EGFP N2a cells incubated with the indicated peptides (10 μM, 1 h), antigen retrieved (10 mM sodium citrate, 0.05% Tween 20, pH 6.0; 1 h at 60 °C) and labelled with anti-TAT (1:20; red). (H) Confocal micrographs (i) of P2X7R-Panx1 clusters (*P2X7R-Panx1; white) in Panx1-EGFP N2a cells pre-incubated with indicated peptides (10 μM, 1 h) prior to vehicle or ATP addition (500 μM; 30 min). (ii) P2X7R-Panx1 clusters were not affected by TAT-conjugated P2X7R-Src interfering peptides ($N = 4$, two-way ANOVA [interaction: $F(3, 24)=0.2707$; $p=0.8439$; TAT peptides: $F(3, 24)=0.8661$, $p=0.4722$; ±ATP: $F(1, 24)=41.33$, $p<0.0001$] with Dunnett's *post-hoc*, *p<0.05, **p<0.01). (D) ATP-evoked Panx1 internalization was unaffected by TAT-conjugated P2X7R-Src interfering peptides ($N = 7$-10, two-way ANOVA [interaction: $F(3, 54)=0.9198$; $p=0.4376$; TAT peptides: $F(3, 54)=1.409$, $p=0.2501$; ±ATP: $F(1, 54)=54.68$, $p<0.0001$] with Dunnett's *post-hoc*, *p<0.05, **p<0.01,**p<0.0001) For imaging experiments, N represents coverslips of independent passage (≥ 30 cells analyzed per coverslip). Representative confocal images were uniformly adjusted for contrast using Adobe Photoshop for display purposes only; no contrast adjustments were made prior to analysis. Hoechst 33342 (blue) was used as a nuclear counterstain. Scale bars, 10 μm.

4.7 Discussion

Here, I demonstrated that extracellular ATP (via both exogenous application and endogenous ATP release) was both necessary and sufficient to stimulate clustering and internalization of P2X7R and Panx1. Clustering initiated at the cell periphery and accumulated in intracellular compartments over time (30 min). P2X7Rs and Panx1 interacted via their respective extracellular domains. Further, alanine-substitution mutation of W74 in Panx1 EL1, previously linked to ATP-mediated channel inhibition

(Qiu & Dahl 2009; Qiu et al. 2012) and internalization (Boyce et al. 2015), disrupted ATP-evoked P2X7R-Panx1 clustering and internalization.

Notably, not all Panx1-positive intracellular compartments were co-positive for P2X7R-Panx1 PLA signal, suggesting there were some compartments where Panx1 existed alone. There are several possible explanations for this phenomenon including (1) co-internalization and differential sorting (reviewed in Jovic et al. 2010) or (2) separate internalization and co-sorting upon meeting in the early endosome (reviewed in Grant & Donaldson 2009). First, P2X7R-Panx1 clusters might co-internalize in response to ATP through a shared pathway, but be sorted to distinct endosomal compartments following internalization; this was a possibility due to the physical proximity induced by ATP and the ATP-sensitive extracellular interaction shared between these two proteins. Interestingly, P2X7R internalized in response to elevated extracellular ATP in other cell types [transformed endocervical epithelial cells, HEK293 cells (Feng et al. 2005), and osteoblasts (Gangadharan et al. 2011)]. The mechanisms described for ATP-induced P2X7R internalization appeared to be dose- and/or cell type-specific. Upon stimulation with 250 μM ATP, P2X7R was internalized in a β-arrestin-, GPCR-kinase 3 (GRK3)-, and clathrin-dependent mechanism to perinuclear vesicles in CaSki and HEK293 cells, respectively (Feng et al. 2005). Here, internalized P2X7R rapidly recycled back to the cell surface (15-30 min). In osteoblasts, 250 μM ATP also stimulated P2X7R internalization through a different mechanism associated with lipid raft localization and caveolin-mediated endocytosis (Gangadharan et al. 2011). Future work is required to determine if the internalization mechanism of P2X7Rs is cell type-specific. If P2X7Rs were sorted to rapidly recycling Rab4-positive endosomes, as observed in epithelial cells

(Feng et al. 2005), it is possible that P2X7R-Panx1 clustering is disrupted upon Panx1 sorting to slow recycling Rab11-/Rab14-positive endosomes (Chapter 3). This would explain the presence of some Panx1-positive compartments that are absent of P2X7R-Panx1 clusters. An alternate explanation for the presence of some internalized Panx1-positive structures absent of P2X7R-Panx1 clusters is that P2X7R and Panx1 internalized through diverse mechanisms in response to ATP and met in the sorting endosome; where again, they shared close proximity. This would be in line with the available evidence that suggested that P2X7R [canonical, clathrin- (Feng et al. 2005) or caveolin-dependent (Gangadharan et al. 2011)] and Panx1 [non-canonical, clathrin-, caveolin-independent (Gehi et al. 2011)] internalized through different mechanisms.

The marked impact of endogenous extracellular ATP removal on clustering was initially surprising, yet confirmed an important role for extracellular ATP in the regulation of Panx1-EGFP subcellular distribution. The exogenously applied ATP concentrations (used in my studies up to this point), although quite high, were well within hypothetical range of extracellular concentrations seen by the membrane regions proximal to ATP release sites. In secretory vesicles, ATP is concentrated up to ~5-50 mM in non-neural cells (Zalk & Shoshan-Barmatz 2006; Bergendorff & Uvnas 1973; Uvnas 1974), while it reached concentrations up to 150-200 mM in synaptic vesicles (Van Der Kloot 2003). With cytosolic ATP concentration in the 1-10 mM range, channel-mediated release or cell lysis could also lead to dramatic increase in extracellular ATP concentrations at discrete locations on the cell membrane (reviewed in Dubyak & el-Moatassim 1993; Pankratov et al. 2006), which would be predicted to cause localized P2X7R-Panx1 clustering and internalization.

N2a cells release ATP, in part through Panx1, under basal conditions (Wicki-Stordeur et al. 2012), which mediates autocrine/paracrine purinergic signalling (Wicki-Stordeur et al. 2012; Iglesias & Spray 2012). The absence of P2X7R-Panx1 clustering following extracellular ATP hydrolysis (apyrase) explained the presence of baseline P2X7R-Panx1 clusters in my vehicle-treated conditions during exogenous ATP application (Chapter 3). Interestingly, although significantly reduced, there was residual intracellular Panx1 following apyrase treatment (24 h; Figure 4.2). Panx1 that was internalized prior to beginning apyrase treatment could explain this observation. In several studies, mature Panx1 possessed a half-life of > 8 h (Penuela et al. 2007; Boassa et al. 2008). Further, where anterograde trafficking was disrupted with BFA (up to 32 h; Penuela et al. 2013) or where newly synthesized Panx1 was tracked through the secretory pathway using fluorophore-based pulse-chase tagging (up to 18 h; Boassa et al. 2007), both a small population of cell surface Panx1 and Panx1 in perinuclear endosomal compartments persisted. Together, these findings in combination with my own suggest that although apyrase treatment was of sufficient duration to disrupt cell surface P2X7R-Panx1 clustering, internalized Panx1 could have persisted in endosomal compartments from prior to the onset of treatment. If ATP-evoked P2X7R-Panx1 clustering were necessary for internalization, increasing the length of apyrase treatments would be expected to further diminish intracellular Panx1.

Pulldown assays with immobilized GST-Panx1^{EL1} identified EL1 as the P2X7R interaction site within Panx1 (Figure 4.3A). Further, we demonstrated that Panx1 harbouring an alanine substitution at W74 prevented ATP-induced P2X7R-Panx1 clustering. Together, these findings suggest that the interaction with P2X7R occurs in the

Panx1 EL1. Importantly, the P2X7R interaction assays (pulldown and PLA) with the Panx1^{EL1} fragment occurred in the absence of exogenous ATP. However, the dependence of the *in cellulo* interaction on the presence of ATP and P2X7R activation suggests, however, that ATP is required to induce a conformational change requisite for interaction. I suspected that, unconstrained by flanking transmembrane domains, the isolated GST-Panx1^{EL1} fragment (present in excess) was able to access the interacting P2X7R residues without the requirement of ATP.

I hypothesized that the lower molecular weight species of P2X7R pulled down by GST-Panx1^{EL1} could be splice variants (Kido et al. 2014; Cheewatrakoolpong et al. 2005) because pull-downs were performed in the presence of protease inhibitors. In mice, two of the variants with the largest differences in protein structure, P2X7RΔ153 and P2X7RΔ430, exhibit truncation of the C-terminus to varying degrees (Kido et al. 2014). The P2X7R antibody used in my study (extracellular epitope, aa 136-152) was potentially capable of detecting both of these truncated isoforms. P2X7RΔ153 possess the N-terminus, TM1, and a portion of the P2X7R extracellular domain, while P2X7RΔ430 contained a portion of the C-terminus, but is truncated upstream of the SH3 domain. Both P2X7RΔ153 and P2X7RΔ430 co-immunoprecipitated with full-length P2X7R channel, and negatively regulated P2X7R function when co-expressed (Kido et al. 2014; Masin et al. 2012). Truncated versions of the human P2X7R also interacted with and negatively regulated full-length P2X7R channel function (Adinolfi et al. 2010). It is possible that the lower molecular weight bands for P2X7R observed in the Western blots are the result of interactions between Panx1 and alternatively spliced P2X7Rs. A potential mechanism for

negative regulation could be via internalization through a Panx1 EL1-mediated interaction.

Although we identified an interaction between the Panx EL1 and P2X7R (Figure 4.3), this is not indicative that this is the sole physical P2X7R-Panx1 interaction site and it remains possible that other domains are capable of mediating an interaction. However, two separate findings suggest that it is the physiological interaction locus. First, mutation of W74 alone disrupted ATP-evoked clustering. Second, the insensitivity of ATP-evoked P2X7R-Panx1 clustering and Panx1 internalization to disruption of P2X7R-Src signalling and SFK inhibition, the C-terminal dependent effectors of P2X7R-Panx1 positive feedback (Suadicani et al. 2009; Iglesias et al. 2008), suggested that internalization occurred in a mechanism independent of previously published intracellular interactions. Further, this combination of data, including the lack of effect by TAT-451P or TAT-451L peptides, suggested that the polymorphism linked to P2X7R-Panx1 crosstalk and pore formation (Suadicani et al. 2009; Sorge et al. 2012; Iglesias et al. 2008) was not involved in the internalization process. I did not identify the interaction site on the extracellular domain of the P2X7R in this study and this should be the focus of future investigations. Importantly, P2X receptors demonstrated strong structural and sequence homology in their ectodomains (Hattori & Gouaux 2012; Kawate et al. 2009; Karasawa & Kawate 2016). If the P2X7R-Panx1 interaction site in P2X7R is partially homologous with other purinergic receptors, it remains possible that other family members may be able to elicit Panx1 internalization to a lesser degree in the absence of P2X7Rs. This could be investigated in future studies using P2X7R knockdown or knockout approaches.

My findings that localized the physical interaction of P2X7R to Panx1 EL1 are relevant to the relationship between Panx1 and other known Panx1 inhibitors. Recent evidence suggested that several Panx1 inhibitors (CBX and ^{10}Panx1) acted at positions in EL1 overlapping or nearby to W74 (Pelegrin & Surprenant 2006; Michalski & Kawate 2016). The fact that W74A mutation disrupted ATP-mediated P2X7R-Panx1 clustering and Panx1 internalization [as well as previously-reported ATP-dependent inhibition (Qiu & Dahl 2009; Qiu et al. 2012)] supported the involvement of this residue in allosteric changes affecting the Panx1 conformation, function, and stability. Additional data supported the involvement of this region in regulating P2X7R-Panx1 interactions as ^{10}Panx1 was initially designed to inhibit P2X7R-mediated Panx1-dependent dye-uptake without disrupting P2X7R dependent ionic currents (Pelegrin & Surprenant 2006). Pre-incubation with ^{10}Panx1 prevented P2X7R-mediated Panx1-dependent activity even 60 min after it was washed out, suggesting a very stable mechanism of inhibition for P2X7R-Panx1 signalling by the inhibitory peptide (Pelegrin et al. 2008). Further investigation into the mechanism of action of these inhibitors will be the focus of future work.

In summary, I tested the hypothesis that *extracellular ATP promotes an extracellular P2X7R and Panx1 interaction, upstream of Panx1 internalization*. I determined that ATP-evoked clustering originated at the cell periphery (5 min) and then accumulated in intracellular compartments (30 min; Figure 4.6). Consistent with previous studies showing the importance of the Panx1 EL1 in ATP-mediated Panx1 inhibition (Qiu et al. 2012; Qiu & Dahl 2009; Boyce et al. 2015), this domain was the locus for a physical interaction with the extracellular domain of P2X7Rs. ATP-evoked P2X7R-

Panx1 clustering was reduced to baseline by an alanine-substitution mutation at W74 in the Panx1 EL1. ATP-evoked P2X7R-Panx1 clustering relied on P2X7R activation, yet was independent of common intracellular signalling pathways associated with P2X7R-Panx1 crosstalk (Ca^{2+} and Src) and pore formation. These findings represent an important advance in understanding the relationship between P2X7Rs and Panx1. This work also provided the first evidence that physiological levels of extracellular ATP are both necessary and sufficient to trigger P2X7R-Panx1 clustering. The following chapter will explore the endocytic machinery involved in P2X7R-Panx1 recruitment and how this couples with internalization to intracellular compartments (chapter 3).

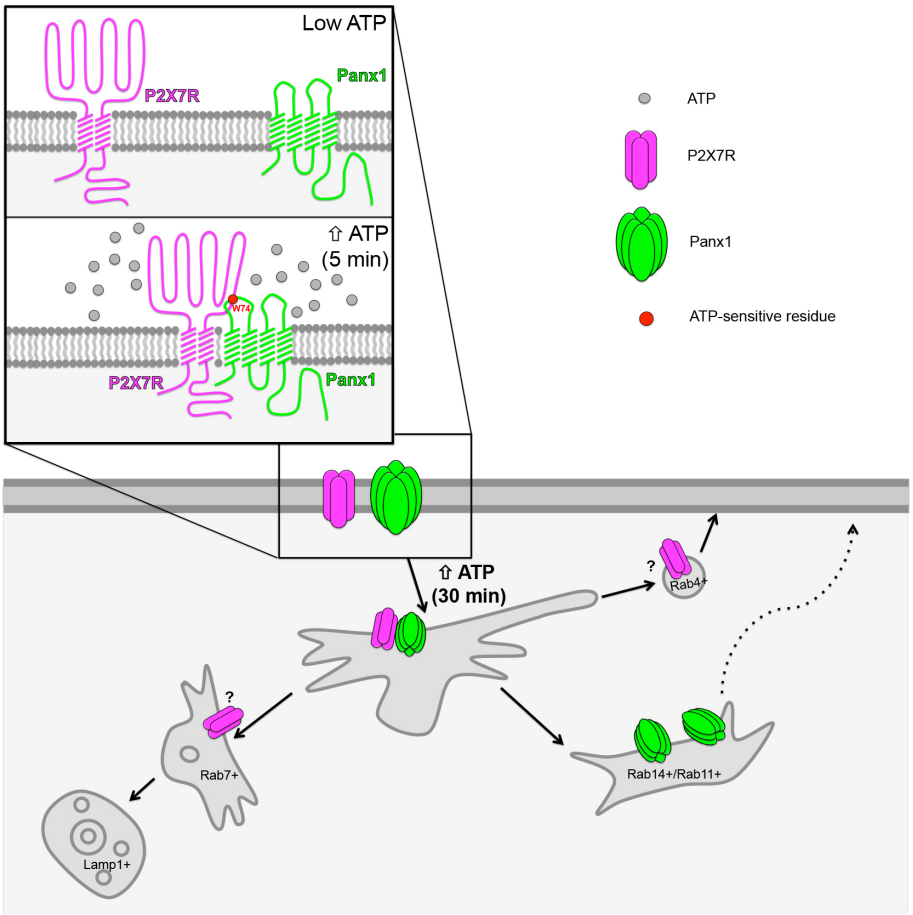

Figure 4.6 ATP triggers an extracellular interaction between P2X7R and Panx1, sensitive to Panx1 W74A mutation, upstream of internalization. Both endogenous ATP release and

exogenous ATP triggered clustering, which occurred first at the cell periphery (5 min) and then accumulated in intracellular compartments (30 min); however, some intracellular compartments contained Panx1 only suggesting differential sorting mechanisms for P2X7R and Panx1. ATP-evoked clustering occurred in part through a physical interaction between the extracellular domains of P2X7R and Panx1, which was disrupted by mutation at W74 in the Panx1 EL1. P2X7R-Panx1 clustering required P2X7R activation yet was independent of common intracellular signalling pathways associated with P2X7R-Panx1 pore formation (Ca^{2+} and Src).

5 Endocytic machinery involved in Panx1 internalization

A portion of the data (Figures 5.1 and 5.2) presented here were published in **Boyce AKJ, Kim MS, Wicki-Stordeur LE, Swayne LA (2015) ATP stimulates pannexin 1 internalization to endosomal compartments. Biochemical Journal 470(3): 319-330.** Figure 5.5 was from **Boyce AKJ, Swayne LA (2017) P2X7 receptor crosstalk regulates ATP-induced pannexin 1 internalization. Biochemical Journal 474(13): 2133-2144.** Data from Figures 5.3, 5.4, and 5.6 are in preparation for a subsequent submission.

5.1 Overview

In this chapter, I bring together the findings I described in Chapters 3 and 4 that demonstrated ATP-sensitive internalization of Panx1 to endosomal compartments mediated through physical coupling with P2X7R. Here, I investigate the endocytic machinery involved in this pathway. Gehi *et al.* observed that Panx1 internalized independent of the canonical endocytic machinery (clathrin, caveolin, and dynamin) in BICR-M1$_k$ and HEK cells (Gehi et al. 2011); however, they did not identify the particular non-canonical endocytic machinery that might be involved in internalization.

Several possible non-canonical endocytic pathways exist that could mediate Panx1 internalization (reviewed in Mayor et al. 2014) including the large-scale pathways, phagocytosis and macropinocytosis, as well as the small-scale endocytic pathways, including Arf6-mediated endocytosis, CLIC/GEEC endocytosis, and flotillin-mediated endocytosis. It was unlikely that Panx1 internalization relied on phagocytosis, as Gehi *et al.* demonstrated that Panx1 was internalized and degraded in the previous study in the non-phagocytic HEK cell line (Gehi et al. 2011), deficient in phagocytic receptors and

related machinery (Licona-Limón et al. 2015) and, in Chapters 3 and 4, there was no evidence of engulfed particles triggering endocytosis. However, macropinocytosis remains a possible internalization mechanism, as well as any of the non-canonical small-scale pathways.

The upstream cell surface clustering of P2X7R and Panx1 preceding internalization provided hints as to the internalization mechanism involved. At the cell surface, several groups had identified two independently distributed P2X7R populations, one localized and the other excluded from lipid microdomains (Garcia-Marcos, Pérez-Andrés, et al. 2006; Bannas et al. 2005; Pfleger et al. 2012; Barth et al. 2007; Barth et al. 2008; Weinhold et al. 2010, reviewed in Robinson & Murrell-Lagnado 2013). Interestingly, localization of P2X7Rs to lipid microdomains required both membrane cholesterol, as cholesterol depletion redistributed P2X7R outside of lipid rafts (Garcia-Marcos, Pérez-Andrés, et al. 2006), and palmitoylation of P2X7R (Gonnord et al. 2009). Not only did P2X7R localize to lipid microdomains, they also regulated lipid metabolism via activation of phospholipases A2, C, and D (reviewed in Garcia-Marcos, Pochet, et al. 2006), processes which are intimately connected with endocytic trafficking (reviewed in Bohdanowicz & Grinstein 2013). Consequently, I hypothesized that **ATP stimulated P2X7R-Panx1 clustering and internalization via non-canonical mechanisms dependent on membrane cholesterol.**

In this chapter, I investigated the endocytic machinery required for ATP-evoked Panx1 internalization. First, I quantitatively determined that, like in HEK and BICR-M1R$_k$ cells (Gehi et al. 2011), Panx1 internalized in a non-canonical mechanism independent of clathrin, caveolin, and dynamin in N2a cells; however, ATP-evoked

Panx1 internalization in N2a cells was disrupted by both cholesterol depletion and aggregation, suggesting a non-canonical, yet cholesterol-dependent, mechanism. In further exploring non-canonical internalization mechanisms, I observed that amiloride, a selective inhibitor of macropinocytic endocytosis, disrupted ATP-evoked Panx1 internalization. In chapter 3, I identified that internalized Panx1 was sorted to recycling endosomes; however, the mechanism was not known. In this chapter, I determined that Arf6, a critical effector of non-canonical endocytic sorting, regulated Panx1 internalization and endosomal sorting, as co-expression with constitutively-active Arf6 Q67L led to accumulation of Panx1 in large intracellular vacuoles. After uncovering the non-canonical mechanism involved in Panx1 internalization, I determined that both depletion and aggregation of membrane cholesterol disrupted peripheral P2X7R-Panx1 clustering upstream of internalization (5 min after stimulation). Prior to beginning this study, Spagnol *et al.* identified that the Panx1 C-terminus contained a putative membrane interaction domain (Spagnol et al. 2014), thus I was interested in whether this region interacted with cholesterol or other specialized lipids. A GST-fused Panx1 C-terminus did not interact with cholesterol directly, yet it did interact significantly with phosphatidic acid (PA), a product of P2X7R-mediated lipid metabolism (reviewed in Garcia-Marcos, Pochet, et al. 2006) and regulator of endocytosis (Kooijman et al. 2003), as well as the phosphoinositides PI(4)P and PI(4,5)P_2 (reviewed in Bohdanowicz & Grinstein 2013). Together, the data presented in this chapter suggested that Panx1 internalization occurred through ATP-evoked cholesterol-dependent macropinocytosis, triggered by P2X7R-mediated phospholipid metabolism, with sorting to recycling endosomes regulated by the Arf6 GTPase.

5.2 ATP-evoked Panx1 internalization is independent of clathrin and caveolin, but dependent on cholesterol

Endocytosis mechanisms are typically grouped into two classes, the canonical clathrin-mediated endocytosis (CME) and clathrin-independent endocytosis (CIE), of which caveolin-mediated endocytosis is the canonical mechanism (reviewed in Maldonado-Baez et al. 2013). As clathrin-mediated endocytosis is the most ubiquitous form of receptor-mediated endocytosis, I first investigated whether clathrin-specific inhibition could disrupt ATP (500 μM)-evoked Panx1 internalization. Chlorpromazine (CLPZ), an established CME inhibitor (Okamoto et al. 2000; Vendeville et al. 2004; Sofer & Futerman 1995) did not attenuate ATP-evoked Panx1 internalization (Figure 5.1A,B). This suggested that clathrin and associated machinery were not involved.

Cholesterol regulates most endocytic mechanisms, particularly those associated with specialized lipid microdomains (reviewed in Kumari et al. 2010), as its integration within the cytofacial leaflet of the plasma membrane impacts membrane curvature and fluidity (Rodal et al. 1999). I investigated whether cholesterol was involved in ATP-evoked Panx1 internalization by using two cholesterol manipulating agents: filipin III (Fil III), which bound to and immobilized cholesterol *in situ* (Rothberg et al. 1990; Rothberg et al. 1992), and methyl-β-cyclodextrin (MβCD), which sequestered cholesterol from membranes (Klein et al. 1995). Following pre-incubation with Fil III (1 μg/mL), ATP-evoked intracellular Panx1 accumulation was disrupted (Figure 5.1C). MβCD pre-incubation (10 mM) also inhibited ATP-evoked accumulation of intracellular Panx1 (Figure 5.1D), which confirmed the critical role of cholesterol in Panx1 internalization.

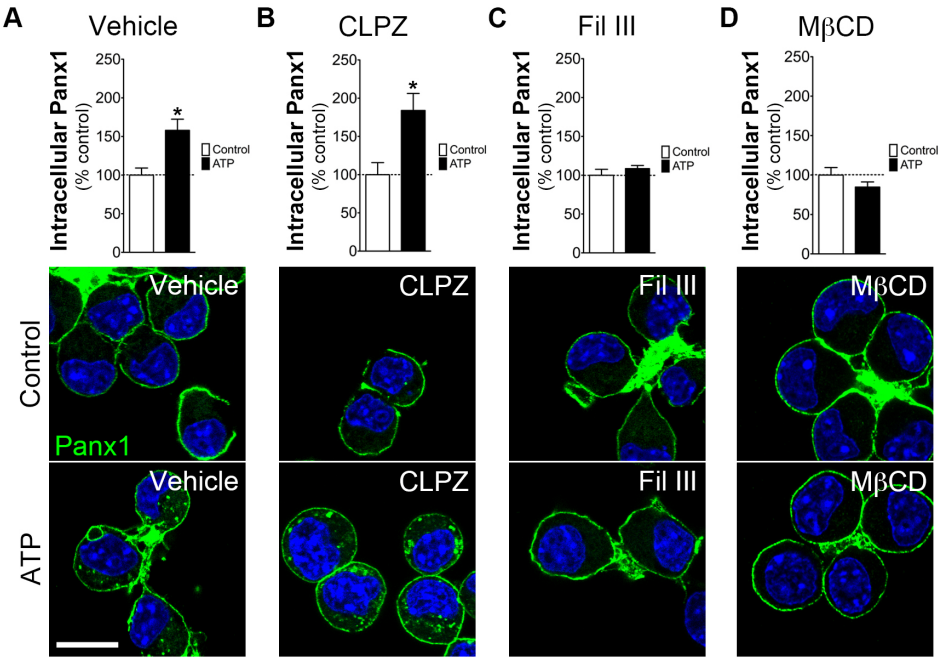

Figure 5.1 Panx1 internalization is clathrin-independent, but sensitive to membrane cholesterol modulation. Intracellular Panx1 relative to control conditions in Panx1-EGFP N2a cells incubated in vehicle control (A; DMSO), CLPZ (B; 10 μg/mL), Fil III (C; 1 μg/mL), or MβCD (D; 10 mM) for 1 h prior to treatment for 30 min with 500 μM ATP or vehicle control. Representative confocal images demonstrate distribution of Panx1-EGFP (green) in ATP and control-treated Panx1-EGFP N2a cells in the presence of each inhibitor or vehicle control. $N = 4$, Student's t test (*$p<0.05$). N refers to the number of coverslips from independent passages (≥ 30 cells analyzed per coverslip). Hoechst (blue) was used as a nuclear counterstain. Scale bars, 10 μm.

As cholesterol is critical for several endocytic mechanisms (reviewed in Mayor et al. 2014), I next aimed to target more specific endocytic machinery. Previous work demonstrated that internalized trans-membrane proteins employing caveolin or clathrin-dependent mechanisms are spatially coupled with caveolin or clathrin (Rappoport & Simon 2009), respectively. Co-distribution of Panx1 with Cav-1 (Figure 5.2A) and clathrin heavy chain (Figure 5.2B) was quantified following vehicle or ATP treatment by

comparing Pearson's correlation coefficients in each condition (as in Chapter 3). Co-distribution with machinery from either of these mechanisms was not enhanced upon ATP stimulation. Additionally, I capitalized on the fact that clathrin and caveolin-dependent mechanisms share a dynamin-scission step (reviewed in Danino & Hinshaw 2001). I observed that Dynasore, an inhibitor of dynamin I, dynamin II and mitochondrial dynamin (Macia et al. 2006; Kirchhausen et al. 2008), had no effect on ATP-induced accumulation of intracellular Panx1 relative to vehicle (Figure 5.2C), despite disrupting dynamin-dependent transferrin internalization. Altogether, these data implicated cholesterol in ATP-stimulated Panx1 internalization in a non-canonical mechanism that is independent of clathrin, caveolin, and dynamin.

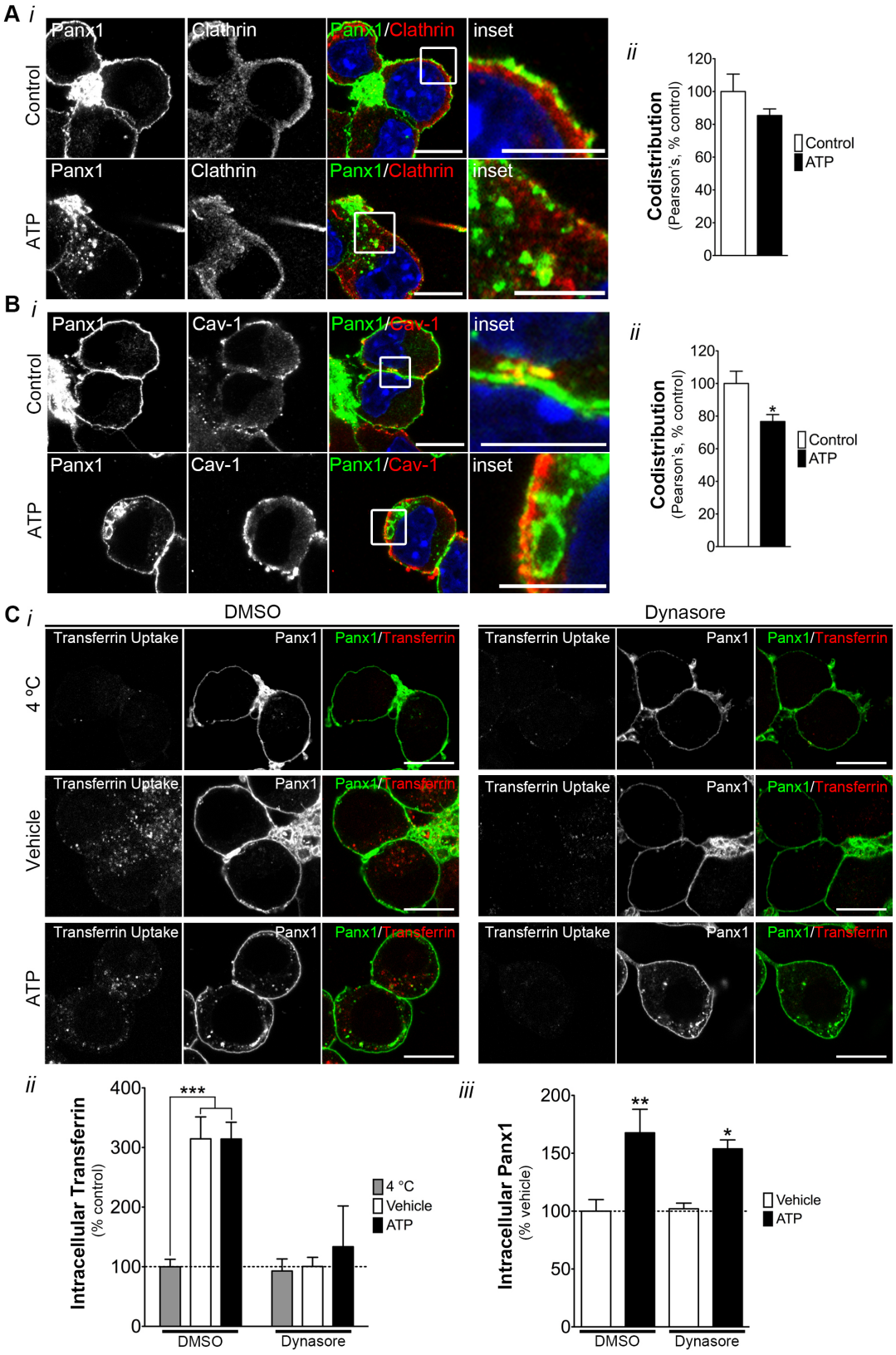
A i
Panx1
Clathrin
Panx1/Clathrin
inset
Control
ATP
ii
Codistribution
(Pearson's, % control)
Control
ATP
B i
Panx1
Cav-1
Panx1/Cav-1
inset
Control
ATP
ii
Codistribution
(Pearson's, % control)
Control
ATP
C i
DMSO
Dynasore
Transferrin Uptake
Panx1
Panx1/Transferrin
4 °C
Vehicle
ATP
ii
Intracellular Transferrin
(% control)
4 °C
Vehicle
ATP
DMSO
Dynasore
iii
Intracellular Panx1
(% vehicle)
Vehicle
ATP
DMSO
Dynasore

Figure 5.2 ATP-evoked Panx1 internalization is clathrin-, caveolin-, and dynamin-independent. (A) Confocal micrographs (*i*) of control (top panels) or ATP-treated (bottom panels) Panx1-EGFP N2a cells immunostained for clathrin heavy chain (clathrin; red). Panx1-EGFP-clathrin co-distribution in control and ATP-treated conditions is quantified in (ii). Inset scale bars = 5 μm. $N = 4$, Student's *t* test. (B) Confocal micrographs (i) of control (top panels) or ATP-treated (bottom panels) Panx1-EGFP N2a cells immunostained for Cav-1 (red). Panx1-EGFP-Cav-1 co-distribution in control and ATP-treated conditions is quantified in (*ii*). $N = 4$, Student's *t* test (*$p<0.05$). *N* refers to the number of coverslips from independent passages (≥ 30 cells analyzed per coverslip). (C) Confocal micrographs (*i*) of Panx1-EGFP N2a cells (green) pre-treated with vehicle (equivalent volume of DMSO) or Dynasore and incubated in 647-transferrin (red) at 4°C, then fixed and imaged immediately after 4°C incubation (top panels) or fixed and imaged after stimulation with vehicle (middle panels) or 500 μM ATP (bottom panels) for 30 min at 37°C. (*ii*) Intracellular 647-transferrin in cells pre-incubated with DMSO or Dynasore was quantified relative to 4°C control. (*iii*) Intracellular Panx1 in cells pre-incubated with DMSO or Dynasore was quantified relative to vehicle control. $N = 4$, one-way ANOVA with Dunnett's *post-hoc* (*$p<0.05$, **$p<0.01$). Hoechst (blue) was used as a nuclear counterstain. Scale bars, 10 μm.

5.3 Amiloride disrupts ATP-evoked Panx1 internalization

ATP-evoked Panx1 internalization in N2a cells occurred coincident with active filopodial dynamics (Movie 3.1, Chapter 3). Macropinocytosis is a cholesterol-dependent internalization mechanism that involves internalization of vesicles between 0.2 and 5 mm in size via membrane ruffling generated by actin-dependent filopodial generation (reviewed in Grimmer et al. 2002). Acidification of the submembranous region by inhibition of the Na^+/H^+ exchanger with amiloride (Koivusalo et al. 2010) disrupts the activity of both kinases and GTPases involved in actin remodelling required for macropinocytosis. In my study, pre-incubation with amiloride (300 μM) abrogated the

ATP-evoked internalization of Panx1 (Figure 5.3), suggesting Panx1 internalized via macropinocytosis.

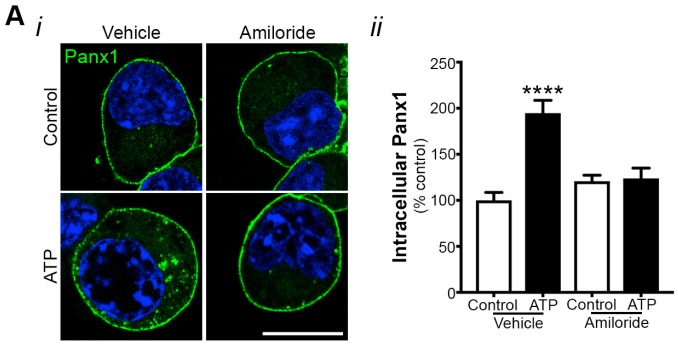

Figure 5.3 Panx1 internalization is amiloride-sensitive. (A) Confocal micrographs (*i*) of Panx1-EGFP (green) N2a cells pre-treated with vehicle (DMSO), or amiloride (300 μM) for 1 h prior to vehicle (water) or ATP (500 μM; 30 min). (*ii*) Intracellular Panx1 was quantified relative to vehicle control. $N = 4$, two-way ANOVA with Dunnett's *post hoc* (interaction: $F[1,12]=19.53$, $p=0.0008$; inhibitor: $F[1,12]=5.825$, $p=0.0327$; ATP: $F[1,12]=22.22$, $p=0.0005$, ****$p<0.0001$). Hoechst (blue) was used as a nuclear counterstain. Scale bars, 10 μm.

5.4 Internalized Panx1 is sorted by Arf6 GTPase

In chapter 3, I demonstrated that internalized Panx1 was targeted to recycling endosomes, following codistribution with early endosome markers (Rab14/Rab11; Figure 3.7). Arf6 is a critical regulator of endosomal sorting in several non-canonical endocytic pathways including macropinocytosis (Brown et al. 2001; Tang et al. 2015, reviewed in Maldonado-Baez et al. 2013). The Arf6 GTPase cycle involves the regulation of membrane phospholipids, which contribute to the recruitment of cytoskeletal elements (reviewed in Bohdanowicz & Grinstein 2013). GTP-bound Arf6 activates the phosphatidylinositol-4-phosphate 5-kinase in internalizing vesicles (Naslavsky et al. 2003). Next, inactivation of Arf6 (to GDP-bound Arf6) is required to reduce $PI(4,5)P_2$

levels to allow internalized vesicles to fuse with the sorting endosome. From here, Arf6 requires reactivation to induce sorting. Thus constitutively-active Arf6 mutants cause accumulation of non-canonical cargo proteins within large intracellular vacuoles upstream of sorting events (Naslavsky et al. 2003). To determine whether internalized Panx1 required Arf6-dependent sorting upon internalization, I co-expressed Arf6-CFP and its constitutively active Arf6Q67L-CFP in Panx1RFP N2a cells. Panx1-positive internalized vesicles were Arf6-positive in cells that co-expressed either the Arf6 or its constitutively active mutant (Figure 5.4Ai). However, Arf6Q67L significantly increased intracellular Panx1 (Figure 5.4Aii) and caused accumulation in large intracellular vacuoles (EEA1+; Figure 5.4Aiii). Together, this suggested that Panx1 internalization and endosomal sorting was regulated by Arf6.

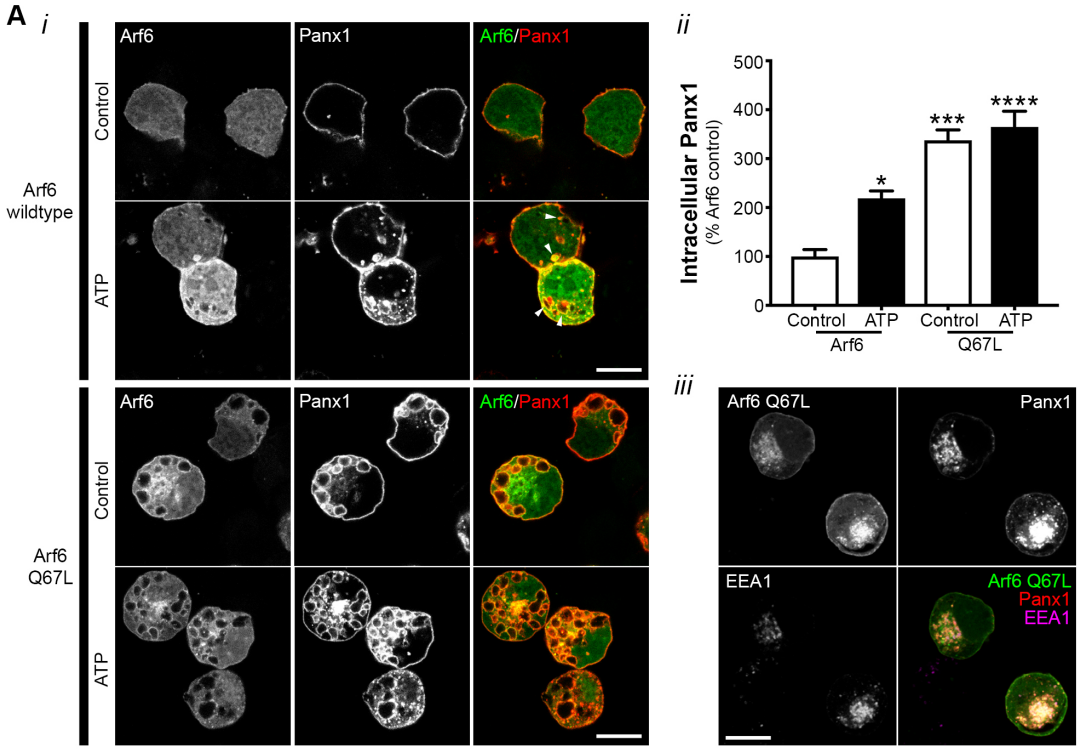

Figure 5.4 Sorting of internalized Panx1 is dependent on Arf6. (A) Confocal micrographs (*i*) of CHX-treated Panx1RFP (red) N2a cells transiently-transfected with Arf6-CFP or Arf6-Q67L-

CFP (48 h) prior to vehicle (water) or ATP (500 μM; 30 min), indicating accumulation of intracellular Panx1 with co-expression of constitutively active Arf6 mutant. White arrows indicate overlap of internalized vesicles. (*ii*) Intracellular Panx1 was quantified relative to Arf6-CFP control. $N = 3$, two-way ANOVA with Dunnett's *post hoc* (interaction: $F[1,8]=4.391$, $p=0.0694$; genotype: $F[1,8]=77.4$, $p<0.0001$; ATP: $F[1,8]=11.23$, $p=0.0101$, *$p<0.05$, ***$p<0.001$, ****$p<0.0001$). (iii) Representative confocal micrographs demonstrating accumulation of Panx1RFP (red) and Arf6-Q67L-CFP (green) in early endosomes (EEA1, magenta). *N* refers to the number of coverslips from independent passages (≥ 30 cells analyzed per coverslip). Scale bars, 10 μm.

5.5 Peripheral P2X7R-Panx1 clustering is regulated by membrane cholesterol

It was known prior to commencing my study that P2X7R-dependent association with lipid microdomains was sensitive to membrane cholesterol depletion (Garcia-Marcos, Pérez-Andrés, et al. 2006). Further, I demonstrated earlier that Panx1 internalization was disrupted by cholesterol immobilization or depletion (Figure 5.1). Following up on these findings, I aimed to determine if cholesterol was required for ATP-induced cell surface clustering of P2X7R-Panx1 (5 min post-treatment), upstream of internalization. ATP (500 μM; 5 min) was unable to induce P2X7R-Panx1 clustering at the cellular periphery following pre-incubation with Fil III (1 μg/mL) and MβCD (10 mM), suggesting that membrane cholesterol was critical for P2X7R-Panx1 signalling events upstream of the internalization process.

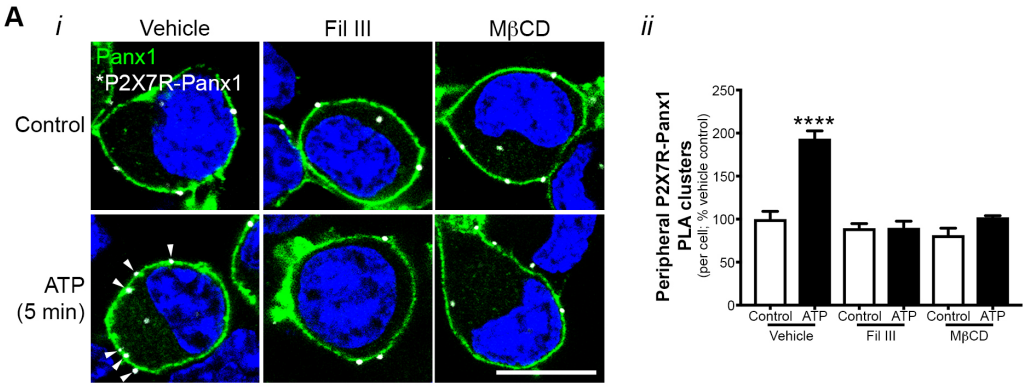

Figure 5.5 Peripheral P2X7R-Panx1 clustering is cholesterol-dependent (A) Representative confocal micrographs (*i*) demonstrating P2X7R-Panx1 clusters (white) in Panx1-EGFP (green) N2a cells pre-treated with vehicle (DMSO), or cholesterol disrupting agents, Fil III (1 μg/mL) and MβCD (10 mM) for 1 h prior to vehicle (water) or ATP (500 μM; 5 min). (*ii*) Peripheral P2X7R-Panx1 clusters were unchanged, in response to ATP (5 min), in the presence of either cholesterol-disrupting agent ($N = 3$, two-way ANOVA [interaction: $F(2, 12)=22.31$; $p<0.0001$; inhibitor: $F(2, 12)=38.99$, $p<0.0001$; ±ATP: $F(1, 12)=40.75$, $p<0.0001$] with Dunnett's *post-hoc*, ****$p<0.0001$). *N* refers to the number of coverslips from independent passages (≥ 30 cells analyzed per coverslip). Hoechst (blue) was used as a nuclear counterstain. Scale bar, 10 μm.

5.6 The Panx1 C-terminus interacts with several phospholipids

Not only have P2X7Rs been associated with lipid microdomains (Garcia-Marcos, Pérez-Andrés, et al. 2006; Bannas et al. 2005; Pfleger et al. 2012; Barth et al. 2007; Barth et al. 2008; Weinhold et al. 2010, reviewed in Robinson & Murrell-Lagnado 2013), they also regulated lipid metabolism (reviewed in Garcia-Marcos, Pochet, et al. 2006). The role of cholesterol in regulating P2X7R-Panx1 clustering and downstream internalization led to my investigation of whether Panx1 interacted with cholesterol or other membrane lipids linked to P2X7R signalling, enriched in lipid rafts, or involved in regulating endocytic events (reviewed in Garcia-Marcos, Pochet, et al. 2006). A putative lipid

interaction domain had previously been identified in the Panx1 C-terminus based on bioinformatics prediction and altered secondary structure of a partial C-terminal fragment in the presence of a mimetic detergent micelles (Spagnol et al. 2014). Thus, I was interested if the C-terminus in particular interacted with membrane lipids. GST-fused Panx1 C-terminus (GST-Panx1^{CT}) and GST alone were incubated with a hydrophobic membrane spotted with 15 different membrane lipids and then probed using GST and Panx1 antibodies (Figure 5.5). Interestingly, GST-Panx1^{CT} did not target cholesterol; however, it significantly interacted with PA, a product of P2X7R-mediated lipid metabolism (Le Stunff et al. 2004) and a regulator of membrane curvature during endocytosis (Kooijman et al. 2003; Kooijman et al. 2005), as well as phosphatinositol-4-monophosphate [PI(4)P] and phosphoinositol-4,5-bisphosphate [PI(4,5)P_2], key phospholipids involved in regulating trafficking events (reviewed in Bohdanowicz & Grinstein 2013).

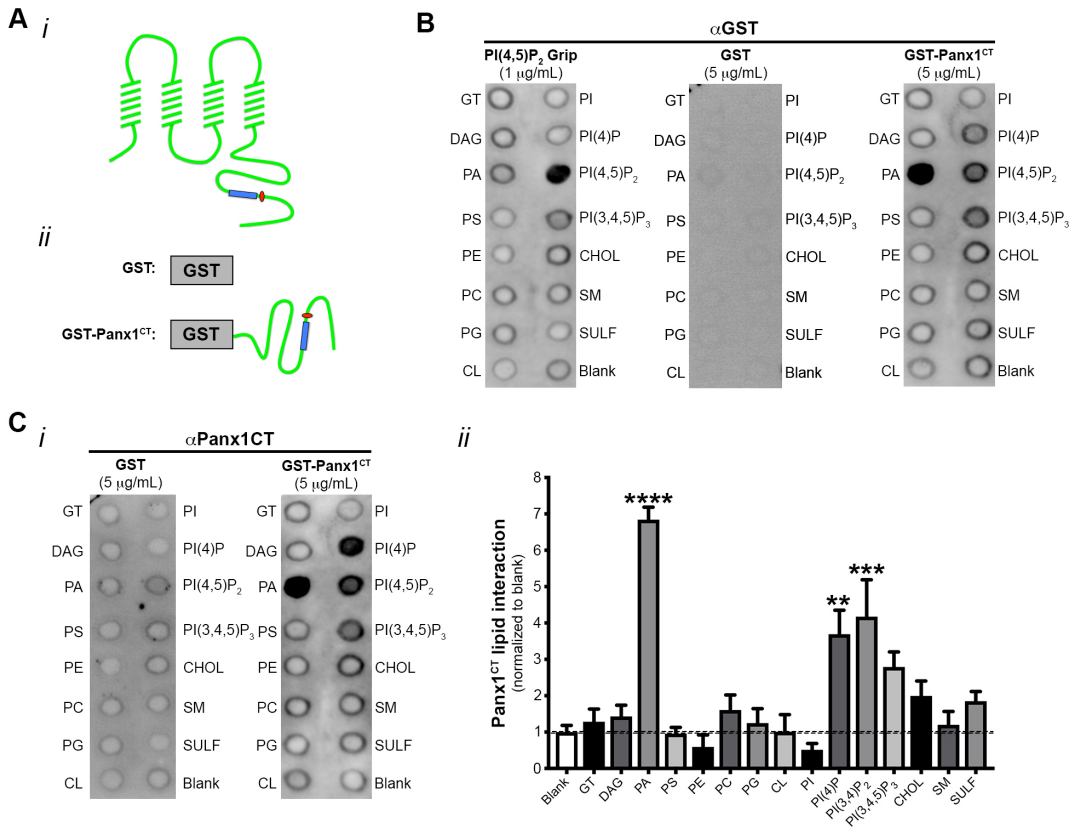

Figure 5.6 The Panx1 C-terminus interacts with phospholipids involved in endocytosis. (A) Schematic of (*i*) full-length Panx1 as well as (*ii*) GST and GST-fused Panx1 C-terminus (GST-Panx1^{CT}) indicating location of putative lipid interaction domain (blue rectangle) relative to the caspase cleavage site (red circle). Western blot (B) of Membrane Lipid Interaction Strip (hydrophobic membrane spotted with 15 different membrane lipids [GT – glyceryl tripalmitate, DAG – diacylglycerol, PA – phosphatidic acid, PS – phosphatidylserine, PE – phosphatidylethanolamine, PC – phosphatidylcholine, PG – phosphatidylglycerol, CL – cardiolipin, PI – phosphatidylinositol, PI(4)P – phosphatidylinositol 4-phosphate, PI(4,5)P_2 – phosphatidylinositol 4,5-bisphosphate, PI(3,4,5)P_3 – phosphatidylinositol 3,4,5-triphosphate, CHOL – cholesterol, SM – sphingomyelin, SULF – 3-sulfogalactosylceramide] and a blank [xylene cyanol FF]) incubated with purified peptides including positive control (PI(4,5)P2 Grip (1 μg/mL)), GST (5 μg/mL) or GST-Panx1^{CT} (5 μg/mL) and probed with GST antibody. (C) Western blot of Membrane Lipid Interaction Strip (*i*) that was pre-incubated with purified GST (5 μg/mL) or GST-Panx1^{CT} (5 μg/mL) and probed with Panx1CT antibody. (ii) Relative GST-Panx1^{CT} lipid interaction enrichment on Western blot, normalized to blank, was quantified using

densitometry. *N* = 3, one-way ANOVA with Dunnett's *post-hoc* (**p<0.01, ***p<0.001, ****p<0.0001).

5.7 Discussion

In this chapter, I identified that ATP-evoked Panx1 internalization occurred via cholesterol-dependent (clathrin, caveolin, and dynamin-independent) macropinocytosis. Cholesterol immobilization or depletion disrupted peripheral P2X7R-Panx1 clustering upstream of internalization. Upon internalization, endosomal sorting of Panx1 was Arf6 GTPase-dependent. The Panx1 C-terminus could be involved in targeting Panx1 to endocytosing vesicles nearby to P2X7R as it interacted with PA, PI(4)P, and PI(4,5)P_2, phospholipids present at the plasma membrane and involved in generating membrane curvature.

It was not surprising that P2X7R-Panx1 clustering and internalization was sensitive to modulation of membrane cholesterol, as there was robust evidence prior to commencing this study that membrane cholesterol regulated P2X7R cell surface distribution and stability in a multitude of cell types (reviewed in (Robinson & Murrell-Lagnado 2013)). Early fractionation evidence in rat submandibular cells suggested that two populations of plasma membrane localized P2X7Rs existed: the first where P2X7Rs were enriched in specialized lipid microdomains (>50% of total P2X7R protein) and a second group of P2X7Rs present in non-raft associated fractions (Garcia-Marcos, Pérez-Andrés, et al. 2006). These diverse P2X7R populations were also observed in lymphoma cells (Bannas et al. 2005), murine heart tissue (Pfleger et al. 2012), and alveolar epithelial cells (Barth et al. 2007; Barth et al. 2008; Weinhold et al. 2010). Following acute cholesterol sequestration with MβCD, P2X7R was eliminated from the lipid raft fraction,

suggesting that membrane cholesterol was critical for recruiting P2X7R to these domains (Garcia-Marcos, Pérez-Andrés, et al. 2006). MβCD treatment had no effect on ATP-evoked Ca^{2+} influx, suggesting the P2X7R was still present in the plasma membrane, but was redistributed outside of lipid-rich microdomains. P2X7R association with cell surface lipid microdomains was dependent on a palmitoylation modification (Gonnord et al. 2009). The functionality and signalling of P2X7R appeared to be different depending on whether it is localized inside or outside lipid raft domains (reviewed in Garcia-Marcos, Pochet, et al. 2006). For instance, P2X7Rs localized to lipid rafts were involved in phospholipid signalling and metabolism (activation of phospholipase A2 (Garcia-Marcos, Pérez-Andrés, et al. 2006), phospholipase D (Humphreys & Dubyak 1996); reviewed in Garcia-Marcos, Pochet, et al. 2006), while P2X7R outside of rafts was incapable of activating these metabolic pathways (Garcia-Marcos, Pérez-Andrés, et al. 2006; Garcia-Marcos, Pochet, et al. 2006). Conversely, depletion of membrane cholesterol led to enhanced P2X7R channel activity, based on cholesterol-sensitive motifs in the N-terminus and proximal C-terminus (Robinson et al. 2014). Consequently, P2X7R-Panx1 positive feedback might occur outside of rafts via pore formation, while targeting of P2X7R-Panx1 clusters to lipid rafts is involved in promoting negative feedback through lipid metabolism. Previous evidence based on changes to glycosylation species and immunofluorescence had suggested that Panx1 internalization occurred independent of cholesterol depletion (Gehi et al. 2011); however, these analyses were not quantitative and cell surface Panx1 immunofluorescence appeared to be enriched following MβCD treatment. Quantitatively revisiting cholesterol dependence in these cell types could be an avenue of future exploration.

ATP-mediated P2X7R activation promoted downstream activation of phospholipase D (PLD) in several studies (Le Stunff et al. 2004; Gargett et al. 1996; Fernando et al. 1999; Le Stunff & Raymond 2007; Hung & Sun 2002; reviewed in Garcia-Marcos, Pochet, et al. 2006). This was particularly relevant to my work because PLD hydrolyzes phosphatidylcholine into PA, the most significant lipid interaction partner of GST-Panx1^{CT} (Figure 5.6), and choline (reviewed in Garcia-Marcos, Pochet, et al. 2006). Although PA made up <2% of the lipid content of the plasma membrane (Vance & Steenbergen 2005), its unique features led to its disproportionately large role in cellular signalling events, including endocytic trafficking (reviewed in Bohdanowicz & Grinstein 2013). Due to its conical shape, focal accumulation of PA in the cytoplasmic leaflet of the plasma membrane promoted negative curvature of the membrane (Gallop et al. 2005). Several groups have described P2X7R-mediated activation of PLD in a number of other cell types including thymocytes (Le Stunff et al. 2004), lymphocytes (Fernando et al. 1999; Gargett et al. 1996), macrophages (Le Stunff & Raymond 2007; El-Moatassim & Dubyak 1992), and astrocyte-like cells (Hung & Sun 2002). The initial discovery of P2X7R-mediated PLD activation was in macrophages, where PLD activation occurred independent of changes in intracellular or extracellular Ca^{2+} levels (El-Moatassim & Dubyak 1992). However, Le Stunff *et al.* later determined that activation of PLD was stunted in thymocytes from P2X7R knockout (P2X7R$^{-/-}$) mice and positively associated with elevation of intracellular Ca^{2+} via ionomycin treatment (45 min) (Le Stunff et al. 2004). Although this suggested that P2X7R-mediated Ca^{2+} influx could modulate PLD activity, it did not demonstrate that it was necessary. In fact, chelation of intracellular Ca^{2+} was observed to potentiate PLD activity in another context

(Gargett et al. 1996). In a different study, coincident Ca^{2+}-dependent and Ca^{2+}-independent P2X7R-mediated PLD activation mechanisms were observed involving tyrosine kinases (Hung & Sun 2002). Interestingly, although prolonged P2X7R activation in thymocytes triggered downstream cell death, PLD inhibition did not disrupt P2X7R-mediated cell death in thymocytes, suggesting the P2X7R-mediated PLD activation had a death-independent function (Le Stunff et al. 2004). In support of this, PA generation via P2X7R-mediated PLD activation in macrophages negatively regulated P2X7R-mediated pore formation and promoted cell survival (Le Stunff & Raymond 2007). Although the authors did not investigate the mechanism of negative regulation (or whether the pore was intrinsic or Panx1-dependent), it is possible that this occurred by promoting Panx1 internalization, as this study was done in 2007 when Panx1 research was in its infancy. It is possible that in my studies, P2X7R-mediated PLD activation led to focal accumulation of PA (and subsequent membrane invagination) in regions where P2X7R and Panx1 were clustered, which triggered endocytosis via Panx1 C-terminus-PA interaction. Consequently future work should explore whether survival of macrophages and other cells co-expressing P2X7R and Panx1 is regulated by P2X7R-mediated PLD-activation of Panx1 internalization. Whether PLD activation and the production of PA are intermediate steps involved in the internalization mechanism is a potential avenue for future study.

Evidence suggested that palmitoylation (Gonnord et al. 2009) and the presence of membrane cholesterol (Garcia-Marcos, Pérez-Andrés, et al. 2006) were required for P2X7R localization to lipid rafts; however, GST-Panx1^{CT} did not directly interact with cholesterol. This indicated that either Panx1 required interaction with an accessory

protein (i.e. P2X7R) for cholesterol association or that there is another, yet to be determined, region of Panx1 that interacts with cholesterol. Depletion of membrane cholesterol is a useful tool to disrupt signalling in cholesterol-rich specialized lipid rafts (Rothberg et al. 1990); however, due to the multitude of roles for cellular cholesterol, this approach alone is not indicative of protein localization to rafts (reviewed in Laude & Prior 2004). Consequently, future work should use a combination of super resolution imaging to resolve Panx1/P2X7R co-distribution with specialized lipid microdomains, and subcellular fractionation to determine if Panx1 and P2X7R co-segregate in detergent-resistant fractions (indicating localization in lipid rafts) in an ATP-dependent manner.

Although the Panx1 C-terminus did not directly interact with cholesterol, it did however significantly interact with PA, mentioned above, as well as PI(4)P and PI(4,5)P_2 (Figure 5.6). Interestingly, these two phosphoinositides are the substrate and product of an enzymatic cycle critically linked to endocytic trafficking through regulated recruitment of GTPases and kinases involved in the cytoskeletal remodelling that underlies many endocytic events (reviewed in Bohdanowicz & Grinstein 2013). PI(4,5)P_2 localizes in and regulates actively-endocytosing regions of the cell surface during several internalization mechanisms including both clathrin- (Padron et al. 2003) and caveolin- (Fujita et al. 2009) mediated endocytosis, phagocytosis (Botelho et al. 2000; Beemiller et al. 2006), macropinocytosis (Grimmer et al. 2002; Haga et al. 2009), CLIC/GEEC endocytosis (Lundmark et al. 2008), and Arf6-mediated endocytosis (Brown et al. 2001) (reviewed in Bohdanowicz & Grinstein 2013). Here, PI(4,5)P_2 also activates PLD leading to the production of PA (reviewed in Weernink et al. 2007), which induces membrane curvature. During Arf6-mediated endocytosis, GTP-bound Arf6 activates PI(4)P 5-K

(Naslavsky et al. 2003), which triggers the conversion of PI(4)P into PI(4,5)P_2. Upon internalization, subsequent dephosphorylation of PI(4,5)P_2 is required for fusion of non-canonical cargo-containing vesicle with the sorting endosome. The constitutively active Arf6 Q67L mutant maintains high levels of PI(4,5)P_2 preventing fusion of these vesicles with the sorting endosome. However, Arf6 Q67L has also been described to facilitate internalization of cargo through other mechanisms of endocytosis, due to the generation of PI(4,5)P_2. The accumulation of Panx1 in Arf6-positive endosomal compartments in both Arf6-CFP and Arf6-Q67L-CFP (Figure 5.4), as well as the pharmacological data described in this chapter (amiloride/MβCD/Fil III-sensitivity, CLPZ-independence) suggested that Arf6 sorting is requisite downstream of Panx1 internalization. Finally, the increase in intracellular Panx1 in Arf6-Q67L-expressing cells (which accumulate internalized cargo prior to sorting into recycling endosomes) above ATP-evoked levels in wildtype Arf6-expressing cells (Figure 5.4) suggested that Panx1 was recycled back to the cell surface in recycling endosomes. Future experiments should explore whether P2X7R-Panx1 clusters are present in these Arf6 Q67L-generated vacuoles to definitively determine if they share an endocytic mechanism in N2a cells.

In chapter 3, I demonstrated that Panx1 was internalized to Rab11-/Rab14-positive endosomal compartments. Interestingly, both Arf6 and PLD have been linked to recycling into Rab14 (Lu & Wilson 2016) and Rab11-positive endosomes (Powelka et al. 2004; Idkowiak-Baldys et al. 2009). Like P2X7R, Arf6 activated PLD (Brown et al. 1993; Jovanovic et al. 2006), leading to the production of PA, which promoted filipodial membrane ruffling during endocytosis (Bohdanowicz et al. 2013; O'Luanaigh et al. 2002). However in work done prior to my studies, recycling of endosomal cargo back to

the plasma membrane also required Arf6-dependent PLD activation. Here, cells expressing an Arf6 mutant incapable of activating PLD (or wildtype Arf6 with disrupted PA generation) accumulated cargo in endosomal membranes that were unable to recycle back to the cell surface (Jovanovic et al. 2006). Recycling was rescued by activating PLD through Arf6-independent mechanism or addition of exogenous PA. Interestingly, it appeared that Rab14 activity was upstream of Arf6-mediated endosomal recycling. Knockdown of Rab14 led to disruption of cell surface targeting of recycling endosomal contents, which was rescued by Arf6 GTPase overexpression (Lu & Wilson 2016). These findings tie together the internalization of Panx1 through macropinocytic membranes and the sorting and possible recycling of Panx1 in Rab14-positive compartments by Arf6.

Macropinocytosis requires dynamic actin remodelling in submembranous regions to initiate filipodial development involved in the internalization process (reviewed in Ridley 2006). The Arp2/3 complex is critical for the generation of filopodia by regulating actin polymerization in the submembrane regions surrounding the site of macropinocytosis (Koivusalo et al. 2010). Our lab (Wicki-Stordeur & Swayne 2013) and others (Bhalla-Gehi et al. 2010) previously identified an interaction with the actin cytoskeleton, as well as the actin-regulatory protein, Arp3 (Wicki-Stordeur & Swayne 2013). Interestingly, co-distribution of Panx1 and both β-actin and Arp3 were most robust in regions of filipodial development (Wicki-Stordeur & Swayne 2013). Future experiments could investigate the regulatory role of the Panx1/Arp3 interaction on the genesis of macropinocytic filipodia. Further, corroboration with additional inhibitors of macropinocytosis is warranted to cement the role for this pathway in Panx1 internalization. Amiloride has off-target sites (including a family of amiloride-sensitive

sodium channels, reviewed in (de la Rosa et al. 2000)); thus, analysis of the consequence of dominant negative BARS expression (Liberali et al. 2008), a regulatory protein involved in macropinosome formation, should be included in future analyses. Further, whether ATP-regulated macropinocytosis was simply a negative feedback mechanism for Panx1 or if Panx1 was a critical component of macropinosome genesis in these cells should be addressed in future studies.

In summary, Panx1 internalization occurred via ATP-evoked cholesterol-dependent macropinocytosis, possibly through P2X7R-generated regulation of lipid metabolism (Figure 5.7). The P2X7R-Panx1 clustering was disrupted by cholesterol immobilization or depletion. Phospholipid-Panx1 interactions (including PA, PI(4)P, and PI(4,5)P_2) potentially regulated the internalization process. Upon internalization, Panx1 sorting to recycling endosomes was Arf6 GTPase-dependent. The impact of this internalization process on the diverse cell types where P2X7R and Panx1 are co-expressed should be the focus of future studies and will be a topic of discussion in chapter 6.

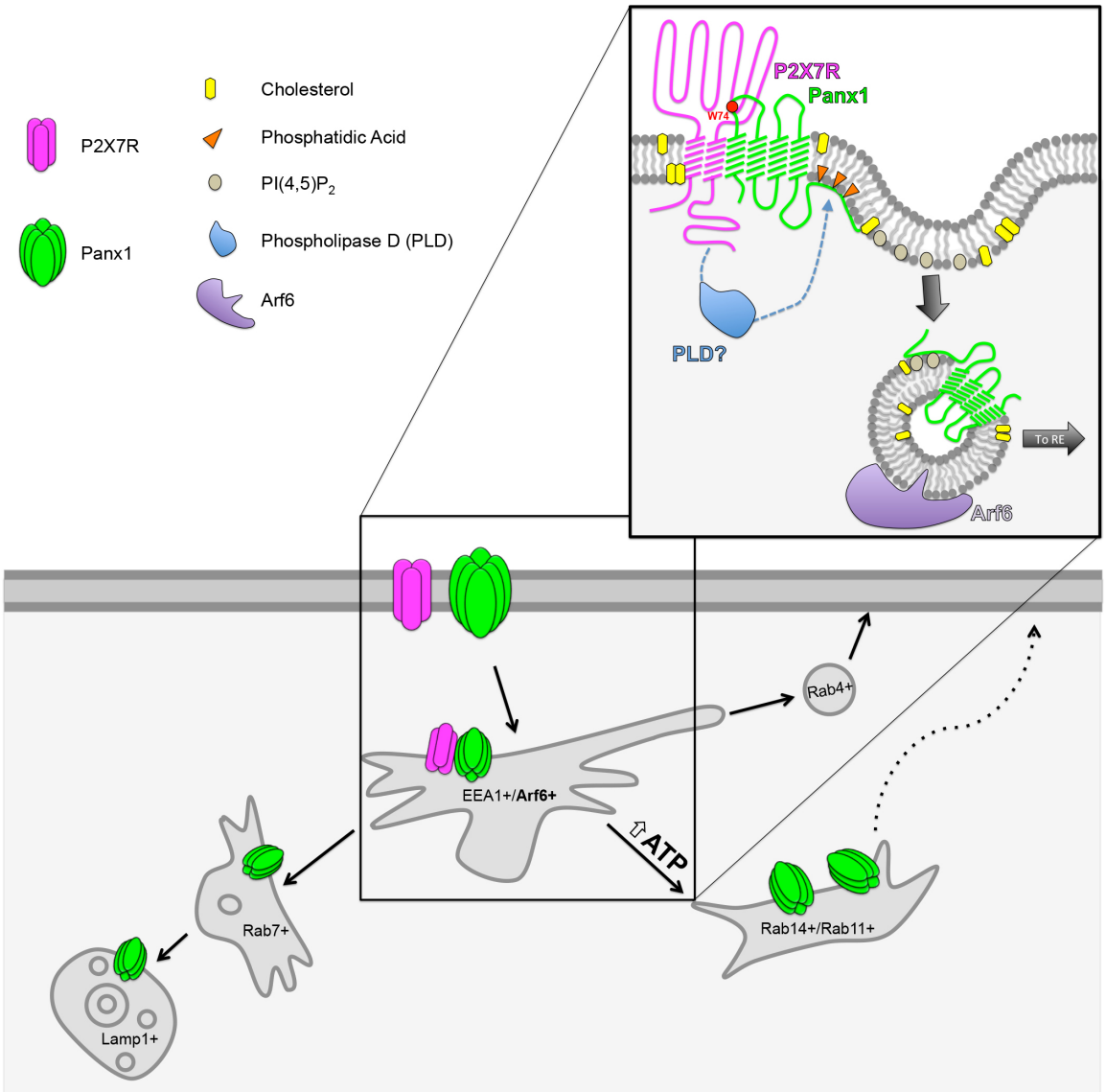

Figure 5.7 ATP triggers P2X7R-dependent macropinocytosis reliant on membrane cholesterol internalizes Panx1 into Arf6-positive vesicles. ATP-evoked P2X7R-Panx1 clustering at the cell periphery required membrane cholesterol. Following this, Panx1 is internalized into macropinosomes positive for Arf6 GTPase. Panx1 interacted through its C-terminus with phospholipid linked to P2X7R-mediated lipid metabolism, which potentially regulated the internalization process by forming membrane invaginations proximal to activated P2X7R-Panx1 clusters.

6 General Discussion:

The work presented in this dissertation revealed that the ATP release channel, Panx1, is endocytosed in response to elevated extracellular ATP in a P2X7R-, cholesterol-dependent macropinocytosis to recycling endosomes (Figure 6.1). P2X7R-Panx1 clustering on the cellular periphery occurred upstream of Panx1 internalization in response to elevated extracellular ATP. Here, I will present a general discussion, relating my findings to other Panxs, as well as detail future directions for exploring additional molecular mechanisms behind this behaviour. Further, I will elaborate on the consequence of some of the identified interactions for regulating other Panx behaviours and finally discuss scenarios where my findings would impact on cellular behaviours with a focus in the nervous system.

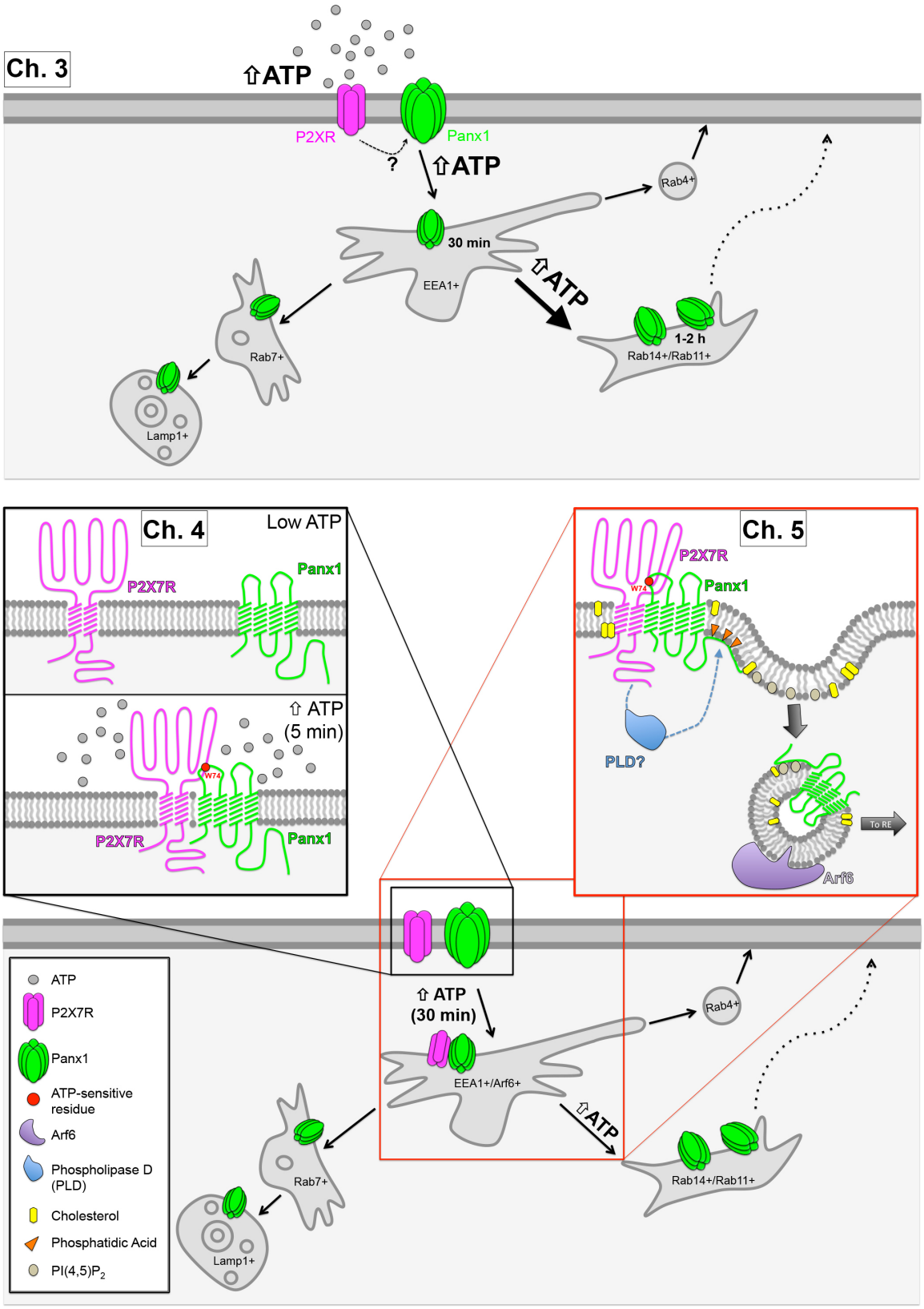
Ch. 3
⇧ATP
P2XR
Panx1
?
⇧ATP
Rab4+
30 min
EEA1+
⇧ATP
1-2 h
Rab14+/Rab11+
Rab7+
Lamp1+
Ch. 4
Low ATP
P2X7R
Panx1
⇧ ATP
(5 min)
W74
P2X7R
Panx1
Ch. 5
P2X7R
W74
Panx1
PLD?
To RE
Arf6
⇧ ATP
(30 min)
EEA1+/Arf6+
⇧ATP
Rab4+
Rab14+/Rab11+
Rab7+
Lamp1+
ATP
P2X7R
Panx1
ATP-sensitive residue
Arf6
Phospholipase D (PLD)
Cholesterol
Phosphatidic Acid
PI(4,5)P2

Figure 6.1 Regulation of Panx1 trafficking by ATP: summary of my dissertation. In chapter 3 (Ch. 3), I demonstrated that ATP stimulates dose- and time-dependent P2XR-mediated Panx1 endocytosis. Once internalized, Panx1 transited through the early endosome (30 min post-treatment) and was later enriched in recycling endosomes (1-2 h post-treatment). In chapter 4, I followed up on the chapter 3 finding that a P2X7R inhibitor (A438079) disrupted internalization and determined that both endogenous ATP release and exogenous ATP triggered P2X7R-Panx1 clustering, beginning at cell periphery (5 min) and then accumulating in intracellular compartments (30 min). ATP-evoked clustering occurred via a physical interaction between the extracellular domains of P2X7R and Panx1, which was disrupted along with downstream internalization by a W74A in the Panx1 EL1. Clustering was inhibited by A438079, yet was independent of common intracellular P2X7R-Panx1 signalling pathways associated with positive feedback mechanisms (Ca^{2+} and Src), suggesting an independent mechanism for negative feedback. In chapter 5, I determined that ATP-evoked P2X7R-Panx1 clustering at the cell periphery required membrane cholesterol. Following this, Panx1 internalized through a clathrin-, caveolin-, and dynamin-independent macropinocytic mechanism. Further, the Panx1 C-terminus interacted with phospholipids linked to P2X7R-activated lipid metabolism, which potentially regulated the internalization process by causing membrane invagination localized to activated or recently active P2X7R-Panx1 clusters.

6.1 ATP-mediated regulation of other Panxs?

The observation that ATP was capable of regulating both Panx1 channel activity (Qiu & Dahl 2009; Qiu et al. 2012; Ma et al. 2009; Kurtenbach et al. 2013) and cell surface stability leads to the question of *whether Panx1 is capable of modulation by extracellular ATP in other mammalian species*, particularly humans for translational impact. Clustal Omega alignment of the Panx1 extracellular loops determined that every ATP-sensitive residue (Figure 6.2A), including W74 (implicated in P2X7R-Panx1 clustering and internalization), was homologous across humans, rats, and mice, suggesting that my findings could be physiologically relevant across mammalian species (Figure 6.2B).

Whether other Panx family members are sensitive to elevated extracellular ATP is also an unresolved question. A Clustal Omega sequence alignment (Figure 6.2C; Sievers et al. 2011) between the extracellular loops of Panx1, Panx2, and Panx3 demonstrated that Panx1 W74, along with downstream ATP-sensitive residues (S93 and L94) of the Panx1 EL1, were not conserved between family members; however, the neighbouring basic and ATP-sensitive residue (R75) was conserved in Panx3 and aligned with position 74 in Panx2. However, unlike Panx1 that is glycosylated on its second extracellular loop, Panx3 is glycosylated at N71 in the Panx3 EL1, while Panx2 is predicted to be glycosylated at N86 of its EL1, as well (Penuela et al. 2009). The proximity of these glycosyl groups to positions aligning with 74/75 of Panx1 could alter the putative interaction between P2X receptors and the other Panx protein involved in triggering endocytosis. In EL2, Panx1 and Panx3 are homologous at Panx1 D240 and I247, while all three share the leucine at Panx1 position 266. Whether these conserved residues are sufficient to allow for ATP-dependent channel regulation is a potential area of future study; however, to date, there is no evidence to my knowledge of interactions between P2 receptors and the other Panx family members, which suggests that this could be a Panx1-specific phenomenon.

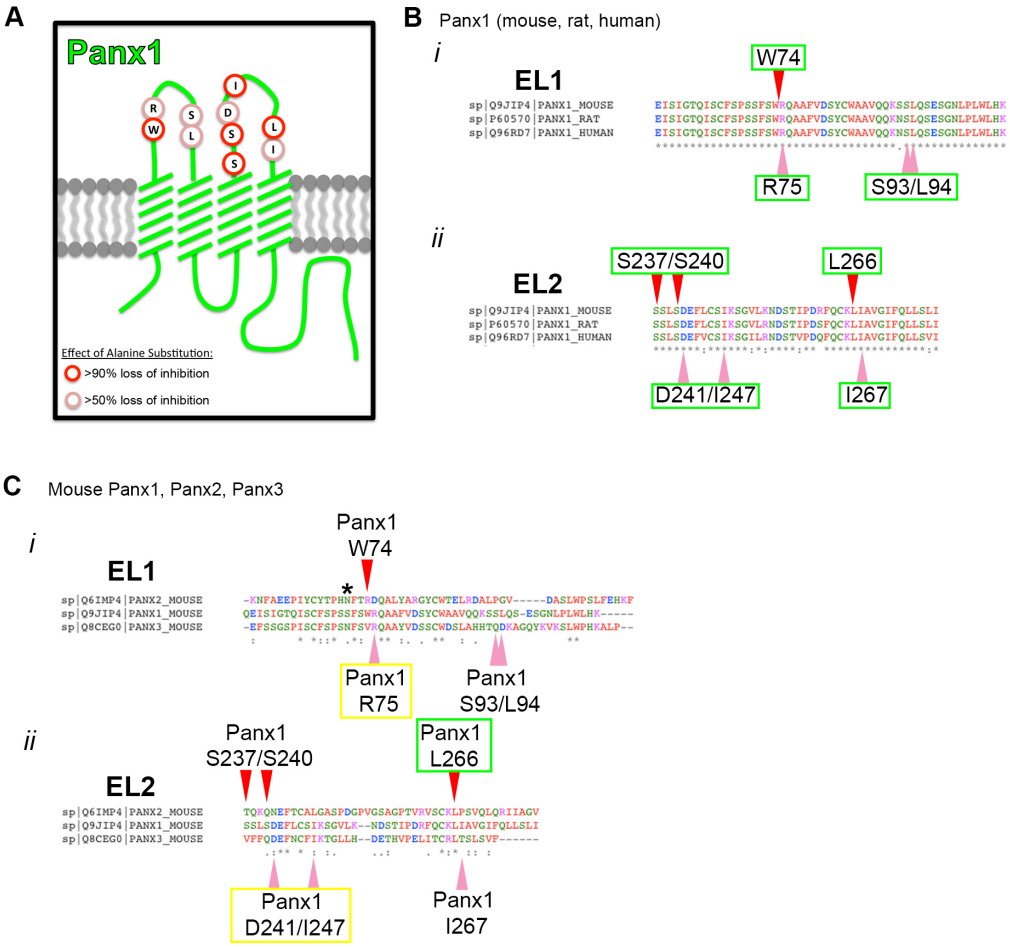

Figure 6.2 Conservation of ATP-sensitive residues between Panxs. (A) Schematic representing ATP-sensitive residues identified in mouse Panx1 by Qiu, Wang, & Dahl (2012), including W74 that regulates internalization. (B) Clustal Omega alignment of the mouse, rat, and human Panx1 (i) EL1 and (ii) EL2 demonstrate conservation of every ATP-sensitive residue between three species (green box). (C) Clustal Omega alignment of the (i) EL1 and (ii) EL2 between mouse Panx1, Panx2, Panx3 demonstrate partial conservation of three ATP-sensitive residues between Panx1 and Panx3 (yellow box; Panx1 R75, D241, I247) and conservation of one ATP-sensitive residue between three species (green box; Panx1 L266). Asterisk indicates the locus of Panx3 glycosylation, and predicted Panx2 glycosylation.

6.2 Role of other P2X receptors in Panx1 internalization?

My findings also generated the question of *whether other P2X receptors are capable of triggering internalization*. As P2X7R was the primary functional expressed at the cell surface of N2a cells (Gomez-Villafuertes et al. 2009), it is possible that other P2X receptors are capable of influencing Panx1 trafficking in different cell types. However, there are several important considerations that could impact on this possibility. First, P2X receptors possessed highly conserved ectodomains (reviewed in Habermacher et al. 2016), allowing for the possibility of a conserved Panx1 interaction site. However in my studies, the selective P2X7R inhibitor A438079 disrupted P2X7R-Panx1 clustering and internalization. Consistent with other selective inhibitors described in a recent high resolution structural study of P2X7R (Karasawa & Kawate 2016), it is likely that A438079 interacts with a P2X7R-specific antagonist binding pocket and 'locks' P2X7R in a resting conformational state. The P2X7R-specific antagonist-binding pocket that was absent in other crystallized P2X receptors [P2X3R (Mansoor et al. 2016), P2X4R (Kawate et al. 2009; Hattori & Gouaux 2012)], suggesting that unique structural elements could be involved in the P2X7R-Panx1 extracellular interaction. However, to confirm this prediction, the precise residues of P2X7R involved in P2X7R-Panx1 interaction should be the focus of future studies. Further, the elongated and unique C-terminus of P2X7R conveys unique signalling capabilities, including its ability to regulate lipid metabolism of the phospholipids I identified to interact with the Panx1 C-terminus (Chapter 5; Garcia-Marcos, Pochet, et al. 2006). Therefore, even if other P2X receptors were able to interact with Panx1 via their ectodomains, they may not provide the local lipid metabolism required to generate endocytosis [i.e. membrane curvature via PA

(Cazzolli et al. 2006; Kooijman et al. 2003) or GTPase/kinase recruitment and cytoskeletal rearrangement via PI(4,5)P_2 (Botelho et al. 2000)].

Despite the inability of other P2X receptors to directly stimulate Panx1 internalization, they could modulate P2X7R-Panx1 crosstalk in this context. It is common for a single cell type to express several subtypes of both P2X receptors (reviewed in North 2002). Although P2X7R formed exclusively homomeric channels, they were capable of interacting in complexes with other P2 receptors, in particular P2X4R (Boumechache et al. 2009; Nicke 2008; Casas-Pruneda et al. 2009; Draganov et al. 2015; Hung et al. 2013). In most cell types, P2X4R was primarily distributed to the lysosome (Huang et al. 2014; Xu et al. 2014; Qureshi et al. 2007); however, P2X4R was identified in a physical complex with P2X7R and Panx1 in gingival epithelial cells (Hung et al. 2013). Selective activation of P2X4R with ivermectin in cells co-expressing P2X4R, P2X7R, and Panx1 potentiated P2X7R activation and downstream Panx1-mediated ATP release (Draganov et al. 2015). This suggested that the addition of P2X4R to P2X7R-Panx1 complexes could also affect internalization cues. Another example occurs during T cell activation, when P2X1R, P2X4R, and Panx1 are recruited to the immune synapse where P2X7R is resident (Woehrle et al. 2010). Not only are diverse P2X receptors present at the immune synapse, these membrane specializations are also rich in specialized phospholipids (reviewed in Harder & Engelhardt 2004), suggesting the potential for crosstalk between P2X7R-Panx1 and other P2X receptors in regulating Panx1 cell surface stability during an immune response. T-cell receptor activation triggers the release of ATP (Filippini et al. 1990), in part through Panx1 channels (Schenk et al. 2008), which mediates T-cell-target cell interactions. Consequently,

interplay between membrane lipids as well as P2X4R could modulate the P2X7R-Panx1 crosstalk involved in T cell activation and subsequent Panx1 internalization may contribute to the resolution of the immune response. Crosstalk between other P2X receptors and P2X7R-mediated Panx1 internalization could occur when cells express a complement of P2 receptors at the cell surface and should be investigated in the future.

6.3 Regulatory roles of the C-terminus in Panx1 trafficking and beyond

The interaction between the Panx1 C-terminus and specialized phospholipids has many implications for not only trafficking, but Panx1 function and related behaviours as well. As the most divergent domain in Panx proteins, the C-terminus has determined several of the unique features of Panx1 (reviewed in Penuela et al. 2013). Not only was it a critical regulator of anterograde trafficking (Gehi et al. 2011; Wicki-Stordeur et al. 2013) and the locus of interaction with the actin cytoskeleton (Bhalla-Gehi et al. 2010), it also contained several critical elements involved in modulating Panx1 function including a Src phosphorylation site (Weilinger et al. 2016) and a caspase 3/7/11 cleavage site (Sandilos et al. 2012; Chekeni et al. 2010; Chiu et al. 2017; Yang et al. 2015, reviewed in Boyce et al. 2017). Experimental evidence suggested that Panx1 inhibition occurs through C-terminal-dependent ball-and-chain interaction with the Panx1 pore (Wang & Dahl 2010; Sandilos et al. 2012; Chiu et al. 2017). Consequently, any interactions localized to the C-terminus of Panx1 have the potential to modulate not only channel trafficking, but also channel activity. Phospholipid-dependent modulation of channel activity, particularly via PI(4,5)P_2, has been observed for other membrane channels

including P2X receptors (Zhao et al. 2007; Bernier et al. 2008, reviewed in Hansen 2015; Hille et al. 2015). Although the precise C-terminal residues in Panx1 involved with each of the interacting phospholipids were not identified, the discovery of a lipid-sensitive region (Figure 6.3A, I360-G370; Spagnol et al. 2014) immediately proximal to the caspase 3/7/11 cleavage site suggested that these residues could mediate the interactions. The precise residues within the Panx1 C-terminus involved in these phospholipid interactions, as well as the effect of C-terminal cleavage and other PTMs on regulating these interactions should be a focus of future investigation. Caspase-dependent cleavage of Panx1 promoted constitutive activation (Chekeni et al. 2010; Sandilos et al. 2012) of the channel, which was proposed to occur through loss of steric hindrance of the pore (Chiu et al. 2017). If phospholipid interactions occurred downstream of the caspase cleavage site in the distal C-terminus (not within the putative membrane interaction domain) and were integral to ATP-mediated Panx1 internalization, it is possible that proteolytic cleavage of Panx1 would disrupt its internalization ability, losing its negative feedback mechanism and supporting constitutive activation.

Transient activation of Panx1 via receptor-mediated interactions (either through physical coupling or PTMs) was speculated to occur by inducing a ‘flapping’ motion of the autoinhibitory C-terminal tail (Chiu et al. 2017). Consequently, many scenarios exist where Panx1 C-terminus-phospholipid interactions could also play a unique modulatory role in receptor-mediated events. An example of this is during NMDAR-mediated activation of Panx1 channels. During investigation of Panx1 expression and subcellular localization in the nervous system, Panx1 was observed in the post-synaptic density of pyramidal neurons of the hippocampus and cortex (Zoidl et al. 2007). There, it has since

been associated with potentiation of NMDAR activity in response to epileptogenic/excitotoxic NMDAR stimulation (Thompson et al. 2008; Weilinger et al. 2016) and ischemia (Thompson et al. 2006; Weilinger et al. 2012) via Src-mediated signalling (Weilinger et al. 2012; Weilinger et al. 2016). Post-synaptic densities shared close proximity to specialized lipid microdomains in the post-synaptic membrane (reviewed in Dotti et al. 2014; Suzuki 2002). Interestingly, more than 85% of Src protein was localized to specialized lipid microdomains in the post-synaptic membrane (Besshoh et al. 2005), suggesting that NMDAR-Panx1 coupling was likely to occur within or proximal to rafts. The NMDAR-mediated Src phosphorylation site in Panx1 was recently localized in the C-terminus [Y308 (Weilinger et al. 2012; Weilinger et al. 2016)]; thus, NMDAR-Panx1 signalling could also be altered by Panx1 C-terminus-phospholipid interactions. Further, Panx1 was implicated in other NMDAR-related behaviours, including bidirectional regulation of synaptic plasticity (Prochnow et al. 2012; Ardiles et al. 2014), where it impacted on learning and memory (Prochnow et al. 2012). These too could be impacted by lipid-Panx1 interactions. Conversely, NMDAR activation also triggers phospholipid metabolism, activating PI(4)P 5-kinase production of PI(4,5)P_2, which promoted modulation of AMPA receptor endocytosis during LTD (Unoki et al. 2012). It is possible that here, NMDARs are also capable of directly or indirectly altering Panx1 cell surface stability by modulating membrane lipid components. Consequently, future experiments should explore the role of Panx1-phospholipid interactions in regulating NMDAR-dependent signalling in the synapse.

The investigation of these aims could begin by disrupting the membrane interacting region using targeted alanine-scanning mutagenesis. Importantly, the role of

this particular region may be more complex than simply interacting with phospholipids. In a review I published in 2014 on Panx1 trafficking (Boyce et al. 2014), I uncovered several potential endosomal-targeting motifs enriched in the Panx1 C-terminus, using a combination of bioinformatics prediction tools (Eukaryotic Linear Motifs; Dinkel et al. 2016) and matching with known targeting motifs (Kelly & Owen 2011; Behnke et al. 2011; Bonifacino & Traub 2003; Figure 6.3A). These motifs interacted with protein effectors of endocytosis and sorting for degradation (reviewed in Bonifacino & Traub 2003). One of the identified motifs (D361PMLL) overlapped with the putative membrane interacting region (I360-G370, Figure 6.3A). Consequently, future studies should use mutagenesis of the membrane interaction domain and the endosomal targeting sequence, or selectively disrupt one of the motifs while maintaining the other. The role of these alanine-substitution mutants in Panx1 function, stability, and trafficking will be the subject of future investigation.

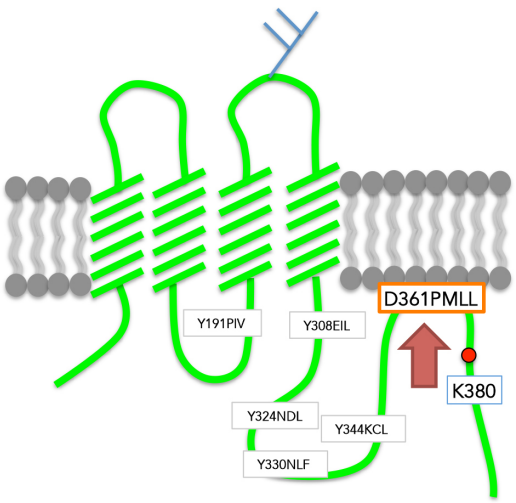

B

Sequence (IDPMLLLTNLG)	Membrane Interacting	Endosomal Targetting
IDEMLLLTNLG	Disrupts	Maintains
IDEMLELTNLG	Disrupts	Disrupts
IEEMLLLTNLG	Disrupts	Maintains
IEPMLLLTNLG	Disrupts	Maintains
EDPMLLLTNLG	Disrupts	Maintains
IDPMLELTNLG	Disrupts	Disrupts
IDPMEELTNLG	Disrupts	Disrupts
IDPMEEETNLG	Disrupts	Disrupts
IDPMLLLENLG	Disrupts	Maintains
IDEMLLLTELG	Disrupts	Maintains
IDEMLLLTNEG	Disrupts	Maintains
IDEMLLLTNLE	Disrupts	Maintains
IDEMAAATNLG	Disrupts	Disrupts
IDEMALATNLG	Disrupts	Disrupts
IDEMAALTNLG	Disrupts	Disrupts
IDEMALLTNLG	Disrupts	Maintains
IAPMAALTNLG	Maintains	Disrupts
IAPMALLTNLG	Maintains	Disrupts
IAPMLLLTNLG	Maintains	Disrupts
IDPMALLTNLG	Maintains	Maintains
IDPMAALTNLG	Disrupts	Disrupts
IDPMAAATNLG	Disrupts	Disrupts
IAPMALATNLG	Maintains	Disrupts
IDAMALATNLG	Maintains	Disrupts
IDPMLLLAAAA	Maintains	Maintains
IDPMLLLAAAG	Maintains	Maintains
IDPMLLLAALG	Maintains	Maintains
IDPMLLLANLG	Maintains	Maintains
ADPMAALAAAA	Maintains	Disrupts

Figure 6.3 Potential regulators of Panx1 trafficking are enriched in the C-terminus. (A) Panx1 contains putative endocytic recognition sequences and endolysosomal targeting sequences and a conserved ubiquitination site (K380; blue box). A combination of known targeting motifs and bioinformatics tools predict that Panx1 contains both an endolysosomal targeting sequence (orange box; "*TRG_LysEnd_APsAcLL"; overlapping with the membrane interaction domain (I360-G370)) and endocytic recognition sequences (grey box; "TRG_ENDOCYTOTIC_2"). Red circle indicates caspase cleavage site (D378). (B) *In silico* analysis of potential alanine substitution mutants for future studies that selectively disrupt either the membrane interaction domain or the endolysosomal targeting sequence or disrupt both.

6.4 Investigation of novel regulators of Panx1 trafficking

Our lab recently discovered interactions between endogenous Panx1 and components of the actin-related machinery involved in macropinocytic endocytosis

(actin, Arp3) using an unbiased proteomics approach (Bhalla-Gehi et al. 2010; Wicki-Stordeur & Swayne 2013). This involved immunoprecipitating Panx1 from N2a cells expressing either EGFP or Panx1-EGFP with subsequent liquid chromatography coupled to tandem mass spectrometry (LC-MS/MS) and confirming with endogenous Panx1 IP (Wicki-Stordeur & Swayne 2013). Amongst the list of putative interactors (480 total) are several proteins involved in lipid metabolism and non-canonical endocytic mechanisms that could inform future research in the field. My dissertation work identified a significant interaction with the phospholipids PA, PI(4)P, and PI(4,5)P_2 localized to the C-terminal region of Panx1 (Chapter 5), so I will focus my discussion on two of the putative interactors directly linked to these specialized lipids.

First, our unbiased proteomics approach identified two subunits (β and δ) of the PI(4,5)P_2 3-kinase, which phosphorylates PI(4,5)P_2 to generate PI(3,4,5)P_3. The elimination of PI(4,5)P_2 and creation of PI(3,4,5)P_3 is a critical regulatory step in the later stages of macropinocytosis, required for the closure of a macropinosome from membrane ruffles (Araki et al. 2007). Future investigation should aim to confirm this interaction and determine whether inhibition of PI(4,5)P_2 3-kinase disrupts Panx1 internalization.

An additional putative interactor may help to identify the role of the C-terminus in promoting cell surface expression. During anterograde trafficking, the C-terminus was required for proper targeting of *de novo* synthesized Panx1. Truncation of the Panx1 C-terminus (Panx1Δ307) led to retention in the ER with subsequent proteasomal degradation (Gehi et al. 2011). Our unbiased proteomics analysis identified the ER-resident lysophosphatidic acid acyltransferase-α (LPAAT-α; Aguado & Campbell 1998), which converts lysophosphatidic acid into PA in the secretory pathway, a process that

promotes negative membrane curvature (Gallop et al. 2005) and ER-Golgi vesicular formation. Consequently, interaction between the Panx1 C-terminus and PA-enriched and budding ER-Golgi vesicles would promote anterograde trafficking. Absent of this C-terminal localized lipid interaction, Panx1Δ307 may have been held up within the ER. However, in a study I co-authored, a Panx2^{Panx1CT} chimer was able to clear the ER, yet was not expressed at the cell surface or the M6PR-positive late endosome (where Panx2 resides in N2a cells) and instead distributed diffusely in intracellular compartments (Wicki-Stordeur et al. 2013). This suggested that there were additional elements in the Panx1 sequence required for cell surface localization. This likely involved the differential regulation of Panx glycosylation (Penuela et al. 2009), as Panx2 does not undergo the complex glycosylation that promotes anterograde trafficking to the cell surface.

Finally, Panx1 was recently identified to contain a ubiquitination site (K380) in the distal C-terminus (Kim et al. 2011), which is conserved in humans and murine species (Boyce et al. 2017). Given the role of mono-ubiquitination in trafficking and turnover of membrane proteins (Schwartz 2003), as well as poly-ubiquitination in proteasomal degradation (Lemus & Goder 2014), the impact of this PTM on trafficking events should be a topic for future investigation.

6.5 P2X7R-Panx1 crosstalk in the nervous system

Not only was extracellular ATP-mediated signalling first discovered in the nervous system (reviewed in Burnstock 2011), it has since been implicated in many physiological and pathophysiological processes in this system including trophic

regulation of neurogenesis (Suyama et al. 2012) or recruiting immune cells to injury loci (Ohsawa et al. 2010), as well as acting as a fast neurotransmitter to modulate synaptic plasticity and pain transmission (reviewed in Chiu et al. 2014; Lohman & Isakson 2014; Baroja-Mazo et al. 2013). As in other tissues, ATP release in the nervous system occurs through either (1) constitutive or regulated vesicular release (Pankratov et al. 2006), (2) activation of Panx1 and other large-pore channels (reviewed in Dubyak & el-Moatassim 1993; Burnstock et al. 2011; Abbracchio et al. 2009; Burnstock 2016), or (3) during cellular lysis following trauma. There are several reasons to expect extracellular ATP to be dynamic and reach particularly high concentrations in the nervous system. First, the nervous system contains several contexts with particularly tight dimensional constraints, including the synaptic cleft, neurogenic niches, and the spinal cord, where the tightly-packed cellular components leads to compaction of the extracellular environment. In the synaptic cleft, taking into account the diffusion of neurotransmitters (Rusakov & Kullmann 1998), as well as the concentration of ATP in synaptic vesicles (150-200 mM (Van Der Kloot 2003)), the peak ATP concentrations proximal to release sites was predicted to be as high as 500 μM (reviewed in Pankratov et al. 2006), which reflected the concentration ranges capable of eliciting internalization used in my studies.

Both P2X7R and Panx1 are expressed in numerous cell types across the nervous system. The expression of Panx1 is developmentally regulated across the nervous system. Panx1 mRNA expression has been detected as early as embryonic day 9.5 (E9.5) in mice (Raslan et al. 2016) and was expressed at a relatively high level during the perinatal period (peaking at E18 in mice (Ray et al. 2005), postnatal day 1 in rats (Vogt et al. 2005)) before decreasing dramatically into adulthood (Vogt et al. 2005). Reduced Panx1

expression in the CNS with age was later paralleled at the protein level in the hippocampus, cortex, and cerebellum (Ardiles et al. 2014). In adult mice, Panx1 was expressed in neural stem and progenitor cells of the subventricular zone (SVZ (Wicki-Stordeur et al. 2012)), as well as in immature neurons (Wicki-Stordeur & Swayne 2013). Although expressed at the highest levels during the developmental period, Panx1 remained widely expressed in diverse populations of mature neurons across the brain (Ray et al. 2005; Vogt et al. 2005; Zoidl et al. 2007). *In situ* hybridization and immunohistochemistry indicated widespread Panx1 expression in most pyramidal cells, as well as GABAergic interneurons (Ray et al. 2005; Vogt et al. 2005) of the adult hippocampus and cortex (Ray et al. 2005; Vogt et al. 2005), the prefrontal cortex (Vogt et al. 2005), as well as the thalamus, hypothalamus, brain stem, cerebellum, and retina (Ray et al. 2005; Vogt et al. 2005). Importantly, immuno-electron microscopy identified enrichment of Panx1 immunolabeling in the post-synaptic density of hippocampal and cortical neurons (Zoidl et al. 2007), accompanied by strong peri-nuclear cytoplasmic staining.

Expression of Panx1 in extra-neuronal populations of the CNS has been a more contentious issue. Initial investigation of Panx1 expression in the CNS, saw no *Panx1* transcripts, or proteins, in astrocytes of the murine nervous system (Vogt et al. 2005; Ray et al. 2005; Zappala et al. 2007). However, more recently, Boassa *et al* observed Panx1 and Panx2 codistribution *in situ* with glial fibrillary acid protein (GFAP), an astrocyte marker in murine hippocampal slices (Boassa et al. 2014). Several groups observed Panx1 expression in cultured astrocytes from diverse regions of the brain and spinal cord (reviewed in Freitas-Andrade & Naus 2016), where Panx1-mediated ATP release was

linked to neuroinflammatory (Garré et al. 2010) and pain-related (Koyanagi et al. 2016) signalling pathways. The differences in astrocytic Panx1 expression *in vivo* versus *in vitro* could have a number of explanations. For instance, as Panx1 is robustly expressed in some neurons, the relatively intense signal from neurons after *in situ* hybridization may have left astrocyte Panx1 transcripts undetected if present at very low levels. It remains possible that Panx1 expression was activated in astrocytes as a stress response and the isolation and culture of astrocytes could have induced Panx1 gene expression. The use of glial cell-specific Panx knockout models for *in vivo* investigations will help to solve these apparent discrepancies. Finally, there is emerging evidence that Panx1 function is present in microglia (Bravo et al. 2014; Burma et al. 2017). This important finding adds to the complexity of extra-neuronal Panx1 expression in the nervous system.

Although P2X7R expression in non-neuronal cells of the CNS is well-accepted (reviewed in Sperlagh & Illes 2014), the cell-type expression of P2X7R in neurons has been a long-standing debate. P2X7R expression at the transcript and protein level was initially detected throughout the mouse brain and spinal cord (Able et al. 2011; Yu et al. 2008). Here, P2X7R was found in the cortex and hippocampus (as well as other brain regions) in neurons, as well as astrocytes and microglia. Early studies into subcellular localization of P2X7R in neurons determined they were primarily localized to presynaptic nerve terminals (Deuchars et al. 2001; Puthussery & Fletcher 2004; Atkinson et al. 2004); however, there was also some evidence for post-synaptic P2X7R expression in retinal and hypothalamic synapses (Puthussery & Fletcher 2004; Gordon et al. 2005). This was questioned by the presence of P2X7R-immunoreactivity in the initial iterations of P2X7R$^{-/-}$ mice (Sim et al. 2004); however this immunolabeling was later determined to

be expression of functional P2X7R splice variants in this initial knockout model (Masin et al. 2012; Nicke et al. 2009). Further complicating the study of neuronal P2X7R, expression of humanized P2X7R in mice (absent of splice variant expression) demonstrated specific neuronal localization to the CA3 region of the hippocampus, as well as in non-neuronal cells throughout the brain (Metzger et al. 2016). However, robust P2X7R expression in the CA3 region was not reflected at the mRNA level in other studies (García-Huerta et al. 2012; Jimenez-Mateos et al. 2015). Further, the gain- and loss- of function attributed to P2X7R splice variants (Masin et al. 2012; Nicke et al. 2009), as well as their potential to alter coupling with Panx1 (Xu et al. 2012), makes their cell-type specific expression a relevant point of investigation. Consequently, neuronal P2X7R expression in the brain has remained a controversial issue. In neurogenic niches, however, P2X7Rs were expressed in neural precursor cells (NPCs) during development (Tsao et al. 2013), as well as in the adult SVZ (Messemer et al. 2013), with some evidence for expression in the SGZ of the hippocampus (Tsao et al. 2013). While in the spinal cord, in glial cells in particular, P2X7R expression was well characterized (reviewed in Cotrina & Nedergaard 2009). Here, P2X7R was observed in both neurons and glia at the transcript and protein levels (Collo et al. 1997; Deuchars et al. 2001; Yu et al. 2008; Xiang & Burnstock 2005; Rappold et al. 2006). Like in neurons of the brain, immunolabeling suggested that P2X7Rs were localized primarily to presynaptic terminals (Deuchars et al. 2001); however, functional evidence suggested they were also present in post-synaptic membranes (reviewed in Cotrina & Nedergaard 2009), which warrants follow-up with immunolabeling experiments. In microglia localized to the spinal cord, P2X7R demonstrated robust expression and were intimately involved in immune

surveillance and inflammatory response (Xiang & Burnstock 2005; Rappold et al. 2006). Taken together, the sum of these studies suggested that P2X7R was likely co-expressed with Panx1 in several cell types throughout the nervous system.

Although there are multiple cell types where P2X7R and Panx1 are co-expressed, for the sake of discussion I will focus on two scenarios where P2X7R and Panx1 expression is less contentious and P2X7R-Panx1 crosstalk and Panx1 internalization could be particularly relevant to neurobiological processes. First, I will discuss regulation of postnatal neurogenesis in the subventricular zone (SVZ) and second, chronic pain signalling surrounding the spinal cord (Figure 6.4). N2a cells have provided an excellent model system for purinergic regulation of NPC behaviours, thanks to their expression of both P2X and P2Y receptors (Gomez-Villafuertes et al. 2009; Masgrau et al. 2009; Chen & Chen 1997) and differentiation capabilities. We observed expression of P2X1-4R and P2X7R transcripts in N2a cells (Chapter 4) and others have demonstrated that P2X4R and P2X7R were the primary isoforms expressed at the protein level, with P2X7R as the predominant functional isoform (Gomez-Villafuertes et al. 2009). Although often used as a model for NPCs, the P2XR expression profile in N2a cells was also very similar to microglia and astrocyte expression, which have typically demonstrated robust expression of P2X4R and P2X7R (reviewed in Inoue & Tsuda 2012; Illes et al. 2011).

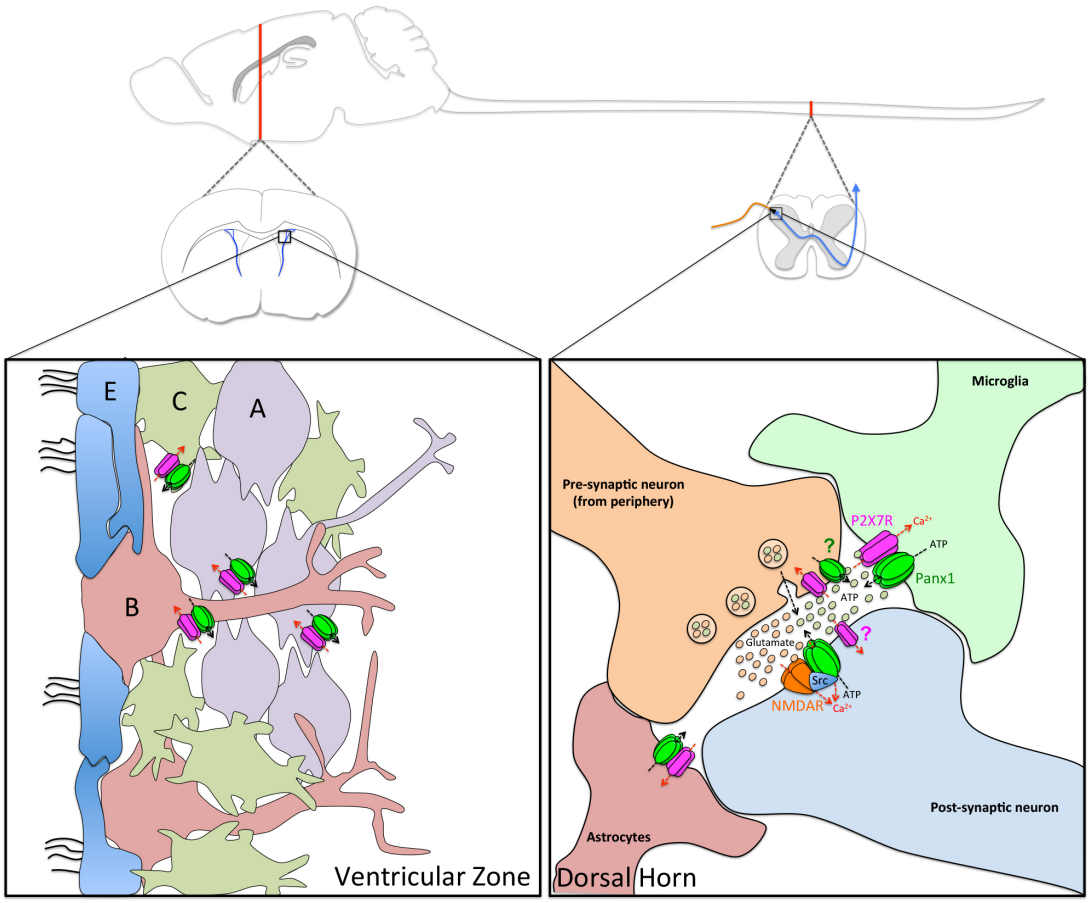

Figure 6.4 Context-specific P2X7R-Panx1 crosstalk in the nervous system. In the adult subventricular zone, P2X7R and Panx1 is expressed in all neural precursor cell types (slowly-dividing radial-glia-like cells (B-type), rapidly-dividing transit-amplifying precursor cells (C-type), and migratory neuroblasts (A-type)), as well as ciliated ependymal cells that border the ventricle, where they regulated NPC proliferation, differentiation, and cell survival. In the dorsal horn of the spinal cord, P2X7R and Panx1 are co-expressed in glial cells and contribute to the inflammatory response, as well as possibly co-expressed in presynaptic and post-synaptic membranes. In this synapse, ATP and glutamate are co-released from the presynaptic neuron, which triggers P2X7R-mediated Panx1 activation in glia and NMDAR-mediated currents in the post-synaptic neuron. Both of these events are potentiated by Panx1, which contributes to hypersensitivity and allodynia in chronic pain.

6.5.1 In the adult SVZ

Post-natal neurogenesis involves the regulation of adult neural stem and progenitor cell proliferation and survival, as well as differentiation into mature neurons (reviewed in Ming & Song 2011). In adults, neurogenesis is restricted to two 'neurogenic niches,' the SVZ of the lateral ventricles and the subgranular zone of the hippocampus. Here, neural precursor cells (NPCs) proceed through three developmental stages: radial-glia-like cells (B-type) that are slow to divide, transit-amplifying precursor cells (C-type) that rapidly divide, and migratory neuroblasts (A-type), which then differentiate into mature neurons (reviewed in Lim & Alvarez-Buylla 2016). In the SVZ, each of these cell types expressed both P2X7R (Tsao et al. 2013; Messemer et al. 2013) and Panx1 (Wicki-Stordeur et al. 2012; Wicki-Stordeur & Swayne 2013; Wicki-Stordeur et al. 2016, reviewed in Sanchez-Arias et al. 2016), as well as P2Y receptors (Suyama et al. 2012; Mishra et al. 2006). Both NPCs (Suyama et al. 2012) and astrocytes (Lacar et al. 2012) contributed to ATP release in this niche; however, the mechanism of release remains unknown. Evidence from our lab suggested that, at least in part, this ATP release was mediated by Panx1 channels (Wicki-Stordeur et al. 2012; Wicki-Stordeur & Swayne 2013; Wicki-Stordeur et al. 2016). Together, P2 receptors and Panx1 regulated NPC proliferation, differentiation, and survival (Wicki-Stordeur et al. 2012; Wicki-Stordeur & Swayne 2013; Wicki-Stordeur et al. 2016). Extracellular ATP impacted on different cellular behaviours in a dose-dependent manner based on interaction with various P2 receptors in this region. At low concentrations, ATP through P2Y1Rs promoted NPC proliferation (Mishra et al. 2006; Suyama et al. 2012); however, at higher concentrations (>100 μM), extracellular ATP activated P2X7Rs (Surprenant et al. 1996, reviewed in North & Surprenant 2000).

At first glance, P2X7R-mediated Panx1 internalization in this scenario could provide a negative feedback mechanism to avoid hyper-proliferation in response to extracellular ATP; however, it is likely not that simple. Although the regulation of NPC proliferation via P2Y receptors is well understood, the role of P2X7Rs in these cells is less clear. Like Panx1 (Wicki-Stordeur & Swayne 2013), in cell culture models for NPCs, P2X7R expression decreased over differentiation (Wu et al. 2009; Orellano et al. 2010; Glaser et al. 2014) and inhibition of both P2X7R activity or knockdown of P2X7R expression promoted neurite outgrowth (Gomez-Villafuertes et al. 2009; Wu et al. 2009), as well as axonal branching in hippocampal neurons (Díaz-Hernandez et al. 2008). Two additional studies demonstrated both pro-death (Orellano et al. 2010) and pro-survival (Gómez-Villafuertes et al. 2015) signalling mediated by P2X7R under differentiation conditions. The role of *in vivo* P2X7R added to the complexity of these studies further, indicating a possible age-dependent role for P2X7Rs. In the embryonic VZ, activation of P2X7Rs promoted differentiation (Tsao et al. 2013); while in the adult VZ, activation of P2X7R controlled the over-proliferation of NPCs by triggering cell death (Messemer et al. 2013). Taken together, these data seemed to suggest that P2X7R played a context-specific role that was developmentally regulated and possibly involved interplay with other proteins, including Panx1. Like P2X7R in most culture models (Wu et al. 2009; Orellano et al. 2010; Glaser et al. 2014), Panx1 was rapidly down-regulated under differentiation conditions (~25% over 24 h (Wicki-Stordeur & Swayne 2013)). As both of these proteins exhibited a comparatively long half-life (Penuela et al. 2007; Boyce et al. 2015; Gonnord et al. 2009), this reduction in expression was likely the result of stimulated protein degradation, which would require internalization from the cell surface. This would have a

similar effect to inhibiting or knocking down either protein, leading to loss of purinergic signalling and ATP release, which was consistent with previous studies *in vitro* (Gomez-Villafuertes et al. 2009; Wu et al. 2009; Wicki-Stordeur & Swayne 2013). This prediction diverges slightly from my findings in Chapter 3. In response to ATP alone, I observed targeting of internalized Panx1 to the slow recycling endosome (Rab11/Rab14+; up to 2 h). Consequently, future studies should investigate P2X7R-Panx1 clustering and internalization under differentiation conditions and extend the time course to >24 h to evaluate the mechanism behind the reduced P2X7R-Panx1 expression in the context of differentiation, particularly whether this involves targeting to the degradation pathway.

6.5.2 In chronic pain

In healthy individuals, pain sensation is typically transient and caused by a noxious stimulus; however, in the context of chronic pain, it is intensified and manifests as hyperalgesia, enhanced and prolonged pain sensation, or allodynia, a pain response to normally benign stimuli, involving complex circuitry in the sensory circuit (reviewed in Baron 2006). Peripheral nerves co-release ATP and glutamate, activating NMDARs (in the post-synaptic neuron) and P2X7Rs (primarily in glial cells) (reviewed in Bravo et al. 2015). Both of these receptors are potentiated by activation of downstream Panx1 channels that leads to enhanced ATP release (reviewed in Isakson & Thompson 2014). Purinergic signalling and P2X7Rs are well-established regulators of both chronic pain (McGaraughty et al. 2007; Chessell et al. 2005; Honore et al. 2006) and spinal cord injury (Wang et al. 2004; Peng et al. 2009, reviewed in Tsuda & Inoue 2016). As P2X7R-Panx1 crosstalk is important for a wide array of cellular behaviours (reviewed in Baroja-Mazo et

al. 2013), this suggested that Panx1 might also play a role in chronic pain. Co-expression/activation of P2X7R and Panx1 was previously linked to inflammasome activation and processing/release of inflammatory cytokines (Pelegrin et al. 2008; Silverman et al. 2009; Pelegrin & Surprenant 2007; Pelegrin & Surprenant 2006), a process pathologically over-activated in chronic pain that contributes to the persistent symptoms.

Recent studies have identified possible Panx1 crosstalk with P2X7R in microglia (Burma et al. 2017; Bravo et al. 2014, review in Bravo et al. 2015). In microglia, enhanced P2X7R activity led to the maintenance of chronic pain by activating the inflammasome and mediating release of pro-inflammatory molecules (McGaraughty et al. 2007; Chessell et al. 2005; Honore et al. 2006). P2X7R-mediated cytokine processing occurred through both Panx1-dependent (Pelegrin & Surprenant 2006) and Panx1-independent (Pelegrin et al. 2008) mechanisms. In Panx1-dependent circumstances, purinergic crosstalk caused by P2X7R-Panx1 activation led to cellular inflammasome activation (Silverman et al. 2009). Here, P2X7R and Panx1 directly interacted with inflammasome components including NRLP1, ASC, and caspase-1 and stimulated caspase-1 activity (Silverman et al. 2009), which triggered proteolytic processing of cytokine precursors and downstream vesicular release of mature cytokines (reviewed in Pelegrin & Surprenant 2009).

In a mouse model of neuropathic pain, mechanical hyperalgesia and allodynia were observed to be mediated by Panx1 activation (Bravo et al. 2014). Panx1 was specifically involved in modulating chronic pain rather than ‘normal’ pain sensitivity, as intrathecal Panx1 inhibition (^{10}Panx1, CBX, Probenecid) transiently reduced the

mechanical nociceptive threshold in neuropathic rats to sham levels, yet had no effect on altering thresholds in sham rats. Later, Panx1 expression in neurons was observed to increase following induction of neuropathic pain in rats (Zhang et al. 2015); however, this occurred in the dorsal root ganglion. The potentiation of NMDAR currents by Panx1 in post-synaptic neurons could also enhance pain sensation. Similarly to previous studies, inhibition and knockdown of Panx1 alleviated pain hypersensitivity in this context (Zhang et al. 2015). However, it is not yet clear whether P2X7R exists in the post-synaptic membrane of these cells allowing for Panx1 internalization. Finally, astrocytic Panx1-mediated ATP release in the spinal cord enhanced diurnal hypersensitivity that exists in neuropathic pain (Koyanagi et al. 2016), adding further complexity to P2X7R-Panx1 crosstalk in this context. In each of these contexts, P2X7R-mediated Panx1 internalization could be expected to reduce the 'ATP load' in synapses of the sensory circuit. ATP release through Panx1 would theoretically lead to ramping P2X7R activation in microglia and astrocytes and exacerbation of the inflammatory response. Here, ATP-evoked Panx1 internalization could dampen the pro-inflammatory response that exacerbates chronic pain, by disrupting the positive feedback loop with P2X7R underlying ramping ATP release. Although functional studies have identified Panx1-mediated microglial behaviours (Burma et al. 2017) and Panx1 protein expression was identified by Western blot in dorsal horn tissue homogenate (Bravo et al. 2014), microglial-specific expression of Panx1 has yet to be determined. Consequently, future studies are needed to determine the precise cell types involved in regulating this phenomenon.

6.6 Summary

Panx1 forms ATP-release channels that crosstalk with purinergic P2 receptors, creating a positive feedback loop underlying several physiological and pathophysiological scenarios. Prior to the onset of my thesis, several groups had identified negative feedback of Panx1 channel activity by elevated extracellular ATP concentrations through an unknown mechanism. Most of the analyses of Panx1 function preceding the studies described in my dissertation focussed on cell surface Panx1; however, there also existed a substantial population of uninvestigated intracellular Panx1. The origin of this intracellular Panx1 could be (1) direct diversion from the secretory pathway or (2) regulated/constitutive internalization from the cell surface. Based on the ubiquitous nature of ATP release and its role as a negative regulator of Panx1 activity at high concentrations, at the onset of my studies, I hypothesized that **ATP stimulated Panx1 internalization to intracellular compartments.** The following findings addressed my hypothesis directly. Upon elevation of extracellular ATP, P2X7R triggered non-canonical internalization of Panx1 via cholesterol-dependent macropinocytosis. This involved upstream clustering of P2X7R-Panx1 through an extracellular interaction and possible contribution of phospholipid interactions localized to the Panx1 C-terminus. Internalized Panx1 was targeted to slow recycling endosomes in an Arf6-dependent mechanism. This was the first evidence of Panx1 cell surface stability being labile to changes in the cellular environment. Further, these data provided an additional layer to P2X7R-Panx1 crosstalk in cells and tissues where these proteins are co-expressed. Finally, in addition to its role as an ATP release channel at the cell surface, Panx1 may play a diverse signalling

role once internalized into endosomal compartments, adding to the complexity of Panx1 function.

Bibliography

Abascal, F. & Zardoya, R., 2012. LRRC8 proteins share a common ancestor with pannexins, and may form hexameric channels involved in cell-cell communication. *Bioessays*, 34, pp.551–560.

Abbracchio, M.P. et al., 2009. Purinergic signalling in the nervous system: an overview. *Trends in Neurosciences*, 32(1), pp.19–29.

Aberer, W. et al., 1978. A characterization of the nucleotide uptake of chromaffin granules of bovine adrenal medulla. *The Biochemical journal*, 172(3), pp.353–360.

Able, S.L. et al., 2011. Receptor localization, native tissue binding and ex vivo occupancy for centrally penetrant P2X7 antagonists in the rat. *British Journal of Pharmacology*, 162(2), pp.405–414.

Adinolfi, E. et al., 2010. Trophic activity of a naturally occurring truncated isoform of the P2X7 receptor. *FASEB J*, 24(9), pp.3393–3404.

Adriouch, S. et al., 2002. Cutting edge: a natural P451L mutation in the cytoplasmic domain impairs the function of the mouse P2X7 receptor. *Journal of immunology (Baltimore, Md. : 1950)*, 169(8), pp.4108–4112.

Aguado, B. & Campbell, R.D., 1998. Characterization of a human lysophosphatidic acid acyltransferase that is encoded by a gene located in the class {III} region of the human major histocompatibility complex. *The Journal of biological chemistry*, 273(7), pp.4096–4105.

Ahmad, S. et al., 2005. Lung epithelial cells release ATP during ozone exposure: Signaling for cell survival. *Free Radical Biology and Medicine*, 39(2), pp.213–226.

Ahmed, S.N., Brown, D.A. & London, E., 1997. On the origin of sphingolipid/cholesterol-rich detergent-insoluble cell membranes: Physiological concentrations of cholesterol and sphingolipid induce formation of a detergent-insoluble, liquid-ordered lipid phase in model membranes. *Biochemistry*, 36(36), pp.10944–10953.

Aït-Slimane, T. et al., 2009. Basolateral internalization of GPI-anchored proteins occurs via a clathrin-independent flotillin-dependent pathway in polarized hepatic cells. *Molecular biology of the cell*, 20(17), pp.3792–800.

Alexander, D.B. & Goldberg, G.S., 2003. Transfer of biologically important molecules between cells through gap junction channels. *Current medicinal chemistry*, 10(19), pp.2045–2058.

Alves, L. et al., 2014. The P2X7 receptor: shifting from a low- to a high-conductance channel - an enigmatic phenomenon? *Biochim Biophys Acta*, 1838(10), pp.2578–2587.

Ambrosi, C. et al., 2010. Pannexin1 and Pannexin2 channels show quaternary similarities to connexons and different oligomerization numbers from each other. *J Biol Chem*, 285(32), pp.24420–24431.

Araki, N. et al., 2007. Phosphoinositide metabolism during membrane ruffling and macropinosome formation in EGF-stimulated A431 cells. *Experimental Cell Research*, 313(7), pp.1496–1507.

Ardiles, A.O. et al., 2014. Pannexin 1 regulates bidirectional hippocampal synaptic

plasticity in adult mice. *Front Cell Neurosci*, 8, p.326.

Armstrong, C.M., Bezanilla, F. & Rojas, E., 1973. Destruction of sodium conductance inactivation in squid axons perfused with pronase. *The Journal of general physiology*, 62(4), pp.375–91.

Aspinwall, C.A. & Yeung, E.S., 2005. Screening populations of individual cells for secretory heterogeneity. *Analytical and Bioanalytical Chemistry*, 381(3), pp.660–666.

Atkinson, L. et al., 2004. Differential co-localisation of the P2X7 receptor subunit with vesicular glutamate transporters VGLUT1 and VGLUT2 in rat CNS. *Neuroscience*, 123(3), pp.761–768.

Avraham, R. & Yarden, Y., 2011. Feedback regulation of EGFR signalling: decision making by early and delayed loops. *Nature reviews. Molecular cell biology*, 12(2), pp.104–17.

Bagatini, M.D. et al., 2011. Enzymes that hydrolyze adenine nucleotides in patients with ischemic heart disease. *Clinica Chimica Acta*, 412(1–2), pp.159–164.

Bannas, P. et al., 2005. Activity and specificity of toxin-related mouse T cell ecto-ADP-ribosyltransferase ART2.2 depends on its association with lipid rafts. *Blood*, 105(9), pp.3663–3670.

Bao, L., Locovei, S. & Dahl, G., 2004. Pannexin membrane channels are mechanosensitive conduits for ATP. *FEBS Lett*, 572(1–3), pp.65–68.

Baranova, A. et al., 2004. The mammalian pannexin family is homologous to the invertebrate innexin gap junction proteins. *Genomics*, 83(4), pp.706–716.

Bargiotas, P. et al., 2012. Functional outcome of pannexin-deficient mice after cerebral ischemia. *Channels*, 6(6), pp.453–456.

Bargiotas, P. et al., 2011. Pannexins in ischemia-induced neurodegeneration. *Proc Natl Acad Sci U S A*, 108(51), pp.20772–20777.

Baroja-Mazo, A., Barbera-Cremades, M. & Pelegrin, P., 2013. The participation of plasma membrane hemichannels to purinergic signaling. *Biochim Biophys Acta*, 1828(1), pp.79–93.

Baron, R., 2006. Mechanisms of disease: neuropathic pain - a clinical perspective. *Nature clinical practice. Neurology*, 2(2), pp.95–106.

Barth, K. et al., 2007. Caveolin-1 influences P2X7 receptor expression and localization in mouse lung alveolar epithelial cells. *FEBS Journal*, 274(12), pp.3021–3033.

Barth, K. et al., 2008. Characterization of the molecular interaction between caveolin-1 and the P2X receptors 4 and 7 in E10 mouse lung alveolar epithelial cells. *International Journal of Biochemistry and Cell Biology*, 40(10), pp.2230–2239.

Beckmann, A. et al., 2016. Pannexin-1 channels show distinct morphology and no gap junction characteristics in mammalian cells. *Cell & Tissue Research*, 363(3), pp.751–763.

Beemiller, P., Hoppe, A.D. & Swanson, J.A., 2006. A phosphatidylinositol-3-kinase-dependent signal transition regulates ARF1 and ARF6 during Fc?? receptor-mediated phagocytosis. *PLoS Biology*, 4(6), pp.0987–0999.

Behnke, J. et al., 2011. Two dileucine motifs mediate late endosomal/lysosomal targeting of transmembrane protein 192 (TMEM192) and a C-terminal cysteine residue is responsible for disulfide bond formation in TMEM192 homodimers. *The Biochemical journal*, 434(2), pp.219–231.

Bergendorff, A. & Uvnas, B., 1973. Storage properties of rat mast cell granules in vitro. *Acta Physiol Scand*, 87, pp.213–222.

Bernier, L.-P. et al., 2008. Phosphoinositides regulate P2X4 ATP-gated channels through direct interactions. *Journal of Neuroscience*, 28(48), pp.12938–12945.

Besshoh, S. et al., 2005. Increased phosphorylation and redistribution of NMDA receptors between synaptic lipid rafts and post-synaptic densities following transient global ischemia in the rat brain. *Journal of Neurochemistry*, 93(1), pp.186–194.

Bhalla-Gehi, R. et al., 2010. Pannexin1 and pannexin3 delivery, cell surface dynamics, and cytoskeletal interactions. *J Biol Chem*, 285(12), pp.9147–9160.

Billaud, M. et al., 2015. A molecular signature in the pannexin1 intracellular loop confers channel activation by the α1 adrenoreceptor in smooth muscle cells. *Science signaling*, 8(364), p.ra17.

Billaud, M. et al., 2011. Pannexin1 regulates alpha1-adrenergic receptor- mediated vasoconstriction. *Circ Res*, 109(1), pp.80–85.

Van der Bliek, A.M. et al., 1993. Mutations in human dynamin block an intermediate stage in coated vesicle formation. *Journal of Cell Biology*, 122(3), pp.553–563.

Boassa, D. et al., 2007. Pannexin1 channels contain a glycosylation site that targets the hexamer to the plasma membrane. *J Biol Chem*, 282(43), pp.31733–31743.

Boassa, D. et al., 2014. Pannexin2 oligomers localize in the membranes of endosomal vesicles in mammalian cells while Pannexin1 channels traffic to the plasma membrane. *Front Cell Neurosci*, 8, p.468.

Boassa, D. et al., 2008. Trafficking dynamics of glycosylated pannexin 1 proteins. *Cell communication & adhesion*, 15, pp.119–132.

Bohdanowicz, M. et al., 2013. Phosphatidic acid is required for the constitutive ruffling and macropinocytosis of phagocytes. *Molecular biology of the cell*, 24(11), pp.1700–12, S1-7.

Bohdanowicz, M. & Grinstein, S., 2013. Role of phospholipids in endocytosis, phagocytosis, and macropinocytosis. *Physiological reviews*, 93(1), pp.69–106.

Bonifacino, J.S. & Traub, L.M., 2003. Signals for sorting of transmembrane proteins to endosomes and lysosomes. *Annu Rev Biochem.*, 72:395-447, pp.395–447.

Botelho, R.J. et al., 2000. Localized biphasic changes in phosphatidylinositol-4,5-bisphosphate at sites of phagocytosis. *Journal of Cell Biology*, 151(7), pp.1353–1367.

Boumechache, M. et al., 2009. Analysis of assembly and trafficking of native P2X4 and P2X7 receptor complexes in rodent immune cells. *Journal of Biological Chemistry*, 284(20), pp.13446–13454.

Boyce, A.K. et al., 2015. ATP stimulates pannexin 1 internalization to endosomal compartments. *Biochem J*, 470(3), pp.319–330.

Boyce, A.K. et al., 2014. Pore positioning: current concepts in Pannexin channel trafficking. *Channels (Austin)*, 8(2), pp.110–117.

Boyce, A.K. et al., 2017. Transcriptional and post-translational regulation of pannexins. *Biochim Biophys Acta*.

Braun, N. et al., 1998. Upregulation of the enzyme chain hydrolyzing extracellular ATP after transient forebrain ischemia in the rat. *The Journal of neuroscience : the official journal of the Society for Neuroscience*, 18(13), pp.4891–900.

Bravo, D. et al., 2015. Interactions of pannexin 1 with NMDA and P2X7 receptors in

central nervous system pathologies: Possible role on chronic pain. *Pharmacol Res*, 101, pp.86–93.

Bravo, D. et al., 2014. Pannexin 1: A novel participant in neuropathic pain signaling in the rat spinal cord. *Pain*, 155(10), pp.2108–2115.

Brown, D.A. & Rose, J.K., 1992. Sorting of GPI-anchored proteins to glycolipid-enriched membrane subdomains during transport to the apical cell surface. *Cell*, 68(3), pp.533–544.

Brown, F.D. et al., 2001. Phosphatidylinositol 4,5-bisphosphate and Arf6-regulated membrane traffic. *Journal of Cell Biology*, 154(5), pp.1007–1017.

Brown, H. a et al., 1993. ADP-ribosylation factor, a small GTP-dependent regulatory protein, stimulates phospholipase D activity. *Cell*, 75(6), pp.1137–1144.

Brown, W.J., Goodhouse, J. & Farquhar, M.G., 1986. Mannose-6-phosphate receptors for lysosomal enzymes cycle between the Golgi complex and endosomes. *J Cell Biol*, 103(4), pp.1235–1247.

Browne, L.E., Jiang, L.H. & North, R.A., 2010. New structure enlivens interest in P2X receptors. *Trends in Pharmacological Sciences*, 31(5), pp.229–237.

Bruzzone, R. et al., 2003. Pannexins, a family of gap junction proteins expressed in brain. *Proc Natl Acad Sci U S A*, 100(23), pp.13644–13649.

Burma, N. et al., 2017. Blocking microglial pannexin-1 channels alleviates morphine withdrawal in rodents. *Nature Medicine*.

Burnstock, G., 1978. A basis for distinguishing two types of purinergic receptor. *Cell Membrane Receptors for Drugs and Hormones: A Multidisciplinary Approach*, pp.107–118.

Burnstock, G., 2011. Introductory overview of purinergic signalling. *Frontiers in bioscience (Elite edition)*, 3, pp.896–900.

Burnstock, G., 1976. Purinergic receptors. *Journal of Theoretical Biology*, 62(2), pp.491–503.

Burnstock, G. et al., 2011. Purinergic signalling: from normal behaviour to pathological brain function. *Progress in neurobiology*, 95(2), pp.229–274.

Burnstock, G., 2016. Purinergic Signalling and Neurological Diseases: An Update. *CNS Neurol Disord Drug Targets*.

Burnstock, G. et al., 1970. Evidence that adenosine triphosphate or a related nucleotide is the transmitter substance released by non-adrenergic inhibitory nerves in the gut. *British Journal of Pharmacology*, 40(4), pp.668–688.

Burnstock, G., Dumsday, B. & Smythe, A., 1972. Atropine resistant excitation of the urinary bladder: the possibility of transmission via nerves releasing a purine nucleotide. *British Journal of Pharmacology*, 44(3), pp.451–461.

Casas-Pruneda, G. et al., 2009. Functional interactions between P2X4 and P2X7 receptors from mouse salivary epithelia. *The Journal of physiology*, 587(Pt 12), pp.2887–901.

Cazzolli, R. et al., 2006. Phospholipid signalling through phospholipase D and phosphatidic acid. *IUBMB life*, 58(8), pp.457–461.

Celetti, S.J. et al., 2010. Implications of pannexin 1 and pannexin 3 for keratinocyte differentiation. *J Cell Sci*, 123(Pt 8), pp.1363–1372.

Chadda, R. et al., 2007. Cholesterol-sensitive Cdc42 activation regulates actin polymerization for endocytosis via the GEEC pathway. *Traffic*, 8(6), pp.702–717.

Chataigneau, T., Lemoine, D. & Grutter, T., 2013. Exploring the ATP-binding site of P2X receptors. *Frontiers in cellular neuroscience*, 7(December), p.273.

Cheewatrakoolpong, B. et al., 2005. Identification and characterization of splice variants of the human P2X7 ATP channel. *Biochemical and Biophysical Research Communications*, 332(1), pp.17–27.

Chekeni, F.B. et al., 2010. Pannexin 1 channels mediate "find-me" signal release and membrane permeability during apoptosis. *Nature*, 467(7317), pp.863–867.

Chen, C. & Chen, W., 1997. P2Y receptor linked to phospholipase C: stimulation of neuro 2A cells by UTP and ATP and possible regulation by protein kinase C subtype epsilon. *J Neurochem*, 69(4), pp.1409–1416.

Chessell, I.P. et al., 2005. Disruption of the P2X7 purinoceptor gene abolishes chronic inflammatory and neuropathic pain. *Pain*, 114(3), pp.386–396.

Chiu, Y.-H. et al., 2017. A quantized mechanism for activation of pannexin channels. *Nature Communications*, 8.

Chiu, Y.H., Ravichandran, K.S. & Bayliss, D.A., 2014. Intrinsic properties and regulation of Pannexin 1 channel. *Channels (Austin)*, 8(2).

Coco, S. et al., 2003. Storage and release of ATP from astrocytes in culture. *Journal of Biological Chemistry*, 278(2), pp.1354–1362.

Collo, G. et al., 1997. Tissue distribution of the P2X7 receptor. *Neuropharmacology*, 36(9), pp.1277–1283.

Cone, A.C. et al., 2013. A comparative antibody analysis of pannexin1 expression in four rat brain regions reveals varying subcellular localizations. *Front Pharmacol*, 4, p.6.

Costa-Junior, H.M., Vieira, F.S. & Coutinho-Silva, R., 2011. C terminus of the P2X7 receptor: Treasure hunting. *Purinergic Signalling*, 7(1), pp.7–19.

Cotrina, M.L. & Nedergaard, M., 2009. Physiological and pathological functions of P2X7 receptor in the spinal cord. *Purinergic Signalling*, 5(2), pp.223–232.

Coussen, F., 2009. Molecular determinants of kainate receptor trafficking. *Neuroscience*, 158(1), pp.25–35.

Crespo Yanguas, S. et al., 2017. Pannexin1 as mediator of inflammation and cell death. *Biochim Biophys Acta*, 1864(1), pp.51–61.

D'hondt, C. et al., 2013. Regulation of connexin- and pannexin-based channels by post-translational modifications. *Biology of the Cell*, 105(9), pp.373–398.

Dahl, G., 2015. ATP release through pannexon channels. *Philosophical Transactions of the Royal Society B: Biological Sciences*, 370(1672), p.20140191.

Dahl, G. et al., 1991. Cell/cell channel formation involves disulfide exchange. *European Journal of Biochemistry*, 197(1), pp.141–144.

Dang, V.C. & Christie, M.J., 2012. Mechanisms of rapid opioid receptor desensitization, resensitization and tolerance in brain neurons. *British Journal of Pharmacology*, 165(6), pp.1704–1716.

Danielsen, E.M. & Hansen, G.H., 2003. Lipid rafts in epithelial brush borders: Atypical membrane microdomains with specialized functions. *Biochimica et Biophysica Acta - Biomembranes*, 1617(1–2), pp.1–9.

Danino, D. & Hinshaw, J.E., 2001. Dynamin family of mechanoenzymes. *Current Opinion in Cell Biology*, 13(4), pp.454–460.

Dedkova, E.N., Sigova, A.A. & Zinchenko, V.P., 2000. Mechanism of action of calcium ionophores on intact cells: ionophore-resistant cells. *Membrane & cell biology*,

13(3), pp.357–68.
Deuchars, S.A. et al., 2001. Neuronal P2X7 receptors are targeted to presynaptic terminals in the central and peripheral nervous systems. *J Neurosci*, 21(18), pp.7143–7152.
Dharmawardhane, S. et al., 2000. Regulation of macropinocytosis by p21-activated kinase-1. *Molecular biology of the cell*, 11(10), pp.3341–3352.
Díaz-Hernandez, M. et al., 2008. Inhibition of the ATP-gated P2X7 receptor promotes axonal growth and branching in cultured hippocampal neurons. *Journal of cell science*, 121, pp.3717–3728.
Diekmann, Y. et al., 2011. Thousands of Rab GTPases for the cell biologist. *PLoS Computational Biology*, 7(10).
Dinkel, H. et al., 2016. ELM 2016 - Data update and new functionality of the eukaryotic linear motif resource. *Nucleic Acids Research*, 44(D1), pp.D294–D300.
Dolmatova, E. et al., 2012. Cardiomyocyte ATP release through pannexin 1 aids in early fibroblast activation. *American Journal of Physiology - Heart and Circulatory Physiology*, 303(10), pp.H1208–H1218.
Dotti, C.G., Esteban, J.A. & Ledesma, M.D., 2014. Lipid dynamics at dendritic spines. *Frontiers in neuroanatomy*, 8(August), p.76.
Dourado, M., Wong, E. & Hackos, D.H., 2014. Pannexin-1 is blocked by its C-terminus through a delocalized non-specific interaction surface. *PLoS ONE*, 9(6).
Draganov, D. et al., 2015. Modulation of P2X4/P2X7/Pannexin-1 sensitivity to extracellular ATP via Ivermectin induces a non-apoptotic and inflammatory form of cancer cell death. *Scientific reports*, 5(October), p.16222.
Dubel, S.J. et al., 2004. Plasma Membrane Expression of T-type Calcium Channel {alpha}1 Subunits Is Modulated by High Voltage-activated Auxiliary Subunits. *Journal of Biological Chemistry*, 279(28), pp.29263–29269.
Dubyak, G.R., 2009. Both sides now: multiple interactions of ATP with pannexin-1 hemichannels. Focus on "A permeant regulating its permeation pore: inhibition of pannexin 1 channels by ATP." *Am J Physiol Cell Physiol*, 296(2), pp.C235-41.
Dubyak, G.R. & el-Moatassim, C., 1993. Signal transduction via P2-purinergic receptors for extracellular ATP and other nucleotides. *Am J Physiol*, 265(3 Pt 1), pp.C577-606.
Dunn, K.W., Kamocka, M.M. & McDonald, J.H., 2011. A practical guide to evaluating colocalization in biological microscopy. *Am J Physiol Cell Physiol*, 300(4), pp.C723-42.
Dvoriantchikova, G. et al., 2006. Expression of pannexin family of proteins in the retina. *FEBS Lett*, 580(9), pp.2178–2182.
Edidin, M., 2003. The state of lipid rafts: from model membranes to cells. *Annual review of biophysics and biomolecular structure*, 32, pp.257–283.
Edwards, F. a, Robertson, S.J. & Gibb, a J., 1997. Properties of ATP receptor-mediated synaptic transmission in the rat medial habenula. *Neuropharmacology*, 36(9), pp.1253–68.
El-Moatassim, C. & Dubyak, G.R., 1992. A novel pathway for the activation of phospholipase D by P2z purinergic receptors in BAC1.2F5 macrophages. *Journal of Biological Chemistry*, 267, pp.23664–23673.
Ellgaard, L. et al., 2016. Co- and Post-Translational Protein Folding in the ER. *Traffic*,

17(6), pp.615–638.
Ennion, S., Hagan, S. & Evans, R.J., 2000. The role of positively charged amino acids in ATP recognition by human P2X1 receptors. *Journal of Biological Chemistry*, 275(38), pp.29361–29367.
Erb, L. et al., 2006. P2 receptors: Intracellular signaling. *Pflugers Archiv European Journal of Physiology*, 452(5), pp.552–562.
Eskelinen, E.L., 2006. Roles of LAMP-1 and LAMP-2 in lysosome biogenesis and autophagy. *Mol Aspects Med*, 27(5–6), pp.495–502.
Evans, R.J., 2009. Orthosteric and allosteric binding sites of P2X receptors. *European Biophysics Journal*, 38(3), pp.319–327.
Feng, W. & Zhang, M., 2009. Organization and dynamics of PDZ-domain-related supramodules in the postsynaptic density. *Nature reviews. Neuroscience*, 10(2), pp.87–99.
Feng, Y.H. et al., 2005. ATP stimulates GRK-3 phosphorylation and beta-arrestin-2-dependent internalization of P2X7 receptor. *Am J Physiol Cell Physiol*, 288(6), pp.C1342-56.
Feranchak, A.P. et al., 2010. Initiation of purinergic signaling by exocytosis of ATP-containing vesicles in liver epithelium. *Journal of Biological Chemistry*, 285(11), pp.8138–8147.
Ferguson, M.A., 1999. The structure, biosynthesis and functions of glycosylphosphatidylinositol anchors, and the contributions of trypanosome research. *Journal of cell science*, 112 Pt 1, pp.2799–2809.
Fernando, K., Gargett, C. & Wiley, J., 1999. Activation of the P2Z/P2X7 receptor in human lymphocytes produces a delayed permeability lesion: involvement of phospholipase D. *Arch Biochem Biophys*, 362(2), pp.197–202.
Filippini, A., Taffs, R.E. & Sitkovsky, M. V, 1990. Extracellular ATP in T-lymphocyte activation: possible role in effector functions. *Proceedings of the National Academy of Sciences of the United States of America*, 87(21), pp.8267–8271.
Fischer, W. et al., 2007. Conserved lysin and arginin residues in the extracellular loop of P2X3 receptors are involved in agonist binding. *European Journal of Pharmacology*, 576(1–3), pp.7–17.
Fiske, C. & Subbarow, Y., 1929. Phosphorus compounds of muscle and liver. *Science*, 70, pp.381–382.
Flannagan, R.S., Jaumouillé, V. & Grinstein, S., 2012. The cell biology of phagocytosis. *Annual review of pathology*, 7, pp.61–98.
Foote, C.I. et al., 1998. The pattern of disulfide linkages in the extracellular loop regions of connexin 32 suggests a model for the docking interface of gap junctions. *Journal of Cell Biology*, 140(5), pp.1187–1197.
Fra, A.M. et al., 1995. A photo-reactive derivative of ganglioside GM1 specifically cross-links VIP21-caveolin on the cell surface. *FEBS Letters*, 375(1–2), pp.11–14.
Freitas-Andrade, M. & Naus, C.C., 2016. Astrocytes in neuroprotection and neurodegeneration: The role of connexin43 and pannexin1. *Neuroscience*, 323, pp.207–221.
Frick, M. et al., 2007. Coassembly of Flotillins Induces Formation of Membrane Microdomains, Membrane Curvature, and Vesicle Budding. *Current Biology*, 17(13), pp.1151–1156.

Fridriksson, E.K. et al., 1999. Quantitative analysis of phospholipids in functionally important membrane domains from RBL-2H3 mast cells using tandem high-resolution mass spectrometry. *Biochemistry*, 38(25), pp.8056–8063.

Fujita, A. et al., 2009. A distinct pool of phosphatidylinositol 4,5-bisphosphate in caveolae revealed by a nanoscale labeling technique. *Proc Natl Acad Sci U S A*, 106(23), pp.9256–9261.

Furlow, P.W. et al., 2015. Mechanosensitive pannexin-1 channels mediate microvascular metastatic cell survival. *Nature Cell Biology*, 17(7), pp.943–952. Available at: http://dx.doi.org/10.1038/ncb3194.

Furthauer, M. & Gonzalez-Gaitan, M., 2009. Endocytic regulation of notch signalling during development. *Traffic*, 10(7), pp.792–802.

Gaitan-Penas, H. et al., 2016. Investigation of LRRC8-Mediated Volume-Regulated Anion Currents in Xenopus Oocytes. *Biophys J*, 111(7), pp.1429–1443.

Gallop, J.L., Butler, P.J. & McMahon, H.T., 2005. Endophilin and CtBP/BARS are not acyl transferases in endocytosis or Golgi fission. *Nature*, 438(7068), pp.675–678.

Gangadharan, V., Nohe, A. & Duncan, R., 2011. ATP Stimulates Caveolar Endocytosis of P2X7R in MC3T3-E1 Osteoblasts. *Biophys J*, 100(3), p.418.

García-Huerta, P. et al., 2012. The specificity protein factor Sp1 mediates transcriptional regulation of P2X7 receptors in the nervous system. *Journal of Biological Chemistry*, 287(53), pp.44628–44644.

Garcia-Marcos, M., Pérez-Andrés, E., et al., 2006. Coupling of two pools of P2X7 receptors to distinct intracellular signaling pathways in rat submandibular gland. *Journal of lipid research*, 47(4), pp.705–14.

Garcia-Marcos, M., Pochet, S., et al., 2006. P2X7 and phospholipid signalling: The search of the "missing link" in epithelial cells. *Cellular Signalling*, 18(12), pp.2098–2104.

Gargett, C.E., Cornish, E.J. & Wiley, J.S., 1996. Phospholipase D activation by P2Z-purinoceptor agonists in human lymphocytes is dependent on bivalent cation influx. *Biochem J*, 313 (Pt 2, pp.529–535.

Garre, J.M. et al., 2016. FGF-1 Triggers Pannexin-1 Hemichannel Opening in Spinal Astrocytes of Rodents and Promotes Inflammatory Responses in Acute Spinal Cord Slices. *Journal of Neuroscience*, 36(17), pp.4785–4801.

Garré, J.M. et al., 2010. FGF-1 induces ATP release from spinal astrocytes in culture and opens pannexin and connexin hemichannels. *Proceedings of the National Academy of Sciences of the United States of America*, 107(52), pp.22659–22664.

de Gassart, A. & Martinon, F., 2015. Pyroptosis: Caspase-11 Unlocks the Gates of Death. *Immunity*, 43(5), pp.835–837.

Gehi, R., Shao, Q. & Laird, D.W., 2011. Pathways regulating the trafficking and turnover of pannexin1 protein and the role of the C-terminal domain. *The Journal of biological chemistry*, 286(31), pp.27639–27653.

Geyti, C.S. et al., 2008. Slow spontaneous [Ca2+]i oscillations reflect nucleotide release from renal epithelia. *Pflugers Archiv European Journal of Physiology*, 455(6), pp.1105–1117.

Ghosh, P., Dahms, N.M. & Kornfeld, S., 2003. Mannose 6-phosphate receptors: new twists in the tale. *Nature reviews. Molecular cell biology*, 4(3), pp.202–212.

Glaser, T. et al., 2014. Modulation of mouse embryonic stem cell proliferation and neural

differentiation by the P2X7 receptor. *PLoS One*, 9(5), p.e96281.
Gomez-Villafuertes, R. et al., 2009. Ca2+/calmodulin-dependent kinase II signalling cascade mediates P2X7 receptor-dependent inhibition of neuritogenesis in neuroblastoma cells. *FEBS Journal*, 276, pp.5307–5325.
Gómez-Villafuertes, R. et al., 2014. Ecto-nucleotide pyrophosphatase/phosphodiesterase (E-NPP) activity in Neuro-2a neuroblastoma cells: expression changes associated with neuronal differentiation. *Journal of neurochemistry*, 131, pp.290–302.
Gómez-Villafuertes, R. et al., 2015. PI3K/Akt signaling pathway triggers P2X7 receptor expression as a pro-survival factor of neuroblastoma cells under limiting growth conditions. *Scientific reports*, 5, p.18417.
Gonnord, P. et al., 2009. Palmitoylation of the P2X7 receptor, an ATP-gated channel, controls its expression and association with lipid rafts. *FASEB J*, 23(3), pp.795–805.
Gordon, G.R.J. et al., 2005. Norepinephrine triggers release of glial ATP to increase postsynaptic efficacy. *Nature neuroscience*, 8(8), pp.1078–1086.
Gowrishankar, K. et al., 2012. Active remodeling of cortical actin regulates spatiotemporal organization of cell surface molecules. *Cell*, 149(6), pp.1353–1367.
Gracia, E. et al., 2011. A2A adenosine receptor ligand binding and signalling is allosterically modulated by adenosine deaminase. *The Biochemical journal*, 435(3), pp.701–9.
Grant, B.D. & Donaldson, J.G., 2009. Pathways and mechanisms of endocytic recycling. *Nature reviews. Molecular cell biology*, 10(9), pp.597–608.
Grimmer, S., van Deurs, B. & Sandvig, K., 2002. Membrane ruffling and macropinocytosis in A431 cells require cholesterol. *Journal of cell science*, 115(Pt 14), pp.2953–62.
Grosshans, B.L., Ortiz, D. & Novick, P., 2006. Rabs and their effectors: achieving specificity in membrane traffic. *Proceedings of the National Academy of Sciences of the United States of America*, 103(32), pp.11821–7.
Gualix, J. et al., 1996. Nucleotide vesicular transporter of bovine chromaffin granules: Evidence for a mnemonic regulation. *Journal of Biological Chemistry*, 271(4), pp.1957–1965.
Gulbransen, B.D. et al., 2012. Activation of neuronal P2X7 receptor–pannexin-1 mediates death of enteric neurons during colitis. *Nature Medicine*, 18(4), pp.600–604.
Habermacher, C. et al., 2016. Molecular structure and function of P2X receptors. *Neuropharmacology*, 104, pp.18–30.
Haga, Y. et al., 2009. CtBP1/BARS is an activator of phospholipase D1 necessary for agonist-induced macropinocytosis. *The EMBO journal*, 28(9), pp.1197–207.
Haga, Y., Ishii, K. & Suzuki, T., 2011. N-glycosylation is critical for the stability and intracellular trafficking of glucose transporter GLUT4. *Journal of Biological Chemistry*, 286(36), pp.31320–31327.
Haitin, Y. & Attali, B., 2008. The C-terminus of Kv7 channels: a multifunctional module. *J Physiol*, 586(7), pp.1803–1810.
Handa, M. & Guidotti, G., 1996. Purification and Cloning of a Soluble ATP-Diphosphohydrolase (Apyrase) from Potato Tubers (Solanum tuberosum). *Biochemical and Biophysical Research Communications*, 218(3), pp.916–923.
Hanke, J.H. et al., 1996. Discovery of a novel, potent, and Src family-selective tyrosine

kinase inhibitor: Study of Lck- and FynT-dependent T cell activation. *Journal of Biological Chemistry*, 271(2), pp.695–701.

Hansen, S.B., 2015. Lipid agonism: The PIP2 paradigm of ligand-gated ion channels. *Biochimica et Biophysica Acta - Molecular and Cell Biology of Lipids*, 1851(5), pp.620–628.

Hanson, P.I. & Whiteheart, S.W., 2005. AAA+ proteins: have engine, will work. *Nature reviews. Molecular cell biology*, 6(7), pp.519–29.

Harder, T. & Engelhardt, K.R., 2004. Membrane domains in lymphocytes - From lipid rafts to protein scaffolds. *Traffic*, 5(4), pp.265–275.

Hattori, M. & Gouaux, E., 2012. Molecular mechanism of ATP binding and ion channel activation in P2X receptors. *Nature*, 485(7397), pp.207–212.

Henley, J.R. et al., 1998. Dynamin-mediated internalization of caveolae. *Journal of Cell Biology*, 141(1), pp.85–99.

Hille, B. et al., 2015. Phosphoinositides regulate ion channels. *Biochimica et Biophysica Acta - Molecular and Cell Biology of Lipids*, 1851(6), pp.844–856.

Hinrichsen, L. et al., 2006. Bending a membrane: how clathrin affects budding. *Proceedings of the National Academy of Sciences of the United States of America*, 103(23), pp.8715–20.

Hjort Ipsen, J. et al., 1987. Phase equilibria in the phosphatidylcholine-cholesterol system. *BBA - Biomembranes*, 905(1), pp.162–172.

Honore, P. et al., 2006. A-740003 [N-(1-{[(cyanoimino)(5-quinolinylamino) methyl]amino}-2,2-dimethylpropyl)-2-(3,4-dimethoxyphenyl)acetamide], a novel and selective P2X7 receptor antagonist, dose-dependently reduces neuropathic pain in the rat. *The Journal of pharmacology and experimental therapeutics*, 319, pp.1376–1385.

Hoppe, A.D. & Swanson, J.A., 2004. Cdc42, Rac1, and Rac2 Display Distinct Patterns of Activation during Phagocytosis. *Molecular biology of the cell*, 15(April), pp.3509–3519.

Hoshi, T., Zagotta, W.N. & Aldrich, R.W., 1990. Biophysical and molecular mechanisms of Shaker potassium channel inactivation. *Science*, 250(4980), pp.533–8.

Huang, P. et al., 2014. P2X4 forms functional ATP-activated cation channels on lysosomal membranes regulated by luminal pH. *Journal of Biological Chemistry*, 289(25), pp.17658–17667.

Huang, Y.J. et al., 2007. The role of pannexin 1 hemichannels in ATP release and cell-cell communication in mouse taste buds. *Proc Natl Acad Sci U S A*, 104(15), pp.6436–6441.

Humphreys, B.D. & Dubyak, G.R., 1996. Induction of the P2z/P2X7 nucleotide receptor and associated phospholipase D activity by lipopolysaccharide and IFN-gamma in the human THP-1 monocytic cell line. *Journal of immunology (Baltimore, Md : 1950)*, 157(12), pp.5627–5637.

Hung, A.C. & Sun, S.H., 2002. The P2X7 receptor-mediated phospholipase D activation is regulated by both PKC-dependent and PKC-independent pathways in a rat brain-derived Type-2 astrocyte cell line, RBA-2. *Cellular Signalling*, 14(1), pp.83–92.

Hung, S.C. et al., 2013. P2X4 Assembles with P2X7 and Pannexin-1 in Gingival Epithelial Cells and Modulates ATP-induced Reactive Oxygen Species Production and Inflammasome Activation. *PLoS ONE*, 8(7).

Huotari, J. & Helenius, A., 2011. Endosome maturation. *EMBO J*, 30(17), pp.3481–3500.

Hwang, T.-C. & Sheppard, D.N., 2009. Gating of the CFTR Cl- channel by ATP-driven nucleotide-binding domain dimerisation. *The Journal of physiology*, 587(Pt 10), pp.2151–61.

Idkowiak-Baldys, J. et al., 2009. Sustained Receptor Stimulation Leads to Sequestration of Recycling Endosomes in a cPKC and PLD-Dependent Manner. *The Journal of biological chemistry*.

Iglesias, R. et al., 2008. P2X7 receptor-Pannexin1 complex: pharmacology and signaling. *Am J Physiol Cell Physiol*, 295(3), pp.C752-60.

Iglesias, R.M. & Spray, D.C., 2012. Pannexin1-mediated ATP release provides signal transmission between Neuro2A cells. *Neurochemical Research*, 37(6), pp.1355–1363.

Illes, P. et al., 2011. P2X Receptors and Their Roles in Astroglia in the Central and Peripheral Nervous System. *The Neuroscientist*, 18(5), pp.422–438.

Inoue, K. & Tsuda, M., 2012. Purinergic systems, neuropathic pain and the role of microglia. *Experimental Neurology*, 234(2), pp.293–301.

Isakson, B.E. & Thompson, R.J., 2014. Pannexin-1 as a potentiator of ligand-gated receptor signaling. *Channels*, 8(2), pp.118–123.

Ishikawa, M. et al., 2011. Pannexin 3 functions as an ER Ca 2+ channel, hemichannel, and gap junction to promote osteoblast differentiation. *Journal of Cell Biology*, 193(7), pp.1257–1274.

Ivanov, D. et al., 2006. Microarray analysis of gene expression in adult retinal ganglion cells. *FEBS Letters*, 580(1), pp.331–335.

Iwamoto, T. et al., 2010. Pannexin 3 regulates intracellular ATP/cAMP levels and promotes chondrocyte differentiation. *Journal of Biological Chemistry*, 285(24), pp.18948–18958.

Jackson, M.F., 2015. Interdependence of ATP signalling and pannexin channels; the servant was really the master all along? *Biochemical Journal*, 472(3), pp.e27–e30.

Jacobson, K.A. et al., 2012. G protein-coupled adenosine (P1) and P2Y receptors: ligand design and receptor interactions. *Purinergic Signal*, 8(3), pp.419–436.

Jaumouille, V. et al., 2014. Actin cytoskeleton reorganization by syk regulates fc?? receptor responsiveness by increasing its lateral mobility and clustering. *Developmental Cell*, 29(5), pp.534–546.

Jiang, L.H. et al., 2000. Identification of amino acid residues contributing to the ATP-binding site of a purinergic P2X receptor. *Journal of Biological Chemistry*, 275(44), pp.34190–34196.

Jimenez-Mateos, E.M. et al., 2015. microRNA targeting of the P2X7 purinoceptor opposes a contralateral epileptogenic focus in the hippocampus. *Scientific reports*, 5(October), p.17486.

Jo, Y.-H. & Role, L.W., 2002. Coordinate release of ATP and GABA at in vitro synapses of lateral hypothalamic neurons. *The Journal of neuroscience : the official journal of the Society for Neuroscience*, 22(12), pp.4794–4804.

Jones, D.T., 1999. Protein secondary structure prediction based on position-specific scoring matrices. *Journal of molecular biology*, 292(2), pp.195–202.

Joseph, S.M. et al., 2004. Methylene ATP analogs as modulators of extracellular ATP metabolism and accumulation. *British journal of pharmacology*, 142(6), pp.1002–

1014.
Jovanovic, O.A., Brown, F.D. & Donaldson, J.G., 2006. An effector domain mutant of Arf6 implicates phospholipase D in endosomal membrane recycling. *Molecular biology of the cell*, 17(1), pp.327–35.
Jovic, M. et al., 2010. The early endosome: A busy sorting station for proteins at the crossroads. *Histology and Histopathology*, 25(1), pp.99–112.
Juranka, P. et al., 2001. Molecular cloning and functional expression of Xenopus laevis oocyte ATP-activated P2X4 channels. *Biochim Biophys Actam*, 1512, pp.111–124.
Jurányi, Z., Sperlágh, B. & Vizi, E.S., 1999. Involvement of P2 purinoceptors and the nitric oxide pathway in [3H]purine outflow evoked by short-term hypoxia and hypoglycemia in rat hippocampal slices. *Brain Research*, 823(1–2), pp.183–190.
Kanjanamekanant, K., Luckprom, P. & Pavasant, P., 2014. P2X7 receptor-Pannexin1 interaction mediates stress-induced interleukin-1 beta expression in human periodontal ligament cells. *J Periodontal Res*, 49(5), pp.595–602.
Kanjanamekanant, K., Luckprom, P. & Pavasant, P., 2014. P2X7 receptor-Pannexin1 interaction mediates stress-induced interleukin-1 beta expression in human periodontal ligament cells. *Journal of Periodontal Research*, 49(5), pp.595–602.
Karasawa, A. & Kawate, T., 2016. Structural basis for subtype-specific inhibition of the P2X7 receptor. *eLife*, 5.
Kawate, T. et al., 2009. Crystal structure of the ATP-gated P2X4 ion channel in the closed state. *Nature*, 460(7255), pp.592–598.
Kelly, B.T. & Owen, D.J., 2011. Endocytic sorting of transmembrane protein cargo. *Current Opinion in Cell Biology*, 23(4), pp.404–412.
Khakh, B.B.S. & Burnstock, G., 2009. The double life of ATP. *Scientific American*, 301(6), pp.84–90, 92.
Khakh, B.S. et al., 2001. International union of pharmacology. XXIV. Current status of the nomenclature and properties of P2X receptors and their subunits. *Pharmacol Rev*, 53(1), pp.107–118.
Khakh, B.S., 2001. Molecular physiology of P2X receptors and ATP signalling at synapses. *Nat Rev Neurosci*, 2(3), pp.165–174.
Khakh, B.S. et al., 1999. Neuronal P2X transmitter-gated cation channels change their ion selectivity in seconds. *Nature neuroscience*, 2(4), pp.322–330.
Kido, Y. et al., 2014. Regulation of activity of P2X7 receptor by its splice variants in cultured mouse astrocytes. *GLIA*, 62(3), pp.440–451.
Kim, J.E. & Kang, T.C., 2011. The P2X7 receptor-pannexin-1 complex decreases muscarinic acetylcholine receptor-mediated seizure susceptibility in mice. *Journal of Clinical Investigation*, 121(5), pp.2037–2047.
Kim, W. et al., 2011. Systematic and quantitative assessment of the ubiquitin-modified proteome. *Molecular cell*, 44(2), pp.325–340.
Kirchhausen, T., Macia, E. & Pelish, H.E., 2008. Use of dynasore, the small molecule inhibitor of dynamin, in the regulation of endocytosis. *Methods Enzymol*, 438, pp.77–93.
Klar, T.A. et al., 2000. Fluorescence microscopy with diffraction resolution barrier broken by stimulated emission. *Proc Natl Acad Sci U S A*, 97(15), pp.8206–8210.
Klebe, R. & Ruddle, F., 1969. Neuroblastoma: Cell culture analysis of a differentiating stem cell system. *J Cell Biol*, 43(69A).

Klein, U., Gimpl, G. & Fahrenholz, F., 1995. Alteration of the myometrial plasma membrane cholesterol content with beta-cyclodextrin modulates the binding affinity of the oxytocin receptor. *Biochemistry*, 34(42), pp.13784–13793.

Van Der Kloot, W., 2003. Loading and recycling of synaptic vesicles in the Torpedo electric organ and the vertebrate neuromuscular junction. *Progress in Neurobiology*, 71(4), pp.269–303.

Koivusalo, M. et al., 2010. Amiloride inhibits macropinocytosis by lowering submembranous pH and preventing Rac1 and Cdc42 signaling. *Journal of Cell Biology*, 188(4), pp.547–563.

Kooijman, E.E. et al., 2003. Modulation of membrane curvature by phosphatidic acid and lysophosphatidic acid. *Traffic (Copenhagen, Denmark)*, 4(3), pp.162–174.

Kooijman, E.E. et al., 2005. Spontaneous curvature of phosphatidic acid and lysophosphatidic acid. *Biochemistry*, 44(6), pp.2097–2102.

Koyanagi, S. et al., 2016. Glucocorticoid regulation of ATP release from spinal astrocytes underlies diurnal exacerbation of neuropathic mechanical allodynia. *Nature Communications*, 7, p.13102.

von Kugelgen, I., 2006. Pharmacological profiles of cloned mammalian P2Y-receptor subtypes. *Pharmacol Ther*, 110(3), pp.415–432.

Von Kügelgen, I. & Hoffmann, K., 2016. Pharmacology and structure of P2Y receptors. *Neuropharmacology*, 104, pp.50–61.

Kuijl, C. et al., 2007. Intracellular bacterial growth is controlled by a kinase network around PKB/AKT1. *Nature*, 450(7170), pp.725–730.

Kumari, S. & Mayor, S., 2008. ARF1 is directly involved in dynamin-independent endocytosis. *Nature Cell Biology*, 10(1), pp.30–41.

Kumari, S., Mg, S. & Mayor, S., 2010. Endocytosis unplugged: multiple ways to enter the cell. *Cell research*, 20(3), pp.256–275.

Kurtenbach, S. et al., 2013. Pannexin1 Channel Proteins in the Zebrafish Retina Have Shared and Unique Properties. *PLoS ONE*, 8(10).

Kyei, G.B. et al., 2006. Rab14 is critical for maintenance of Mycobacterium tuberculosis phagosome maturation arrest. *The EMBO journal*, 25(22), pp.5250–5259.

de la Rosa, D.A. et al., 2000. Structure and Regulation of Amiloride-Sensitive Sodium Channels. *Annual Review of Physiology*, 62(1), pp.573–594.

Lacar, B. et al., 2012. Neural progenitor cells regulate capillary blood flow in the postnatal subventricular zone. *J Neurosci*, 32(46), pp.16435–16448.

Lai, C.P. et al., 2007. Tumor-suppressive effects of pannexin 1 in C6 glioma cells. *Cancer Res*, 67(4), pp.1545–1554.

Laird, D.W., 2006. Life cycle of connexins in health and disease. *The Biochemical journal*, 394(Pt 3), pp.527–543.

Lall, P. et al., 2015. Structure-function analyses of the interactions between Rab11 and Rab14 small GTPases with their shared effector Rab coupling protein (RCP). *Journal of Biological Chemistry*, 290(30), pp.18817–18832.

Langlois, S. et al., 2014. Pannexin 1 and pannexin 3 channels regulate skeletal muscle myoblast proliferation and differentiation. *Journal of Biological Chemistry*, 289(44), pp.30717–30731.

Laude, A.J. & Prior, I. a, 2004. Plasma membrane microdomains: organization, function and trafficking. *Molecular membrane biology*, 21(3), pp.193–205.

Lazarowski, E.R., 2012. Vesicular and conductive mechanisms of nucleotide release. *Purinergic Signalling*, 8(3), pp.359–373.

Lee, M.C.S. & Miller, E.A., 2007. Molecular mechanisms of COPII vesicle formation. *Seminars in Cell and Developmental Biology*, 18(4), pp.424–434.

Leithe, E. & Rivedal, E., 2007. Ubiquitination of gap junction proteins. *The Journal of membrane biology*, 217(1–3), pp.43–51.

Lemus, L. & Goder, V., 2014. Regulation of Endoplasmic Reticulum-Associated Protein Degradation (ERAD) by Ubiquitin. *Cells*, 3(2), pp.824–847.

Li, H. et al., 2008. Rab4 and Rab11 coordinately regulate the recycling of angiotensin II type I receptor as demonstrated by fluorescence resonance energy transfer microscopy. *Journal of biomedical optics*, 13(3), p.31206.

Liberali, P. et al., 2008. The closure of Pak1-dependent macropinosomes requires the phosphorylation of CtBP1/BARS. *The EMBO journal*, 27(7), pp.970–81.

Licona-Limón, I. et al., 2015. CD13 mediates phagocytosis in human monocytic cells. *Journal of leukocyte biology*, 98(1), pp.85–98.

Lim, D.A. & Alvarez-Buylla, A., 2016. The adult ventricular-subventricular zone (V-SVZ) and olfactory bulb (OB) neurogenesis. *Cold Spring Harbor Perspectives in Biology*, 8(5).

Lin, J.H. et al., 2007. Purinergic signaling regulates neural progenitor cell expansion and neurogenesis. *Dev Biol*, 302(1), pp.356–366.

Linford, A. et al., 2012. Rab14 and its exchange factor FAM116 link endocytic recycling and adherens junction stability in migrating cells. *Dev Cell*, 22(5), pp.952–966. Available at: http://www.ncbi.nlm.nih.gov/pubmed/22595670.

Lippincott-Schwartz, J. et al., 1991. Brefeldin A's effects on endosomes, lysosomes, and the TGN suggest a general mechanism for regulating organelle structure and membrane traffic. *Cell*, 67(3), pp.601–616.

Lippincott-Schwartz, J. et al., 1989. Rapid redistribution of Golgi proteins into the ER in cells treated with brefeldin A: Evidence for membrane cycling from Golgi to ER. *Cell*, 56(5), pp.801–813.

Locovei, S. et al., 2007. Pannexin1 is part of the pore forming unit of the P2X(7) receptor death complex. *FEBS Lett*, 581(3), pp.483–488.

Locovei, S., Bao, L. & Dahl, G., 2006. Pannexin 1 in erythrocytes: function without a gap. *Proc Natl Acad Sci U S A*, 103(20), pp.7655–7659.

Locovei, S., Wang, J. & Dahl, G., 2006. Activation of pannexin 1 channels by ATP through P2Y receptors and by cytoplasmic calcium. *FEBS Lett*, 580(1), pp.239–244.

Lohman, A.W., Billaud, M., et al., 2012. Expression of pannexin isoforms in the systemic murine arterial network. *J Vasc Res*, 49(5), pp.405–416.

Lohman, A.W. et al., 2015. Pannexin 1 channels regulate leukocyte emigration through the venous endothelium during acute inflammation. *Nature Communications*, 6, p.7965.

Lohman, A.W., Weaver, J.L., et al., 2012. S-nitrosylation inhibits pannexin 1 channel function. *J Biol Chem*, 287(47), pp.39602–39612.

Lohman, A.W. & Isakson, B.E., 2014. Differentiating connexin hemichannels and pannexin channels in cellular ATP release. *FEBS Lett*, 588(8), pp.1379–1388.

Lu, R. & Wilson, J.M., 2016. Rab14 specifies the apical membrane through Arf6-mediated regulation of lipid domains and Cdc42. *Scientific Reports*, 6(August),

p.38249.
Lundmark, R. et al., 2008. The GTPase-Activating Protein GRAF1 Regulates the CLIC/GEEC Endocytic Pathway. *Current Biology*, 18(22), pp.1802–1808.
Lunkes, G.I. et al., 2003. Enzymes that hydrolyze adenine nucleotides in diabetes and associated pathologies. *Thrombosis Research*, 109(4), pp.189–194.
Ma, W. et al., 2009. Pharmacological characterization of pannexin-1 currents expressed in mammalian cells. *J Pharmacol Exp Ther*, 328(2), pp.409–418.
Ma, Z. et al., 2016. Calcium homeostasis modulator (CALHM) ion channels. *Pflugers Archiv European Journal of Physiology*, 468(3), pp.395–403.
Macia, E. et al., 2006. Dynasore, a cell-permeable inhibitor of dynamin. *Dev Cell*, 10(6), pp.839–850.
Maeda, S. et al., 2009. Structure of the connexin 26 gap junction channel at 3.5 A resolution. *Nature*, 458(7238), pp.597–602.
Maldonado-Baez, L., Williamson, C. & Donaldson, J.G., 2013. Clathrin-independent endocytosis: a cargo-centric view. *Exp Cell Res*, 319(18), pp.2759–2769.
Mansoor, S.E. et al., 2016. X-ray structures define human P2X3 receptor gating cycle and antagonist action. *Nature*, 538, pp.66–71.
Masgrau, R. et al., 2009. BM88/Cend1 regulates stimuli-induced intracellular calcium mobilization. *Neuropharmacology*, 56(3), pp.598–609.
Masin, M. et al., 2012. Expression, assembly and function of novel C-terminal truncated variants of the mouse P2X7 receptor: Re-evaluation of P2X7 knockouts. *British Journal of Pharmacology*, 165(4), pp.978–993.
Maslieieva, V. & Thompson, R.J., 2014. A critical role for pannexin-1 in activation of innate immune cells of the choroid plexus. *Channels*, 8(2), pp.131–141.
Mayor, S., Parton, R.G. & Donaldson, J.G., 2014. Clathrin-independent pathways of endocytosis. *Cold Spring Harbor Perspectives in Biology*, 6(6).
Mayor, S. & Riezman, H., 2004. Sorting GPI-anchored proteins. *Nature reviews. Molecular cell biology*, 5(2), pp.110–20.
McGaraughty, S. et al., 2007. P2X7-related modulation of pathological nociception in rats. *Neuroscience*, 146(4), pp.1817–1828.
McMahon, H.T. & Boucrot, E., 2011. Molecular mechanism and physiological functions of clathrin-mediated endocytosis. *Nat Rev Mol Cell Biol*, 12(8), pp.517–533.
McMahon, H.T. & Gallop, J.L., 2005. Membrane curvature and mechanisms of dynamic cell membrane remodelling. *Nature*, 438(7068), pp.590–596.
van Meer, G. & Simons, K., 1988. Lipid polarity and sorting in epithelial cells. *Journal of Cellular Biochemistry*, 36(1), pp.51–58.
Melani, A. et al., 2005. ATP extracellular concentrations are increased in the rat striatum during in vivo ischemia. *Neurochem Int*, 47(6), pp.442–448.
Messemer, N. et al., 2013. P2X7 receptors at adult neural progenitor cells of the mouse subventricular zone. *Neuropharmacology*, 73, pp.122–137.
Metzger, M.W. et al., 2016. Genetically dissecting P2rx7 expression within the central nervous system using conditional humanized mice. *Purinergic Signalling*, pp.1–18.
Michalski, K. & Kawate, T., 2016. Carbenoxolone inhibits Pannexin1 channels through interactions in the first extracellular loop. *The Journal of General Physiology*, 147(2), pp.165–174.
Ming, G.L. & Song, H., 2011. Adult neurogenesis in the mammalian brain: significant

answers and significant questions. *Neuron*, 70(4), pp.687–702.
Mishra, S.K. et al., 2006. Extracellular nucleotide signaling in adult neural stem cells: synergism with growth factor-mediated cellular proliferation. *Development*, 133(4), pp.675–684.
Mochida, S. et al., 2008. Regulation of Presynaptic CaV2.1 Channels by Ca2+ Sensor Proteins Mediates Short-Term Synaptic Plasticity. *Neuron*, 57(2), pp.210–216.
Morel, N. & Meunier, F. -M, 1981. Simultaneous Release of Acetylcholine and ATP from Stimulated Cholinergic Synaptosomes. *Journal of Neurochemistry*, 36(5), pp.1766–1773.
Munro, S., 2003. Lipid Rafts: Elusive or Illusive? *Cell*, 115(4), pp.377–388.
Murata, M. et al., 1995. VIP21/caveolin is a cholesterol-binding protein (membrane microdomains/intracellular transport/membrane reconstitution). *Cell Biology*, 92, pp.10339–10343.
Naslavsky, N., Weigert, R. & Donaldson, J.G., 2003. Convergence of Non-clathrin-and Clathrin-derived Endosomes Involves Arf6 Inactivation and Changes in Phosphoinositides. *Molecular Biology of the Cell*, 14, pp.417–431.
Negoro, H. et al., 2014. Pannexin 1 channels play essential roles in urothelial mechanotransduction and intercellular signaling. *PLoS ONE*, 9(8).
Neher, E. & Almers, W., 1986. Fast calcium transients in rat peritoneal mast cells are not sufficient to trigger exocytosis. *EMBO J*, 5(1), pp.51–53.
Nelson, D.W. et al., 2006. Structure-activity relationship studies on a series of novel, substituted 1-benzyl-5-phenyltetrazole P2X7 antagonists. *J Med Chem*, 49(12), pp.3659–3666.
Nicke, A. et al., 2009. A functional P2X7 splice variant with an alternative transmembrane domain 1 escapes gene inactivation in P2X7 knock-out mice. *Journal of Biological Chemistry*, 284(38), pp.25813–25822.
Nicke, A., 2008. Homotrimeric complexes are the dominant assembly state of native P2X7 subunits. *Biochemical and Biophysical Research Communications*, 377(3), pp.803–808.
North, R.A., 2002. Molecular physiology of P2X receptors. *Physiol Rev*, 82(4), pp.1013–1067.
North, R.A., 2002. Molecular physiology of P2X receptors. *Physiological reviews*, 82(4), pp.1013–1067.
North, R.A. & Surprenant, A., 2000. Pharmacology of cloned P2X receptors. *Annual review of pharmacology and toxicology*, 40, pp.563–80.
O'Luanaigh, N. et al., 2002. Continual production of phosphatidic acid by phospholipase D is essential for antigen-stimulated membrane ruffling in cultured mast cells. *Molecular biology of the cell*, 13(10), pp.3730–46.
Odin, J.A. et al., 1991. Regulation of phagocytosis and [Ca2+]i flux by distinct regions of an Fc receptor. *Science*, 254(5039), pp.1785–1788.
Ogiso, H., Taniguchi, M. & Okazaki, T., 2015. Analysis of lipid-composition changes in plasma membrane microdomains. *Journal of Lipid Research*, 56, pp.1–34.
Ohbuchi, T. et al., 2011. Possible contribution of pannexin channel to ATP-induced currents in vitro in vasopressin neurons isolated from the rat supraoptic nucleus. *Brain Research*, 1394, pp.71–78.
Ohno, H. et al., 1995. Interaction of tyrosine-based sorting signals with clathrin-

associated proteins. *Science (New York, N.Y.)*, 269(5232), pp.1872–1875.

Ohsawa, K. et al., 2010. P2Y12 receptor-mediated integrin-beta1 activation regulates microglial process extension induced by ATP. *Glia*, 58(7), pp.790–801.

Okamoto, Y. et al., 2000. Cholesterol oxidation switches the internalization pathway of endothelin receptor type A from caveolae to clathrin-coated pits in Chinese hamster ovary cells. *J Biol Chem*, 275(9), pp.6439–6446.

Orellano, E.A. et al., 2010. Inhibition of neuronal cell death after retinoic acid-induced down-regulation of P2X7 nucleotide receptor expression. *Molecular and Cellular Biochemistry*, 337(1–2), pp.83–99.

Oshima, A. et al., 2007. Three-dimensional structure of a human connexin26 gap junction channel reveals a plug in the vestibule. *Proceedings of the National Academy of Sciences*, 104(24), pp.10034–10039.

Otto, G.P. & Nichols, B.J., 2011. The roles of flotillin microdomains--endocytosis and beyond. *J Cell Sci*, 124(Pt 23), pp.3933–3940.

Oude Weernink, P.A., López De Jesús, M. & Schmidt, M., 2007. Phospholipase D signaling: Orchestration by PIP2 and small GTPases. *Naunyn-Schmiedeberg's Archives of Pharmacology*, 374(5–6), pp.399–411.

Padron, D. et al., 2003. Phosphatidylinositol phosphate 5-kinase Iβ recruits AP-2 to the plasma membrane and regulates rates of constitutive endocytosis. *Journal of Cell Biology*, 162(4), p.693.

Pan, H.-C., Chou, Y.-C. & Sun, S.H., 2015. P2X7 R-mediated Ca(2+) -independent d-serine release via pannexin-1 of the P2X7 R-pannexin-1 complex in astrocytes. *Glia*, 63(5), pp.877–93.

Panchin, Y. et al., 2000. A ubiquitous family of putative gap junction molecules. *Curr Biol*, 10(13), pp.R473-4.

Panchin, Y. V., 2005. Evolution of gap junction proteins - the pannexin alternative. *Journal of Experimental Biology*, 208(8), pp.1415–1419.

Pankratov, Y. et al., 2006. Vesicular release of ATP at central synapses. *Pflugers Archiv European Journal of Physiology*, 452(5), pp.589–597.

Paukert, M., Hidayat, S. & Grunder, S., 2002. The P2X(7) receptor from Xenopus laevis: formation of a large pore in Xenopus oocytes. *FEBS Lett.*, 513, pp.253–258.

Payne, C.K. et al., 2007. Internalization and trafficking of cell surface proteoglycans and proteoglycan-binding ligands. *Traffic*, 8(4), pp.389–401.

Pelegrin, P. et al., 2006. Pannexin-1 mediates large pore formation and interleukin-1β release by the ATP-gated P2X7 receptor. *The EMBO Journal*, 25(21), pp.5071–5082.

Pelegrin, P., Barroso-Gutierrez, C. & Surprenant, A., 2008. P2X7 receptor differentially couples to distinct release pathways for IL-1beta in mouse macrophage. *J Immunol*, 180(11), pp.7147–7157.

Pelegrin, P. & Surprenant, A., 2007. Pannexin-1 couples to maitotoxin- and nigericin-induced interleukin-1beta release through a dye uptake-independent pathway. *J Biol Chem*, 282(4), pp.2386–2394.

Pelegrin, P. & Surprenant, A., 2009. The P2X(7) receptor-pannexin connection to dye uptake and IL-1beta release. *Purinergic Signal*, 5(2), pp.129–137.

Peng, W. et al., 2009. Systemic administration of an antagonist of the ATP-sensitive receptor P2X7 improves recovery after spinal cord injury. *Proceedings of the*

National Academy of Sciences of the United States of America, 106(30), pp.12489–93.

Penuela, S. et al., 2008. Diverse subcellular distribution profiles of pannexin 1 and pannexin 3. *Cell Commun Adhes*, 15(1), pp.133–142.

Penuela, S. et al., 2009. Glycosylation regulates pannexin intermixing and cellular localization. *Mol Biol Cell*, 20(20), pp.4313–4323.

Penuela, S. et al., 2012. Loss of pannexin 1 attenuates melanoma progression by reversion to a melanocytic phenotype. *J Biol Chem*, 287(34), pp.29184–29193.

Penuela, S. et al., 2007. Pannexin 1 and pannexin 3 are glycoproteins that exhibit many distinct characteristics from the connexin family of gap junction proteins. *J Cell Sci*, 120(21), pp.3772–3783.

Penuela, S., Gehi, R. & Laird, D.W., 2013. The biochemistry and function of pannexin channels. *Biochim Biophys Acta*, 1828(1), pp.15–22.

Pfleger, C. et al., 2012. Detection of caveolin-3/caveolin-1/P2X7R complexes in mice atrial cardiomyocytes in vivo and in vitro. *Histochemistry and Cell Biology*, 138(2), pp.231–241.

Pike, L.J. et al., 2002. Lipid rafts are enriched in arachidonic acid and plasmenylethanolamine and their composition is independent of caveolin-1 expression: A quantitative electrospray ionization/mass spectrometric analysis. *Biochemistry*, 41(6), pp.2075–2088.

Pike, L.J. & Casey, L., 1996. Localization and turnover of phosphatidylinositol 4,5-bisphosphate in caveolin-enriched membrane domains. *Journal of Biological Chemistry*, 271(43), pp.26453–26456.

Poornima, V. et al., 2012. P2X7 receptor-pannexin 1 hemichannel association: effect of extracellular calcium on membrane permeabilization. *Journal of molecular neuroscience : MN*, 46(3), pp.585–594.

Powelka, A.M. et al., 2004. Stimulation-dependent recycling of integrin β1 regulated by ARF6 and Rab11. *Traffic*, 5(1), pp.20–36.

Praetorius, H.A. & Leipziger, J., 2009. ATP release from non-excitable cells. *Purinergic Signalling*, 5(4), pp.433–446.

Prochnow, N. et al., 2009. Pannexin1 in the outer retina of the zebrafish, Danio rerio. *Neuroscience*, 162(4), pp.1039–1054.

Prochnow, N. et al., 2012. Pannexin1 stabilizes synaptic plasticity and is needed for learning. *PLoS One*, 7(12), p.e51767.

Puthussery, T. & Fletcher, E.L., 2004. Synaptic Localization of P2X7 Receptors in the Rat Retina. *Journal of Comparative Neurology*, 472(1), pp.13–23.

Qiu, F. & Dahl, G., 2009. A permeant regulating its permeation pore: inhibition of pannexin 1 channels by ATP. *American journal of physiology. Cell physiology*, 296, pp.C250–C255.

Qiu, F., Wang, J. & Dahl, G., 2012. Alanine substitution scanning of pannexin1 reveals amino acid residues mediating ATP sensitivity. *Purinergic signalling*, 8(1), pp.81–90. Available at: http://www.ncbi.nlm.nih.gov/pubmed/21987098.

Qureshi, O.S. et al., 2007. Regulation of P2X4 receptors by lysosomal targeting, glycan protection and exocytosis. *J Cell Sci*, 120(Pt 21), pp.3838–3849.

Racoosin, E.L. & Swanson, J.A., 1989. Macrophage colony-stimulating factor (rM-CSF) stimulates pinocytosis in bone marrow-derived macrophages. *J Exp Med*, 170(5),

pp.1635–1648.
Radhakrishna, H. & Donaldson, J.G., 1997. ADP-ribosylation factor 6 regulates a novel plasma membrane recycling pathway. *Journal of Cell Biology*, 139(1), pp.49–61.
Ransford, G.A. et al., 2009. Pannexin 1 contributes to ATP release in airway epithelia. *Am J Respir Cell Mol Biol*, 41(5), pp.525–534.
Rappold, P.M., Lynd-Balta, E. & Joseph, S.A., 2006. P2X7 receptor immunoreactive profile confined to resting and activated microglia in the epileptic brain. *Brain Research*, 1089(1), pp.171–178.
Rappoport, J.Z. & Simon, S.M., 2009. Endocytic trafficking of activated EGFR is AP-2 dependent and occurs through preformed clathrin spots. *J Cell Sci*, 122(Pt 9), pp.1301–1305.
Raslan, A. et al., 2016. Pannexin-1 expression in developing mouse nervous system: new evidence for expression in sensory ganglia. *Cell & Tissue Research*, 364, pp.29–41.
Ray, A. et al., 2005. Site-specific and developmental expression of pannexin1 in the mouse nervous system. *Eur J Neurosci*, 21(12), pp.3277–3290.
Reigada, D. et al., 2003. Control of neurotransmitter release by an internal gel matrix in synaptic vesicles. *Proceedings of the National Academy of Sciences of the United States of America*, 100(6), pp.3485–3490.
Ridley, A.J., 2006. Rho GTPases and actin dynamics in membrane protrusions and vesicle trafficking. *Trends in Cell Biology*, 16(10), pp.522–529.
Riento, K. et al., 2009. Endocytosis of flotillin-1 and flotillin-2 is regulated by Fyn kinase. *Journal of cell science*, 122, pp.912–918.
Riquelme, M.A. et al., 2013. The ATP required for potentiation of skeletal muscle contraction is released via pannexin hemichannels. *Neuropharmacology*, 75, pp.594–603.
Roberts, J.A. et al., 2008. Cysteine substitution mutagenesis and the effects of methanethiosulfonate reagents at P2X2 and P2X4 receptors support a core common mode of ATP action at P2X receptors. *Journal of Biological Chemistry*, 283(29), pp.20126–20136.
Robinson, L.E. et al., 2014. Plasma Membrane Cholesterol as a Regulator of Human and Rodent P2X7 Receptor Activation and Sensitization. *The Journal of biological chemistry*, 289(46), pp.31983–31994.
Robinson, L.E. & Murrell-Lagnado, R.D., 2013. The trafficking and targeting of P2X receptors. *Front Cell Neurosci*, 7, p.233.
Rodal, S.K. et al., 1999. Extraction of cholesterol with methyl-beta-cyclodextrin perturbs formation of clathrin-coated endocytic vesicles. *Mol Biol Cell*, 10(4), pp.961–974.
Rollet-Labelle, E. et al., 2004. Recruitment of the cross-linked opsonic receptor CD32A (FcgammaRIIA) to high-density detergent-resistant membrane domains in human neutrophils. *The Biochemical journal*, 381(Pt 3), pp.919–928.
Romanello, M. et al., 2005. Autocrine/paracrine stimulation of purinergic receptors in osteoblasts: Contribution of vesicular ATP release. *Biochemical and Biophysical Research Communications*, 331(4), pp.1429–1438.
Römer, W. et al., 2010. Actin Dynamics Drive Membrane Reorganization and Scission in Clathrin-Independent Endocytosis. *Cell*, 140(4), pp.540–553.
Rothberg, K.G. et al., 1992. Caveolin, a protein component of caveolae membrane coats. *Cell*, 68(4), pp.673–682.

Rothberg, K.G. et al., 1990. Cholesterol controls the clustering of the glycophospholipid-anchored membrane receptor for 5-methyltetrahydrofolate. *J Cell Biol*, 111(6 Pt 2), pp.2931–2938.

Rusakov, D. a & Kullmann, D.M., 1998. Extrasynaptic glutamate diffusion in the hippocampus: ultrastructural constraints, uptake, and receptor activation. *The Journal of neuroscience : the official journal of the Society for Neuroscience*, 18(9), pp.3158–3170.

Sabharanjak, S. et al., 2002. GPI-anchored proteins are delivered to recycling endosomes via a distinct cdc42-regulated clathrin-independent pinocytic pathway. *Developmental Cell*, 2(4), pp.411–423.

Sahu, G., Sukumaran, S. & Bera, A.K., 2014. Pannexins form gap junctions with electrophysiological and pharmacological properties distinct from connexins. *Scientific reports*, 4, p.4955.

Sallusto, F. et al., 1995. Dendritic cells use macropinocytosis and the mannose receptor to concentrate macromolecules in the major histocompatibility complex class II compartment: downregulation by cytokines and bacterial products. *The Journal of experimental medicine*, 182(2), pp.389–400.

Sanchez-Arias, J.C., Wicki-Stordeur, L.E. & Swayne, L.A., 2016. Perspectives on the role of Pannexin 1 in neural precursor cell biology. *Neural Regen Res*, 11(10), pp.1540–1544.

Sandilos, J.K. et al., 2012. Pannexin 1, an ATP release channel, is activated by caspase cleavage of its pore-associated C terminal autoinhibitory region. *J Biol Chem*.

Sandilos, J.K. & Bayliss, D.A., 2012. Physiological mechanisms for the modulation of pannexin 1 channel activity. *J Physiol*, 590(Pt 24), pp.6257–6266.

Sannerud, R. et al., 2011. ADP ribosylation factor 6 (ARF6) controls amyloid precursor protein (APP) processing by mediating the endosomal sorting of BACE1. *Proc Natl Acad Sci U S A*, 108(34), pp.E559–E568.

Santiago, M.F. et al., 2011. Targeting pannexin1 improves seizure outcome. *PLoS ONE*, 6(9), p.e25178.

Sawada, K. et al., 2008. Identification of a vesicular nucleotide transporter. *Proc Natl Acad Sci U S A*, 105(15), pp.5683–5686.

Schenk, U. et al., 2008. Purinergic control of T cell activation by ATP released through pannexin-1 hemichannels. *Sci Signal*, 1(39), p.ra6.

Schetinger, M.R.C. et al., 2007. NTPDase and 5???-nucleotidase activities in physiological and disease conditions: New perspectives for human health. *BioFactors*, 31(2), pp.77–98.

Schindelin, J. et al., 2012. Fiji: an open-source platform for biological-image analysis. *Nature Methods*, 9(7), pp.676–82.

Schindelin, J. et al., 2015. The ImageJ ecosystem: An open platform for biomedical image analysis. *Molecular Reproduction and Development*, 82(7–8), pp.518–529.

Schneider-Poetsch, T. et al., 2010. Inhibition of eukaryotic translation elongation by cycloheximide and lactimidomycin. *Nature chemical biology*, 6(3), pp.209–217.

Schneider, A. et al., 2008. Flotillin-dependent clustering of the amyloid precursor protein regulates its endocytosis and amyloidogenic processing in neurons. *J Neurosci*, 28, pp.2874–2882.

Schoonderwoert, V.T. et al., 2013. Huygens STED Deconvolution Increases Signal-to-

Noise and Image Resolution towards 22 nm. *Microscopy Today*, 21(6), pp.38–44.
Schroeder, R., London, E. & Brown, D., 1994. Interactions between saturated acyl chains confer detergent resistance on lipids and glycosylphosphatidylinositol (GPI)-anchored proteins: GPI-anchored proteins in liposomes and cells show similar behavior. *Proc Natl Acad Sci USA*, 91(25), pp.12130–4.
Schwartz, J.H., 2003. Ubiquitination, protein turnover, and long-term synaptic plasticity. *Science's STKE : signal transduction knowledge environment*, 2003(190), p.pe26.
Seref-Ferlengez, Z. et al., 2016. P2X7R-Panx1 complex impairs bone mechanosignaling under high glucose levels associated with type-1 diabetes. *PLoS ONE*, 11(5).
Sesti, C. et al., 2002. EctoNucleotidase in cardiac sympathetic nerve endings modulates ATP-mediated feedback of norepinephrine release. *The Journal of pharmacology and experimental therapeutics*, 300(2), pp.605–611.
Sharma, P. et al., 2004. Nanoscale Organization of Multiple GPI-Anchored Proteins in Living Cell Membranes. *Cell*, 116(4), pp.577–589.
Shoji, K.F. et al., 2014. Pannexin1 channels act downstream of P2X receptors in ATP-induced murine T-cell death. *Channels (Austin)*, 8(2).
Shrimal, S., Cherepanova, N. & Gilmore, R., 2015. Cotranslational and posttranslocational N-glycosylation of proteins in the endoplasmic reticulum. *Semin Cell Dev Biol*, 41, pp.71–78.
Siebert, A.P. et al., 2013. Structural and functional similarities of calcium homeostasis modulator 1 (CALHM1) ion channel with connexins, pannexins, and innexins. *Journal of Biological Chemistry*, 288(9), pp.6140–6153.
Sievers, F. et al., 2011. Fast, scalable generation of high-quality protein multiple sequence alignments using Clustal Omega. *Molecular systems biology*, 7(1), p.539.
Sikora, J. et al., 2014. Hemolysis is a primary ATP-release mechanism in human erythrocytes. *Blood*, 124(13), pp.2150–2157.
Silverman, W., Locovei, S. & Dahl, G., 2008. Probenecid, a gout remedy, inhibits pannexin 1 channels. *Am J Physiol Cell Physiol*, 295(3), pp.C761-7.
Silverman, W.R. et al., 2009. The pannexin 1 channel activates the inflammasome in neurons and astrocytes. *J Biol Chem*, 284(27), pp.18143–18151.
Sim, J. a et al., 2004. Reanalysis of P2X7 receptor expression in rodent brain. *The Journal of neuroscience : the official journal of the Society for Neuroscience*, 24(28), pp.6307–14.
Simons, K. & Gerl, M.J., 2010. Revitalizing membrane rafts: new tools and insights. *Nature reviews. Molecular cell biology*, 11(10), pp.688–699.
Simons, K. & Ikonen, E., 1997. Functional rafts in cell membranes. *Nature*, 387, pp.569–572.
Singer, S.J. & Nicolson, G.L., 1972. The Fluid Mosaic Model of the structure of cell membranes. *Science*, 175, pp.720–731.
Snyder, P.M., 2005. Minireview: Regulation of epithelial Na+ channel trafficking. *Endocrinology*, 146(12), pp.5079–5085.
Söderberg, O. et al., 2006. Direct observation of individual endogenous protein complexes in situ by proximity ligation. *Nature Methods*, 3(12), pp.995–1000.
Sofer, A. & Futerman, A.H., 1995. Cationic amphiphilic drugs inhibit the internalization of cholera toxin to the Golgi apparatus and the subsequent elevation of cyclic AMP. *J Biol Chem*, 270(20), pp.12117–12122.

Sonnichsen, B. et al., 2000. Distinct membrane domains on endosomes in the recycling pathway visualized by multicolor imaging of Rab4, Rab5, and Rab11. *J Cell Biol*, 149(4), pp.901–914.

Sorge, R.E. et al., 2012. Genetically determined P2X7 receptor pore formation regulates variability in chronic pain sensitivity. *Nature medicine*, 18(4), pp.595–599.

Sorkin, A. & von Zastrow, M., 2009. Endocytosis and signalling: intertwining molecular networks. *Nature reviews. Molecular cell biology*, 10(9), pp.609–22.

Sosinsky, G.E. et al., 2011. Pannexin channels are not gap junction hemichannels. *Channels*, 5(3), pp.193–197.

Spagnol, G., Sorgen, P.L. & Spray, D.C., 2014. Structural order in Pannexin 1 cytoplasmic domains. *Channels*, 8(2), pp.157–166.

Sperlagh, B. & Illes, P., 2014. P2X7 receptor: an emerging target in central nervous system diseases. *Trends Pharmacol Sci*, 35(10), pp.537–547.

Sridharan, M. et al., 2010. Pannexin 1 is the conduit for low oxygen tension-induced ATP release from human erythrocytes. *American journal of physiology. Heart and circulatory physiology*, 299(4), pp.H1146-52.

Stenmark, H., 2009. Rab GTPases as coordinators of vesicle traffic. *Nature reviews. Molecular cell biology*, 10(8), pp.513–25.

Stjärne, L., 2001. Novel dual “small” vesicle model of ATP- and noradrenaline-mediated sympathetic neuromuscular transmission. *Autonomic Neuroscience: Basic and Clinical*, 87(1), pp.16–36.

Strauss, K. et al., 2010. Exosome secretion ameliorates lysosomal storage of cholesterol in Niemann-Pick type C disease. *Journal of Biological Chemistry*, 285(34), pp.26279–26288.

Le Stunff, H. et al., 2004. The Pro-451 to Leu Polymorphism within the C-terminal Tail of P2X7 Receptor Impairs Cell Death but Not Phospholipase D Activation in Murine Thymocytes. *Journal of Biological Chemistry*, 279(17), pp.16918–16926.

Le Stunff, H. & Raymond, M., 2007. P2X7 receptor-mediated phosphatidic acid production delays ATP-induced pore opening and cytolysis of RAW 264.7 macrophages. *Cell Signal*, 19(9), pp.1909–1918.

Suadicani, S. et al., 2009. Point mutation in the mouse P2X7 receptor affects intercellular calcium waves in astrocytes. *ASN Neuro*, 1(1).

Surprenant, A. et al., 1996. The cytolytic P2Z receptor for extracellular ATP identified as a P2X receptor (P2X7). *Science (New York, N.Y.)*, 272(5262), pp.735–8.

Suyama, S. et al., 2012. Purinergic signaling promotes proliferation of adult mouse subventricular zone cells. *The Journal of neuroscience : the official journal of the Society for Neuroscience*, 32(27), pp.9238–9247. Available at: http://www.ncbi.nlm.nih.gov/pubmed/22764232.

Suzuki, T., 2002. Lipid rafts at postsynaptic sites: Distribution, function and linkage to postsynaptic density. *Neuroscience Research*, 44(1), pp.1–9.

Swanson, J.A. & Watts, C., 1995. Macropinocytosis. *Trends in Cell Biology*, 5(11), pp.424–428.

Swayne, L.A. & Bennett, S.A., 2016. Connexins and pannexins in neuronal development and adult neurogenesis. *BMC Cell Biol*, 17 Suppl 1, p.10. Available at: http://www.ncbi.nlm.nih.gov/pubmed/27230672.

Swayne, L.A., Sorbara, C.D. & Bennett, S.A., 2010. Pannexin 2 is expressed by postnatal

hippocampal neural progenitors and modulates neuronal commitment. *J Biol Chem*, 285(32), pp.24977–24986.

Tadross, M.R., Tsien, R.W. & Yue, D.T., 2013. Ca2+ channel nanodomains boost local Ca2+ amplitude. *Proc Natl Acad Sci U S A*, 110(39), pp.15794–15799.

Tang, W. et al., 2015. Arf6 controls beta-amyloid production by regulating macropinocytosis of the Amyloid Precursor Protein to lysosomes. *Molecular Brain*, 8(1), p.41.

Taylor, K.A. et al., 2014. Amplification of human platelet activation by surface pannexin-1 channels. *Journal of Thrombosis and Haemostasis*, 12(6), pp.987–998.

Thompson, R.J. et al., 2008. Activation of pannexin-1 hemichannels augments aberrant bursting in the hippocampus. *Science*, 322(5907), pp.1555–1559.

Thompson, R.J., Zhou, N. & MacVicar, B.A., 2006. Ischemia Opens Neuronal Gap Junction Hemichannels. *Science*, 312(5775), pp.924–927.

Thomsen, A.R.B. et al., 2016. GPCR-G Protein-β-Arrestin Super-Complex Mediates Sustained G Protein Signaling. *Cell*, 166(4), pp.907–919.

Timóteo, M.A. et al., 2014. ATP released via pannexin-1 hemichannels mediates bladder overactivity triggered by urothelial P2Y6 receptors. *Biochemical Pharmacology*, 87(2), pp.371–379.

Torreno-Pina, J.A. et al., 2014. Enhanced receptor-clathrin interactions induced by N-glycan-mediated membrane micropatterning. *Proceedings of the National Academy of Sciences of the United States of America*, 111(30), pp.11037–42.

Traub, L.M., 2009. Tickets to ride: selecting cargo for clathrin-regulated internalization. *Nature reviews. Molecular cell biology*, 10(9), pp.583–96.

Tsao, H.K., Chiu, P.H. & Sun, S.H., 2013. PKC-dependent ERK phosphorylation is essential for P2X7 receptor-mediated neuronal differentiation of neural progenitor cells. *Cell Death Dis*, 4, p.e751.

Tsuda, M. & Inoue, K., 2016. Neuron-microglia interaction by purinergic signaling in neuropathic pain following neurodegeneration. *Neuropharmacology*, 104, pp.76–81.

Turmel, P. et al., 2011. Characterization of pannexin1 and pannexin3 and their regulation by androgens in the male reproductive tract of the adult rat. *Molecular Reproduction and Development*, 78(2), pp.124–138.

Ullrich, O. et al., 1996. Rab11 regulates recycling through the pericentriolar recycling endosome. *Journal of Cell Biology*, 135(4), pp.913–924.

Unoki, T. et al., 2012. NMDA Receptor-Mediated PIP5K Activation to Produce PI(4,5)P 2 Is Essential for AMPA Receptor Endocytosis during LTD. *Neuron*, 73(1), pp.135–148.

Uvnas, B., 1974. The molecular basis for the storage and release of histamine in rat mast cell granules. *Life Sci*, 14(12), pp.2355–2366.

Vance, J.E. & Steenbergen, R., 2005. Metabolism and functions of phosphatidylserine. *Progress in Lipid Research*, 44(4), pp.207–234.

Vanden Abeele, F. et al., 2006. Functional implications of calcium permeability of the channel formed by pannexin 1. *J Cell Biol*, 174(4), pp.535–546.

Van Rossum 1976. The effects of oligomycin on energy metabolism and cation transport in slices of rat liver. Inhibition of oxidative phosphorylation as the primary action. *Biochim Biphys Acta,* 423 (1):111-121.

Le Vasseur, M. et al., 2014. Pannexin 2 protein expression is not restricted to the CNS.

Frontiers in cellular neuroscience, 8(392), pp.1–13.
Vendeville, A. et al., 2004. HIV-1 Tat enters T cells using coated pits before translocating from acidified endosomes and eliciting biological responses. *Mol Biol Cell*, 15(5), pp.2347–2360.
Vial, C., Roberts, J.A. & Evans, R.J., 2004. Molecular properties of ATP-gated P2X receptor ion channels. *Trends in Pharmacological Sciences*, 25(9), pp.487–493.
Vitelli, R. et al., 1997. Role of the small GTPase Rab7 in the late endocytic pathway. *J Biol Chem*, 272(7), pp.4391–4397.
Vogt, A., Hormuzdi, S.G. & Monyer, H., 2005. Pannexin1 and Pannexin2 expression in the developing and mature rat brain. *Brain Res Mol Brain Res*, 141(1), pp.113–120.
Volonté, C. et al., 2012. P2X7 Receptors : Channels , Pores and More. *CNS & Neurological Disorders - Drug Targets*, 11(November 2016), pp.705–721.
Vroman, R. et al., 2014. Extracellular ATP Hydrolysis Inhibits Synaptic Transmission by Increasing pH Buffering in the Synaptic Cleft. *PLoS Biology*, 12(5).
Walker, J.E. et al., 1982. Distantly related sequences in the alpha- and beta-subunits of ATP synthase, myosin, kinases and other ATP-requiring enzymes and a common nucleotide binding fold. *The EMBO Journal*, 1(8), pp.945–951.
Wang, J. & Dahl, G., 2010. SCAM analysis of Panx1 suggests a peculiar pore structure. *The Journal of general physiology*, 136, pp.515–527.
Wang, X. et al., 2004. P2X7 receptor inhibition improves recovery after spinal cord injury. *Nature medicine*, 10(8), pp.821–7.
Wang, X.H. et al., 2009. Identification and characterization of pannexin expression in the mammalian cochlea. *J Comp Neurol*, 512(3), pp.336–346.
Wei, R. et al., 2015. Probenecid protects against cerebral ischemia/reperfusion injury by inhibiting lysosomal and inflammatory damage in rats. *Neuroscience*, 301, pp.168–177.
Weilinger, N.L. et al., 2016. Metabotropic NMDA receptor signaling couples Src family kinases to pannexin-1 during excitotoxicity. *Nat Neurosci*, 19(3), pp.432–442.
Weilinger, N.L., Tang, P.L. & Thompson, R.J., 2012. Anoxia-induced NMDA receptor activation opens pannexin channels via Src family kinases. *J Neurosci*, 32(36), pp.12579–12588.
Weinhold, K. et al., 2010. Interaction and interrelation of P2X7 and P2X4 receptor complexes in mouse lung epithelial cells. *Cellular and Molecular Life Sciences*, 67(15), pp.2631–2642.
Weisman, G.A. et al., 2012. P2Y receptors in the mammalian nervous system: pharmacology, ligands and therapeutic potential. *CNS Neurol Disord Drug Targets*, 11(6), pp.722–738.
Weisman, G.A. et al., 2012. P2Y receptors in the mammalian nervous system: pharmacology, ligands and therapeutic potential. *CNS & neurological disorders drug targets*, 11(6), pp.722–38.
West, M.A. et al., 2000. Rac is required for constitutive macropinocytosis by dendritic cells but does not control its downregulation. *Current Biology*, 10(14), pp.839–848.
West, M.A., Bretscher, M.S. & Watts, C., 1989. Distinct endocytotic pathways in epidermal growth factor-stimulated human carcinoma A431 cells. *Journal of Cell Biology*, 109(6 I), pp.2731–2739.
Wicki-Stordeur, L.E. et al., 2016. Pannexin 1 Differentially Affects Neural Precursor Cell

Maintenance in the Ventricular Zone and Peri-Infarct Cortex. *Journal of Neuroscience*, 36(4), pp.1203–1210.

Wicki-Stordeur, L.E. et al., 2012. Pannexin 1 regulates postnatal neural stem and progenitor cell proliferation. *Neural development*, 7(1), p.11. Available at: http://www.ncbi.nlm.nih.gov/pubmed/22458943.

Wicki-Stordeur, L.E., Boyce, A.K. & Swayne, L.A., 2013. Analysis of a pannexin 2-pannexin 1 chimeric protein supports divergent roles for pannexin C-termini in cellular localization. *Cell communication & adhesion*, 20(3–4), pp.73–79.

Wicki-Stordeur, L.E. & Swayne, L.A., 2012. Large Pore Ion and Metabolite-Permeable Channel Regulation of Postnatal Ventricular Zone Neural Stem and Progenitor Cells: Interplay between Aquaporins, Connexins, and Pannexins? *Stem cells international*, 2012, p.454180.

Wicki-Stordeur, L.E. & Swayne, L.A., 2013. Panx1 regulates neural stem and progenitor cell behaviours associated with cytoskeletal dynamics and interacts with multiple cytoskeletal elements. *Cell communication and signaling : CCS*, 11(1), p.62.

Wilkinson, W.J. et al., 2006. Role of ectodomain lysines in the subunits of the heteromeric P2X2/3 receptor. *Molecular pharmacology*, 70(4), pp.1159–1163.

Woehrle, T. et al., 2010. Pannexin-1 hemichannel-mediated ATP release together with P2X1 and P2X4 receptors regulate T-cell activation at the immune synapse. *Blood*, 116(18), pp.3475–3484.

Woo, S.K. et al., 2013. Complex n-Glycosylation stabilizes surface expression of transient receptor potential melastatin 4b protein. *Journal of Biological Chemistry*, 288(51), pp.36409–36417.

Worthington, R. et al., 1999. Localisation of P2X receptors in human salivary gland epithelial cells and human embryonic kidney cells by sodium dodecyl sulfate-polyacrylamide gel electrophoresis/Western blotting and immunofluorescence. *Electrophoresis*, 20, pp.2065–2070.

Wu, P.Y. et al., 2009. Functional decreases in P2X7 receptors are associated with retinoic acid-induced neuronal differentiation of Neuro-2a neuroblastoma cells. *Cell Signal*, 21(6), pp.881–891.

Xia, J. et al., 2012. Neurons respond directly to mechanical deformation with pannexin-mediated ATP release and autostimulation of P2X7 receptors. *The Journal of physiology*, 590(Pt 10), pp.2285–2304.

Xiang, Z. & Burnstock, G., 2005. Expression of P2X receptors on rat microglial cells during early development. *GLIA*, 52(2), pp.119–126.

Xu, J. et al., 2014. Imaging P2X4 receptor subcellular distribution, trafficking, and regulation using P2X4-pHluorin. *The Journal of general physiology*, 144(1), pp.81–104.

Xu, X.J. et al., 2012. Splice variants of the P2X7 receptor reveal differential agonist dependence and functional coupling with pannexin-1. *J. Cell Sci.*, 125, pp.3776–89.

Yamamoto, H. et al., 2010. Functional cross-talk between Rab14 and Rab4 through a dual effector, RUFY1/Rabip4. *Mol Biol Cell*, 21(15), pp.2746–2755.

Yan, Z. et al., 2010. Experimental characterization and mathematical modeling of P2X7 receptor channel gating. *The Journal of neuroscience : the official journal of the Society for Neuroscience*, 30(42), pp.14213–24.

Yan, Z. et al., 2006. Participation of the Lys313-Ile333 sequence of the purinergic P2X4

receptor in agonist binding and transduction of signals to the channel gate. *Journal of Biological Chemistry*, 281(43), pp.32649–32659.

Yan, Z. et al., 2008. The P2X7 receptor channel pore dilates under physiological ion conditions. *The Journal of general physiology*, 132(5), pp.563–73.

Yang, D. et al., 2015. Caspase-11 Requires the Pannexin-1 Channel and the Purinergic P2X7 Pore to Mediate Pyroptosis and Endotoxic Shock. *Immunity*, 43(5), pp.923–932.

Yu, Y. et al., 2008. Cellular localization of P2X7 receptor mRNA in the rat brain. *Brain Research*, 1194, pp.45–55.

Yudowski, G.A. et al., 2010. Cargo-Mediated Regulation of a Rapid Rab4-Dependent Recycling Pathway. *Molecular Biology of the Cell*, 82(4), pp.327–331.

Zalk, R. & Shoshan-Barmatz, V., 2006. Characterization of DIDS-sensitive ATP accumulation in brain synaptic vesicles. *FEBS Letters*, 580(25), pp.5894–5898.

Zappala, A. et al., 2007. Expression of pannexin2 protein in healthy and ischemized brain of adult rats. *Neuroscience*, 148(3), pp.653–667.

Zemkova, H. et al., 2007. Role of aromatic and charged ectodomain residues in the P2X4 receptor functions. *Journal of Neurochemistry*, 102(4), pp.1139–1150.

Zhang, S. et al., 1995. Rho family GTPases regulate p38 mitogen-activated protein kinase through the downstream mediator Pak1. *Journal of Biological Chemistry*, 270(41), pp.23934–23936.

Zhang, Y. et al., 2015. Pannexin-1 up-regulation in the dorsal root ganglion contributes to neuropathic pain development. *Journal of Biological Chemistry*, 290(23), pp.14647–14655.

Zhao, Q. et al., 2007. PIP(2) regulates the ionic current of P2X receptors and P2X(7) receptor-mediated cell death. *Channels (Austin, Tex.)*, 1(1), pp.46–55.

Zoidl, G. et al., 2007. Localization of the pannexin1 protein at postsynaptic sites in the cerebral cortex and hippocampus. *Neuroscience*, 146(1), pp.9–16.

Appendix 1

Taylor & Francis
Taylor & Francis Group

Our Ref: JB/ICAC/P17/951

14TH July 2017

Dear Andrew Boyce

Thank you for your correspondence requesting permission to reproduce the following article published in our journal in your printed thesis and to be posted in your university's repository at the University of Victoria.

Figure 1 'Analysis of a pannexin 2-pannexin 1 chimeric protein supports divergent roles for pannexin Ctermini in cellular localization' by Leigh E. Wicki-Stordeur, Andrew K. J. Boyce & Leigh Anne Swayne *Cell Communication & Adhesion* Vol 20:3 pp. 73-79 (2013).

We will be pleased to grant permission on the sole condition that you acknowledge the original source of publication and insert a reference to the article on the Journals website:

This is the authors accepted manuscript of an article published as the version of record in Cell Communication & Adhesion Research 10th May 2013.
http://www.tandfonline.com/ http://dx.doi.org/10.3109/15419061.2013.791681

Please note that this license does not allow you to post our content on any third-party websites or repositories.

Thank you for your interest in our Journal.

Yours sincerely

Jo Bateman
Routledge, Taylor & Francis Group.
4 Park Square, Milton Park, Abingdon, Oxon, OX14 4RN, UK.
Tel: +44 (0)20 7017 7617
Fax: +44 (0)20 7017 6336
Web: www.tandfonline.com
Email: Joanne.bateman@tandf.co.uk

2&4 Park Square, Milton Park, Abingdon, Oxfordshire
OX14 4RN
Tel: +44 (0) 20 7017 6000; Fax: +44 (0) 20 7017 6336

www.tandf.co.uk

Registered in England and Wales. Registered Number: 1072954
Registered Office: 5 Howick Place, London, SW10 1WG

an informa business